



Ullah, Ihsan (2014) *The role of autophagy in infection with S. pneumoniae*. PhD thesis.

<http://theses.gla.ac.uk/5648/>

Copyright and moral rights for this work are retained by the author

A copy can be downloaded for personal non-commercial research or study, without prior permission or charge

This work cannot be reproduced or quoted extensively from without first obtaining permission in writing from the author

The content must not be changed in any way or sold commercially in any format or medium without the formal permission of the author

When referring to this work, full bibliographic details including the author, title, awarding institution and date of the thesis must be given

Enlighten:Theses
<http://theses.gla.ac.uk/>
theses@gla.ac.uk

**The Role of Autophagy in Infection with
*S. pneumoniae***

IHSAN ULLAH

MBBS, PGD EBM&Ed

A thesis submitted to the College of Medical, Veterinary and Life Sciences,
University of Glasgow in fulfilment of the requirements for the degree of
Doctor of Philosophy

Institute of Infection, Immunity and Inflammation
University of Glasgow
120 University Place
Glasgow G12 8TA

October 2014

Abstract

Streptococcus pneumoniae is a common commensal of the human upper respiratory tract flora living peacefully without causing any harm to the host in normal conditions. *S. pneumoniae* can cause serious life threatening diseases in certain circumstances and usually affects children, the elderly and immunocompromised people. *S. pneumoniae* is a highly transformable pathogen and newly emerging antibiotic resistant strains are becoming commoner. Developing multi-drug resistant strains is a serious threat to the community, and the available drug treatment and vaccines do not provide full protection. Some newer strategies such as harnessing the immunological response to *S. pneumoniae* must be adopted to overcome this invasive pathogen.

The human immune system has evolved in a way to successfully detect, isolate and eliminate invading pathogens. It provides a generalised and rapid response during invasion of infectious agents and is usually enough to stop infections. Normally immunological and inflammatory responses against invading pathogens and foreign antigens are under strict control. However, they are potentially dangerous and may cause autoimmune diseases.

Autophagy is an emerging pathway associated with the innate immune system. It has an important role in infection control and maintains a fine balance in inflammatory responses to protect the host from harmful effects. Autophagy is basically a homeostatic pathway for degradation of unwanted protein aggregates at a cellular level, but has an important role in innate immunity. Autophagy-related (Atg) proteins have a crucial role in the body's immune system and take part in innate and adaptive immunity. This pathway is considered to prevent the body's immune system from attacking self-tissues and suppression of the auto-immune inflammatory responses.

In this thesis I present that infection with *S. pneumoniae* strain D39 WT and its pneumolysin deficient counter-part D39 Δ Ply induces autophagy in primary murine bone marrow derived macrophages and human neutrophils *in-vitro* and *in-vivo*. We confirmed autophagy by a classical marker protein LC3 through immunofluorescence and western blot. The associated inflammasome activation in *S. pneumoniae* infection has an inhibitory effect on autophagy

induction as was observed using WT and pneumolysin deficient strains. Similarly inflammasome inhibition with pharmacological and genetic methods up-regulates autophagy in *S. pneumoniae* infection.

I also present here that autophagy is associated with phagocytosis and intracellular killing of *S. pneumoniae* and both these pathways are used as innate immune mechanisms for clearing infection. Previous research links autophagy and phagocytosis, and the phagocytosed microbe is targeted to the lysosome for degradation and killing. Our findings here in this thesis demonstrate that these pathways are also influenced by the virulence factors of *S. pneumoniae*. Pneumolysin have some inhibitory effects on autophagy induction and phagocytosis which may be a direct effect or indirectly through the inflammasome activation.

Next, I present here a novel extracellular killing pathway in human neutrophils, the neutrophil extracellular traps generation or NETosis. *S. pneumoniae* infection induces NET generation, that is autophagy-dependent and can be inhibited by blocking autophagy pharmacologically or genetically. NET generation is morphologically the same in *S. pneumoniae* D39 WT and D39 Δ Ply but pneumolysin helps in pathogen escape from NET entrapment which is a novel finding and needs further exploration.

I present here the role of different pattern recognition receptors in *S. pneumoniae* induced autophagy signalling. *S. pneumoniae* infection induces autophagy independent of TRIF, MyD88, TLR4, TLR2 and NOD2 pathways. P38MAP kinase was also explored and has no association with autophagy induction in *S. pneumoniae* infection. Autophagy induction in *S. pneumoniae* infection may be associated with some unknown signalling pathway which needs further exploration.

Table of Contents

The Role of Autophagy in Infection with <i>S. pneumoniae</i>	1
Abstract	2
Table of Contents.....	4
List of Tables	8
List of Figures	9
Dedication	13
Acknowledgement.....	14
Author’s Declaration.....	16
Abbreviations.....	17
List of publications and presentations	22
1 Introduction.....	23
1.1 <i>Streptococcus pneumoniae</i>	24
1.1.1 <i>S. pneumoniae</i> infections	25
1.1.2 Virulence factors and toxins of <i>S. pneumoniae</i>	27
1.2 Immune defences against <i>S. pneumoniae</i>	29
1.2.1 Innate immune system	30
1.3 Macrophages and the mononuclear phagocyte system.....	47
1.3.1 Identification of macrophages	48
1.3.2 Activation of Macrophages	48
1.3.3 Macrophage host defence during <i>S. pneumoniae</i> infection	49
1.4 Human polymorphonuclear neutrophils	52
1.4.1 Functions of neutrophils.....	53
1.5 Autophagy	60
1.5.1 Molecular mechanism of autophagosome formation	61
1.5.2 Role of autophagy in Infection.....	66
1.5.3 Role of autophagy in immunity.....	68
1.5.4 Role of autophagy in inflammatory and autoimmune diseases	70
1.6 Project Aim, Objectives and Implications	72

1.6.1	Aim	72
1.6.2	Objectives	72
1.6.3	Implications	73
2	Materials and Methods	74
2.1	Materials	75
2.1.1	Mouse strains used in this study	75
2.1.2	Cell Culture.....	76
2.1.3	Bacterial cultures.....	89
2.2	Methods	93
2.2.1	Cell viability assay.....	93
2.2.2	<i>S. pneumoniae</i> CFU counting and bacterial dose optimisation (MOI).....	93
2.2.3	Immunofluorescence slide preparation and fluorescent microscopy	94
2.2.4	Neutrophil activation, NET staining and immunoblotting	95
2.2.5	Bacterial staining in the NETs and confocal microscopy	96
2.2.6	Western blot analysis	97
2.2.7	Enzyme linked Immunosorbent Assay (ELISA)	99
2.2.8	Flow cytometry (FACS).....	100
2.2.9	siRNA transfection in primary murine BMDMs	100
2.2.10	Human neutrophil electroporation	101
2.2.11	Gentamicin protection assay	101
2.2.12	Neutrophil phagocytosis and killing assay	102
2.2.13	LDH cytotoxicity assay	103
2.2.14	Animal model used in this study (<i>in vivo</i> experiments)	105
2.3	Statistical analysis of data	118
3	Infection with <i>S. pneumoniae</i> induces autophagy in primary murine bone marrow derived macrophages (BMDMs)	120
3.1	Introduction	121
3.2	Results	125
3.2.1	Autophagy induction in primary murine BMDMs infected with <i>S. pneumoniae</i> using immunofluorescence (IF) and western blot (WB) techniques	125
3.2.2	Autophagy induction in primary murine BMDMs infected with <i>S. pneumoniae</i> is dose dependent	127
3.2.3	Monitoring autophagy flux with lysosomal inhibitors.....	129
3.2.4	Effects of antibodies to pneumococcal surface protein A (<i>PspA</i>) on autophagy induction with <i>S. pneumoniae</i> infection	135
3.2.5	Blocking autophagy pathway by chemical and genetic methods in murine BMDMs	137

3.2.6	Phagocytosis (internalization) of <i>S. pneumoniae</i> by primary murine BMDMs	146
3.2.7	Relationship of autophagy with inflammasome activation	154
3.2.8	Effects of inflammasome activation on autophagy induction in primary murine BMDMs	156
3.2.9	Influence of autophagy inhibition on inflammasome activation in <i>S. pneumoniae</i>	160
3.2.10	The role of TIR-domain-containing adapter-inducing interferon- β (TRIF) in autophagy induction	166
3.2.11	Autophagy induction in murine BMDMs from <i>Myd88</i> knock-out mice infected with <i>S. pneumoniae</i>	170
3.2.12	Role of TLR4 in autophagy induction in primary murine BMDMs in infection with <i>S. pneumoniae</i>	172
3.2.13	Role of TLR2 in autophagy induction in murine BMDMs infected with <i>S. pneumoniae</i>	175
3.2.14	Role of NOD2 in autophagy induction in primary murine BMDMs	177
3.2.15	Influence of a P38MAP Kinase Inhibitor on Autophagy induction in primary murine BMDMs infected with <i>S. pneumoniae</i>	179
3.3	Discussion and Conclusion	181
3.3.1	Discussion	181
3.3.2	Conclusion	183
4	<i>In vivo</i> Studies of Autophagy following <i>S. pneumoniae</i> Infection	184
4.1	Introduction	185
4.2	Results	186
4.2.1	Autophagy induction in <i>in vivo</i> mouse model of <i>S. pneumoniae</i> infection	186
4.2.2	Role of autophagy in <i>S. pneumoniae</i> clearance during <i>in vivo</i> infection	188
4.2.3	Influence of autophagy in <i>S. pneumoniae</i> induced inflammasome activation <i>in vivo</i>	191
4.2.4	Influence of autophagy on protein content of peritoneal fluid in <i>S. pneumoniae</i> infection	193
4.3	Discussion	194
5	Infection with <i>S. pneumoniae</i> induces autophagy, phagocytosis and neutrophil extracellular traps in human neutrophils	196
5.1	Introduction	197
5.2	Results	199
5.2.1	Autophagy induction in human neutrophils infected with <i>S. pneumoniae</i> using immunofluorescence (IF) and western blot (WB) techniques	199
5.2.2	Dependence of autophagy on multiplicity of infection	201

5.2.3	Autophagy flux is increased following infection of neutrophils with <i>S. pneumoniae</i>	203
5.2.4	Blocking autophagy by chemical and genetic methods	206
5.2.5	Relationship of autophagy with inflammasome activation	211
5.2.6	Phagocytosis and killing of <i>S. pneumoniae</i> by human neutrophils ..	215
5.2.7	Neutrophil extracellular trap (NET) generation by human neutrophils following infection with <i>S. pneumoniae</i>	224
5.2.8	Inhibition of autophagy attenuates NET generation in human neutrophils following infection with <i>S. pneumoniae</i>	226
5.3	Discussion and conclusion	231
6	General Discussion and Conclusions	234
6.1	Discussion	235
6.2	Conclusion	241
6.3	Future Plans	243
	References	245

List of Tables

Table 1.1 Mouse TLRs with their PAMPs and adaptor proteins.....	38
Table 1.2 Different NLRs subfamilies and their structure	42
Table 1.3 Cell surface markers and genes expressed by tissue macrophages	51
Table 1.4 Directly acting neutrophil proteins and their antimicrobial actions...	57
Table 2.1 Antibodies used in this study along with working concentration.....	106
Table 2.2 siRNA controls used in this study.....	110
Table 2.3 siRNA used in this study	111
Table 2.4 Solutions, Buffers, chemicals, drugs and other material and equipment used in this study.....	113

List of Figures

Figure 1.1 Schematic representation of basic structure of PRRs	34
Figure 1.2 Schematic representation of Autophagy pathway	65
Figure 2.1 Primary murine BMDMs surface marker F4/80 staining	79
Figure 2.2 Rapid Romanowski staining of human neutrophils.....	82
Figure 2.3 Optimisation of siRNA transfection with siGLO Green transfection indicator in murine BMDMs	84
Figure 2.4 Optimisation of siRNA transfection with siGLO Green transfection indicator in human neutrophils.....	86
Figure 2.5 7AAD staining of human neutrophils after electroporation	88
Figure 2.6 LDH (Cytotoxicity) Assay of murine BMDMs infected with <i>S. pneumoniae</i>	104
Figure 3.1 Autophagy induction in primary murine BMDMs following <i>S. pneumoniae</i> infection.....	126
Figure 3.2 Dependence of autophagy on multiplicity of infection (MOI) in primary murine BMDMs.....	128
Figure 3.3 Cell cytotoxicity assay (% LDH released by the cells)	130
Figure 3.4 Lysosomal inhibitors of autophagy E64d and Pepstatin A increased accumulation of autophagy flux.....	132
Figure 3.5 Inhibition of lysosomal degradation by Bafilomycin A1 increases levels of LC3 II	134
Figure 3.6 Effects of anti- <i>PspA</i> antibody on autophagy induced by <i>S. pneumoniae</i> infection	136
Figure 3.7 3-MA inhibits autophagy in primary murine BMDMs	139
Figure 3.8 <i>S. pneumoniae</i> induced autophagy in primary murine BMDMs is LC3 dependent.	141
Figure 3.9 <i>S. pneumoniae</i> induced autophagy is Atg5 dependent.....	143
Figure 3.10 <i>S. pneumoniae</i> induced autophagy is Atg7 dependent.	145
Figure 3.11 <i>S. pneumoniae</i> strain D39 WT is resistant to phagocytosis when compared to its pneumolysin deficient counter-part	147

Figure 3.12 Antibody to <i>PspA</i> up-regulates phagocytosis of <i>S. pneumoniae</i> by murine BMDMs.....	149
Figure 3.13 3-MA down regulates phagocytosis of <i>S. pneumoniae</i> by murine BMDMs	151
Figure 3.14 Autophagy gene <i>Lc3b</i> knock down in murine BMDMs down-regulates phagocytosis of <i>S. pneumoniae</i>	153
Figure 3.15 Inflammasome activation by <i>S. pneumoniae</i> strains D39 WT and D39 Δ Ply.....	155
Figure 3.16 Autophagy is up-regulated in the presence of the caspase-1 inhibitor Z-YVAD-FMK in murine BMDM infected with <i>S. pneumoniae</i>	157
Figure 3.17 <i>Caspase-1</i> gene Knock down in primary murine BMDMs up-regulates autophagy in <i>S. pneumoniae</i> infection	159
Figure 3.18 Activation of the Inflammasome by <i>S. pneumoniae</i> infection in primary murine BMDM pre-treated with 3MA.....	161
Figure 3.19 Inflammasome activation is up-regulated by knock down of autophagy genes <i>LC3b</i> and <i>Atg5</i> in murine BMDMs	163
Figure 3.20 Inflammasome activation is up-regulated in <i>Vav-Atg7</i> ^{-/-} primary murine BMDMs infected with <i>S. pneumoniae</i>	165
Figure 3.21 Autophagy induction following infection with <i>S. pneumoniae</i> is not dependent on TRIF pathway.	167
Figure 3.22 TRIF is not required as adaptor protein for autophagy induction in murine BMDMs infected with <i>S. pneumoniae</i>	169
Figure 3.23 MYD88 is not required for autophagy induction in murine BMDMs with <i>S. pneumoniae</i> infection.	171
Figure 3.24 Autophagy induction is not affected in TLR4- defective LPS hypo-responsive murine BMDMs in infection with <i>S. pneumoniae</i>	173
Figure 3.25 Role of TLR4 in autophagy induction in primary murine BMDMs infected with <i>S. pneumoniae</i>	174
Figure 3.26 TLR2 is not required for autophagy induction in murine BMDMs infected with <i>S. pneumoniae</i>	176
Figure 3.27 NOD2 has no role with the induction of autophagy in primary murine BMDMs	178
Figure 3.28 P38-mitogen activated protein kinase inhibitor has no effect on autophagy induction in murine BMDMs infected with <i>S. pneumoniae</i>	180

Figure 4.1 3MA inhibits <i>S. pneumoniae</i> induced Autophagy <i>in vivo</i>	187
Figure 4.2 Inhibition of Autophagy increased CFU of <i>S. pneumoniae</i> in the peritoneal lavage	189
Figure 4.3 Autophagy up-regulates phagocytosis of <i>S. pneumoniae in vivo</i>	190
Figure 4.4 Autophagy induction down regulates cytokine production in <i>in vivo</i> infection with <i>S. pneumoniae</i>	192
Figure 4.5 Autophagy inhibition increases protein content of peritoneal fluid in <i>S. pneumoniae</i> infection.....	193
Figure 5.1 Autophagy induction in human neutrophils infected with <i>S. pneumoniae</i>	200
Figure 5.2 Dependence of autophagy on multiplicity of infection	202
Figure 5.3 Infection with <i>S. pneumoniae</i> increases autophagocytic flux in human neutrophils	204
Figure 5.4 Infection with <i>S. pneumoniae</i> increases autophagocytic flux in human neutrophils	205
Figure 5.5 3-Methyl-adenine inhibits autophagy in human neutrophils	207
Figure 5.6 <i>S. pneumoniae</i> induced autophagy is Atg5 dependent.....	210
Figure 5.7 Inflammasome activation by <i>S. pneumoniae</i> strains D39 WT and D39 Δ Ply.....	212
Figure 5.8 Inflammasome activation by <i>S. pneumoniae</i> strains D39 WT and D39 Δ Ply in neutrophils knocked down for autophagy.....	214
Figure 5.9 Phagocytosis and killing of <i>S. pneumoniae</i> strains D39 WT and D39 Δ Ply by human neutrophils.....	217
Figure 5.10 Effect of 3-MA on phagocytosis and killing of <i>S. pneumoniae</i> strain D39 WT by human neutrophils.....	220
Figure 5.11 Phagocytosis and killing of <i>S. pneumoniae</i> D39 WT by human neutrophils knocked down for (<i>Atg5</i>) autophagy gene.....	223
Figure 5.12 Human neutrophils generate NETs in infection with <i>S. pneumoniae</i>	225
Figure 5.13 NET generation in human neutrophils following infection is down regulated by inhibition of autophagy with 3MA.	227

Figure 5.14 Autophagy gene <i>Atg5</i> knock down in human neutrophils down-regulates NETs generation in infection with <i>S. pneumoniae</i>	228
Figure 5.15 NET trapping of <i>S. pneumoniae</i> D39 WT and D39 Δ Ply in human neutrophils	230
Figure 6.1 Schematic representation of autophagy, phagocytosis and NETosis .	243

Dedication

This work is dedicated to my dear parents and family whose prayers, encouragement and never ending love enabled me to achieve every dream of my life. Without their support and help, the completion of this work would not have been possible.

Acknowledgement

First of all I am extremely thankful to my creator and sustainer, the ALMIGHTY ALLAH, the most beneficent and the most merciful for granting me the courage and health to complete my PhD and this thesis.

I am very much thankful to my supervisor Professor T J Evans for his endless guidance, encouragement, motivation, enthusiasm and support during my lab work and during writing this thesis. I consider myself very lucky to have Professor T J Evans as my supervisor. You are truly a brilliant academician, a great scientist with extensive publications in molecular microbiology and immunology and a reputed clinician. I believe that ALLAH has gifted you with extraordinary skills and a very caring, loving and sincere personality. You are an excellent mentor and have guided me through all the phases of my PhD: in the first year to get my head round the basic lab skills and experimental work; in the second year to work on my project independently under your kind guidance and encouragement; and in 3rd year to become an independent researcher and an academic writer. I must say that you have not only provided me the vision and direction in my PhD but have enormously helped me in developing my personality. I hope we will stay in touch in future.

I would also like to acknowledge the people who helped me during my PhD, all members of the Evans lab, past and present. I am very thankful to Dr Alexandra Macpherson, Dr Neil Ritchie, Dr Hannah Byes, Dr Majid Jabir, Dr Sharon Irvine and Dr Ruth McCartney. Without you guys it would not be worth it. It is a great department and I feel privileged to have worked with all of you. I would be happy to have anyone of you on a break to my country Pakistan.

I would also like to acknowledge some people in the Institute of Infection, Immunity and Inflammation who helped me during my PhD, the technicians especially Mr Robert Thomson, Ms Helen Arthur, Mr Jim Scot and Ms Diane Vaughan and all other supporting staff of this institute. You were always there to help me and spared your precious time for me for which I am thankful.

I am also grateful to Khyber Medical University Peshawar, Pakistan and Higher Education Commission of Pakistan for funding my studies here at the University

of Glasgow, UK. I highly appreciate the efforts of Professor M Hafeez Ullah, Prof. Shad Muhammad, Prof. Jawad Ahmad, Col. Ehtesham, Mr. Arshad, and all KMU PhD Scholars. I am thankful to Charles Wallace Trust Pakistan and the University of Glasgow for their financial support during the last period of my project.

I would also like to thank my parents for everything. You are the best parents in the world and I am here because of you and your endless help and prayers for me. The encouragement and prayers from my parents and family members throughout my whole career have been invaluable. I pray ALMIGHTY ALLAH for your good health and long life. I am also grateful to my mother-in-law who took care of my son Arsal during the early days of my PhD.

Finally and foremost a massive thank to my sweet wife Dr Humera Adeeb for encouraging me from the beginning of my PhD. Thank you for moving with me to Glasgow and taking care of our sweet and lovely children Arsal and Hamdan. I would also like to apologize to you, Arsal and Hamdan for not giving proper attention and love which you deserved during my PhD. This really would not have been possible without your patience. I love you, my sons Arsal and Hamdan.

Author's Declaration

This work represents original work carried out by the author, unless otherwise stated, and has not been submitted in any form to any other University.

Ihsan Ullah _____

October 2014

Abbreviations

ACD	Acid-citrate dextrose
AIM2	Absent in melanoma 2
Ambra1	Activating molecule in Beclin-1 regulating autophagy
ANOVA	Analysis Of Variance
ASC	Apoptosis-associated speck-like protein containing a CARD
APC	antigen presenting cells
ATG	Autophagy-related
BCA	Bicinchoninic acid
BHI	Brain heart infusion
BIR	Baculoviral inhibitory repeat- like domain
BLP	bacterial lipoprotein
BM	bone marrow
BMDM	bone marrow derived macrophage
BSA	Bovine serum albumen
CARD	Caspase activation and recruitment domain
Cat	Catalogue
CD	Cohn's disease
CFU	Colony forming unit
CLRs	C- type lectin receptors
COX2	Cyclo-oxygenase type- II
CSF	cerebrospinal fluid
CNS	central nervous system
DAPI	4',6-diamidino-2-phenylindole
DC	dendritic cells

DAMP	danger-associated molecular pattern
dH ₂ O	Distilled water
DC	Dendritic cells
DMEM	Dulbecco's modified Eagle's medium
DMSO	Dimethyl sulfoxide
DNA	Deoxyribonucleic acid
DTT	Di-thiothreitol
ECL	Enhanced Chemiluminescence
EDTA	Ethylene diamine tetra acetic acid
ELISA	enzyme-linked immunosorbent assay
ER	Endoplasmic reticulum
FACS	fluorescence activated cell sorting
FCS	foetal calf serum
FITC	fluorescein isothiocyanate
FSC	forward scatter
GFP	green fluorescent protein
GM-CSF	granulocyte macrophage colony stimulating factor
HIV	human immuno- deficiency virus
HRP	Horseradish peroxidase
IF	Immunofluorescence
IFN	interferon
Ig	Immunoglobulin
IL	interleukin
iNOS	Inducible nitric oxide synthase
Ip	Intra-peritoneal
IRF	interferon regulatory factor

KCl	Potassium Chloride
LC3 (MAP LC3)	microtubule-associated protein light chain-3
LDH	Lactate dehydrogenase
LDS	lithium dodecyl sulfate
LIR	LC3- interacting region
LPS	lipopolysaccharide
M1	classically activated macrophages
M2	alternatively activated macrophages
M-CSF	monocyte-stimulating factor
MDR	multi-drug resistant
MDP	Muramyl di-peptide
MES	2-(N-morpholino) ethane sulfonic acid
MHC	major histocompatibility complex
μ F	Micro Farad
MOI	Multiplicity of infection
MPO	Myeloperoxidase
mTOR	Mammalian target of rapamycin
MYD88	myeloid differentiation factor 88
NaCl	Sodium chloride
NADPH	nicotinamide adenine dinucleotide Phosphate-oxidase
NAIP	Neuronal apoptosis inhibitory protein
NGS	Normal goat serum
NET	neutrophil extracellular trap
NF- κ B	nuclear factor kappa- B
NK	natural killer
NLR	Node-like receptor

NO	nitric oxide
NOD	nucleotide-binding oligomerisation domain
OD	Optical density
Ply	pneumolysin
PavA	Pneumococcal adherence and virulence factor A
PAGE	Poly Acrylamide Gel Electrophoresis
PE	Phosphatidyl ethanolamines
PFA	Paraformaldehyde
PspA	Pneumococcal surface protein A
PspC	Pneumococcal surface protein C
PAMP	pathogen associated molecular pattern
PBS	phosphate buffered solution
PCR	polymerase chain reaction
PCV	Polyvalent conjugate vaccines
PI(3)K	Phosphoinositide-3-kinase
PtdIns(3)p	Phosphatidylinositol 3- phosphate
PPV	Polyvalent polysaccharide vaccines
PG	prostaglandins
PFA	Para formaldehyde
PRR	pattern recognition receptor
PVDF	polyvinylidene difluoride
P38MAPK	P38 mitogen-activated protein kinase
ROS	Reactive oxygen species
RPMI	Roswell Park Memorial Institute - 1640 medium
RIPA	Radio immuno-precipitation assay
SEM	Standard error mean

7-AAD	7- amino- actinomycin
SD	standard deviation
SDS	sodium dodecyl sulfate
SLE	systemic lupus erythematosus
siRNA	Small interfering RNA
SSC	side scatter
3MA	3-methyl- adenine
TGF	transforming growth factor
TRAF	TNF receptor activated factor
TRIF	TIR domain containing adapter-inducing interferon- β
TLR	Toll like receptor
TNF	tumor necrosis factor
WB	Western blot
WHO	World health organization
WT	Wild type

List of publications and presentations

Meeting abstracts

- 1 Ihsan Ullah and T J Evans., Autophagy in Infection with *S. pneumoniae*, Oral presentation, Annual Health Symposium, Khyber Medical University Peshawar, Pakistan December, 2012.
- 2 Ihsan Ullah and T J Evans., Induction of autophagy in *S. pneumoniae* infection down regulates inflammasome activation, Oral presentation. Scottish society for experimental medicine Edinburgh, March 2013.

Presentations

- 1 Ihsan Ullah and T J Evans., The Role of Autophagy in Infection with *S. Pneumoniae*. Poster presented at the Institute of Infection, Immunity and Inflammation University of Glasgow, May 2012.
- 2 Ihsan Ullah and T J Evans., Autophagy in Infection with *S. pneumoniae*, Oral presentation. Annual Health Symposium, Khyber Medical University Peshawar, Pakistan, Feb, 2013.
- 3 Ihsan Ullah and T J Evans., Induction of Autophagy in *S. pneumoniae* infection down regulates inflammasome activation. Poster presented at Institute of Infection, Immunity and Inflammation University of Glasgow, May, 2013.

1 Introduction

1.1 *Streptococcus pneumoniae*

S. pneumoniae is a fastidious oval or club shaped pathogen, occurring singly, in pairs or short chains. It is an inhabitant of the normal flora of the human upper respiratory tract (Gray et al., 1980). Normally it lives as a commensal in the pharynx along with other microbes and causes no harm to the host, but unfortunately in some circumstances can cause a number of diseases ranging from otitis media to severe life threatening conditions e.g. pneumonia, meningitis, septicaemia and sinusitis (Cartwright, 2002, Cornick et al., 2011).

S. pneumoniae is currently the leading cause of invasive bacterial disease in children under 5 years and in elderly people. It is more prevalent in the developing world (Rudan et al., 2008, O'Brien et al., 2009). It is responsible for a considerable economic burden. According to the World Health Organization estimates in 2005, around 1.6 million people died of these diseases every year including children with a mortality of almost 0.7 to 1 million (WHO, 2008).

Treatment options for pneumococcal diseases are limited because of emerging new strains which are resistant not only to the traditional antibiotics but also to second-line drugs such as chloramphenicol, Tetracycline and Sulphonamides (Bouza et al., 2005). *S. pneumoniae* is a highly transformable organism, which enables it to develop resistance against antimicrobial drugs by producing new resistant strains. Recent studies demonstrate that *S. pneumoniae* is becoming less susceptible to treatment throughout the world. Its resistance is increasing at an alarming rate with the emergence of multi- drug resistant (MDR) strains (Zhanet al., 2003, Song et al., 2004, Lee et al., 2001).

The growing threat of pneumococcal diseases and the emergence of MDR strains is a big problem worldwide. Polyvalent polysaccharide vaccines (PPV) were successful in the beginning to combat common serotypes causing invasive pneumococcal diseases, but gradually a decline has appeared in the effectiveness of these vaccines due to the emerging new strains (Brueggemann et al., 2007). Polyvalent conjugate vaccines (PCV) provide full protection from the vaccine serotypes but transformable pneumococci may switch their genes to non-capsular serotypes and allow the microbe to escape vaccine-induced immunity (Hsieh et al., 2008).

1.1.1 *S. pneumoniae* infections

S. pneumoniae infections are of two types; invasive and non- invasive. Invasive pneumococcal infections involve a major organ for example meningitis, bacteraemia, pneumonia and septic arthritis, whereas non-invasive infections remain outside the major organs for examples bronchitis, otitis media and sinusitis.

1.1.1.1 Meningitis

Inflammation of the brain and spinal cord protective membranes along with invasion of cerebrospinal fluid (CSF) as a result of pneumococcal infection is called pneumococcal meningitis. It is a serious life threatening condition and is characterized by a range of symptoms including headache, stiffening of the neck, seizures, and coma which can lead to death. Mortality ranges from 16 - 37%, with residual neurological sequelae in 32- 50 % (Ostergaard et al., 2005, Kastenbauer and Pfister, 2003). Pneumococcal meningitis is the second largest cause of bacterial meningitis in the United Kingdom.

S. pneumoniae invades the blood stream and gains access to the meninges. Meningitis is generally preceded by initial pneumococcal infection elsewhere, in about 30 % of cases of acute otitis media and about 18 % cases with pneumonia (Ostergaard et al., 2005). *S. pneumoniae* also has the ability to invade and infect the central nervous system directly through the olfactory neurons (van Ginkel et al., 2003).

1.1.1.2 Bacteraemia

Bacteraemia is a condition in which bacteria gain access to the blood stream by any means and invade normally sterile sites i.e. blood and CSF. Non-invasive pneumococcal infections may lead to bacteraemia, which can lead to sepsis and death. Bacteraemia can develop independently without prior non-invasive pneumococcal diseases. It has been shown that bacteraemia is the most common type of invasive pneumococcal disease worldwide (Laterre et al., 2005, Myers and Gervaix, 2007).

1.1.1.3 Pneumococcal pneumonia

Pneumococcal pneumonia is characterized by inflammation of the lung parenchyma with consolidation and exudation into the alveolar spaces which blocks gaseous exchange between the lungs and bloodstream. *S. pneumoniae* is the most common bacterium that causes community acquired pneumonia in children and is responsible for up to 35 % of cases in adults. It is responsible for approximately 11-12 % of all childhood deaths, mostly in developing countries (Moine et al., 1995, O'Brien et al., 2009).

The organism colonises the nasopharynx and spreads directly to the respiratory tract through airways. *S. pneumoniae* can also penetrate epithelial surfaces and produces bacteraemia and other invasive diseases. Important predisposing factors of pneumococcal pneumonia are extremes of age, pulmonary, cardiac, hepatic or neurological diseases, smoking, cancer, HIV, diabetes, alcohol abuse, recent hospitalization and previous pneumonia (Dockrell et al., 2012, Cardozo et al., 2008).

1.1.1.4 Acute otitis media

Acute otitis media is a common pneumococcal infection and is relatively a benign problem. It is characterized by pneumococcal growth in the middle ear and is a common disease of children. Infections are generally transmitted through the colonization of the nasopharynx. Its incidence is 10.85 % acute and 4.7 % chronic otitis media of which almost 51 % of cases occur in children under 5 years. Each year 21,000 people die worldwide due to complications of otitis media (Hausdorff et al., 2002, Monasta et al., 2012).

1.1.1.5 Sinusitis

Inflammation of the para-nasal sinuses is commonly caused by an allergic response or viral infection. A small proportion of sinusitis cases progress to secondary bacterial infection. *S. pneumoniae* causes acute purulent sinusitis in children and adults along with some other gram positive and gram negative bacteria (Brook, 2011).

1.1.1.6 Other pneumococcal infections

S. pneumoniae is also responsible for some relatively less important clinical conditions. Generally non-typable pneumococci are considered to cause pneumococcal conjunctivitis (Williamson et al., 2008). *S. pneumoniae* also causes inflammation of the endocardium, which may involve the heart valves and inter-ventricular septum, showing the invasive nature of *S. pneumoniae* (Tsang et al., 2013). Some rare diseases like cerebral abscess are also caused by *S. pneumoniae* (Belodu et al., 2013).

1.1.2 Virulence factors and toxins of *S. pneumoniae*

1.1.2.1 Pneumolysin (Ply)

Pneumolysin (Ply) is an important toxin of *S. pneumoniae* belonging to the pore-forming toxin group and plays an important role in the pathogenesis of disease. Ply can lyse host cells through its action on the cholesterol component of the cell membranes in the tissues coverings of pulmonary and cerebral surfaces. It can attack the immune system of the body and disrupts functions of the immune molecules as well as induce necrosis and apoptosis of the immune cells (Marriott et al., 2008, Molloy, 2011).

Ply is a strong inducer of inflammasome activation leading to the release of inflammatory cytokine IL-1 β from different murine and human inflammatory cells (Shoma et al., 2008, Littmann et al., 2009). It also has inhibitory effects on monocyte degranulation and induction of IL-1 β and TNF- α secretion to prevent pneumococcal clearance from the infection site (Houldsworth et al., 1994). Ply can activate the complement system in the host through classical pathway by binding the Fc portion of IgG (Mitchell et al., 1991). Ply along with other virulence factors *PspA* and *PspC* helps in nasopharyngeal colonization of *S. pneumoniae* (Ogunniyi et al., 2007).

Ply interacts with Toll-like receptor 4 (TLR4) and induces innate immune response against *S. pneumoniae* (Malley et al., 2003) but can also activate NLRP3 inflammasome independent of the TLR4 pathway (McNeela et al., 2010). The role of Ply and its associated inflammasome activation will be studied in this thesis.

1.1.2.2 *S. pneumoniae* capsule

S. pneumoniae has a capsular covering composed of polysaccharide and the available polyvalent vaccines are based on it. The capsule helps to protect *S. pneumoniae* from phagocytosis, action of opsonins and the activity of complement system (Hyams et al., 2010). Over 90 capsular serotypes of *S. pneumoniae* have been recognised. The capsular polysaccharide consists of multiple sugar side chains attached to a sugar backbone. The monosaccharides include α or β -D-glucose, D- galactose, L- rhamnose and N-acetyl- α or β -D-glucosamine.

Sequencing of the capsular locus (*cps*) has revealed its genetic diversity and the genes lie between the *dexB* and *aliA* genes with sizes from 10,337 base pairs in serotype 3 to 30,298 base pairs in serotype 38. Analysis of the *cps* loci also show multiple enzyme classes including 40 groups of polysaccharide polymerases, 13 flippases, and a large number of transferases responsible for variable expression of different components of the capsule (Bentley et al., 2006).

S. pneumoniae can switch capsular type by horizontal gene transfer. It is the transfer of genes between organisms via a bacteriophage or plasmid, which might have a positive or negative effect on their virulence. *S. pneumoniae* escapes from the effects of vaccines by horizontal gene transfer (Hiller et al., 2010, Kelly et al., 1994). Almost 70 % of invasive diseases are caused by 6 - 11 serotypes and 7 serotypes (1, 6A, 5, 14, 6B, 19F, 23F) are more common globally (Johnson et al., 2010). In this thesis we studied highly virulent capsular serotype 2 strain D39, which is most frequently used in current pneumococcal studies (Lanie et al., 2007).

1.1.2.3 *S. pneumoniae* surface protein A (*PspA*)

Pneumococcal surface protein A (*PspA*) is a choline binding protein and a good candidate for protein based vaccines. It is a variable protein and inhibits bacterial uptake by complement mediated phagocytosis (Arulanandam et al., 2001, Ren et al., 2012). *PspA* protects *S. pneumoniae* by preventing deposition and activation of the complement system of the host. It binds to lactoferrin and

protects *S. pneumoniae* from killing by apolactoferrin (Mukerji et al., 2012, Shaper et al., 2004), and also helps in nasopharyngeal colonisation (Ogunniyi et al., 2007).

1.1.2.4 *S. pneumoniae* surface protein C (*PspC*)

PspC is a highly variable choline binding protein present on the surface of *S. pneumoniae* and may have a role in the development of sepsis (Iannelli et al., 2004). *PspC* is an important virulence factor required for nasopharyngeal colonisation and multiplication of the *S. pneumoniae* in lung tissue (Balachandran et al., 2002, Ogunniyi et al., 2007).

1.1.2.5 Other pneumococcal proteins

There are multiple other pneumococcal surface proteins and molecules which add to the virulence of *S. pneumoniae* (reviewed by Mitchell and Mitchell, 2010). The pneumococcal pilus mediates bacterial binding to the cells and induces inflammatory response. There are multiple (Leucine-Proline & Threonine-Glycine) LPXTG-anchored surface proteins including hyaluronidases, neuraminidases, and serine proteases. Hyaluronidases are secreted by most of pneumococcal isolates which break down the hyaluronic acid and aid in the bacterial spread, colonization and pulmonary inflammation. Neuraminidase cleaves N-acetylneuraminic acid from glycolipids, lipoproteins and oligosaccharides on cell surface which directly damage the host tissues or unmask binding sites of the bacterium aiding in colonisation. Serine proteases are also important and aid in tissue damage and facilitate bacterial growth (Mitchell and Mitchell, 2010). Adherence and virulence factor A (*PavA*) is another important protein associated with adherence and colonisation of *S. pneumoniae* (Pracht et al., 2005).

1.2 Immune defences against *S. pneumoniae*

The immune system of the body detects dangerous stimuli and eliminates invading pathogens. It consists of two subsystems; the innate immune system and the adaptive immune system, both working in tandem to protect the body efficiently. Generally the immune system tolerates some foreign antigens such as dietary components, environmental antigens and commensal and mutualistic

bacteria, and an immune response against these antigens would be dangerous to the body tissues.

1.2.1 Innate immune system

The innate immune system is the first line of defence against invading pathogens, and is usually sufficient to clear infection. It provides a robust early response to different pathogenic stimuli. It provides a generalised protection against all types of dangers. Innate immunity includes a range of processes against diverse pathogens such as viruses, bacteria, fungi and parasites. The important features of innate immune system are barriers at different levels such as anatomic, physiologic and chemical barriers, generalised inflammatory response, cellular response and phagocytosis by macrophages and neutrophils, complement system and synthesis of antimicrobial products.

1.2.1.1 Mucosal immunity against *S. pneumoniae*

The nasopharyngeal mucosal surfaces prevent the entry of *S. pneumoniae* into the body as first line of defence. A breach in the mucosal integrity can provide a route of entry for the pathogens. Mucosal surfaces and respiratory mucous secretion prevent microbes from entering in to the body (Boyton and Openshaw, 2002). Mucus traps the invading microbe and expels it from the respiratory airways.

S. pneumoniae entrapment in the luminal mucus is the first defence mechanism faced during entry into the nasopharynx to colonise. Capsular *S. pneumoniae* are resistant to the mucosal clearance. The polysaccharide present in mucus contains negatively charged sialic acid which repels the polysaccharide capsule of *S. pneumoniae* (Nelson et al., 2007).

1.2.1.2 Nasopharyngeal colonisation of *S. pneumoniae*

S. pneumoniae is transmitted via aerosol or respiratory droplets from one individual to another. On arrival in to the nasopharynx, *S. pneumoniae* establishes viable colonies on the surface in favourable conditions which continues until cleared by the host innate immune responses. In this colonisation

period, viable bacteria can be cultured from nasopharyngeal samples (Bogaert et al., 2004).

Predisposing factors for colonisation includes smoking, low immunity and some prior viral infections especially influenza virus. Following colonisation of the nasopharynx, *S. pneumoniae* can spread to various sites locally causing otitis media and sinusitis while its aspiration can lead to pneumonia, meningitis and septicaemia (Bogaert et al., 2004).

On entering into the nasopharynx, *S. pneumoniae* traverses the mucus barrier and binds to the apical surface of the respiratory tract epithelium. Virulence factors of *S. pneumoniae* aid in the process of colonisation. The capsule provides protection from negatively charged mucus polysaccharides and *S. pneumoniae* strains lacking capsule are expelled easily with mucus due to their greater binding (Nelson et al., 2007). Virulence factors help *S. pneumoniae* to invade the superficial tissues during mucosal attachment and colonisation (Briles et al., 2005). *PspA* binds to mucosal apolactoferrin to prevent killing of *S. pneumoniae* and aid in colonisation (Shaper et al., 2004).

PavA described earlier, also binds with fibronectin and aid in colonization of *S. pneumoniae* (Pracht et al., 2005). Structural abnormalities in the airways for example chronic obstructive pulmonary disease (COPD) can lead to pneumococcal spread and colonisation of the bronchial tree (Patel et al., 2002).

Beside the mucus trapping of *S. pneumoniae*, the host immune system adopts multiple strategies to prevent colonisation. Mucosal epithelium constitutes the first barrier and the induction of IgA antibodies prevents colonisation of *S. pneumoniae*. Mucosal immunisation with certain Lactobacillus strains can induce IgA antibodies (Oliveira et al., 2006). Moreover some soluble mucosal antimicrobial peptides including lysozyme and β -defensin-2 act synergistically and inhibit *S. pneumoniae* colonisation and infection (Lee et al., 2004).

1.2.1.3 Inflammation

Inflammation is a nonspecific response of the body to any type of injury such as cellular damage, infection and irritation. The word inflammation is derived from a Latin word “inflammatio” meaning, to set on fire. Generally inflammation is marked by five cardinal signs: redness, swelling, increased temperature, pain and loss of function described by Cornelius Celsus and Rudolf Virchow. Elevated cellular metabolism increases blood flow with vasodilatation and release of inflammatory mediators with extravasation of fluids. Inflammation is aimed to clear the injurious agent and start healing but in some circumstances it may progress to chronic inflammation (Puchta et al., 2014) .

During *S. pneumoniae* nasopharyngeal colonisation, the host immune cells release inflammatory mediators which lead to inflammation and activation of other inflammatory cells including macrophages and lymphocytes. The severity of inflammatory response depends upon the virulence of *S. pneumoniae* strain (Puchta et al., 2014). Alveolar macrophages and epithelial cells play important role in initiating the host response against *S. pneumoniae*. The release of pro-inflammatory cytokine in *S. pneumoniae* infection depends upon p38 MAP Kinase which is a potential molecular target to modulate overwhelming lung inflammation (Xu et al., 2008).

A previous study demonstrates that *S. pneumoniae* induced inflammasome activation and the release of inflammatory mediators are related to more complication in bacterial meningitis. ASC and NLRP3 inflammasome knock-out mice showed decreased systemic inflammatory responses and there was decreased bacterial growth as compared to wild type mice (Geldhoff et al., 2013). This indicates that inflammation might have no effect in the clearance of invading pathogens and it suppresses bacterial clearance by other immune mechanisms including autophagy.

1.2.1.4 Pattern recognition receptors (PRRs) involved in *S. pneumoniae* infection

When pathogens cross the first line of defence, a variety of innate immune cells are activated in the body by specialised molecules and receptors. Pattern-recognition molecules or receptor (PRRs) recognise pathogen-associated

molecular patterns (PAMPs) and initiate a signalling cascade. PAMPs are highly conserved small molecular motifs released by the microorganisms while danger-associated molecular patterns (DAMPs) are non-infectious nuclear and cytoplasmic cell products, which can initiate immune responses (Ferrero-Miliani et al., 2007, Matzinger, 2002, Janeway Jr, 1992).

Pathogens can escape the immune system by changing their PAMPs; however, the immune system recognises their essential structure. PAMPs include peptidoglycans, LPS, flagellin and pathogen related sugars while DAMPs include double stranded DNA and uric acid from tissue damage (Martinon et al., 2009, Martinon et al., 2006).

PRRs were first identified in plants and they are classified according to their location, function, ligand specificity or some other aspects. Different cell types such as macrophages, monocytes, neutrophils, dendritic cells and epithelial cells express PRRs (Martinon et al., 2009). PRRs may be cell surface and endosome related i.e. Toll-like receptors (TLRs) or soluble pentraxins and cytosolic i.e. Nod like receptors (Martinon et al., 2009). Cell surface PRRs include Toll-like receptors (Akira et al., 2006), and C-type lectins (CLRs) (Brown, 2006) while cytosolic PRRs include NLRs, RIG like helicases RLRs (Nakhaei et al., 2009) and some DNA sensors (Hornung et al., 2009, Fernandes-Alnemri et al., 2009).

Some researchers believe that PRRs are not actual receptors, and they name them (PRMs) pattern recognition molecules (Hausdorff et al., 2002). This thesis includes investigation of some TLRs and NLRs in autophagy induction and hence they are discussed in detail. The schematic representation of basic structure of TLRs and NLRs is shown in (Fig. 1.1).

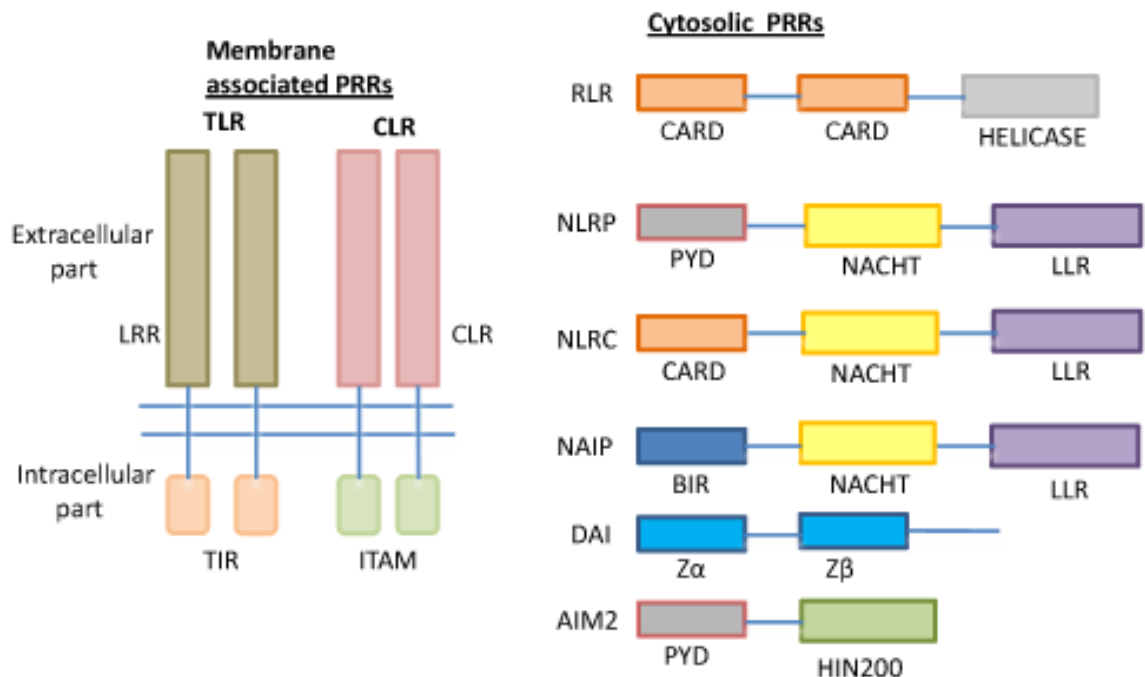


Figure 1.1 Schematic representation of basic structure of PRRs

A basic structure and different parts of PRRs is shown: TLR; Toll-like receptor, LRR; Leucine-rich repeat domain, TIR; Toll-interleukin-1 receptor (TIR) domain, CLR; C-type lectin receptor domain, ITAM; Immunoreceptor tyrosine-based activation motif, RLR; Rig-I-like receptor, CARD; Caspase recruitment and activation domain, Helicase; helicase domain, NLRP; NOD-like receptor protein, PYD; Pyrin domain, NACHT; NAIP (neuronal apoptosis inhibitor protein), CIITA (MHC class II transcription activator), HET-E (incompatibility locus protein from *Podospora anserina*) and TP1 (telomerase associated protein), NLRC; NLR family card domain containing protein, NAIP; Neuronal apoptosis inhibitory protein domain, BIR; Baculovirus inhibitor of apoptosis repeat, DAI; DNA-dependent activator of interferon regulatory factor, AIM2; Absent in melanoma 2 protein, HIN200; Haemopoietic expression, interferon-inducibility nuclear localization 200 domain, Z = Z-DNA binding domain, figure adapted from (Bryant and Fitzgerald, 2009).

1.2.1.5 Toll- like receptors (TLRs) involved in *S. pneumoniae* infection

TLRs are cell membrane and endosomal PRRs and play an important role in innate immunity. TLRs were discovered as homologues of *Drosophila* Toll protein which mediates an immune response in adult *Drosophila* (Medzhitov et al., 1997). They are type-1 trans-membrane proteins present in macrophages, monocytes, neutrophils and endothelial cells. TLRs have an extracellular leucine- rich repeat domain (LRR) which senses pathogens and transmits signals through the cytoplasmic Toll-interleukin-1 (IL-1) receptor (TIR) domain (Akira and Takeda, 2004). The TIR domain acts as a platform for downstream signalling which recruits and interacts with adaptor proteins containing a TIR- domain i.e. myeloid differentiation primary response gene (Myd88), and TIR domain-containing adaptor inducing IFN-beta, TRIF (Ishii et al., 2008, Lord et al., 1990).

MyD88 is a universal adaptor protein used by different TLRs except TLR3 (Arancibia et al., 2007). These adaptor proteins ultimately lead to the activation of transcription factor nuclear factor kappa-B (NF-kB), activator protein AP-1 and interferon regulatory factor IRF (Martinon et al., 2009). The Myd88 pathway controls inflammatory responses while the TRIF pathway mainly mediates type-I interferon (IFN) responses (Kawai and Akira, 2006).

Currently, around 13 mouse and 10 human TLRs have been identified. Cell membrane TLRs include 1, 2, 4, 5, 6, and 10, while endosomal TLRs are 3, 7, 8, 9 (Akira et al., 2006). TLRs located at the cell surface sense cell wall components of bacteria, fungi and viral proteins while those associated with endosomes recognize viral DNA and RNA (Kumar et al., 2009).

S. pneumoniae infection is associated with the activation of multiple TLRs. The cell wall component lipoteichoic acid (LTA) activates TLR2 leading to induction of inflammatory responses and activation of coagulation pathway *in vivo* which was amplified by treating with a TLR4 ligand (Dessing et al., 2008). Pneumolysin was previously believed to induce inflammasome activation independent of TLR4. A study by Malley et al. demonstrated that TLR4 activation is involved in Ply induced innate immune responses and the release of inflammatory cytokines from murine macrophages (Malley et al., 2003).

Another important receptor TLR9 (associated with endosomes) is activated by pneumococcal DNA containing un-methylated CpG motifs. *S. pneumoniae* induced TLR9 activation is involved in enhancement of phagocytosis and early clearance of bacteria from the lower respiratory tract (Albiger et al., 2007).

TLR2 activation is also believed to play an important role during *S. pneumoniae* colonisation by impairing the integrity of epithelial barrier and enhancing pneumococcal translocation across the epithelium (Clarke et al., 2011). A single pathogen can activate several TLRs leading to the most appropriate immune responses against that particular pathogen. Similarly a single TLR could be activated by multiple pathogens including bacteria, viruses, fungi and parasites. In this project we studied the role of TLR2 and TLR4 in *S. pneumoniae* induced autophagy. The schematic representation of basic structure of TLRs is shown in (Fig. 1.1). Different TLRs, their associated adaptor proteins and activating PAMPs are shown in (Table 1.1).

Cell membrane associated TLRs		
TLR	Activating PAMPs	Adaptors
TLR1/2	Bacterial and Mycobacterial tri-acyl lipopeptides	MyD88, TIRAP
TLR2	Bacterial: porins from Neisseria Lipoarabinomannan from Mycobacteria Viral: Hemagglutinin from measles virus Fungi: Phospholipomannan from Candida	MyD88 TIRAP
TLR4	Bacterial: LPS from Gram (-) bacteria Fungi: Mannan from Candida Virus :Envelope proteins from RSV Trypanosoma: Glycoinositolphospholipids	MyD88 TIRAP TRAM TRIF
TLR5	Bacterial flagellin	MyD88
TLR6/2	Bacteria: lipoteichoic acid from <i>Streptococcus</i> Saccharomyces cervisiae: zymosan Mycoplasma: lipopeptides	MyD88 TRIF
TLR11	Uropathogenic bacteria: Profilin like molecules from toxoplasma gondii	MyD88

Endosomal TLRs		
TLR3	Virus: polyinosinic: polycytidylic acid (Poly I:C) double stranded RNA, Reovirus: ssRNA from West Nile Virus	TRIF
TLR7	Bacteria: RNA Virus: ssRNA from Influenza virus and vesicular stomatitis virus	MyD88
TLR9	Bacteria: CpG-DNA motifs. Viral dsDNA from Herpes Simplex Virus and murine Cytomegalovirus Plasmodium: Hemozoin	MyD88
TLR8	Probably inactive in mice	MyD88
TLR12	Toxoplasma profilin	MyD88
TLR13	Bacterial RNA	MyD88

Table 1.1 Mouse TLRs with their PAMPs and adaptor proteins

TLR; Toll-like receptor, MyD88; Myeloid differentiation primary response gene, TRIF; TIR- domain-containing adapter-inducing interferon- β , TIRAP; Toll-interleukin 1 receptor (TIR) domain containing adaptor protein, TRAM; TRIF-related adaptor molecule, adapted from (Kumar et al., 2009, Blasius and Beutler, 2010, Hochrein and Kirschning, 2013).

1.2.1.6 NOD- like receptors (NLRs) involved in *S. pneumoniae* infection

Nucleotide- binding oligomerization domain (NOD)- like receptors (NLRs) are extensively studied cytosolic microbial sensors . Presently 23 NLRs have identified in humans and 34 in mice (Bryant and Fitzgerald, 2009). Nod1, the first identified NLR is a homologue of *C. elegans* protein (CED-4), a regulator of apoptosis (Inohara et al., 1999).

When activated, Nod1 and Nod2 start activation of receptor-interacting protein2 (RIP2) caspase-like apoptosis-regulator protein kinase (RICK) via CARD interactions leading to NF- κ B activation (Tattoli et al., 2007). Nod1 (NLRC1) and Nod2 (NLRC2) detect muropeptides from bacterial peptidoglycans. Nod1 is activated by meso- diaminopimelic acid (meso-DAP) found predominantly in Gram-negative bacteria while Nod2 is activated by muramyl dipeptides (MDP) from all bacteria (Girardin and Philpott, 2004, McDonald et al., 2005).

NLRs are multi-domain proteins with a C-terminal leucine - rich repeat (LRR), a central nucleotide domain and an N-terminal effector domain (Fig.1.1). The C-terminal LRRs sense ligands from pathogens via an unknown mechanism. Most LRRs have 20-30 amino acids with 2 or more repeats forming a horse shoe shaped molecule with tandem repeats of a β -strand and α -helix (Bella et al., 2008, Song et al., 2014). The oligomerization of central NACHT (NAIP; neuronal apoptosis inhibitor protein, CIITA; MHC class II transcription activator, HET-E; incompatibility locus protein from *Podospora anserina* and TP1; telomerase-associated protein) domain is important for the activation of NLRs which form active multimeric complexes such as the Nod signalosome and inflammasome (Franchi et al., 2012, Faustin et al., 2007).

The N-terminal effector domain divides NLRs into different sub-families i.e. NLRC which contains a caspase recruitment domain (CARD), NLRP contains a pyrin domain (PYD) and the NAIP contains three baculovirus inhibitors of apoptosis protein repeat domains (BIRs). The N-terminal domain mediates signal transduction to their targets such as activation of caspases and NF- κ B, and has a death domain (DD) and the death effector domain DED which form homologous dimers and trimmers to bind receptors to the adaptors and recruit other CARD or PYD containing proteins (Park et al., 2007, Bonardi et al., 2012).

Currently, five NLR subfamilies have been described and each has a specific molecular structure. NLRP is the largest with 14 genes in the human genome (Proell et al., 2008, Ting et al., 2008, Tschopp et al., 2003). NLRP1-3 proteins are present in the inflammasome complexes while NLRC subfamily contains NOD1,-2 and NLRC3-5 (Proell et al., 2008, Ting et al., 2008, Martinon and Tschopp, 2005). NLRA, NLRB and NLRX are the remaining subfamilies which contain immune regulatory proteins class-II transcriptional activator domain (CIITA), neuronal apoptosis inhibitory protein domain (NAIP) and NLRX1 respectively (Ting et al., 2008).

These NLRs have important functions and lead to inflammasome activation and production of pro-inflammatory cytokines (Wen et al., 2013). Peptidoglycan from *S. pneumoniae* is sensed by Nod2 which on activation releases inflammatory mediator by immune cells. This role of Nod2 is required for the *S. pneumoniae* clearance (Davis et al., 2011). Pneumolysin activates NLRP3 inflammasome in *S. pneumoniae* infection which induces protective immunity against respiratory infections (McNeela et al., 2010).

The schematic representation of basic structure of different NLRs is shown in figure 1.1. Different NLR subfamilies in humans and mice, their nomenclature and structure are shown in (Table 1.2). In this project we studied the role of Nod2 in autophagy induction.

NLRs Subfamilies	Nomenclature (Mouse)	Nomenclature (Human)	Structure
NLRA	CIITA	CIITA	CARD- AD- NACHT- NAD- LRR
NLRB	NAIP a-g	NAIP	BIR- BIR- BIR- NACHT- LRR
NLRC	Nod1	Nod1	CARD- NACHT- NAD- LRR
-	Nod2	Nod2	CARD- CARD- NACHT- NAD-LRR
-	NLRC3	NLRC3	CARD- NACHT- NAD- LRR
-	NLRC4	NLRC4	CARD- NACHT- LRR
-	NLRC5	NLRC5	CARD- NACHT- LRR
NLRP	NLRP1a		NACHT- NAD- LRR- FIIND-CARD
		NLRP1	PYD- NACHT- NAD- LRR- FIIND- CARD
	NLRP2	NLRP2	PYD- NACHT- NAD- LRR
	NLRP3	NLRP3	PYD- NACHT- NAD- LRR
	NLRP4 a-g	NLRP4	PYD- NACHT- NAD- LRR
	NLRP5		NACHT- NAD- LRR

		NLRP5	PYD- NACHT- NAD- LRR
	NLRP6	NLRP6	PYD- NACHT- NAD- LRR
		NLRP7	PYD- NACHT- NAD- LRR
		NLRP8	PYD- NACHT- NAD- LRR
	NLRP9 a-c	NLRP9	PYD- NACHT- NAD- LRR
	NLRP10	NLRP10	PYD- NACHT- NAD
		NLRP11	PYD- NACHT- NAD- LRR
	NLRP12	NLRP12	PYD- NACHT- NAD- LRR
		NLRP13	PYD- NACHT- NAD- LRR
	NLRP14	NLRP14	PYD- NACHT- NAD- LRR
NLRX	NLRX1	NLRX1	X- NACHT- LRR

Table 1.2 Different NLRs subfamilies and their structure

NLRP; NOD-like receptor protein, CIITA; Class-II transcriptional activator domain, AD; Acidic activation domain, NAD; Nicotinamide adenine dinucleotide, LRR; Leucine-rich repeat domain, NOD; Nucleotide-binding oligomerization domain, CARD; Caspase recruitment and activation domain, PYD; Pyrin domain, NACHT; NAIP (neuronal apoptosis inhibitor protein), CIITA (MHC class II transcription activator), HET-E (incompatibility locus protein from *Podospora anserina*) and TP1 (telomerase associated protein), NLRC; NLR family card domain containing protein, NAIP; Neuronal apoptosis inhibitory protein domain, BIR; Baculovirus inhibitor of apoptosis repeat, adapted from (Jacobs and Damania, 2012, Martinon et al., 2009, Ting et al., 2008).

1.2.1.7 Caspases

Caspases are cysteine-aspartate proteases secreted as a pro-form and then proteolytically activated. The activated enzyme subunits are named following their molecular size i.e. (caspase-1 p10 & p20). Currently, 13 mammalian and 11 human caspases have been identified that play essential biological roles in inflammation and apoptosis (Cohen, 1997, Earnshaw et al., 1999).

Caspases are classified according to their role in apoptosis and inflammation. Caspases associated with apoptosis are caspase-3, -6, -7, -8 and -9 (in mammals) and inflammatory caspases are caspases-1, -4, -5, -12 (in humans) and caspase-1, -11 and -12 (in mice) while caspase-2, -10 and -14 could not be categorized (Martinon et al., 2009).

Caspases involved in apoptosis are further classified into initiator caspases i.e. (caspase-8 and -9) and executioner caspases i.e. (caspase-3, -6, and -7). The initiator caspases have an N-terminal death-fold domain like NLR-proteins which is required for the C-terminal activation. The initiator caspases are activated through different platforms i.e. caspase-9 is activated by the apoptosome at the onset of apoptosis while the executioner caspases are activated by initiator caspases (Martinon et al., 2009). Caspases are activated via inflammasome activation to process and activate different cytokines.

1.2.1.8 Interleukin-1 β (IL-1 β)

The Interleukin-1 (IL-1) family plays a central role in inflammation and consists of 11 cytokines. IL-1 α and IL-1 β were the first to be discovered among all members of this family and possess strong pro-inflammatory properties. Interleukin-1 receptor antagonist (IL-1Ra), another member of IL-1 family is a regulator for pro-inflammatory activity of IL-1 α and IL-1 β by blocking their binding sites. These cytokines bind to IL-1receptor type-1(IL-1RI) followed by recruitment of the co-receptor IL-1 receptor accessory protein (IL-1RAcP) which form (IL-1 + IL-1RI + IL-1RAcP) complex (Dinarello, 2011).

This complex initiates a signal for the recruitment of adaptor protein MyD88 to the Toll-IL-1 receptor (TIR) domain similar to the TLR signalling

pathway. Inflammasome activation therefore leads to TLR-like receptor activation and phosphorylation of several kinases which translocate NF- κ B to the nucleus and starts a cascade of inflammatory cytokines (Dinarello, 2011). The data presented in this thesis will concentrate on IL-1 β released from inflammasome activation in *S. pneumoniae* infection, so we will focus on this cytokine.

Interleukin-1 β is an important and powerful pro-inflammatory cytokine and a key initiator of pro-inflammatory reactions during tissue injury. It is produced by a variety of cell types in the body but most research studies focus on innate immune cells including blood monocytes, macrophages and dendritic cells (Ferrero-Miliani et al., 2007). IL-1 β production is stimulated by either PAMPs or DAMPs and involves multiple steps. It is synthesized as pro-IL-1 β and then activated to the mature and biologically active form by the action of caspase-1, and subsequently released to the extracellular milieu.

Researchers have suggested five different pathways for the release of IL-1 β i.e. exocytosis of secretory lysosomes, shedding of microvesicles from plasma membrane, shedding of IL-1 β containing exosomes, export through specific membrane transporters or release after cell lysis. The exact mechanism of IL-1 β production is not known and further exploration may help in development of strategies against inflammatory and autoimmune diseases (Eder, 2009).

IL-1 β produces multiple systemic effects on the central nervous system, vascular system, metabolism and blood. These effects include fever, increased sleep, anorexia, hypotension, neutrophilia, increased leukocyte adherence, release of adrenocorticotrophic hormones (ADH), release of neuropeptides and hepatic proteins (Dinarello, 1988).

The systemic effects are due to the induction of cyclooxygenase type-2 (COX-2), type-II phospholipase A and inducible nitric oxide synthase (iNOS) mediated by IL-1 β release. IL-1 β is also believed to mediate inflammation in periodic fever syndrome caused by mutations in the NLRP3 gene and treatment with IL-1inhibitor relieves disease symptoms (Dinarello, 2009, Hoffman et al., 2004).

1.2.1.9 The Inflammasomes in *S. pneumonia* infection

Inflammasomes are large multi-protein complexes in the cytoplasm formed by NLR proteins and caspases i.e. caspase-1, PYCARD (ASC), NALP and caspase-11. Inflammasomes are activated by microbial ligands and metabolic stress which leads to proteolytic activation of pro-inflammatory cytokines, including IL-1 β and IL-18 through the activation of caspase-1 (Martinon et al., 2002, Tsuchiya and Hara, 2014).

After the discovery of NLRP1 as the first inflammasome, several other inflammasomes have been recognized in the recent years. Four inflammasomes including NLRP1, NLRP3, NLRC4 and AIM2 have been studied extensively (Martinon et al., 2007). Some of the NLRs including neuronal apoptosis inhibitory protein (NAIP) and Nod2 are also involved in pathogen sensing and form complexes but the exact mechanism is not known (Leavy, 2011, Franchi et al., 2008).

Inflammasome activation mainly depends upon the adaptor proteins. The apoptosis-associated speck-like protein containing a CARD (ASC) is an adaptor protein which is recruited to the NLRP proteins via PYD-PYD interactions, and is essential for inflammasome formation (Srinivasula et al., 2002, Martinon et al., 2002). The CARD domain of ASC adaptor protein interacts with the CARD domain of caspase-1 leading to its activation and inflammasome formation. Similarly NLRC4 inflammasome also uses ASC protein as an adaptor and recruits pro-caspase-1 directly via CARD-CARD interactions, but the exact mechanism is unknown (Poyet et al., 2001).

Inflammasomes respond to different signals and microbial ligands including PAMPs and DAMPs. The NLRP3 inflammasome is activated by a variety of signals including bacterial ligands and toxins, danger signals, muramyl dipeptide (MDP) and viral DNA. Similarly AIM2 (absent in melanoma 2) is a sensor for the double stranded cytoplasmic DNA which results in inflammasome formation together with ASC and caspase-1. Both NLRP3 and AIM2 inflammasomes activate apoptosis and pyroptosis via adaptor protein ASC (Martinon et al., 2009, Sagulenko et al., 2013).

When activated, the inflammasome activates pro-caspase-1 by increased proteolysis. The activated caspase-1 then processes the inflammatory cytokines pro-IL-1 β and pro-IL-18. Activation of these pro-inflammatory cytokines is an important process which starts an inflammatory response. Secretion of mature IL-1 β requires two signals. Firstly activation of TLRs leads to the transcription of the IL-1 β gene and production of pro-IL-1 β . Secondly the accumulated inactive pro-IL-1 β is then activated following the activation of NLR proteins and activation of inflammasome and caspase-1. In addition to cytokine maturation, inflammasome activation also leads to a type of cell death called pyroptosis which means death due to the release of pro-inflammatory cytokines (Eder, 2009, Fink and Cookson, 2005).

Inflammasome activation is important in *S. pneumoniae* infection. Previous research demonstrates that ASC inflammasomes including NLRP3 and AIM2 are essentially required for the caspase-1 activation during *S. pneumoniae* infection. Caspase-1 activation was significantly decreased in AIM2 knockdown and knockout mice while partially impaired in NLRP3^{-/-} macrophages in infection with *S. pneumoniae*. Furthermore, ASC^{-/-} mice were more susceptible to *S. pneumoniae* infection with impaired inflammatory response and lower IL-1 β and IL-18 production (Fang et al., 2011).

Previous studies also demonstrate that inflammasome activation during *S. pneumoniae* infection is due to its virulence factor pneumolysin. IL-1 β secretion by *S. pneumoniae* infection and by Ply treated dendritic cells was shown to require the NLRP3 inflammasome. This indicates the importance of Ply during inflammasome activation and the inflammatory response. Furthermore, NLRP3 was also required for protective immunity against respiratory infection with *S. pneumoniae* which adds significantly to our understanding of the interactions between Ply and the immune system (McNeela et al., 2010).

The pneumolysin deficient strain was unable to activate caspase-1 and induce production of inflammatory cytokines, when macrophages were stimulated with *S. pneumoniae* D39 WT and D39 Δ Ply. Cell stimulation with recombinant Ply induced inflammasome activation and the release of inflammatory cytokines. Ply toxin released by *S. pneumoniae* activates the TLR4 pathway to activate the inflammasome and caspase-1 which leads to production

of inflammatory cytokines (Shoma et al., 2008). The influence of *S. pneumoniae* induced inflammasome activation on autophagy, phagocytosis and NETosis is studied and presented in this thesis.

1.3 Macrophages and the mononuclear phagocyte system

Macrophages and mononuclear phagocytic cells are the first line of defence, described by Elie Metchnikoff in the 19th century. Macrophages are present in almost every tissue of the body. They are large myeloid origin cells that display stellate morphology and are characterized by the presence of pseudopodia, nonspecific esterases and phagocytic granules which give them a foamy appearance.

Macrophages are effector cells of the innate immune system and play a wider role in the body. They are highly efficient phagocytes and help in maintenance of the tissue homeostasis through the clearance of damaged and apoptotic cells generated during the process of wear and tear. Phagocytosis of dead material also helps in organogenesis and macrophages are highly concentrated at embryonic development sites to clear the huge number of dead cells (Hopkinson-Woolley et al., 1994).

Macrophages are also involved in wound healing during tissue injury. They perform some tissue specific functions i.e. liver macrophages (Kupffer cells) help in toxin removal from the circulation, alveolar macrophages engulf and eliminate inhaled antigenic particles, and bone macrophages are essential for bone remodelling. Macrophages secrete soluble mediators which help in tissue homeostasis and maintenance of enzymes, cytokines, chemokines, glycoproteins such as fibronectin and arachidonic acid derivatives (Takemura and Werb, 1984).

Macrophages are located near the epithelial surfaces in most of the tissues and detect microbial ligands i.e. PAMPs and DAMPs through their PRRs. The invading pathogens are phagocytosed by macrophages, degraded and finally eliminated from the body.

1.3.1 Identification of macrophages

Macrophages are identified by protein markers on their surface as shown in table 1.3. In mouse macrophages, the best and commonly used marker is F4/80, and a monoclonal antibody directed specifically against this protein is used for identification (Austyn and Gordon, 1981). Murine macrophages express some other markers as well. Human macrophages do not express F4/80 predominantly and this marker is useful in human eosinophils (Hamann et al., 2007). Some CD markers are useful to characterize human macrophages e.g. CD68 and CD14.

1.3.2 Activation of Macrophages

Macrophages are activated by any disturbance in tissue homeostasis which leads to phenotypic and functional changes in the cells. Macrophages are activated by two different pathways.

1.3.2.1 Classical pathway for macrophage activation (M1)

In the classical pathway, macrophages sense PAMPs released by Gram positive and Gram negative bacteria. This triggers the release of pro-inflammatory cytokines and chemokines including IL-1, IL-6, IL-12, IL-23, TNF- α , CXCL9 and CXCL10 (Mosser and Edwards, 2008, Murray and Wynn, 2011). Classically activated macrophages also generate reactive oxygen species (ROS) and nitric oxide (NO) which further enhance the killing of pathogens. ROS production is mediated by NADPH oxidase, while NO is produced by inducible NO synthase (iNOS) from L-arginine (Wink et al., 2011).

They also express major histocompatibility complex (MHC) class-II and co-stimulatory molecules which allow them to act as antigen presenting cells and induce T helper type-1 and T helper-17 responses (Krausgruber et al., 2011).

1.3.2.2 Alternate pathway of macrophage activation (M2)

This pathway was originally described in 1990. Macrophages are activated by cytokines produced by type-2 helper (Th-2) cell responses i.e. IL-4 and IL-13 instead of an interferon- γ (IFN- γ) Th-1 response (Stein et al., 1992). These

macrophages contribute in tissue repair. Th-2 cells cytokines including IL-4, IL-13, IL-25 and IL-33 promote activation of different transcription factors such as Kruppel-like factor-4 (KLF4), signal transducer and activator of transcription 6 (STAT6), the nuclear receptors including peroxisome proliferator-activated receptors (PPAR- δ) and (PPAR- γ) (Gordon and Martinez, 2010, Sica and Mantovani, 2012).

These macrophages also express some specific markers i.e. arginase-1 (Arg1), IL-4R etc. (Gordon and Martinez, 2010) and chemokines such as CCL24, CCL22, CCL18, CCL17, CCL14, and CCL13. Arginase-1 expression in mouse macrophages promotes the production of ornithine and polyamines which make these M2 macrophages highly efficient in wound healing and elimination of parasites (Martinez et al., 2009). They also secrete immunosuppressive cytokine IL-10 and tumour growth factor- β (TGF- β) which help in tissue repair (Fairweather and Cihakova, 2009).

1.3.3 Macrophage host defence during *S. pneumoniae* infection

Macrophages response to bacterial infections mainly involves the up-regulation of genes encoding cytokines during M1 polarization. These up-regulated genes encode indoleamine- pyrrole 2-3 di-oxygenase and nitric oxide synthase 2 (NOS2) involved in antimicrobial activity. However prolonged M1 polarization in some condition can lead to self-tissue injury. M2 activated macrophages play an important role in the resolution of inflammation by producing anti-inflammatory mediators (Benoit et al., 2008).

Macrophages detect invading pathogens, releasing chemical mediators to the blood and body fluids and initiate a strong signal to other immune cells. They are more efficient phagocytes than other immune cells and phagocytose invading pathogens including *S. pneumoniae* (Robertson et al., 1939). Innate immune response to pneumococcal infection activates macrophages via the classical pathway as reviewed by (Gordon et al., 2013).

Macrophage activation takes place following interaction with pneumococcal PAMPs or stimulation by natural killer (NK) cells leading to ROS production. Ply released during *S. pneumoniae* infection functions via TLR2 and

TLR4 as described earlier. Macrophages can also be activated by IFN- γ released by CD4⁺ lymphocytes. This mode of activation results in increased expression of major histocompatibility complex class-II (MHC-II), antigen presentation, phagocytosis, and microbial killing functions of macrophages. This is important in pulmonary defence against pneumococci (Gordon et al., 2013).

When macrophages are stimulated with *S. pneumoniae* infection, nitric oxide (NO) is produced. Ply acts on macrophages and induces the release of IFN- γ which then activates iNOS and NO production. Furthermore, Ply knockout *S. pneumoniae* was unable to produce NO during macrophage infection. NO is an essential element in macrophage antimicrobial activity but may cause host-induced tissue injury, hypotension and shock. Similarly macrophages with knockout of IFN- γ receptors or interferon regulatory factor 1 (IRF-1; a transcription factor) are also unable to express iNOS and NO production (Braun et al., 1999).

A previous study demonstrated that ply released in *S. Pneumoniae* infection of macrophages induces pro-inflammatory cytokines IL-1 α , IL-1 β , and IL-18 while there is no effect on TNF- α and IL-12p40 (Shoma et al., 2008). Along with the release of pro-inflammatory cytokines, *S. pneumoniae* infection also induces other immune responses in macrophages including phagocytosis, microbial killing and apoptosis. Different macrophage receptors including complement receptors, Fc receptors, platelet-activating factor receptors, scavenger receptors, and toll-like receptor (TLR) complexes which recognize *S. pneumoniae*. Opsonisation of *S. pneumoniae* via Fc receptors up-regulates bacterial phagocytosis (Dockrell et al., 2001).

In this thesis we study the induction of autophagy, phagocytosis and the associated inflammasome activation in murine BMDM infected with *S. pneumoniae*.

Marker	Gene	Expression/ Comments
F4/80	Emr1	Expressed on most tissue macrophages in mouse. Limited usefulness in humans for eosinophils
CD11b	Itgam	Expressed on all myeloid cell types including neutrophils
CD11c	Itgax	Expressed on monocytic- derived cells including macrophages, but typically associated with DCs
CD68	Cd68	Expressed on all mouse and human macrophages Useful for IHC. It has limited usefulness
CD163	Cd163	Expressed on most tissue macrophages, Useful for IHC including human paraffin embedded tissues
CSF1R	Csf1r	Expressed on all monocytic- derived cells including macrophages and osteoclasts
MAC2 galectin 3	Lgals3	Useful for IHC
LY6C	Ly6c1	Expressed on monocytic myeloid cells. Useful when used together with LY6G to determine relative number of granulocytes and monocytes
LY6G	Ly6g	Expressed on granulocytes. Useful when used with LY6C to determine relative number of granulocytes and monocytes.
IL- 4R α	Il4ra	Expressed on most macrophages but also lymphocytes and other cell types responsive to IL-4 and IL13

Table 1.3 Cell surface markers and genes expressed by tissue macrophages

CD; Cluster of differentiation, CSF1R; Colony stimulating factor 1 receptor, MAC2; Macrophage galactose- specific lectin 2, LY; lymphocyte antigen, adapted from (Murray and Wynn, 2011).

1.4 Human polymorphonuclear neutrophils

Polymorphonuclear neutrophils (PMN) or simply neutrophils make up approximately 40- 75 % of all white blood cells in mammals and they are one of the principal effectors cells of the immune system. Neutrophils spend most of their life span in circulation and are the first leukocytes recruited to the site of any breach in the body's defence. Neutrophils develop in the bone marrow and are exported to the blood stream on maturity. Their major function is protection from invading pathogens. In normal conditions, the lifespan of neutrophil is approximately 4.5 days, if not activated by inflammation (Nathan, 2006, Pillay et al., 2010).

Neutrophils were first described by Elie Metchnikoff, a Russian biologist (Nobel laureate in medicine, 1908) in 1882, when he inserted rose thorns into starfish larvae and found that wandering mesodermal cells accumulated at the puncture site. He named these cells phagocytes and described the larger cells as macro-phagocytes, or macrophages, and the smaller as micro-phagocytes, now known as granulocytes, of which the most numerous are the neutrophils (Segal, 2005). Later on neutrophils were further discussed and characterized by Nobel laureate Paul Ehrlich, who realized the potential importance of the neutrophil granules in the inflammatory process.

Pathogen invasion is detected by tissue resident macrophages and then signalled to circulating neutrophils. Neutrophils are rapidly recruited to the site of infection and start their actions including phagocytosis, degranulation and neutrophil extracellular traps (NETs) generation to control the invading pathogen. These leukocytes adopt a diverse array of strategies to provide protection against a broad range of pathogens by limiting their spread (Papayannopoulos and Zychlinsky, 2009).

Structurally neutrophils have multi-lobed (2-5) nuclei and are divided into segmented and banded types. The nuclear structure allows easy emigration of neutrophils through narrow junctions between endothelial cells. They have multiple cytoplasmic pink staining granules containing different potent molecules through which they communicate with the macrophages and dendritic

cells for killing and lysis of pathogens. Sometimes these molecules can become dangerous causing injury to the host tissues.

1.4.1 Functions of neutrophils

Neutrophils are the first cells to be recruited to the site of infection through a process called chemotaxis and provide the first line of defence against invading pathogens.

1.4.1.1 Neutrophil chemotaxis

Chemotaxis is a process used by the leukocytes in which they crawl towards the infection site in response to certain chemicals. Chemo-attractant molecules are released by pathogens that induce rapid changes in the neutrophil shape which results in cell orientation to migrate up a gradient of attractant molecules to the site of infection (Bourne and Weiner, 2002). This help in the accumulation of neutrophils at the site of infection.

1.4.1.2 Neutrophil phagocytosis and Intracellular Killing

Elie Metchnikoff described neutrophil phagocytosis, as a process of endocytosis where solid particles including microorganisms are taken up by these cells. On arrival at the site of infection, neutrophils bind and internalize the invading microbes by a receptor-mediated process called phagocytosis. The microorganism is trapped in a vacuolated structure called a phagosome which undergoes maturation and fuses with the intracellular granules containing a variety of antimicrobial factors for clearance (Steinberg and Grinstein, 2007).

The contents of the phagosome are then subjected to several potent antimicrobial molecules i.e. antimicrobial peptides, reactive oxygen species (ROS) and some hydrolytic enzymes which kill and degrade the phagocytosed microbe. Microbial killing and degradation inside the phagosome is important to prevent their release into the cytosol and surround tissue (Brinkmann et al., 2004).

1.4.1.3 Neutrophil extracellular microbial killing

When neutrophils are activated, they kill pathogens using different controlled strategies. They have an array of antimicrobial mechanisms, including antimicrobial proteins, release of reactive oxygen species neutrophil extracellular traps which are used to kill microbes.

1.4.1.4 Neutrophil granules

Neutrophils contain four types of granules which release their toxic contents at specific times for microbial killing (Amulic et al., 2012).

Primary azurophilic granules are the first to appear during neutrophil maturation. They are the largest peroxidase positive granules and stain with azure A. They contain myeloperoxidase (MPO), defensins, lysozyme, bacterial permeability-increasing protein (BPI), and some serine proteases including neutrophil elastase (NE), proteinase 3 (PR3), and cathepsin G (Amulic et al., 2012).

The secondary granules are smaller, MPO negative and are formed after azurophilic granules. They contain glycoprotein, lactoferrin and lysozymes. The third class consists of the smallest gelatinase granules. They are also MPO negative and contain few antimicrobial molecules, but mainly act as storage location for the metalloproteases i.e. gelatinase and leukolysin. Most of the granular proteins play a potent role in microbial killing (Amulic et al., 2012).

A fourth class of neutrophil granules family consists of the secretory granules which appear during the last stage of maturation. These granules do not bud from the Golgi apparatus but instead are formed through endocytosis and contain plasma derived proteins such as albumen (Amulic et al., 2012).

1.4.1.5 Neutrophil antimicrobial proteins

Neutrophils produce some proteins which act directly or indirectly as antimicrobial molecules. Three different categories of neutrophil antimicrobial proteins have been described i.e. cationic peptides which bind to microbial membranes and alter their membrane functions, enzymes which directly destroy

microbes and chelating proteins which deprive microbes from essential nutrients. Neutrophil antimicrobial proteins are shown in (Table 1.4).

Proteins/peptides	Antimicrobial mechanism
Cationic peptides	
<p>α-defensins (human neutrophil peptides) HNP-1, -2, -3, -4</p>	<p>-Permeabilize membrane bilayers which contain negatively charged phospholipids</p> <p>-Inhibit DNA, RNA as well as protein biosynthesis</p> <p>-Inhibit bacterial cell wall synthesis</p>
LL-37	A trans-membrane pore-forming protein
BPI (permeability increasing protein)	Increases bacterial permeability and hydrolysis of bacterial phospholipids by binding to LPS
Histones	Its mechanism of action is unknown
Proteolytic enzymes	
Lysozyme	Degradation of bacterial cell wall
Proteinase-3 (PR3)	It has an independent non proteolytic mechanism and binds to the bacterial membrane
<p>Neutrophil elastase (NE), Cathepsin G (CG)</p>	Cleaves bacterial virulence factors and outer membrane proteins independent of a proteolytic activity by binding to the membrane
Azurocidin	Bind to the bacterial outer membrane independent of a proteolytic activity

Metal chelators	
Lactoferrin	<ul style="list-style-type: none"> -Bind to iron, an essential bacterial nutrient and alter bacterial activity -Releases LPS from the cell wall by binding with lipid-A part of LPS and increases membrane permeability
Calprotectin	Sequesters manganese and zinc leading to alteration in bacterial growth

Table 1.4 Directly acting neutrophil proteins and their antimicrobial actions

adapted from (Amulic et al., 2012).

1.4.1.6 Reactive oxygen species

Neutrophils activation produce reactive oxygen species (ROS) through a process called the respiratory burst. ROS are important for the antimicrobial activity of neutrophils. Defective ROS production in chronic granulomatous diseases leads to poor antimicrobial action of neutrophils (Amulic et al., 2012).

1.4.1.7 Neutrophil Extracellular Traps (NETs)

Neutrophils were previously considered to kill microbes via phagocytosis and secretion of antimicrobial molecules and free radicals. A novel strategy of trapping and killing microbes, the neutrophil extracellular trap (NET) generation was identified by Brinkmann and his co-workers when they treated neutrophils with phorbol myristate acetate (PMA), interleukin 8 (IL-8) and lipopolysaccharide *in vitro* (Brinkmann et al., 2004).

A NET consists of neutrophil nuclear material along with granular and cytoplasmic proteins released into the cytosol. NETs are thought to limit the spread of microbes and promote the effectiveness of neutrophils by limiting diffusion of protein molecules from the infection site. This also prevent the host tissues from damage by the granular proteins (Papayannopoulos and Zychlinsky, 2009).

NETs are associated with neutrophil elastases and histones which can be used as identification markers. An individual NET is approximately 15 nm in diameter, derived from the unfolded chromatin components. Scanning electron microscopy revealed that NET threads have globular components and multiple threads wound up to make a 100nm diameter cable, and several cables form a complex web-like structure. Experiments on NETs have shown that they are flexible structures and surround the neutrophils from whom they originate (Brinkmann et al., 2004).

Studies demonstrate that TLRs may play important role in NET generation. Stimulation of neutrophils with intact pathogen produced more NETs as compared to stimulation of a single TLR. Furthermore, NET generation is an active process and require the release of ROS. On stimulation, neutrophils are

converted into motile phagocytes with higher oxidative burst in the first hour (Fuchs et al., 2007).

There are few nuclear changes in the first hour but their chromatin remodels into active and inactive parts and lose its lobular appearance later on. After almost 2 hours the nuclear membrane dissolves allowing the chromatin to mix with other components of the cell. Simultaneously the granules in the neutrophils are dissolved and at about 3 hours, the mixture of chromatin and granules is released into the extracellular environment (Fuchs et al., 2007).

1.4.1.8 Mechanisms of neutrophil microbial killing

Neutrophils use oxygen-independent and oxygen-dependent mechanisms for killing pathogens. In the oxygen-independent method, neutrophils release antimicrobial cationic proteins and peptides i.e. BPI, defensins, and cathelicidins into the phagosome containing pathogen (Lehrer and Ganz, 1999). These molecules bind directly to the microbe and disrupt their cell membrane integrity to cause death.

In the oxygen- dependent method, NADPH oxidase and myeloperoxidase is produced which leads to production of the potent antimicrobial superoxide anions hydrogen peroxide (H_2O_2) and hypochlorite (HOCl) (Segal, 2005). Electron transfer occurs from the cytoplasmic NADPH to oxygen on the inside of phagosome to produce superoxide and other free radicals (Segal and Abo, 1993).

Mutations in the genes encoding NADPH oxidase complex in chronic granulomatous disease (CGD) lead to severe life threatening infections due to inability of neutrophils to kill microorganism through these free radicals (Heyworth et al., 2003). Free radicals oxidize proteins and DNA of microorganism and kill them. On completion of phagocytosis and microbial digestion neutrophils undergo apoptosis mediated by caspases (Fadeel et al., 1998). The neutrophil apoptotic bodies are quickly removed by macrophages to shorten the inflammatory process (Serhan and Savill, 2005).

1.5 Autophagy

Autophagy, derived from Greek words meaning “self- eating”, was coined by Deter and de-Duve for the first time almost 50 years ago. They described this ancient homeostatic process according to their observations in experiments on rat hepatocytes perfused with a hormone glucagon (Deter and De Duve, 1967).

Autophagy-related (Atg) proteins are responsible for this important pathway and their molecular machinery, the *Atg* genes have been identified in the yeast, with their orthologues well conserved in the eukaryotes (Heath and Xavier, 2009). Atg proteins form functional complexes to control this important pathway and degrade large cellular components, protein aggregates and pathogens which cannot be degraded by the Ubiquitin-proteasome pathway (Deretic et al., 2009b, Virgin and Levine, 2009).

Previously autophagy was considered as a process for cell survival during starvation, but recent studies link this pathway to many pathological conditions including microbial infections, inflammatory diseases, cancers, neurodegenerative diseases and ageing (Mizushima et al., 2008). Autophagy is activated during cellular starvation and growth factor deprivation as an adaptation process and involves lysosomal degradation of cellular components and protein aggregates (Levine, 2005).

It is interesting that despite abundant extra-cellular nutrients, deprivation of growth factors in the cells can activate autophagy for their ATP production from the intracellular substrate, highlighting the importance of autophagy for sustaining viability and cell survival during starvation and growth factor withdrawal (Lum et al., 2005). This pathway also plays an important role during birth and nutrient deprivation due to placental disruption (Levine, 2005).

Autophagy and Atg proteins are important for their crucial role in infection, immunity and inflammation. The role of autophagy in both innate and adaptive immunity has been recognized at different levels ranging from highly specialized immunologic effector and regulatory function (type-I immunophagy) to generic homeostatic influence on immune cells (type-II immunophagy). The concept of understanding the relation of autophagy with immunity is that it is an

evolutionary ancient microbial clearance mechanism for the defence of eukaryotic cells against intracellular pathogens. Different receptors and proteins involved in autophagy are also linked to immune systems and they form the link between these two processes (Deretic, 2006).

Autophagy plays an important role in infection control and is thought to be the only effective mechanism for removal of intracellular pathogens. Studies have demonstrated that different microbial ligands trigger autophagy and autophagy-related pathways through the activation of PRRs on the cell surface and cytoplasm i.e. TLRs and NLRs (Delgado et al., 2008, Saitoh et al., 2008). Another molecule, the inhibitory complement receptor CD46, a type-1 glycoprotein, expressed by nucleated cells in humans can bind to multiple pathogens, and is thought to be direct inducer of autophagy in microbial infections (Meiffren et al., 2010).

The discovery of Atg proteins helped in understanding the relationship between autophagy, immunity and Inflammation in the last decade. The autophagy pathway maintains a balance between the beneficial and harmful effects of the host response to infection, and is implicated in either the pathogenesis or response to a wide variety of diseases including chronic bacterial and viral infections (Kundu et al., 2008).

Autophagy proteins function both in induction and suppression of immune and inflammatory responses. Similarly, immune and inflammatory signals also function in both induction and suppression of autophagy pathway (Levine and Kroemer, 2008).

1.5.1 Molecular mechanism of autophagosome formation

The most important feature of autophagy is autophagosome formation. It is a double membrane-bound compartment for sequestering cytosolic materials through a distinct process. Autophagosome membrane formation is a complex process controlled by multiple Atg proteins. The exact mechanism and source of autophagosome membrane formation is not clearly understood. It is believed to initiate with the isolation membrane followed by elongation and autophagosome

formation surrounding the cytosolic components. On closure, the autophagosome fuses with lysosome to form mature autophagosome (Fig. 1.2).

1.5.1.1 Initiation

The first important event in autophagosome formation is induction or nucleation. It is initiated by the formation of isolation membrane or phagophore. The exact mechanism is not known but recent research demonstrates that endoplasmic reticulum (ER) and mitochondria may provide membrane (Tooze and Yoshimori, 2010). According to some studies, plasma and nuclear membranes may also contribute to autophagosome membrane formation but no evidence is available for specific markers of these structures (Hailey et al., 2010, Ravikumar et al., 2010).

Mammalian target of rapamycin (mTOR), a serine/threonine kinase plays an important role in autophagy. Inhibition of mTOR activity leads to autophagy induction in eukaryotic cells. This is mediated by Atg1 in yeast and Ulk1 (Unc-51-like kinase) and Ulk2 in mammals (Chan et al., 2007). The mTOR substrate complex i.e. (ULK1/2, ATG13, focal adhesion kinase family-interacting protein 200 (FIP200), retinoblastoma1-inducible coiled coil protein1 (RB1CC1) and ATG101) is translocated from cytosol to the endoplasmic reticulum or other nearby structures (Itakura and Mizushima, 2010). This leads to recruitment of Class-III phosphatidylinositol-3-kinase complex i.e. (VPS34, VPS15 or p150, beclin 1 and ATG14) to the ER (Matsunaga et al., 2009).

The class-III PI3K complex produces phosphatidylinositol-3-phosphate (PI3P) leading to recruitment of the effector molecules i.e. double FYVE-containing protein 1 (DFCP1) and WD repeat domain phospho-inositide-interacting (WIPI) proteins. DFCP1 is found diffusely on the ER and golgi complex. It translocates to the site of autophagosome membrane formation in a PI3P-dependent manner and starts omegasome (Ω -like structure) formation (Axe et al., 2008). WIPI-2 protein is the major form of WIPI family which promotes the development of omegasome to form isolation membrane and autophagosome (Polson et al., 2010).

1.5.1.2 Elongation

The phagophore elongation leads to autophagosome formation which requires Atg proteins. Beclin-1 with class-III PI3K complex not only plays an important role in vesicle nucleation, but may also help in autophagosomal elongation. The elongation process is controlled by two protein conjugation systems. The Atg-12 is conjugated with Atg-5 and then to Atg-16L1 which continues from the initiation site. LC3 (Atg8) is conjugated with phosphatidylethanolamine (PE) at its C-terminus. This lipid modification is denoted as a change from LC3 I to LC3 II (Fujita et al., 2008, Matsunaga et al., 2009).

Both these conjugation processes are controlled by Atg7, Atg3 and Atg10. Atg7 acts like E1 enzyme of ubiquitin system, and Atg3 and Atg10 acts like E2 of the ubiquitin system and localize to the developing autophagosome. The Atg12-Atg5 complex has an important role in LC3 lipidation. The LC3-PE complex is believed to help in autophagosome elongation and can be detected within the membranes and lumen of autophagosome (Fujita et al., 2008, Matsunaga et al., 2009).

Atg4 is another important protein identified to help in LC3 conjugation. Atg4B cleaves a peptide at the C-terminal of LC3 and processes LC3 I to LC3 II. Similarly another protein, formin-binding protein-1-like (FNBP1L) is thought to be an Atg3 interacting protein and helps in autophagosome formation (Huett et al., 2009).

Activating molecule in Beclin1-regulated autophagy (Ambra1) and ultraviolet irradiation resistance-associated gene (UVRAG) also associate with the PI3K complex and regulate the process of autophagy (Liang et al., 2006, Fimia et al., 2007, Liang et al., 2008). UVRAG-Beclin1-VPS34 complex functions as a promoter for the autophagosome maturation, but the same complex with the addition of another protein rubicon (Rubicon-UVRAG-Beclin1-VPS34) suppresses autophagosome maturation (Liang et al., 2008).

1.5.1.3 Closure and maturation

Autophagosome closure and fusion with the lysosome is less well understood as compared to the early stages. Researchers believe that

autophagosomal maturation also requires Atg proteins. Vacuole-membrane protein1 (VMP1) is an ER-associated multi-spanning protein. It interacts with beclin1 and functions in the later stages of autophagosome formation (Itakura and Mizushima, 2010, Tian et al., 2010). After closure, the autophagosome is transferred to the peri-nuclear region of the cell for fusion with the lysosome. This process is controlled by microtubules and a motor protein called dynein (Kimura et al., 2008).

The Atg12-Atg5 and Atg16 complex dissociates from autophagosome after closure but the LC3 remains attached. It is presumed that LC3 also plays an important role in closure and fusion of autophagosome (Noda et al., 2009). When the autophagosome outer membrane fuses with the lysosome, it forms mature autophagosome leading to lysis and degradation of the autophagosome contents with the lysosomal enzymes.

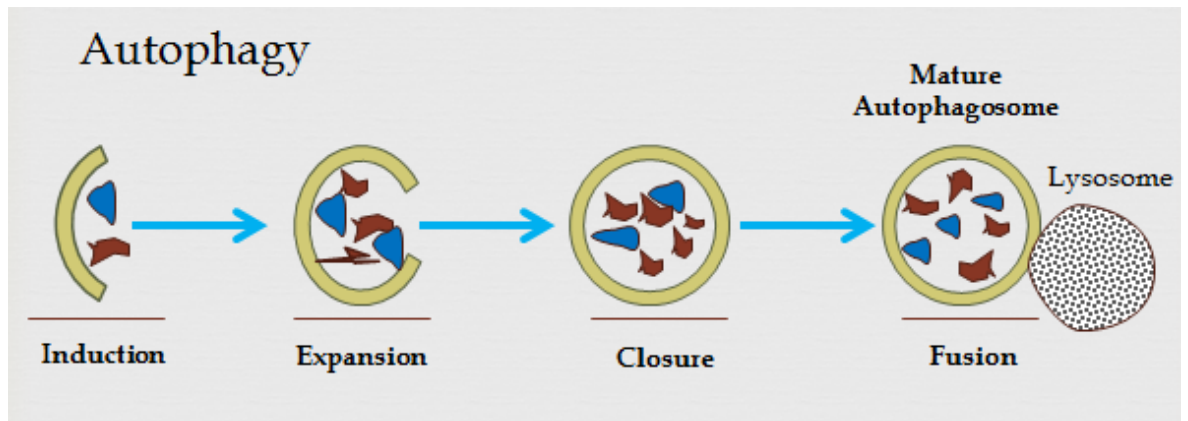


Figure 1.2 Schematic representation of Autophagy pathway

Autophagosome formation starts with induction, the isolation membrane expands surrounding the cargo. Mature autophagosome is formed after closure and fusion with the lysosome. Each step in this pathway is controlled by Atg protein complexes, figure adapted from (Kirkegaard et al., 2004).

1.5.2 Role of autophagy in Infection

1.5.2.1 Autophagic degradation of pathogens

Autophagy was considered a non-selective bulk degradation pathway in the past. Now it is quite clear that autophagy can degrade invading pathogens in selective manner. Pathogens are taken up and degraded inside a double membrane autophagosome, a process called xenophagy. Autophagy can also restrict pathogen invasion independent of autophagosome formation (Gomes and Dikic, 2014). The exact mechanism of xenophagy and its membrane dynamics is not known but pathogen killing and degradation process has been investigated up to some extent.

Cytoplasmic vacuoles containing internalized bacteria are quite similar to the autophagosome and use the same autophagy machinery (Atg proteins). The diameter of the bacteria containing vacuole is larger than the autophagosome. It is formed by Rab7 dependent fusion of small isolation membranes in the cytoplasm (Yamaguchi et al., 2009, Hyttinen et al., 2013). The Rab proteins belong to Ras-like GTPase superfamily involved in various stages of autophagy. Rab7, Rab8B, and Rab24 control maturation of autophagosome (Ao et al., 2014).

It is believed that ubiquitin-p62 dependent and independent molecular mechanisms may have role in targeting microbes to the vacuolar compartments in the cytosol. The p62 adaptor protein targets microbes for autophagy i.e. in *Shigella flexneri* infection the phagocytosed pathogen breaks the phagosome to get access to the cytosol. The broken vacuole membrane remnants contain polyubiquitinated proteins which recruit p62 and LC3 proteins. It is then targeted for autophagic degradation. This vacuole membrane rupture by an invading bacterium acts as a signalling node for autophagy (Dupont et al., 2009).

The LC3 protein in combination with another adaptor, the nuclear dot protein 52 (NDP52) also plays an important role in clearance of *Salmonella* and restricts its invasion and intracellular replication (Thurston et al., 2009). A lipid second messenger, di-acylglycerol (DAG) is also necessary for microbial autophagy. It localizes to the phagosome prior to autophagy and mediates the functions of protein kinase C in *Salmonella* induced autophagy (Shahnazari et

al., 2010). A microbial sensor protein, the self-ligand cell-surface receptor (SLAM) has a dual function. It acts as a microbial sensor and co-stimulatory molecule for autophagy in gram negative bacterial infection. Slamf1 regulates the activity of NOX2 enzyme and maturation of the phagosome. It recruits Vps34 producing PI3P and facilitates phagosome-lysosome fusion (Ma et al., 2012).

Recent studies demonstrate that autophagy functions as an innate defence mechanism in mycobacterial infections. Mycobacterial autophagy is induced through the activation of PRRs especially TLRs. T helper cell responses play an important role. Th1 cytokines activate autophagy while Th2 cytokines inhibit it. Immunity-related GTPases were found to play important role in Mycobacterial autophagy (Deretic et al., 2009a). Human genetic studies also provide evidence that IRGM, a human immunity related GTPase-1 (*Irgm-1*) orthologue is important for the regulation of autophagy-dependent clearance of Mycobacteria (Singh et al., 2006).

Autophagy not only plays important role in bacterial infection but also viral, protozoan and parasitic infections. Selective autophagy of viruses is exactly the same as cellular protein aggregates. In *Drosophila*, a mutation in *Atg* genes increased susceptibility to viral and bacterial infection. *Atg5* gene knock-out animals were found more susceptible to *Sindbis virus* infection of central nervous system (Orvedahl et al., 2010). Infection of human fibroblasts with cytomegalovirus (HCMV) resulted in autophagy induction and increased lipidation of LC3 protein. This demonstrates the importance of autophagy as a cellular response to early virion and foreign DNA in human cells (McFarlane et al., 2011).

1.5.2.2 Autophagic survival of pathogens

Pathogens have developed different strategies to protect themselves from immune responses and autophagy. *Listeria monocytogenes*, a gram positive pathogen escapes from phagosome by lysing phagosomal membrane with its pore-forming toxin listeriolysin. It replicates in the cytoplasm and can spread to surrounding tissues (Pareja and Colombo, 2013). A recent study demonstrated that autophagy in infection with *Salmonella typhimurium* facilitated replication

of pathogen. A subset of *Salmonella* associated with autophagy components p62 and LC3 replicated very quickly in Hela cells (Yu et al., 2014).

Autophagy proteins are believed to play important role in viral replication but the exact mechanism is not clear. Atg proteins may have some role in remodelling ER membrane or fusion of multi-vesicular bodies. One possibility is that Atg proteins may provide membrane for viral replication or translation machinery. Infection of a hepatocarcinoma cell line (Huh7) with hepatitis C virus showed that its replication is dependent on Beclin-1, Atg4B, Atg5 and Atg12 proteins. Knock down of these proteins decreased replication of hep-C virus (Dreux et al., 2009). Similarly intracranial injection of *Dengue virus 2 (DV2)* to 6 days old mice induced autophagy which led to increased viral replication. Treatment with rapamycin enhanced the disease symptoms and viral replication while 3MA inhibited autophagy and down regulated viral replication (Lee et al., 2013).

Inhibition of autophagy with 3MA or Atg7 knock down in Huh7 cell line decreased replication of hepatitis B (DNA) virus. (Sir et al., 2010). RNA viruses like coronavirus, measles virus, HIV and hepatitis C virus use immunity associated GTPase M (IRGM) to interact with Atg proteins and induce formation of a double membrane ER-derived vesicle for their replication (Grégoire et al., 2011). Thus autophagy induction is not always protective to the host, because some pathogens might use this pathway for their own benefit.

In this thesis, we demonstrate autophagy induction in *S. pneumoniae* infection which is a novel finding. The exact molecular mechanism of autophagy induction in this extracellular pathogen is not known and requires further investigation.

1.5.3 Role of autophagy in immunity

Autophagy and Atg proteins play an important role in inflammation, immunity and antigen presentation. Autophagy balances the beneficial and harmful effects of immune system and provide protection from autoimmunity (Levine et al., 2011).

Recent research links autophagy with innate immunity through its effects on inflammasome activation. Autophagy down regulates inflammasome activation by an unknown mechanism. Some direct interaction between Atg proteins and inflammasome components may be present. Autophagy induction in macrophages reduces serum level of inflammatory cytokine (IL-1 β) which demonstrates its association with inflammasome. IL-1 β production may be controlled by two separate mechanisms i.e. targeting pro-IL-1 β for lysosomal degradation and regulating NLRP3 inflammasome (Harris et al., 2011).

Autophagy and innate immunity overlap each other at molecular level. There are multiple connections between autophagy and innate immune system through different proteins and receptors including IL-1 β , high mobility group B1 protein (HMGB1), TLRs, NLRP4, NLRC3, NLRC4 and RLRs. Autophagy adaptor protein, sequestosome 1/p62- like receptors (SLRs) are a category of PRRs. They facilitate autophagic elimination of pathogens as well as serving as a platform for immune signalling. SLRs play important role in autophagy against intracellular microbes including *Salmonella*, *Shigella*, *Listeria*, *Mycobacterium tuberculosis*, *HIV-1* and *Sindbis virus* (Deretic, 2012).

Autophagy is also linked with phagocytosis, an innate immune process for the elimination of invading pathogens and apoptotic cells. A proteomic analysis of phagosomal membrane from macrophages demonstrated that phagosomal proteins are association with TLR signalling, secretory processes, and autophagy. The induction of autophagy changed several proteins in the phagosomal membrane fraction and demonstrated a relationship (Shui et al., 2008). Autophagy is also associated with clearance of dying apoptotic cells during programmed cell death. Autophagy inhibition by knock down of *Atg5* gene is associated with defective clearance of apoptotic bodies (Qu et al., 2007).

Autophagy has an important role in adaptive immunity. Antigens are loaded onto major histocompatibility complex class II (MHC II) molecules in dendritic cells and cross-present to CD8 $^+$ T lymphocytes. Autophagy is also essential for homeostasis and cell survival of T lymphocytes and modulates selection of some clones of CD4 $^+$ T cells in thymus. B-lymphocytes also need autophagy for their development at specific stages in the bone marrow (Puleston and Simon, 2014).

Autophagy plays a role during self-antigen presentation in the thymic epithelium to MHC II molecules and is believed to participate in the delivery of these molecules. Genetic knock down of *Atg5* in thymic epithelial cells can lead to abnormal selection of certain MHC II T-cell specificities (Nedjic et al., 2008). These findings suggest that autophagy induction controls multiple innate and adaptive immune functions. Further work is needed to study the molecular basis of the relationship with the immune system.

1.5.4 Role of autophagy in inflammatory and autoimmune diseases

Inflammatory and autoimmune diseases are very common worldwide. A defect in the autophagy pathway may lead to multiple inflammatory and autoimmune diseases. Genome-wide association studies have linked autophagy genes, i.e. *ATG16L1* with Crohn's disease (CD). It is a chronic inflammatory bowel disease caused by a defect in the innate immunity against enteric pathogens. Invasive strains of *E.coli* have been consistently isolated from patients with CD. They are considered to play an important role in the pathogenesis of CD (Henderson and Stevens, 2012).

Some studies associate multiple autophagy genes including *ATG16L1* and immunity-related GTPase- M (*IRGM*) to inflammatory bowel diseases. An innate immune receptor Nod2 is believed to induce autophagy. Nod2 interacts with *ATG16L1* which indicates the importance of this protein in the autophagic clearance of pathogens (Fritz et al., 2011).

Another study demonstrates that Nod1 and Nod2 both are necessary for the autophagic response against invading pathogens. They recruit *ATG16L1* to the bacterial entry site of the plasma membrane. Mutations in *Nod2* and *ATG16L1* genes inhibit autophagosome formation. This indicates that autophagy proteins play an important role in the development of CD (Travassos et al., 2010).

The autophagy pathway also plays an important role in the pathogenesis of systemic lupus erythematosus (SLE). This is a multifactorial autoimmune disease affecting multiple systems of the body. The exact pathogenesis of SLE is not clearly understood. Multiple genome-wide association studies demonstrate that

genetic variants of *Atg5* gene show strong association with this disease. This indicates that autophagy may play important role in the pathogenesis of SLE which needs further investigation (Zhou and Zhang, 2012).

Autophagy also plays an important role in generation of functional and self-tolerant CD4⁺ T cells stock. Autophagy is required for the MHC class-II molecules on the thymic epithelial cells in mice to generate self-tolerant T cells. Genetic interference with autophagy in thymic epithelial cells leads to abnormal selection of some MHC II restricted T cells which results in severe colitis and multi-organ inflammatory diseases in mice (Nedjic et al., 2008).

Autophagy also controls energy balance of the body. Obesity is a physiological stressor to ER in the β -cell of pancreas which may lead to dysfunction and insulin resistance. Mice with β -cell-specific *Atg7* knock-out developed severe diabetes which suggested that autophagy-deficient β -cells cannot cope with increased metabolic stress. Autophagy also plays an important role in hypothalamic control of appetite, energy expenditure, and body weight. Any defect in autophagy may contribute to metabolic disorders including diabetes (Quan et al., 2013). Thus autophagy is an important pathway that not only controls body homeostasis but also infections, inflammatory and autoimmune conditions.

1.6 Project Aim, Objectives and Implications

As described in the above sections, *S. pneumoniae* is a common human pathogen and a major cause of multiple life threatening diseases in children and elderly. The recent increase in the MDR strains of *S. pneumoniae* may need some newer treatment strategies. Autophagy is a potential target for development of a new treatment option to eradicate this pathogen. This project will identify autophagy induction in *S. pneumoniae* infection and its association with other immune mechanisms. Our main focus is the clearance of pathogen from the body through innate immune system without any harm to the host.

1.6.1 Aim

The overall aim of this project is to investigate the induction of autophagy in *S. pneumoniae* infection and the influence of autophagy manipulation on associated inflammasome activation and antimicrobial mechanisms. Autophagy induction could possibly be used as a newer strategy for tempering the harmful inflammatory responses during infection which may eliminate microbes by a non-inflammatory process.

1.6.2 Objectives

The following is a list of specific objectives of this project;

- i. To explore autophagy induction in *S. pneumoniae* infection using primary murine BMDMs, human neutrophils and a mouse model.
- ii. To find the relationship between autophagy and inflammasome activation, and assess the influence of autophagy induction on inflammasome activation.
- iii. To study the induction of phagocytosis and associated intracellular killing of *S. pneumoniae* by primary murine BMDMs and human neutrophils.
- iv. To assess the role of autophagy in phagocytosis of *S. pneumoniae* by neutrophils.

- v. To investigate the role of *S. pneumoniae* virulence factors in induction of phagocytosis in murine BMDMs and human neutrophils.
- vi. To investigate neutrophil extracellular trap (NET) generation in *S. pneumoniae* infection.
- vii. To investigate the role of autophagy in NET generation following *S. pneumoniae* infection.
- viii. To explore the influence of *S. pneumoniae* virulence factor pneumolysin in NET trapping of microbes.
- ix. To explore the role of different PRRs and adaptor proteins in autophagy induction with *S. pneumoniae* infection.

1.6.3 Implications

The treatment of pneumococcal diseases is a challenge in resistant cases. Autophagy induction could potentially prove useful in treating this important human pathogen through enhancing its clearance by innate immune cells. Reinforcing autophagy may help in decreasing the hazards of *S. pneumoniae* induced inflammatory response.

2 **Materials and Methods**

2.1 Materials

2.1.1 Mouse strains used in this study

2.1.1.1 C57BL / 6 and BALB /c mice

C57BL/6 and BALB/c mice were purchased from Harlan (Bicester, UK) and maintained in the University of Glasgow Biological services facilities under Home office UK guidelines. Mice were used aged 6-12 weeks and weight approximately 20-25 grams.

2.1.1.2 C3H/ HeNHsd and C3H/ HeJolaHsd-TLR4 Lps-d mice

These are lipopolysaccharide (LPS) hypo-responsive TLR4-defective and control strains of mice purchased from Harlan (Bicester, UK). Mice were maintained in the University of Glasgow Biological services facilities under Home office, UK guidelines. Mice were used aged 6-12 weeks and weight approximately 20-25 grams.

2.1.1.3 *Atg7*^{-/-} (*Atg7* gene knock out) mice

Femurs from these mice were kindly gifted by Dr. K. Simon, University of Oxford, UK.

2.1.1.4 *TLR4*^{-/-} (*Tlr4* gene knock out) mice

Femurs from these mice were kindly gifted by T. Mitchell, University of Glasgow.

2.1.1.5 *Myd88*^{-/-} (*Myd88* gene knock out) mice

Femurs from these mice were kindly gifted by Prof D. Gray, University of Edinburgh.

2.1.1.6 *TRIF*^{-/-} (*Trif* gene knock out) mice

Femurs from these mice were kindly gifted by Professor C. Bryant, University of Cambridge.

2.1.2 Cell Culture

2.1.2.1 J774A-1 cell line

This is a murine macrophage cell line which was stored long-term in cryovials (Alpha lab ltd, Cat. LW3532, UK) placed in liquid nitrogen. Thawing of the cryovials was performed quickly. Cryovials were transferred in dry ice into a 37 °C water bath for a minute shaking slowly. When about 80 % thawed, the cell suspension was quickly transferred to RPMI 1640 medium (Sigma Aldrich, Cat. R8758, USA).

The medium was supplemented with 2mM L- glutamine (Invitrogen, Cat.no.25030, USA), 10 % heat inactivated filtered fetal bovine serum (Invitrogen, Cat. no.15561020, USA), 100 µg/ ml Streptomycin, and 100IU/ ml Penicillin (Sigma Aldrich, Cat. P0781 USA). Cells were incubated at 37 °C, 5 % CO₂ in 25 cm² vented culture flasks (Sigma Aldrich, Cat. 430639, USA).

The RPMI 1640 medium was changed after 24 hours incubation to remove the non-adherent dead cells and traces of dimethyl sulfoxide (DMSO) from the storage medium. To maintain culture, cells were split at around 80-90% confluence and transferred to larger tissue culture flasks (Sigma Aldrich). About 6-8 hours before infection, cells were washed three times with 1X PBS (Invitrogen, Cat.14190-094, USA). Cells were re-suspended in complete RPMI 1640 medium without antibiotics (Penicillin & Streptomycin) to remove any traces of antibiotics.

Cell culture was maintained throughout in incubator at 37 °C temperature and 5 % CO₂. Cells were seeded at a concentration 1×10⁶ cell/ ml/ well of 12 well plates (Sigma Aldrich, Cat. 3513 USA) in complete RPMI 1640 medium. When the cells were fully adherent, they were washed once and then infected according to the required multiplicity of infection (MOI) and time course.

2.1.2.2 L929 cell line

The murine cell line L929 was used for monocyte-colony stimulating factor (M-CSF) production. M-CSF is required for growth of primary macrophages. These cells produce M-CSF in cell culture when grown in flasks containing media.

L929 cells aliquots were grown from cryostock in 25 cm² tissue culture flasks (Sigma Aldrich, Cat. 430639, USA) in RPMI 1640 medium. The medium was supplemented with 2mM L-glutamine, 10 % heat inactivated filtered fetal bovine serum, 100 µg/ ml of Streptomycin and 100 IU/ ml Penicillin.

When the cells were around 80-90 % confluent, the medium was washed out and the adherent cells were treated with 0.05 % Trypsin with EDTA (Sigma Aldrich, Cat. T3924, USA) just to cover the cells. The culture flask was incubated for (5-10) min at 37° C until most of the adherent cells had detached. Complete RPMI 1640 media was added to stop the action of trypsin. The cell suspension was spun at 1500rpm for 5-7 minutes and the pellet was re-suspended in fresh RPMI 1640 medium without antibiotics.

When culturing to obtain M-CSF, cells were split into large 150 cm² tissue culture flasks (Sigma Aldrich, Cat. 430825, USA) and incubated at 37° C, 5 % CO² for 7-8 days following full confluency. After incubation, the cell supernatant was taken off and sterile filtered with 0.2 µm, 25 mm diameter syringe filter (Sartorius, Cat. 16534). It was then stored at -20° C temperature until used for culturing of primary bone marrow derived macrophages (BMDMs).

2.1.2.3 Storage and long term maintenance of cell lines

Cell lines from the above groups were cryopreserved for long term maintenance using liquid nitrogen. Cryopreservation of cells was performed when the cells were at maximum growth rate and confluent. Cells were grown to maximum number, treated with 0.05 % Trypsin with EDTA (Sigma Aldrich, Cat. T3924, USA) to detach and then washed twice with RPMI 1640 medium. After centrifugation, the pellet was re-suspended in complete RPMI medium supplemented with 20 % FBS.

The cells were counted with haemocytometer, and viability confirmed with Trypan blue (Sigma Aldrich, Cat. T8154, USA) (Legrand et al., 1992). The cell suspension was supplemented with 5-10 % of dimethyl sulfoxide (DMSO). The concentration of cells in storage medium was adjusted to 1X10⁶ cells/ ml/ vial and stored at -20° C for one hour. The vials were then transferred to -80° C for overnight and finally stored and maintained in liquid nitrogen for future use.

2.1.2.4 Primary Murine bone marrow derived macrophages

Different strains of mice were used for the isolation of primary bone marrow derived macrophages (BMDMs). All animals used in this study were kept and maintained according to the Glasgow University Institutional and National (UK Home Office and European Union) guidelines.

BMDMs were isolated using a modified method described by (Lutz et al., 1999, Manzanero, 2012) for generation of bone marrow dendritic cells and macrophages. Briefly, mice were sacrificed by cervical dislocation or CO₂ inhalation. Femurs and tibias were dissected out aseptically. Muscles, cartilages and both ends of the bones were dissected.

The bone marrow was flushed with complete RPMI 1640 medium using 5 ml syringe (Becton Dickinson, Cat. 302187, Spain) and 25G 1” needle (BD Microlane, 3, Cat. 300600, Spain). Bone marrow was then suspended in RPMI medium and mixed by gentle pipetting to obtain mononuclear phagocytic precursor cells. To remove tissues and debris, the cell suspension was passed through a sterile nitex mesh (Cadisch Sons, London, UK).

Cells were then cultured in complete RPMI 1640 medium. It was supplemented with 10 % heat inactivated filtered FBS, Streptomycin (100 µg/ml), Penicillin (100 IU/ml), L-glutamine (2mM), M-CSF 10ng/ml (Peprotech, Cat. 315-02, UK) in 9 cm petri dishes (Sterilin, Cat. 24998, UK). Cells concentration was maintained at 3×10^6 cells/ petri dish/ 10ml of medium. In some experiments, we used sterile filtered supernatant from L929 cell line instead of commercial M-CSF at 20 % of the RPMI 1640 medium used for cell growth.

Petri- dishes with cultured cells were incubated at 37° C, 5 % CO₂ and grown for 6-9 days before they were ready to use. Fresh complete RPMI 1640 medium was added on the fourth day of incubation to feed the growing cells. Under these conditions, the resultant cell population was > 90 % macrophages when confirmed by staining with the macrophage marker F4/80 (Fig. 2.1; experiment performed by Dr Majid Jabir).

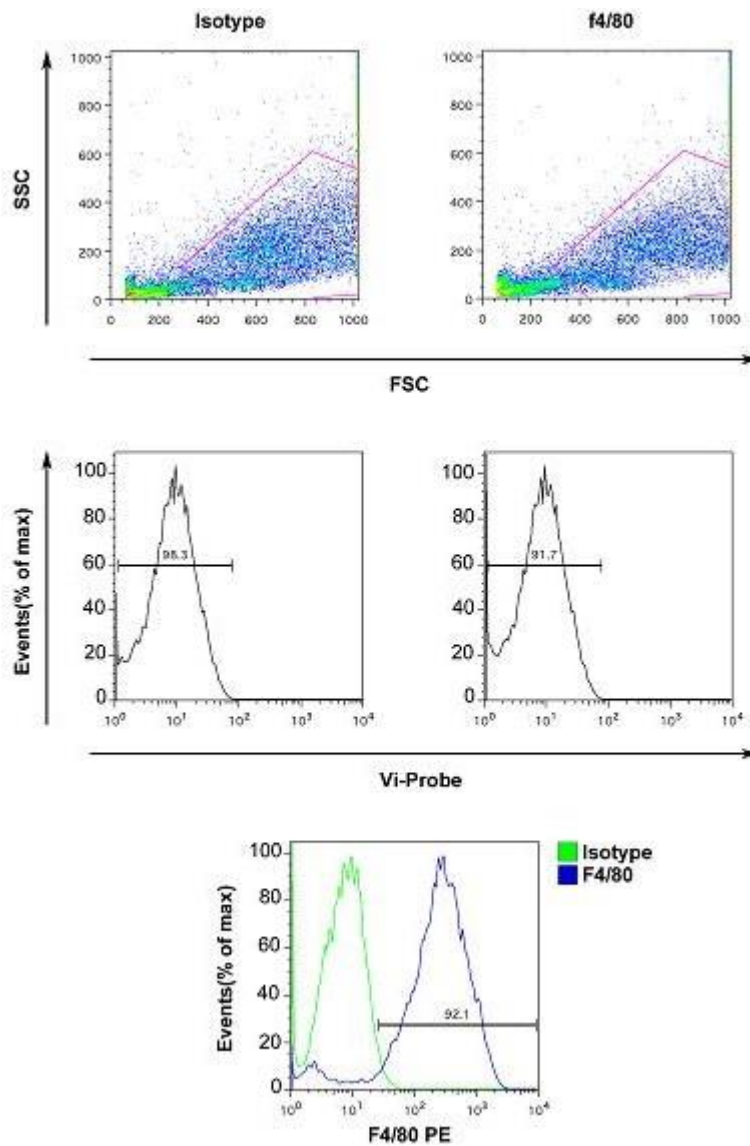


Figure 2.1 Primary murine BMDMs surface marker F4/80 staining

Murine BMDMs were analysed for the F4/80 marker using purified anti-mouse F4/80 antibody (Biolegend, Cat. 122602 USA). This is a marker for mature mouse macrophages (Leenen et al., 1994). The anti-F4/80 staining was compared with its isotype antibody by flowcytometry (FACS). Cells were gated based on the forward and side scatters. These results show that > 90 % of cells were F4/80 positive. Experiment performed by Dr Majid Jabir.

2.1.2.5 Human polymorphonuclear neutrophils (PMN) isolation

Human neutrophils were isolated from fresh venous blood obtained from healthy volunteers using a modified method adapted from (Nauseef, 2014). All procedures were performed under Glasgow University Institutional ethical approval.

Briefly neutrophil isolation was performed by dextran sedimentation method. This method separated leukocytes from erythrocytes. Hypotonic lysis was performed for the residual erythrocytes. Finally Ficoll-Paque sedimentation was performed for separation of neutrophils from the rest of leukocytes. Blood and neutrophils were maintained on ice most of the time to prevent neutrophil activation. The purity of neutrophils using this method was > 90 % with minimum activation.

Blood was collected aseptically and mixed with (ACD) acid- citrate dextrose (Sigma Aldrich) at (9:1) ratio in 50 ml centrifuge tubes (Sigma Aldrich, Cat. 210261, USA). The tubes were gently inverted several times to mix and prevent clotting of the blood. 8 ml of the blood was transferred to 15 ml centrifuge tubes (Sigma Aldrich, Cat. 188271, USA). Then 4 ml (50 % of the blood volume) from pre-prepared 6 % sterile filtered Dextran (Sigma Aldrich, Cat. 31392-10MG, USA) in 0.9 % NaCl (Merck, Cat. 1.06404.500) solution was added into 8 ml of ACD mixed blood. The tube was inverted gently 10-15 times to ensure adequate mixing. The tubes were then left to stand for 45- 60 minutes at room temperature.

Next, the yellowish supernatant was collected in a 15 ml centrifuge tube and spun at 1150 rpm for 12 min at 4°C without brake. The supernatant was discarded in this step and the pellet was re-suspended in 2 ml of ice-cold PBS. The residual RBCs were lysed by a rapid hypotonic shock by adding 6 ml of ddH₂O for 20-30 seconds. The tonicity of cell suspension was quickly restored by adding 0.6 M Potassium Chloride (KCl) solution (Sigma Aldrich, Cat. P9333-500G). The cells suspension was centrifuged again at 1300 rpm for 7 min at 4°C with full brake.

Finally, the cell pellet was re-suspended in 3 ml of PBS and layered slowly drop-by-drop over 3 ml of Ficoll- Paque plus (GE Healthcare, Cat. 17-1440-02, UK) in 15ml centrifuge tubes. The tube was spun at 1500 rpm for 30 min at 4 °C using no brake. Next, the pellet containing neutrophils was re-suspended in complete RPMI 1640 medium containing 10 % heat inactivated human serum. Cell concentration was determined using a haemocytometer. The neutrophil purity was confirmed by rapid Romanowski staining before using for experiment.

2.1.2.6 Neutrophil cytopsin and Rapid Romanowski staining

Cytopsin and Romanowski staining of human neutrophils were performed after cell isolation. Approximately 2×10^5 cells were washed with PBS and re-suspended in 200 μ l of cold 1 % BSA- PBS buffer. Clean glass slides and filters were placed into appropriate slots in the cytopsin centrifuge. 100 μ l of cell suspension was added to the cytopsin wells and spun at 500 rpm for 4-5 minutes. Cells were transferred to glass slides (VWR, Cat. 631-0113, UK) by cytopsin (Shandon Cytopsin II, centrifuge, USA). Filters were removed carefully without contacting the smear on the slides. The slides were then air dried and stained.

Neutrophils were stained with rapid Romanowsky stain (TCS Bioscience, Cat. HS705, UK), according to the manufacturer's instructions. Briefly, slides were flooded with solution "A" (Cat. HS705A; methanol fixation), for 30 seconds. Washed gently with tap water and then flooded with solution "B" (Cat. HS705B; acidic eosin dye) for 30 seconds. The slides were washed again and finally flooded with solution "C" (Cat. HS705C; methylene blue polychrome) for 30 seconds. The excess dye was removed by washing once again, edges of the slides were mopped off with tissue paper and air dried.

The slides were examined under a light microscope. The percentage of neutrophils in all experiments was maintained throughout at > 90 % of all cells (Fig. 2.2).

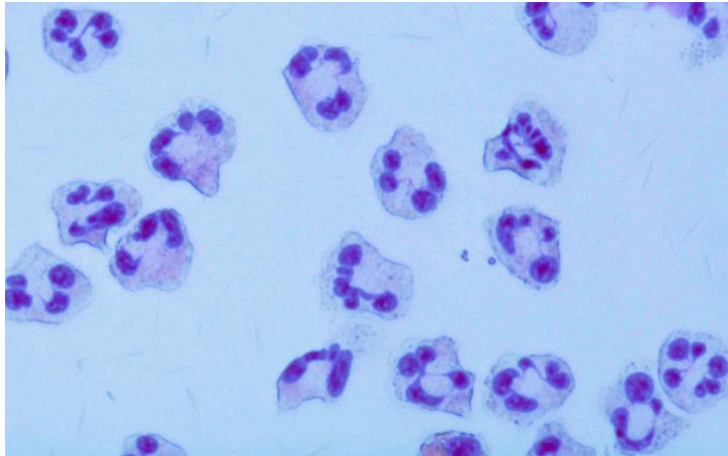


Figure 2.2 Rapid Romanowski staining of human neutrophils

Human neutrophils were isolated and cytopsin performed. Cells were stained with rapid Romanowski stain. Cell purity was confirmed by counting cells in different views during light microscopy. Neutrophils purity was maintained at > 90 % in all experiments.

2.1.2.7 Optimisation of siRNA dose with siGLO green transfection indicator in murine BMDMs

Transfection of siRNA into BMDMs was optimised using siGLO Green transfection indicator (Thermoscientific, Dharmacon RNAi Technologies, Cat. D-001630-01-05, UK). Hi-Perfect transfection reagent (Qiagen, Cat. 301704, UK), was used according to the manufacturer's instructions.

Briefly, cells were plated at a density of 0.5×10^6 cells/ well of a 12-well plate in 500 μ l complete RPMI 1640 culture medium. Transfection indicator siGLO Green was diluted in 90 μ l RPMI 1640 medium using different concentrations. Then 10 μ l of Hi-perfect transfection reagent was added to the mixture. It was gently mixed and then incubated at room temperature for 20 minutes to form complexes of transfection indicator and reagent. The siGLO Green and Hi-Perfect transfection reagent mixture was then added to the appropriate wells of a 24-well culture plate containing murine BMDMs. The plate was incubated at 37°C and 5 % CO₂ for 24-72 hours.

siGLO Green is a fluorescent oligonucleotide that localises to the nucleus of the mammalian cells. Fluorescent transfection signal was visualized and quantified using flowcytometry (FACS). The best results obtained showed transfection efficiency greater than 94 % (Fig. 2.3).

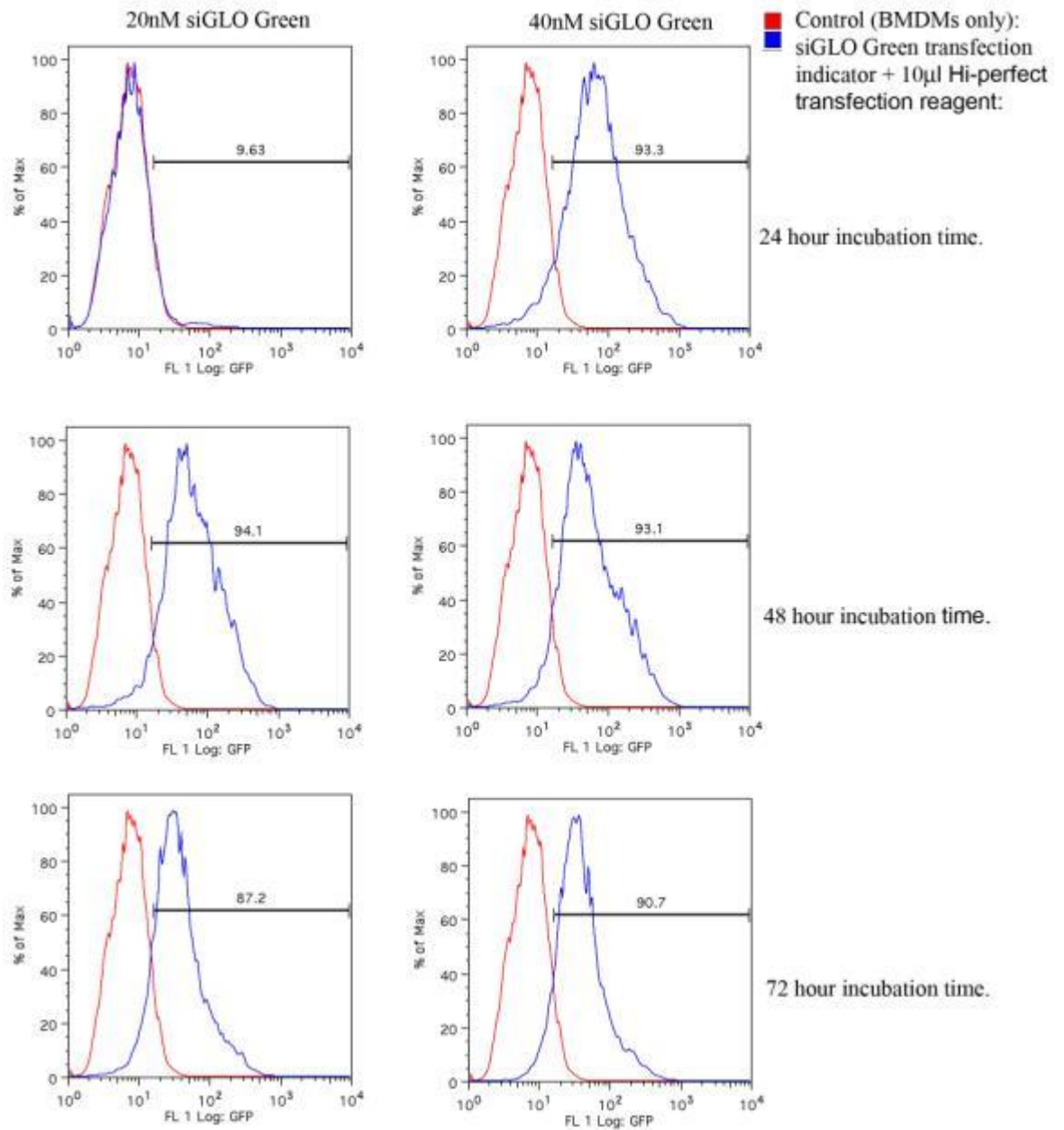


Figure 2.3 Optimisation of siRNA transfection with siGLO Green transfection indicator in murine BMDMs

Transfection of siGLO Green was performed using different conditions and time courses as shown. siGLO Green (20nM & 40nM) along with 10µl of Hi- perfect transfection reagent were incubated for 24, 48 and 72 hours. Transfection efficiency was highest at 48 hours incubation with 20nM siGLO Green transfection indicator and 10µl Hi- Perfect transfection reagent.

2.1.2.8 Optimisation of siRNA dose with siGLO green transfection indicator in human neutrophils

Neutrophils were washed and re-suspended in Gene pulser electroporation buffer (Bio-Rad Laboratories, Cat. 165-2676, CA) at approximately 5×10^6 cells/ml. Different concentrations (10 nM- 100 nM) of siGLO Green transfection indicator (Thermoscientific, Cat. D-001630-01-05, UK) were added to each 350 μ l of cell suspension in small eppendorf tubes and gently vortexed.

The cell suspension along with siGLO Green transfection indicator was then transferred to 0.4 cm electrode gap sterile Gene- Pulser electroporation cuvettes (Bio-Rad, Cat. 165-2088, CA), keeping on ice. Electroporation of human neutrophils was performed using X-cell Gene- Pulser machine (Bio- Rad, Canada). The electroporation cuvettes were placed one-by-one in the shock pad and pulsed at the following settings;

1. Capacitance 1000 μ F, Resistance 1000 Ohm and Voltage 250 v.
2. Capacitance 500 μ F, Resistance 1000 Ohm and Voltage 250 v.

Cells were quickly washed with and re-suspended in complete RPMI 1640 medium after electroporation. The medium was supplemented with 10 % heat-inactivated human serum and GM-CSF (10ng/ ml). The cells were incubated at 37°C, 5 % CO₂ overnight.

The siGLO Green fluorescent signal was then quantified using flow cytometry (Fig. 2.4). The best results were obtained with 100 nm transfection indicator with the 1000 μ F capacitance; these conditions were used for all transfections of neutrophils by electroporation.

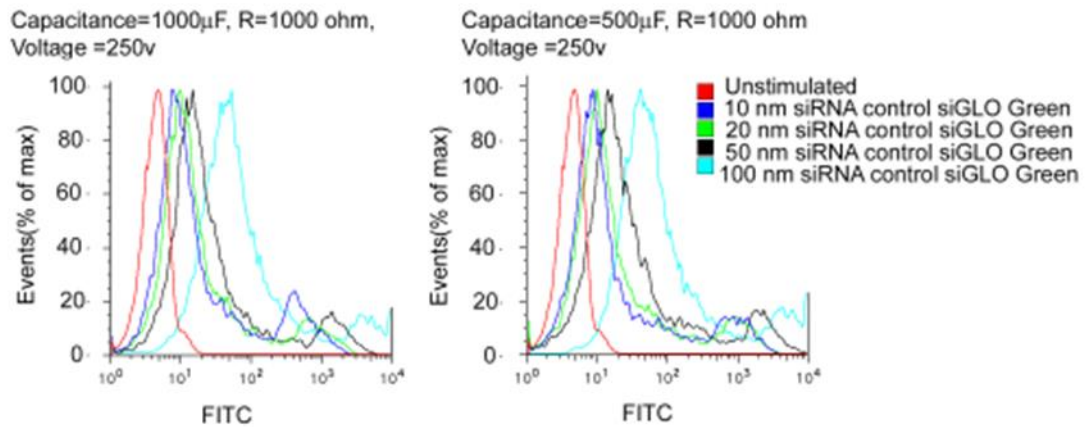


Figure 2.4 Optimisation of siRNA transfection with siGLO Green transfection indicator in human neutrophils

Human neutrophil electroporation was performed under the indicated conditions. siGLO Green (10 nM -100 nM) was added in electroporation buffer and X-cell gene pulser machine was used at two different settings i.e. Capacitance (500 μ F or 1000 μ F), Resistance 1000 (Ohm) and Voltage 250 (v). Cells were pulsed and then incubated overnight at 37 $^{\circ}$ C and 5 % CO $_2$. Transfection was observed by flow cytometry. The best results obtained with 100 nM siGLO Green, 1000 μ F capacitance, 1000 Ohm resistance and 250 volts were followed throughout neutrophil transfection.

2.1.2.9 7- AAD viability staining of neutrophils

Neutrophil viability was determined by 7-Aminoactinomycin D (7-AAD) after electroporation and overnight incubation. It is a fluorescent compound which can be detected by flow- cytometry (FACS) in fluorescence channel 3. The stain strongly binds to DNA of dead cells. It cannot penetrate membranes of the living cells, which makes it a useful live/dead cell marker. Living cells are visible as 7-AAD low cells and the dead cell takes high amount of stain.

Cells were washed and re-suspended in FACS buffer. 5 µl of 7-AAD stain solution (BD Pharmingen, Cat. 559925, UK) was added to the cell suspension for approximately 10-15 minutes. The cells were analysed on the FACSCalibur. Unstained cell suspension was used as negative control.

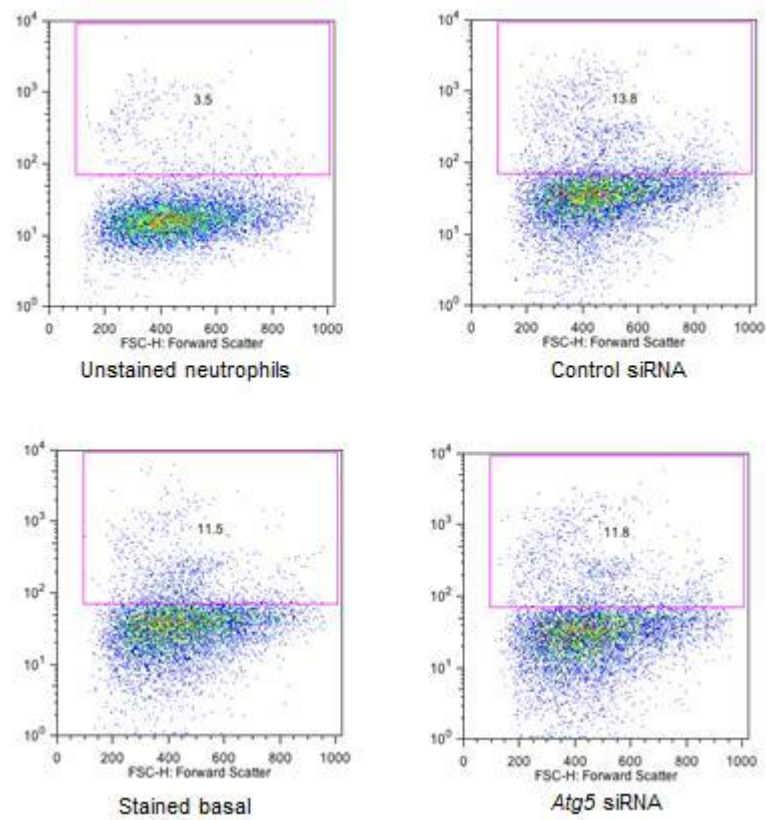


Figure 2.5 7AAD staining of human neutrophils after electroporation

7-AAD staining was performed for neutrophils after electroporation and *Atg5* gene transfection to confirm their viability. Cells were left un-transfected (stained basal), unstained control or stained (control siRNA and *Atg5* siRNA) and then visualized with flow cytometer. 7-AAD stained dead cells were determined and cell viability was maintained at > 80 % after electroporation. It was comparable in all experiments in both control and *Atg5* siRNA.

2.1.3 Bacterial cultures

2.1.3.1 *Streptococcus pneumoniae*

S. pneumoniae strains were kindly gifted by Dr Alexandra Macpherson, Institute of Infection, Immunity and Inflammation University of Glasgow. Bacteria were grown on sterile blood agar plates and used for infection.

The blood agar plates were freshly prepared using petri-dishes (Thermo-Scientific) and blood agar base (Sigma Aldrich, Cat. 70133-500G, USA). Blood agar base was thoroughly mixed in dH₂O, heated and sterilized. It was then supplemented with 5-10 % de-fibrinated horse blood (H&O Laboratories Ltd, Cat. DHB100, Scotland). Approximately 20-25 ml of the agar- blood mixture was transferred into each petri-dish and air dried in the culture hood.

Bacteria were streaked on the blood agar plates from frozen stock and grown overnight. Purified isolated colonies were transferred to sterile brain heart infusion (BHI) broth (Oxoid, Cat. CM1135). Bacteria were incubated in the water bath at 37°C for about 6 - 8 hours until grown to the mid-log phase (OD⁶⁰⁰, 0.4-0.6).

After confirming the OD, bacteria were centrifuged at 3500g and 4°C for 20 minutes, and the pellet washed twice with sterile PBS. The bacteria were re-suspended in ice-cold complete RPMI 1640 medium without antibiotics (Penicillin & Streptomycin). The bacteria were then used for infecting cells according to the required multiplicity of infection (MOI).

2.1.3.2 D39 WT

D39 WT is encapsulated virulent strain of *S. pneumoniae* which is used in laboratory experiments. The genome of this stain has been sequenced (Lanie et al., 2007). We used this strain for most of our *in-vitro* and *in-vivo* experiments in comparison to its pneumolysin deficient counterpart.

2.1.3.3 D39 Δ Ply

D39 Δ Ply is deficient in pneumolysin toxin. Its virulence is less as compared to D39 WT strain.

2.1.3.4 Confirmation of *S. pneumoniae*

S. pneumoniae was further confirmed by colony morphology, alpha haemolysis on the blood agar, Gram staining and Optochin sensitivity test. To confirm D39 Δ Ply strain from D39 WT, we performed haemolysis activity assay to observe the action of associated pneumolysin.

2.1.3.5 Gram staining

Before transferring bacteria from blood agar into the BHI, a few single colonies were transferred to a glass slide (Tissue-Tek, Ca. 9545) with a sterile loop along with a drop of dH₂O. Bacteria were mixed thoroughly with a wooden stick to make a thin circular smear about 1.5 cm and left to air-dry. The slide was passed through a Bunsen burner flame a few times to accelerate drying and enhance adhesion of the bacteria to the slide.

The following steps were followed for gram staining;

First, the slide was flooded with Gram crystal violet stain (Becton Dickinson & Co. BD, Cat. 212525, USA) for 60 seconds. The slide was gently rinsed with a slow stream of tap water using a plastic water bottle to wash away the excess stain. The slide was flooded with stabilized Gram iodine (BD, Cat. 212542, USA) for 60 seconds and rinsed with tap water.

Next, the slide was flooded with acetone decolouriser (BD, Cat. 212527) for 4-5 seconds and quickly washed as above. Counterstain was applied using a basic dye, safranin solution (BD, Cat. 212531, USA) for 60 seconds. The excess solution was washed off with tap-water and the slide was air dried.

Finally, the slide was examined under light microscope (Leitz, Germany) using oil immersion lens (OEL) with (10x100) magnification. Gram positive purple stained *S. pneumoniae* colonies were confirmed.

2.1.3.6 Optochin sensitivity test

Optochin sensitivity is one of the important characteristics of *S. pneumoniae*. It differentiates *S. pneumoniae* from other α -haemolytic

streptococci (Fenoll et al., 1994). Ethyl hydrocupreine hydrochloride (Optochin) is a chemical substance toxic to *S. pneumoniae* while other α -haemolytic streptococci are rarely sensitive to it.

Optochin impregnated discs (Sigma Aldrich, Cat. 74042-50DISKS-F, USA) were placed in blood agar plates streaked with bacteria and incubated overnight. The next day, bacterial growth was observed. There was a clear zone of growth inhibition around the optochin disc due to diffusing chemical to blood agar. This confirmed *S. pneumoniae* as α -haemolytic bacterium sensitive to optochin.

2.1.3.7 Haemolysis activity assay

S. pneumoniae (D39 WT & D39 Δ Ply) were grown on the blood agar overnight. Single colonies were transferred into 10 ml of sterile filtered BHI and grown for 6- 8 hours up to mid-log growth phase (OD^{600} 0.4- 0.6). The bacterial suspension was spun down at 3500g for 15- 20 min, washed three times and re-suspended in sterile ice-cold PBS. Bacteria were sonicated using (Soniprep- 150, Henderson Biomedical Ltd, UK) for 30 seconds 4- 5 times, keeping on ice. They were again spun down at 3500g for 15- 20 minutes. The supernatants were collected from both strains and stored on ice.

Next, erythrocyte solution was prepared by diluting 1.8 % v/v of horse blood in PBS. It was spun down at 500g for 7 min and the supernatant was discarded. Cells pellet was re-suspended in PBS after washing 3-4 times carefully to remove any lysed cells and residual haemoglobin.

The bacterial culture supernatant was serially diluted into a 96- well plate in duplicate using PBS. 10 mM of (DTT) Di- thiothreitol (Melford laboratories Ltd, Cat. mb1015, UK) and 0.1 % FBS were added to a total volume of 100 μ l/ well. The first well was taken as a 2x dilution of supernatant and assay diluent and prepared down to 1: 406 dilutions. 100 μ l of erythrocyte suspension was added to each supernatant dilution, mixed well and incubated at 37° C for 60 minutes.

Control was prepared by adding dH₂O into erythrocyte suspension. It lyses red blood cells (100 %) by hypotonic shock. Control was added into the appropriate well as 100 %, 50 % and 0 % concentration.

The plate was then centrifuged at 3000g for 5 min to remove any erythrocytes. The supernatant was transferred to another plate and OD was measured at 591 nm. The highest OD in D39 WT was almost equal to the top standard and the highest OD in D39 Δ Ply was less than 50 % of the top standard at 1.8 % of erythrocyte solution.

2.2 Methods

2.2.1 Cell viability assay

Macrophages (cell line and primary murine BMDMs) were grown for 7-8 days. They were detached from petri-dish using cell scrapers (Greiner bio-one, Cat. 541070, Germany) or treated with 0.05 % Trypsin with EDTA (Sigma Aldrich, Cat. T3924, USA). Cells were collected, re-suspended in complete RPMI 1640 medium and mixed by gentle pipetting.

Cell viability was determined using Trypan blue (Legrand et al., 1992). This dye is taken up by the dead cells. Approximately 50 μ l of the cell suspension was mixed with equal volume of 0.04 % (w/v) Trypan blue (Sigma Aldrich, Cat.T8154, USA) in PBS.

The cells and dye mixture was incubated at 37°C for 5- 7 minutes. The number of viable cells was counted per 100 cells using a haemocytometer (Superior, Germany). Cell viability in all assays was maintained at > 85 % of all cells and throughout different cell types. The viabilities of the cells used in experimental work remained comparable throughout all time points.

2.2.2 *S. pneumoniae* CFU counting and bacterial dose optimisation (MOI)

S. pneumoniae D39 WT and D39 Δ Ply were grown in BHI for 6-8 hours at 37°C. 10 ml bacterial suspension was taken at mid-log phase (OD^{600} , 0.4- 0.6) in 15 ml centrifuge tube for each strain. Bacteria were spun at 3500g for 15- 20 min at 4°C. The pellet was washed 2- 3 times with ice-cold PBS and re-suspended in 10 ml PBS. Serial dilutions of bacterial suspensions were made using a sterile 96- well plate. 10 μ l of each bacterial suspension was plated in triplicate onto blood agar from each dilution. Plates were incubated at 37°C overnight.

Colony counting was performed the next day. The adjusted numbers of bacterial counts were approximately 100 million/ ml (1×10^8) in both strains. Colony counting was performed at three different occasions and the mean was used for infecting the cells.

To infect the cells with appropriate multiplicity of infection (MOI) and time course, we prepared a ready to use bacterial suspension. 10 ml of original bacterial suspension was spun at 3500g, 4 °C for 15- 20 minutes. The pellet was washed three times and then re-suspended in 1 ml of complete RPMI 1640 without antibiotics. 1- 20 µl of this bacterial suspension was used for infection which provided an MOI of 1- 20. The best results were obtained at an MOI of 10 with less cytotoxicity.

Similarly we used different time courses (1 hour - 8 hours). The best results were obtained at 4 hours incubation with less cytotoxicity.

2.2.3 Immunofluorescence, slide preparation and fluorescent microscopy

Cells (BMDMs) were grown and then seeded in to Lab-Tek™ chamber slides (Thermoscientific, Cat.177399, USA) in RPMI-1640 complete medium without antibiotics. Cell were incubated at 37 °C, 5 % CO₂ for an hour and then infected as described. After the required infection and treatments, cells were washed 3 times with sterile PBS and fixed.

Cells were fixed in 4 % paraformaldehyde (VWR, Cat. 30525-89-4, UK) in PBS for 30- 45 minutes at room temperature. Fixed cells were washed 3 times with PBS and then permeabilized in 0.2 % Triton X-100 (Sigma Aldrich, Cat. 9002-93-1, USA) in PBS for approximately 20 minutes at room temperature. Cells were washed three times with PBS. Cells were then blocked with 10 % normal goat serum (NGS) in PBS (Sigma Aldrich, Cat. G9023, USA) for approximately 60 minutes.

Cells were then incubated with primary antibody i.e. 1.25 µg/ ml rabbit polyclonal anti LC3 antibody (Abgent, Cat. AP1802a, USA) in 10 % NGS in PBS for 60 minutes at room temperature. In some conditions primary antibody was incubated overnight at 4 °C. Cells were washed three times with PBS for 5 minutes and incubated with secondary antibody i.e. 1µg/ ml Alexa Fluor-488 conjugated goat anti- rabbit IgG (Invitrogen, Cat. A11034, USA). Cells were washed again three times with PBS. The chambers of the slides were removed,

and cover slips mounted using Vectashield mounting medium with DAPI (Vector Laboratories, Cat. H1500, USA).

Slides were viewed using a Zeiss Axiovert S100 microscope (Germany) using Open Lab software (PerkinElmer). In some of experiments, slides were viewed with laser confocal microscope (Carl Zeiss, Germany) using Meta 510 software. Pictures were taken from different sites of the slides randomly and LC3 puncta were quantified using Image J (NIH, Maryland, USA) software. All results show values of mean number of puncta per cell in pictures taken. At least 60 cells were analysed for each result.

2.2.4 Neutrophil activation, NET staining and immunoblotting

Purified human neutrophils were suspended in RPMI 1640 medium. A 24-well tissue culture plate (Corning, Cat. 3524) was prepared by putting sterile 13 mm (no. 1, 5 1) round glass cover slips (VWR, Cat. 631-0150, USA) into the wells of the plate. Approximately 2×10^5 cells were seeded into each well in 500 μ l of complete RPMI 1640 medium (Sigma Aldrich, Cat. R8758 USA) containing 2 % heat inactivated human serum.

Cells were infected with bacterial strains according to the required multiplicity of infection (10 MOI). Phorbol-myristate acetate (PMA; Invivogen, Cat. 16561-29-8) was used at 1 μ g/ ml as positive control to stimulate cell for NETs generation. The plate was incubated at 37 °C and 5 % CO₂ for 4 hours.

Next, cells were fixed in approximately 300 μ l of 4 % paraformaldehyde (PFA; Alfa Aesar, Cat. 43368, USA) in PBS for about 60- 90 minutes. Cover slips were carefully removed from the plate wells using curved needle and fine forceps. It was inverted on a drop of PBS on parafilm sheet covering a test tube stand. The coverslips were then transferred to further drops of PBS after 5 minutes to wash three times.

The coverslips were incubated on a drop of 0.5 % Triton- X 100 (Sigma-Aldrich, Cat. 9002-93-1, USA) for 15 minutes. Washed as above and then blocked in 10 % NGS (Sigma Aldrich, Cat. G9023, USA) for 30 min at room temperature. The blocked cells were then incubated with primary antibodies: anti-histone H2B

(Abcam, Cat. Ab1790 UK) and anti-neutrophil Elastase (Abcam, Cat. Ab21595 UK) for 60- 90 minutes at room temperature in a humidified chamber. The antibodies were diluted in blocking buffer (1: 50). Coverslips were washed as above and then incubated with secondary antibody, Alexa Fluor 488 goat anti rabbit IgG (H+L) antibody (Invitrogen, Cat. A11034, USA) diluted (1: 500) in blocking buffer. The antibody was incubated for 60-90 minutes at room temperature using a humidified chamber in the dark.

Finally, cover slips were washed and transferred onto glass slides on a drop of Vecta-shield mounting medium with DAPI (Vector Laboratories, Cat. H1500, USA). Cover slips were sealed to the glass slides with nail polish. Slides were air dried and examined for NETs under fluorescent or confocal microscope using oil immersion lens.

2.2.5 Bacterial staining in the NETs and confocal microscopy

S. pneumoniae strains were stained before using for infection. Bacteria were washed with PBS to remove any serum and stained with 40 μ M cell proliferation dye eFluor 450 (eBioscience, Cat. 65-0842, USA) for 15 minutes according to the manufacturer's instructions. Bacteria were washed twice and re-suspended in RPMI 1640 medium containing serum to stop the staining reaction.

Neutrophils were stimulated with the required multiplicity of stained bacteria to induce NETs generation. Cover slips were fixed with 4 % PFA, blocked with 10 % NGS and incubated with primary and secondary antibodies (Table 2.1) as before. Finally cells were washed, incubated with SYTOX orange nucleic acid stain (Invitrogen, Cat. S11368, USA) diluted in PBS (1:10,000) for 15 minutes keeping in dark. Cover slips were mounted with Fluoromount-G (eBioscience, Cat. 00-4958-02) and sealed with nail polish.

The slides were viewed with laser confocal microscope (Carl Zeiss, Germany) using Meta 510 software. DAPI, FITC and Cy3 channels were used to view the slides. Pictures were analysed with LSM software.

2.2.6 Western blot analysis

Western blot analysis was performed for different proteins according to the manufacturer's instructions. Briefly, cells were infected and treated according to the requirements of experiment. Cells were washed with ice- cold PBS and then lysed with ice-cold RIPA lysis buffer (Thermo Scientific, Cat. 89900, USA) for 30 min keeping on ice. Protease inhibitor cocktail EDTA-free (Roche, Cat. 04693159001, Germany) was added to the lysis buffer. Cell lysates were collected in ice-cold eppendorf tubes and spun down. Supernatants were collected for western blot analysis.

2.2.6.1 Determination of protein concentration in cell lysates

Protein concentration of samples was determined using Micro BCA Protein Assay kit (Pierce proteins, ThermoScientific, Cat. 23235, USA) according to the manufacturer's instructions. Proteins were adjusted to equal concentrations across different samples. The volume required for each sample was then calculated using Microsoft Excel.

2.2.6.2 Sample preparation and SDS Gel Electrophoresis

Cell lysates were mixed with NuPAGE lithium dodecyl sulphate (LDS) sample buffer (Invitrogen, Cat. NP0007, USA). NuPAGE sample reducing agent (Invitrogen, Cat. NP0004, USA) was added to LDS (1: 10). Samples were heated with LDS at 70°C for 15 minutes.

Approximately 25µg each sample was loaded on to precast Nu-PAGE Bis-Tris gels (Invitrogen, Cat. NP0322, NP0341, USA). Gels were placed in X Cell SureLock electrophoresis cell (Invitrogen, USA) using 1x NuPAGE MES SDS running buffer (Invitrogen, Cat. NP0002). Electrophoresis was performed at a voltage of 100 volts and 125 mA current for 120-150 minutes until the blue dye reached the base of the gel.

2.2.6.3 Protein transfer to membrane using transfer tank

Proteins were transferred from Gel to nitrocellulose or polyvinylidene difluoride (PVDF) membrane after separation by electrophoresis. Hybond- P (GE

Healthcare, Cat. RPN303F, UK) membrane was placed with Gel in the transfer cassette according to the manufacturer's instructions.

Protein transfer was performed using a transfer Tank (Hoefer Incorporation, Cat. TE22, USA) and 1X NuPAGE transfer buffer (Invitrogen, Cat. NP0006-1, USA). Transfer buffer was supplemented with 20 % methanol (Fisher chemicals, Cat. M/4000/PC17, UK). Protein transfer was performed at a voltage of 30v and 125 mA current for 2 hours.

2.2.6.4 iBLOT transfer system

In some experiments, protein transfer was performed using a rapid dry blotting system, the iBlot gel transfer device (Invitrogen, Cat. IB1001UK). The device was pre-set for 6-7 minutes transfer time. The gel was quickly transferred into the iBlot gel transfer stack containing a nitrocellulose membrane (Invitrogen, Cat. IB301001). Protein transfer was performed according to the manufacturer's instruction. This is a quick protein transfer method which require only 6-7 minutes.

2.2.6.5 Visualizing protein of interest and blot stripping

The presence of protein bands on the blot were observed by Ponceau's solution (Sigma Aldrich, Cat. P7170, USA) and then washed. The blot was blocked with 5 % skimmed milk (Marvel, Cat. 92962, Ireland) in PBS for 60 minutes. It was incubated with primary antibody (Table 2.1) as indicated for 60-90 minutes at room temperature or overnight at 4 °C according to the manufacturer's instructions.

The unbound primary antibody was washed three times with PBS-T (Phosphate buffer saline + 0.5 % Tween 20). The blot was then incubated with secondary antibody (Table 2.1) as indicated for 60 - 90 minutes at room temperature. The unbound secondary antibody was washed as above.

The blot was subjected to immunoblotting using Enhanced Chemiluminescence (ECL) kit (GE Healthcare, Cat. RPN2209, UK) according to the manufacturer's instructions. Proteins were visualized by exposure to photographic film.

To look for other proteins of interest, the blot was subjected to re-probing using Restore plus Western Blot Stripping Buffer (Thermoscientific, Cat. 46430, USA) according to the manufacturer instructions. Briefly, the blot was washed with PBS- T and incubated in stripping buffer for 15 minutes. It was washed again with PBS-T and blocked again with 5 % skimmed milk for 60 minutes at room temperature. The blot was incubated with primary and secondary antibodies as above. Finally it was subjected to immunoblotting with Enhanced Chemiluminescence (ECL) kit and then visualized as above.

2.2.7 Enzyme linked Immunosorbent Assay (ELISA)

The concentration of inflammatory cytokines i.e. IL-1 β in cell culture supernatant was determined by ELISA using a kit (R & D, Cat. DY401, USA) according to the manufacturer's standard protocol.

ELISA flat bottom 96- well plates (Coring Costar, Cat. 9018, USA) were coated with 50 μ l capture antibody at concentration 4 μ g/ ml diluted in PBS. The plate was sealed and incubated overnight at room temperature. The plate was washed five times with wash buffer (PBS + 0.05 % Tween 20). It was blocked with 1 % (BSA) bovine serum albumen (Sigma Aldrich, Cat. A7030-50, USA) in PBS for 60-90 minutes at room temperature. The plate was washed as above and then 50 μ l of standards and samples applied to the appropriate wells. Standards were added with a top standard of 1000 pg/ml and serially diluted (1:2) down to 10 times of the original concentration. The plate was sealed and incubated for 2 hours at room temperature.

The plate was washed again and incubated with detection antibody at a concentration of 2.5 μ g/ ml. It was diluted in reagent diluent (0.1 % BSA, 0.05 % Tween 20 in Tris- buffered saline, pH 7.4) and incubated for 2 hours at room temperature. In the next step after washing, the plate was incubated with Streptavidin-HRP. It was used at 1: 200 dilution in reagent diluent for 20 minutes at room temperature keeping in the dark.

Finally after further washing, TMB Micro-well Peroxidase substrate solution (KPL, Cat. 52-00-00,USA) was added for approximately 20 minutes at room temperature in the dark. The reaction was then stopped by adding 25 μ l of

TMB stop solution (KPL, Cat. 52-58-04, USA). The plate was read at 570 nm using a Tecan sunrise plate reader and analysed by Magellan and MS Excel software.

TNF- α concentration in the cell culture supernatants was measured by ELISA kit (eBiosciences, Cat. 88-7324-22, USA) according to the manufacturer's standard protocol, essentially as for IL-1 β .

To determine the concentrations of IL1 β and TNF α in the cell supernatants of human neutrophils, ELISA kits (eBiosciences, USA) were used according to the manufacturer's instructions.

2.2.8 Flow cytometry (FACS)

Flow cytometry was performed to determine viability and optimization of the siRNA transfection. All procedures were performed according to the manufacturer's standard protocols. Briefly cells were treated, washed and re-suspended in FACS buffer (PBS+ 1 % Fetal bovine serum). Analysis of the cells was performed using a FACSCalibur flow cytometer (BD) or CyAn ADP (Beckman Coulter). Flow cytometry data was analysed with Flowjo software (Tree Star Incorporation).

2.2.9 siRNA transfection in primary murine BMDMs

siRNA transfection of murine BMDMs was performed using Hi-Perfect transfection reagent according to the manufacturer's instructions. Briefly, control siRNA and siRNAs to different genes were obtained from Thermoscientific, Dharmacon RNAi Technologies, UK. On-target plus SMART pool of different siRNAs were introduced into the cells with Hi-Perfect transfection reagent (Qiagen, Cat. 301704, UK). The siRNA dose was adjusted through optimization with siGLO Green as discussed earlier (Fig. 2.3).

Cells were plated at a density of 0.5×10^6 cells/ well of a 12-well plate in 500 μ l of complete RPMI 1640 medium. siRNA was diluted in RPMI medium and mixed with Hi-Perfect transfection reagent. It was incubated for 20 minutes at room temperature to allow it to make complexes of siRNA and transfection reagent. siRNA along with transfection reagent was then added to the cells drop-

wise swirling the plate slowly. The plate was incubated for 48 hours at 37° C and 5 % CO₂.

After transfection, the cells were processed and treated according to the requirements of individual experiment.

2.2.10 Human neutrophil electroporation

Human neutrophils were washed and re-suspended in electroporation buffer (BIO-RAD, Cat. 165-2676, USA) at a concentration of 5 x 10⁶ cells/ ml. Electroporation was performed according to a modified protocol used by Dr Schaff from Bio-Rad (Schaff, 2008).

ON-Target plus human *Atg 5* (9474) siRNA SMART pool (Thermoscientific RNAi technologies, Cat. L-004374-00-0005) and control siRNA were used at optimized concentrations. siRNA was slowly mixed in the buffer containing cells and then transferred to 0.4 cm Gene Pulser cuvettes (BIO-RAD, Cat.165-2088) in 300 µl buffer/ cuvette. Electroporation was performed using the Gene Pulser X-cell electroporation system (BIO-RAD, USA) with resistance of 1000 ohm, voltage 250 V, capacitance 1000 µF and exponential decay pulse.

Immediately following electroporation, the cells were spun at 1100 rpm for 7 minutes. The cells were washed with and re-suspended in ice-cold complete RPMI 1640 medium containing recombinant human GM-CSF (10 ng/ ml) and incubated overnight. The next day, cells were washed and infected according to the requirement of experiments.

2.2.11 Gentamicin protection assay

Gentamicin protection assay was performed to determine viable intracellular bacterial counts. Murine BMDMs were infected with the indicated multiplicity of infection (MOI) and incubated at 37° C and 5 % CO₂ for 1-4 hours. Cells were washed three times with RPMI 1640 medium to remove bacteria.

Next, cells were incubated in RPMI 1640 medium containing gentamicin (100µg/ ml) for a further 90 minutes to kill the extracellular bacteria. Cells were then washed 2-3 times with RPMI 1640 medium and lysed with 0.1 % Triton X

100. Viable internalized bacteria were enumerated by colony counting after culturing on blood agar plates overnight (Vaudaux and Waldvogel, 1979, Arlehamn et al., 2010).

2.2.12 Neutrophil phagocytosis and killing assay

Neutrophil phagocytosis and killing assay was performed using a modification of methods described by (Hampton and Winterbourn, 1999).

Briefly, human neutrophils were isolated according to the protocol discussed earlier. Cells were re-suspended in centrifuge tubes at 1×10^6 cells/ ml in complete RPMI 1640 medium containing heat inactivated human serum. Cells were infected with *S. pneumoniae* at 10 multiplicity of infection (MOI) and incubated at 37°C and 5 % CO₂. The same numbers of bacteria were grown in a second tube in complete RPMI 1640 medium as a control.

The tubes were rotated end to end slowly and 1 ml of infected neutrophils and bacterial suspension were collected at different time points (0 - 120 min). Infected neutrophils were centrifuged at 100g for 5 minutes. The supernatant containing bacteria was collected in a tube and the neutrophil pellet was washed twice with PBS to remove any extracellular bacteria. The above procedure was repeated during each time point.

Next, infected neutrophils were re-suspended in 1 ml of PBS containing 0.05 % (w/v) saponin (Sigma Aldrich, Cat. 47036-50G-F, USA) on ice. Saponin lyse neutrophils and does not affect the viability of bacteria at this concentration (Hamers et al., 1984). The cell lysates were homogenized by gentle pipetting, serially diluted and incubated on the blood agar overnight. The number of bacteria in each sample from control, supernatant and cell lysates was enumerated by colony counting.

The same protocol was followed for different strains of *S. pneumoniae* and for cells pre-treated with 3MA and for siRNA transfected cells.

The data were analysed using an Excel spread sheet as described by Parker et al and available from:

<http://www.otago.ac.nz/christchurch/research/freeradical/assays/index.html>

The neutrophil uptake and killing assay was analysed using a two-step kinetic model that separates uptake of bacteria and their subsequent killing within the neutrophil. The spread sheet calculates the rate constants for these separate processes as k_p , the rate of phagocytosis, and k_k , the rate of killing.

2.2.13 LDH cytotoxicity assay

Lactate dehydrogenase (LDH) assay was performed to determine the cytotoxicity of bacterial infection during experiments. LDH is a soluble cytosolic enzyme present in eukaryotic cells. It is released into the culture medium due to cell lysis. The increase in LDH activity in the culture supernatant of infected cells is proportional to the number of lysed cells. It appears as red colour from a reaction cocktail, and is measured at 490 nm using a spectrophotometer.

Cells were incubated in RPMI 1640 medium lacking Phenol red (Invitrogen, Cat. 11835-030, UK). LDH release was measured using CytoTox-96 cytotoxicity assay kit (Promega, Cat. G1781, USA). It quantitatively measures LDH enzyme. Assay was performed on the cell supernatants using 96 well plates (Corning, Cat. 3799) according to the manufacturer's instructions. Control was prepared by treating cells with 1 % Triton X 100 (Sigma Aldrich, Cat. T8787, USA) and incubated for 60 minutes at 37°C and 5 % CO₂ (Legrand et al., 1992). Fresh controls were prepared for each experiment.

The data was presented as bar graphs according to the following formula; $[(\text{OD of the sample} / \text{OD of the standard}) \times 100]$. Sample data from such a calculation are shown in Figure 2.6. The LDH released by infected cells was maintained at < 20 % in all experiments.

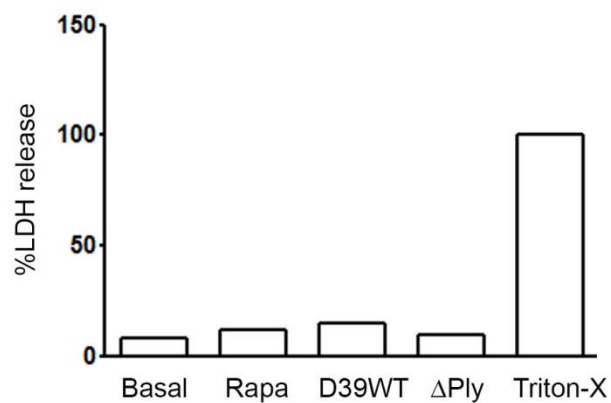


Figure 2.6 LDH (Cytotoxicity) Assay of murine BMDMs infected with *S. pneumoniae*

Bar graph showing % LDH released by murine BMDMs. Cells were left uninfected (Basal), treated with Rapamycin (25 μ g/ ml) and infected with *S. pneumoniae* strains D39 WT and D39 Δ Ply for 4 hours. The LDH release was compared with positive control (Cells treated with 1 % Triton- X100).

2.2.14 Animal model used in this study (*in vivo* experiments)

Animal model experiments were designed to test my *in vitro* observations. An intraperitoneal (i.p) infection model was used.

Initially, bacterial dose was optimised using six mice in 3 groups of (n= 2) per group. 5, 10, 20 million bacteria/ animal were injected to find the most effective dose. Female C57BL/6 mice aged 7- 8 weeks were obtained from Harlan UK and used in this model. 1×10^7 bacteria per animal gave the most effective onset of infection.

Mice were randomly divided into six groups (n=3 per group). Mice from the three control groups were injected (i.p) with sterile PBS, rapamycin alone (1.5 mg / kg body weight) or 3-MA (30 mg / kg of body weight) (Harris et al., 2011, Kim et al., 2012). Experimental groups were all injected (i.p) with *S. pneumoniae* strain D39 WT (1×10^7) alone and in addition in separate groups with rapamycin 1.5 mg / Kg body weight or with 3-MA 30 mg / Kg body weight. The infected mice were left for 6 hours.

Blood and peritoneal lavage were collected after infection and analysed. Peritoneal lavage was analysed for bacterial colony counting. Macrophages in the peritoneal lavage were analysed for autophagy by western blotting. Serum and peritoneal lavage were analysed for inflammatory cytokines by ELISA and protein concentration.

Table 2.1 Antibodies used in this study along with working concentration

Antibody	Manufacturer	Catalogue number	Application	Working conc.
Purified Rabbit polyclonal antibody Pab, LC3 antibody (APG8B) (N-term).	Abgent (USA)	AP 1802a	IF	1.25µg/ ml
LC3 Antibody, Autophagosome marker	Novus Biological (UK)	NB100-2220	WB FACS	1µg/ ml
Anti-Atg5 Antibody.	Novus Biological (UK)	NB110-53818SS	WB	0.5µg/ ml
Alexa flour 488 goat anti- rabbit IgG (H+L).	Invitrogen (USA)	A11034	IF FACS	1µg/ ml
Alexa flour 568 goat anti- mouse IgG (H+L).	Invitrogen (USA)	A11031	IF	1µg/ ml
Rabbit immunoglobulin fraction (solid-phase absorbed) (Negative control)	Dako, (Denmark)	X0936	IF FACS	1.25µg/ ml
Monoclonal Anti-β-Tubulin antibody produced in	Sigma-Aldrich (USA)	T8328	WB	1µg/ ml

mouse				
Anti-rabbit IgG HRP- linked antibody.	Cell signalling technology (UK)	7074	WB	1: 2000
Anti-Mouse IgG HRP- linked antibody.	Cell signalling technology (UK)	7076	WB	1: 2000
Anti-pneumococcal surface protein-A Antibody (Anti- <i>PspA</i>)	Abcam UK	ab63330	Opsonizing bacteria for WB and Phagocytosis	8µg/ ml
Capture Antibody (ELISA)	R and D system (USA)	80134	ELISA	4µg/ ml
Detection Antibody.	R and D system (USA)	80135	ELISA	600ng/ ml
Caspase -1 p10 (M-20) Antibody.	Santa Cruz biotechnology (UK)	sc-514	WB	1µg/ ml
Caspase -1 (A-19) Antibody.	Santa Cruz biotechnology (UK)	sc-622	WB	1µg/ ml
Rabbit polyclonal to IL-1 β antibody	Abcam (UK)	ab9722	WB	1µg/ ml

Rabbit polyclonal anti-TRIF antibody	abcam (UK)	ab13810	WB	1µg/ ml
Monoclonal Anti-FLAG, M2, Clone M2.	Sigma (USA)	F1804	WB	1µg/ ml
Mouse Anti-rabbit IgG .mAb (HRP conjugate).	Cell signalling technology (UK)	5127	WB	1: 2000
Capture Ab purified anti-mouse TNF -α.	eBioscience (UK)	14-7423-67A	ELISA	1: 250
Detection Ab Biotin-conjugate anti-mouse TNF -α polyclonal.	eBioscience (UK)	13-7341-67A	ELISA	1: 250
Capture Ab purified anti-human IL-1β.	eBioscience (UK)	14-7018-68	ELISA	1: 250
Detection Ab Biotin-conjugate anti-human IL-1 β TNF -α polyclonal	eBioscience (UK)	33-7016-68	ELISA	1: 250
Purified mouse IgG2a, Isotype control 0.5mg/ml	BD Pharmingen (UK)	553459	NETs	1µg/ ml
Anti-TLR2 antibody	Invivogen (USA)	mabg-mtlr2	For blocking TLR2	1µg/ ml

			receptors	
Human Anti-neutrophils Elastase Antibody	Abcam (UK)	Ab21595	IF (NETs)	1: 50
Anti-histone H2B antibody	Abcam (UK)	Ab1790	IF (NETs)	1: 100

Table 2.2 siRNA controls used in this study

siRNA	Catalogue number	Manufacturer
Transfection indicator (siGLO green)	D-001630-01-05	Dharmacon RNAi Technology, USA
ON-Target plus-NON- Targeting pool (control siRNA)	D-001810-10-05	Dharmacon RNAi Technology, USA

Table 2.3 siRNA used in this study

Mouse siRNA	Cat. number/ Manufacturer	Target sequences in the pool
<i>LC3b</i>	L-040989-01-0005 Dharmacon RNAi technology USA	5' -ACUAUGGUGCGAUCAGUAA-3' 5' -CAUCCUAAGUUGCCAAUAA-3' 5' -GGAUUAAGCUCUAAGCCGG-3' 5' -CUAAUAAAGGCACAACGAA-3'
<i>Atg5</i>	L-064838-0005 Dharmacon RNAi technology USA	5' - GCAUAAAAGUCAAGUGAUC-3' 5' - CCAAUUGGUUUACUAUUUG-3' 5' - CGAAUCCAACUUGCUUUA-3' 5' - UUAGUGAGAU AUGGUUUGA-3'
<i>Caspase-1</i>	L-048913-00-0005 Dharmacon RNAi technology USA	5' - GAAUACAACCACUCGUACA-3' 5' - GCCAAAUCUUUAUCACUUA-3' 5' - GGUAUACCGUGAAAGUGAA-3' 5' - GCAUUAAGAAGGCCCAUUA-3'
<i>Ticam-1 (Trif)</i>	L-055987-00-0005 Dharmacon RNAi technology USA	5' -GAUCGGUGCAGUUCAGAAU-3' 5' -GAACAGCCUUACACAGUCU-3' 5' -GGAAAGCAGUGGCCUUAUUA-3' 5' -GAGAU AAGCUGGCCUCCA U-3'

Human siRNA		
<i>Atg5</i> (9474)	L-004374-00-0005 Dharmacon RNAi technology USA	5'-ACAAAGAUGUGCUUCGAGA-3' 5'-UGACAGAUUUGACCAGUUU-3' 5'-GCAGAACCAUACUAAUUUGC-3' 5'-GGCAUUAUCCAAUUGGUUU-3'

Table 2.4 Solutions, Buffers, chemicals, drugs and other material and equipment used in this study

Solutions / Buffers etc.	Catalogue number	Manufacturer
Albumin Standards for detection of protein concentration in cell lysates	23209	Pierce, Thermo-scientific, USA
Bovine serum albumen	A7030-50	Sigma Aldrich, USA
Brain Heart Infusion (BHI)	CM1135	Oxoid, USA (Thermoscientific)
Bafilomycin A1 (Drug)	B1793	Sigma Aldrich, USA
Caspase-1 inhibitor Z-YVAD-FMK	ALX-260-154-R020	Enzo Life Science, USA
Calbiochem, SB203580 (EMD Millipore) 5 mg	559389	Merck, Kga A, Germany
Cell proliferation dye (500µg) (eFlour 450) - for bacterial stain	65-0842-85	eBioscience, USA
De-fibrinated Horse Blood	DHB100	E&O Labs Ltd, Scotland
Dried skimmed milk	92962	Marvel, Ireland
Dimethyl sulfoxide (DMSO)	D5879-500G	Sigma Aldrich, USA
Dextran from leuconostoc spp.	31392-10g	Sigma Aldrich, USA

E64d (drug)	BML- PI107-0001	Enzo Life sciences, USA
ECL protein detection Kit: Lumigen P5-3 reagent A, Lumigen P5-3 reagent B	RPN 2132 V1 RPN 2132 V2	GE Healthcare, UK
ELISA KIT (Mouse IL-1 beta/ IL-1F2 DuoSet, 5 Plate)	DY401-05	R & D System, USA
ELISA substrate solution (R&D)	DY999	R & D System, USA
ELISA stop solution 2N H ₂ SO ₄ (R&D)	DY994	R & D System, USA
Human IL-1 β ELISA Ready- SET - Go	88-7010	eBioscience, USA
Fetal Bovine serum	15561020	Invitrogen, USA
Gene - Pulser Electroporation buffer	165-2676	Bio - Rad Laboratories, USA
Human GM-CSF (Recombinant)	300-03	PeptoTech, USA
HRP- Streptavidin Horseradish Peroxidase Conjugate.	43-4323,	Invitrogen, USA
Hi - Perfect Transfection Reagent	301705	Qiagen, USA
Inoculating loop	18388-500EA	Sigma Aldrich, USA

KCl (Potassium Chloride)	P9333-500G	Sigma Aldrich, USA
LDH cytotoxicity assay kit		
LDH Assay Buffer.	G 180	Promega, USA
Substrate mix	G 179	
LDS (Loading) buffer, 4X (Nuphage)	NP0007	Invitrogen, USA
Murine M-CSF	315-02	PeptoTech, USA
Micro BCA Reagent, A 240 ml	23231	Pierce, USA
Micro BCA Reagent, B 240ml	23232	Pierce, USA
Micro BCA Reagent C, 12ml	23234	Pierce, USA
MES SDS Running Buffer 20X	NP0002	Invitrogen, USA
Normal goat serum (NGS)	G9023	Sigma Aldrich, USA
Nuphage sample reducing agent 10 X	NP0004	Invitrogen, USA
Nuphage MES SDS , Running Buffer 20X	NP0002	Invitrogen, USA
Nuphage Transfer buffer 20X for western blotting	NP0006-1	Invitrogen, USA
NOVEX BT GEL 12 % 1.0MM	NP0341BOX	Invitrogen, USA

10W		
NOVEX BT GEL 4-12 % 1.0MM 10W	NP0321BOX	Invitrogen, USA
NOVEX BT GEL 12 % 1.0 MM 12W	NP0342BOX	Invitrogen, USA
Optochin discs	74042-50	Sigma Aldrich, USA
Phosphate buffer saline	14190-094	Gibco, Life technologies, UK
Protease inhibitor cocktail tablet (Complete mini EDTA-free)	04693 159 001	Roche, Germany
Pepstatin A	P5318	Sigma Aldrich, USA
Para- formaldehyde (PFA)	43368	Vwr (Alfa Aesar), USA
Ponceau S solution (stain)	P7170, USA	Sigma Aldrich, USA
Pam3 CSK4 1mg / ml- used 100ng/ ml	112208-00-1	Invivogen, USA
Rapid Romanowski stain pack	HS705	TCS Biosciences Ltd. Buckingham, UK
Rapamycin	BML-A275-0005	Enzo life- sciences incorporation UK
RIPA Buffer (Pierce TM)	89900	Thermoscientific, USA

Mammalian cell lysis buffer		
Sample reducing agent 10X	NP0004	Invitrogen, USA
Stop solution for LDH assay	G 183	Promega, USA
Stripping buffer (Restore Plus Western blot)	46430	Thermoscientific USA
siRNA buffer 5X	B-002000-UB-100	Dharmacon, UK
Sterile RNase - free water for siRNA Buffer dilution	B-002000-WB-100	Dharmacon, UK
7-AAD viability stain	420404	Bio- Legend, USA
SYTOX™ Orange, 5mM Solution (Nucleic acid stain)	S11368	Invitrogen, USA
Tween- 20	P2287	Sigma Aldrich, USA
Trypan blue stain	T8154	Sigma Aldrich, USA
Triton X-100	9002-93-1	Sigma Aldrich, USA
3-methyladenine	M9281-100MG	Sigma Aldrich, USA
Vectashield Mounting medium with DAPI.	H -1500	Vector, USA

2.3 Statistical analysis of data

All experiments in this study were repeated independently at least three times. Statistical analysis of data was performed using GraphPad Prism 5 software and Microsoft Excel.

Data are presented in the form of bar and line graphs and expressed as mean, \pm standard deviation (SD) or \pm standard error of the mean (SEM).

Mean is the average number of different observations during an experiment. In statistics, mean and expected values are used for one measure of the central tendency obtained from different observations.

Standard deviation measures the amount of variation or dispersion of data points from the average. A low standard deviation indicates that the data points are very close to the mean (expected value), while a higher SD indicates that the data points are far apart from the mean value.

SEM is the standard deviation of means of different samples drawn from a certain population. It takes into account the values of SD and the sample size. It is an indication of how well the mean of a certain sample estimates the mean of a population. The SEM can provide a rough estimate of the interval in which the population mean is likely to fall. SEM decreases with an increase in the sample size.

Unpaired t-test, also known as student's t-test, was performed to make comparison between two groups at one time point assuming unequal variances. Unpaired t-test is applied to two independent groups. It compares the means of two groups and calculates the mean difference, if it is a positive or negative value. This test is used to determine if two sets of data are significantly different from each other or equal. It is applied if the data is normally distributed. The criterion for statistical significance was taken as $p < 0.05$ (2 sided).

Two way analysis of variance (ANOVA) was used for complex grouping of data. It is used for more than two groups, because multiple t-tests may result in

increased chance of incorrectly rejecting a true null hypothesis (a type1 error). It can be used for several groups whether the means of data are equal or not. Comparison between groups over time was performed by 2 way ANOVA using GraphPad Prism and statistical significance was taken as p value < 0.05 in each case.

Figures were prepared using Image J (NIH), LSM, Photoshop CS6 software and Microsoft Power Point.

- 3 Infection with *S. pneumoniae* induces autophagy in primary murine bone marrow derived macrophages (BMDMs)**

3.1 Introduction

Macrophages are one of the most important cells in the body and form the first line of defence against infection. They are present in almost all body tissues. They provide strong immunity by eliminating invading pathogens through different strategies. Macrophages are large myeloid origin cells characterized by the presence of pseudopodia, nonspecific esterases and phagocytic granules. They are one of the principal effector and regulator cells of the innate immune system and play a much wider role in the body (Hopkinson-Woolley et al., 1994).

Macrophages are mainly associated with generalized immunity. They also provide help in adaptive immunity via antigen presentation. They are considered large phagocytes maintaining tissue homeostasis by engulfing damaged and apoptotic cells and foreign bodies. They also detect invading pathogens, release chemical mediators to blood and body fluids, and initiate a strong signal to other immune cells. They are more efficient phagocytes than other immune cells and can phagocytose invading pathogens including *S. pneumoniae*. There is a strong relationship between autophagy and phagocytosis by macrophages. The autophagy protein LC3 is recruited to the phagosome forming a phagolysosome which kills pathogens through lysosomal degradation (Robertson et al., 1939, Sanjuan et al., 2007).

Invading pathogens also activate the inflammasome in macrophages which is a cytoplasmic platform for the activation of caspase-1 and processing of pro IL-1 β and IL-18 to their active forms (Franchi et al., 2012). Inflammasome activation and autophagy induction are both important pathways in host defence. The effects of the inflammasome activation on the induction of autophagy are not clearly understood.

Autophagy induction is shown to down regulate inflammasome activation through the sequestration of defective mitochondria (mitophagy). This inhibits the release of mitochondrial DNA and reactive oxygen intermediates required for the activation of NLRP3 inflammasome (Sun et al., 2014). Similarly autophagy proteins are also associated with inflammasome activation and innate immunity

in multi-cellular organisms. They directly interact with multiple immune signalling molecules (Deretic et al., 2009, Saitoh and Akira, 2010).

S. pneumoniae is an extracellular pathogen with multiple virulence factors and toxins. Pneumolysin (Ply) is one of the most important virulence factors of this pathogen. Ply is believed to activate the NLRP3 inflammasome in macrophages and dendritic cells (Shoma et al., 2008, McNeela et al., 2010). These innate immune cells attack and kill *S. pneumoniae* but the bacterium is capable of adopting strategies to escape its killing. Virulence factors and toxins play a vital role in the protection of *S. pneumoniae*. Virulence factors enable *S. pneumoniae* to cause persistent infection (Campoy and Colombo, 2009) and complete its infectious cycle.

We hypothesized that *S. pneumoniae* infection induces autophagy in primary murine BMDMs and that this pathway is associated with phagocytosis and inflammasome activation which has not been previously demonstrated. To test our hypothesis, we infected primary murine BMDMs with *S. pneumoniae* strain D39 WT and D39 Δ Ply (pneumolysin deficient strain). We observed the effects of *S. pneumoniae* strains on autophagy induction, phagocytosis and inflammasome activation.

We used these encapsulated virulent strains and demonstrated a different pattern of autophagy induction in each strain. D39 strain of *S. pneumoniae* belongs to serotype 2 virulent group, which is completely sequenced (Lanie et al., 2007). D39 strain of *S. pneumoniae* is a classic representative of this invasive human pathogen.

We used different techniques to demonstrate autophagy induction in primary murine BMDMs including immunofluorescence and western blot analysis. We used different time courses of infection and observed the effects of incubation time. We also observed the effect of *S. pneumoniae* strains at different multiplicities of infection (MOI). During each experiment, we observed cytotoxicity by measuring the LDH released during infection and maintained at a low level.

Our study revealed that autophagy is induced in infection with *S. pneumoniae* in primary murine BMDMs through a process involving multiple autophagy proteins including Atg8 (LC3), Atg5 and Atg7. These are important proteins and classical markers of autophagy. These autophagy proteins form complexes and function in association with other Atg proteins during autophagosome formation (Chew and Yip, 2014). Furthermore, autophagy induction in *S. pneumoniae* infection was also studied indirectly via chemical inhibition or genetic knock-down of autophagy genes.

We further studied phagocytosis in primary murine BMDMs infected with *S. pneumoniae*. We also demonstrated the effect of autophagy on phagocytosis of *S. pneumoniae*. We studied the influence of pneumococcal virulence factors pneumolysin and antibodies to pneumococcal surface protein A (PspA) on phagocytosis of *S. pneumoniae*. Next, we studied inflammasome activation in association with autophagy induction in murine BMDMs. We found that inhibition of autophagy by pharmacological and genetic methods up-regulated inflammasome activation. We also demonstrated that inhibition of the inflammasome by pharmacological or genetic methods increased autophagy in *S. pneumoniae* infection.

To find how autophagy is triggered by an extracellular pathogen to the interior of the cell, we studied different cell surface and cytoplasmic receptors. Research demonstrates that not only TLR4 but other TLR family members are also involved in autophagy but our experiments on *Tlr4*^{-/-} mice revealed that this pathway is not associated with autophagy induction in *S. pneumoniae* infection.

Similarly we also studied the effect of TRIF and MyD88 pathways which is believed to recruit Beclin 1 into TLR signalling complex and induce autophagy in macrophages (Shi and Kehrl, 2008). Our results demonstrated that knock out of TRIF and MyD88 did not affect autophagy induction following infection with *S. pneumoniae*. This showed that there might be some other pathway involved in autophagy induction in *S. pneumoniae* infection.

Next, we investigated TLR2 pathway which is known to induce autophagy in *Staph. aureus* (Fang et al., 2014). We blocked TLR2 receptors in primary

murine BMDMs and then infected with *S. pneumoniae*. Inhibition of TLR2 did not affect autophagy induction in *S. pneumoniae* infection. We also studied the role of the intracellular pattern recognition receptor NOD2. Its activation is believed to induce autophagy in macrophages (Homer et al., 2010). We stimulated macrophages with muramyl dipeptide (MDP) and its control (MDPc). MDP is a peptidoglycan from gram positive and gram negative bacteria activating NOD2. Our results demonstrated that there was no autophagy induction following MDP stimulation of macrophages.

Next, we studied the effect of p38MAP kinase which is believed to induce autophagy (Matsuzawa et al., 2014). We treated murine BMDMs with p38 MAP kinase inhibitor and then infected with *S. pneumoniae*. We found that *S.pneumoniae* induced autophagy in in both inhibitor treated and untreated cells. This demonstrated that p38MAP Kinase is not involved in autophagy induction in murine BMDM with *S. pneumoniae* infection.

All our experiments presented in this chapter provide useful information for understanding this important pathway associated with the innate immune system and infection control. *S. pneumoniae* infection especially multi-drug resistant strains are difficult to treat. They could possibly be controlled with some treatment strategies based on autophagy induction and our study might prove helpful.

3.2 Results

3.2.1 Autophagy induction in primary murine BMDMs infected with *S. pneumoniae* using immunofluorescence (IF) and western blot (WB) techniques

S. pneumoniae has not previously been shown to induce autophagy in macrophages. We determined the induction of autophagy with two different strains of *S. pneumoniae* (D39 WT and D39 Δ Ply) in primary murine BMDMs. We confirmed our results with IF and WB techniques using different incubation conditions and treatments. Autophagosome formation was observed in murine BMDMs by immunofluorescence (Fig. 3.1a) and the conversion of LC3 I to its lipidated form LC3 II (Fig. 3.1c).

Our results clearly demonstrated a marked increase in the absolute amount of LC3 II relative to β - tubulin following infection, to levels observed in positive control rapamycin, a classic inducer of autophagy. Moreover, the ratio of LC3 II to β - tubulin following infection with *S. pneumoniae* was slightly greater in these experiments with D39 Δ Ply, a pneumolysin deficient counterpart of the D39 strain (Fig. 3.1d).

During the time and dose course experiments we observed that both strains of *S. pneumoniae* induced autophagy which could be detected as early as 1 hour incubation and increased with time to about 4 hours incubation. Although we got the same signal at incubations more than 4 hours but the cytotoxicity of infection was increased when observed by LDH assay (discussed in material and methods section).

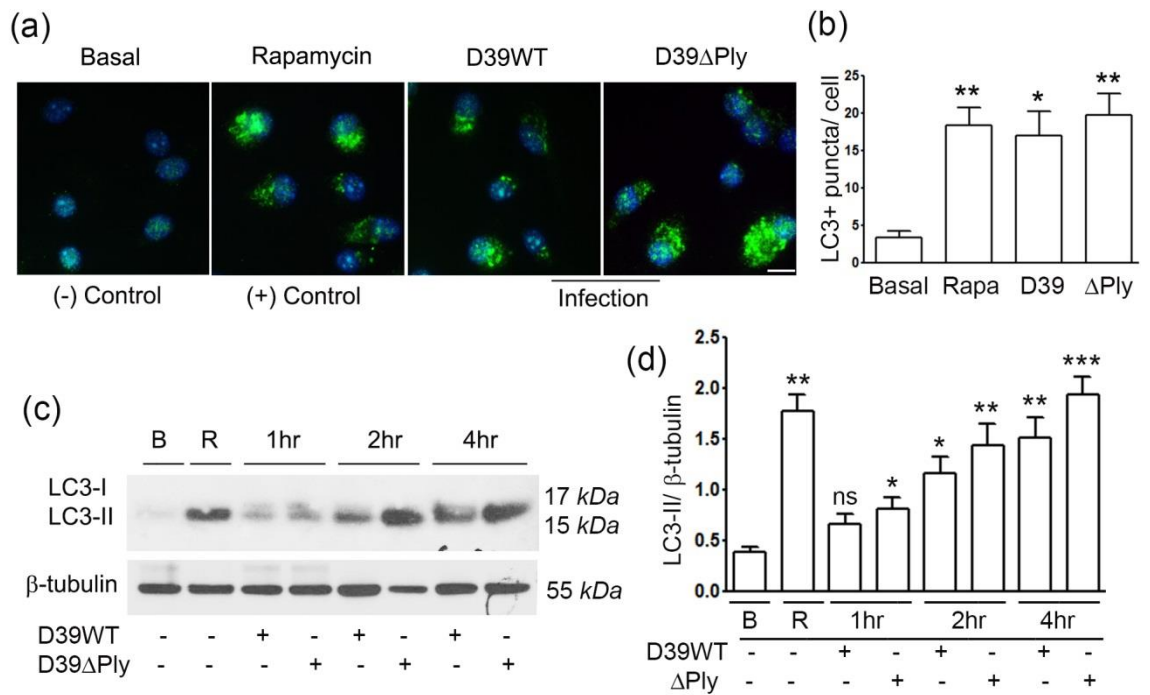


Figure 3.1 Autophagy induction in primary murine BMDMs following *S. pneumoniae* infection

(a) Immunofluorescence was performed for LC3 protein levels in untreated (Basal) murine BMDMs as negative control, treated with Rapamycin (50 μ g/ml) as positive control of autophagy and infected with *S. pneumoniae* strains D39 WT and D39 Δ Ply at an MOI of 10 for 4 hours. Fluorescent microscopy was performed to visualize LC3 (green) and nuclear (DAPI, blue) staining. Scale bar is 50 μ m.

(b) Numbers of LC3 puncta /cell (counted in 60 cells in different views). Columns show mean; error bars are SEM. Asterisks indicate statistical significance from basal: *, $p < 0.05$; **, $p < 0.01$; ***, $p < 0.001$.

(c) Western blot analysis of LC3 I and LC3 II proteins in murine BMDMs. Cells were left unstimulated (B), treated with Rapamycin (R; 50 μ g/ml) as positive control of autophagy and infected with *S. pneumoniae* strains D39 WT and D39 Δ Ply at an MOI of 10 for the time indicated. The same blot was stripped and re-probed for β - tubulin protein as loading control as shown in panel.

(d) Densitometry measurement of the ratio of LC3 II/ β - tubulin (three representative blots from independent experiments). Asterisks denote level of significance from basal as shown in (b).

3.2.2 Autophagy induction in primary murine BMDMs infected with *S. pneumoniae* is dose dependent

Next, we determined the relationship between the infecting dose of bacteria and the induction of autophagy by repeating these experiments using different multiplicities of infection (MOI), as shown in Figure 3.2. We found that there was a relationship between MOI and induction of autophagy. However, the data show that at MOI below 5 there was minimal induction of autophagy and that a MOI of 10 was required to produce a significant increase in autophagy, as shown by the increase in relative amounts of LC3 II. This suggests that there is a threshold of about an MOI of 5, below which no autophagy is produced.

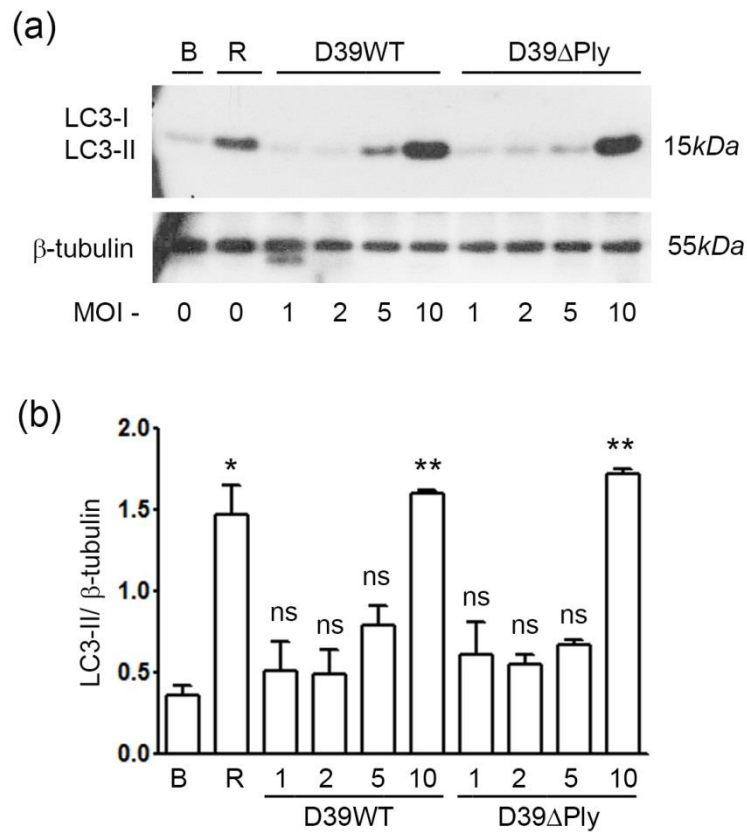


Figure 3.2 Dependence of autophagy on multiplicity of infection (MOI) in primary murine BMDMs

(a) Representative western blot images of LC3 II protein using primary murine BMDMs infected with *S. pneumoniae* at different MOIs. Cells were left uninfected (B), treated with Rapamycin (R; 25 μ g/ml) or infected with *S. pneumoniae* strains D39 WT and D39 Δ Ply at MOI of 1, 2, 5 and 10 as shown.

(b) Densitometry analysis of LC3 II/ β -tubulin (two independent experiments). Columns are mean values; error bars are SEM. Asterisks show level of significant difference from basal: * $p < 0.05$; ** $p < 0.01$.

3.2.3 Monitoring autophagy flux with lysosomal inhibitors

To determine if infection with *S. pneumoniae* increases flux through the autophagocytic pathway, lysosomal proteases were inhibited with E64d and Pepstatin A or by preventing fusion of autophagosomes with lysosomes using Bafilomycin A1 (Tanida et al., 2005, Yamamoto et al., 1998). Conversion of LC3 I to LC3 II (lipidation) is not affected by these drugs and the LC3 II accumulates as the various drugs block LC3 II degradation.

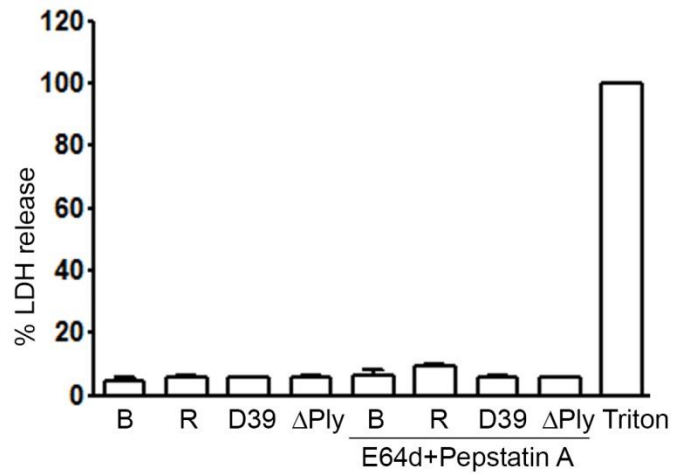


Figure 3.3 Cell cytotoxicity assay (% LDH released by the cells)

Representative bar graph from cell supernatant assayed for LDH released in two different experiments. Supernatant from cells treated with and without E64d and Pepstatin A and then left untreated (B), treated with Rapamycin (R) and infected with *S. pneumoniae* D39 WT and D39 ΔPly. The cytotoxicity was compared with cells treated with 1 % Triton- X100 (control). The columns are means of % LDH released and error bars are SEM.

3.2.3.1 Autophagy flux using lysosomal inhibitors E64d and Pepstatin A

The lysosomal degradation of LC3 was blocked by pre-treating primary murine BMDMs with E64d and Pepstatin A (Tanida et al., 2005). Cells were then infected with *S. pneumoniae* strain D39 WT and D39 Δ Ply without changing culture medium containing lysosomal inhibitor drugs. This increased the amount of LC3 II produced following infection as shown in (Fig. 3.4). This indicated that autophagy flux was increased in the infected cells, although the increase in LC3 II levels in the presence of E64d and pepstatin A was not large though it was reproducible (Fig. 3.4b).

Importantly under these conditions, there was not any significant increase in cell death due to cytotoxicity of the drugs. This was measured by the release of lactate dehydrogenase (LDH) from both treated and untreated cells as shown (Fig. 3.3).

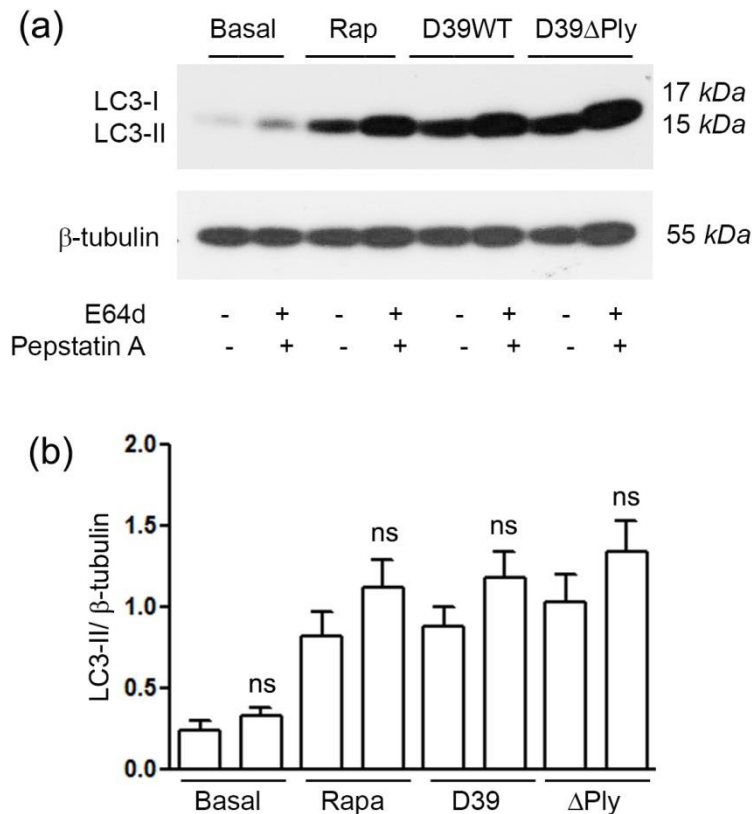


Figure 3.4 Lysosomal inhibitors of autophagy E64d and Pepstatin A increased accumulation of autophagy flux.

(a) Representative western blot analysis of LC3 I and LC3 II levels in primary murine BMDMs pre- treated as indicated with E64d (10 μ g/ ml) and Pepstatin A (10 μ g/ml) and compared to untreated cells infected with *S. pneumoniae*. Cells were left un-stimulated (Basal), treated with Rapamycin (Rapa; 25 μ g/ml), or infected with *S. pneumoniae* strains D39 WT and D39 Δ Ply at an MOI of 10 for 4 hours in the presence (+) or absence (-) of inhibitor drugs.

(b) Densitometry analysis of LC3 II/ β tubulin from (two independent experiments). Columns are mean values; error bars are SEM. These results indicate that there is some increase in autophagy flux in cells treated with lysosomal inhibitor drugs but the results are non- significant (ns).

3.2.3.2 Autophagy flux with lysosomal inhibitor Bafilomycin A1

Bafilomycin A1 is another specific inhibitor of the late phase of autophagy pathway which blocks fusion of the autophagosome with lysosome (Yamamoto et al., 1998). Primary murine BMDMs were pre-treated with Bafilomycin A1 and then infected with *S. pneumoniae* D39 WT and D39 Δ Ply as shown in (Fig. 3.5). Bafilomycin A1 treatment increased the amounts of LC3 II produced following infection, indicating an increase in autophagocytic flux.

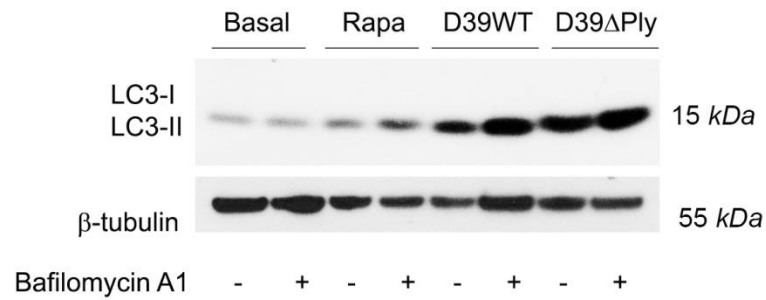


Figure 3.5 Inhibition of lysosomal degradation by Bafilomycin A1 increases levels of LC3 II

Representative western blot analysis of LC3 II levels in murine BMDMs pre- treated with Bafilomycin A1 (50nM) as indicated. The cells were then left un-stimulated (Basal), treated with Rapamycin (Rapa; 25µg/ ml), or infected with *S. pneumoniae* D39 WT and D39 ΔPly (10MOI) for 4 hours with (+) or without (-) inhibitor drug.

3.2.4 Effects of antibodies to pneumococcal surface protein A (*PspA*) on autophagy induction with *S. pneumoniae* infection

Pneumococcal surface protein A (*PspA*) is an important virulence factor of *S. pneumoniae* expressed by all capsular serotypes and exposed on the surface. It is believed to inhibit complement activation and thus prevents the clearance of *S. pneumoniae* by host immune cells (Tu et al., 1999). Previously it has been demonstrated that blocking *PspA* by genetic knock down or by anti-*PspA* antibodies enhances phagocytosis of *S. pneumoniae* (Ren et al., 2012). The effect of antibodies to this virulence factor on autophagy induction has not been demonstrated.

Our aim was to find the effect of antibody to *PspA* on the induction of autophagy in primary murine BMDMs following pneumococcal infection. *S. pneumoniae* strain D39 WT and D39 Δ Ply were pre-treated with anti-*PspA* antibody and then used for infection of primary murine BMDMs. Autophagy induction was observed by Western blot analysis of LC3 II levels (Fig. 3.6). Autophagy was slightly enhanced in cells infected with anti-*PspA* antibody treated *S. pneumoniae* as compared to untreated bacteria but this increase was non-significant.

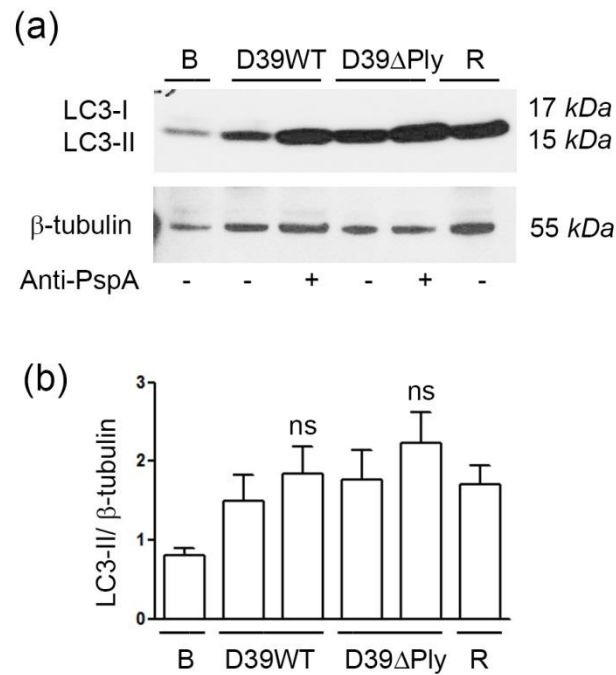


Figure 3.6 Effects of anti-*PspA* antibody on autophagy induced by *S. pneumoniae* infection

Representative western blot analysis of LC3 II levels in primary murine BMDMs infected with *S. pneumoniae* D39 WT and D39 DPly pre-treated with anti-*PspA* (1µg/ ml) and compared with untreated bacteria. Cells were left un-stimulated (B), treated with Rapamycin (R; 25µg/ ml), as positive control of autophagy or, infected with *S. pneumoniae* strains D39 WT and D39 ΔPly (10 MOI; 4 hours) in the presence (+) or absence (-) of anti-*PspA* antibody.

(b) Densitometry analysis of LC3 II/ B-tubulin from (two independent experiments). Columns are mean values; error bars are SEM. These results indicate that there is a non-significant (ns) difference between the two groups.

3.2.5 Blocking autophagy pathway by chemical and genetic methods in murine BMDMs

Next, we studied the functional effects of autophagy in primary murine BMDMs by inhibiting the process using chemical inhibitors of this pathway and siRNA knock down of different autophagy genes. We also used gene knockout animals to study the induction of autophagy with *S. pneumoniae* infection. Under these conditions, there was not any significant increase in cell death due to cytotoxicity of 3MA or siRNA as measured by the release of LDH from both treated and untreated cells (data not shown).

3.2.5.1 Autophagy inhibition with 3-methyladenine (3MA)

Primary murine BMDMs were treated with 3MA, a pharmacological agent known to block autophagosome formation by inhibiting class- III phosphatidylinositol-3-kinase (PI-3K III). Cells were pre-treated with 3MA (Seglen and Gordon, 1982, Wu et al., 2010) and then infected with *S. pneumoniae* strains D39 WT and D39 Δ Ply.

Immunofluorescence and western blot techniques were performed on 3MA treated and untreated cells. Fluorescent microscopy was performed to observe LC3 puncta and cell lysates were analysed by western blot for LC3 I and II isoforms. As shown in (Fig. 3.7), 3MA produced a marked inhibition of autophagy, in both assay of LC3 puncta formation, and in inhibiting the formation of LC3 II.

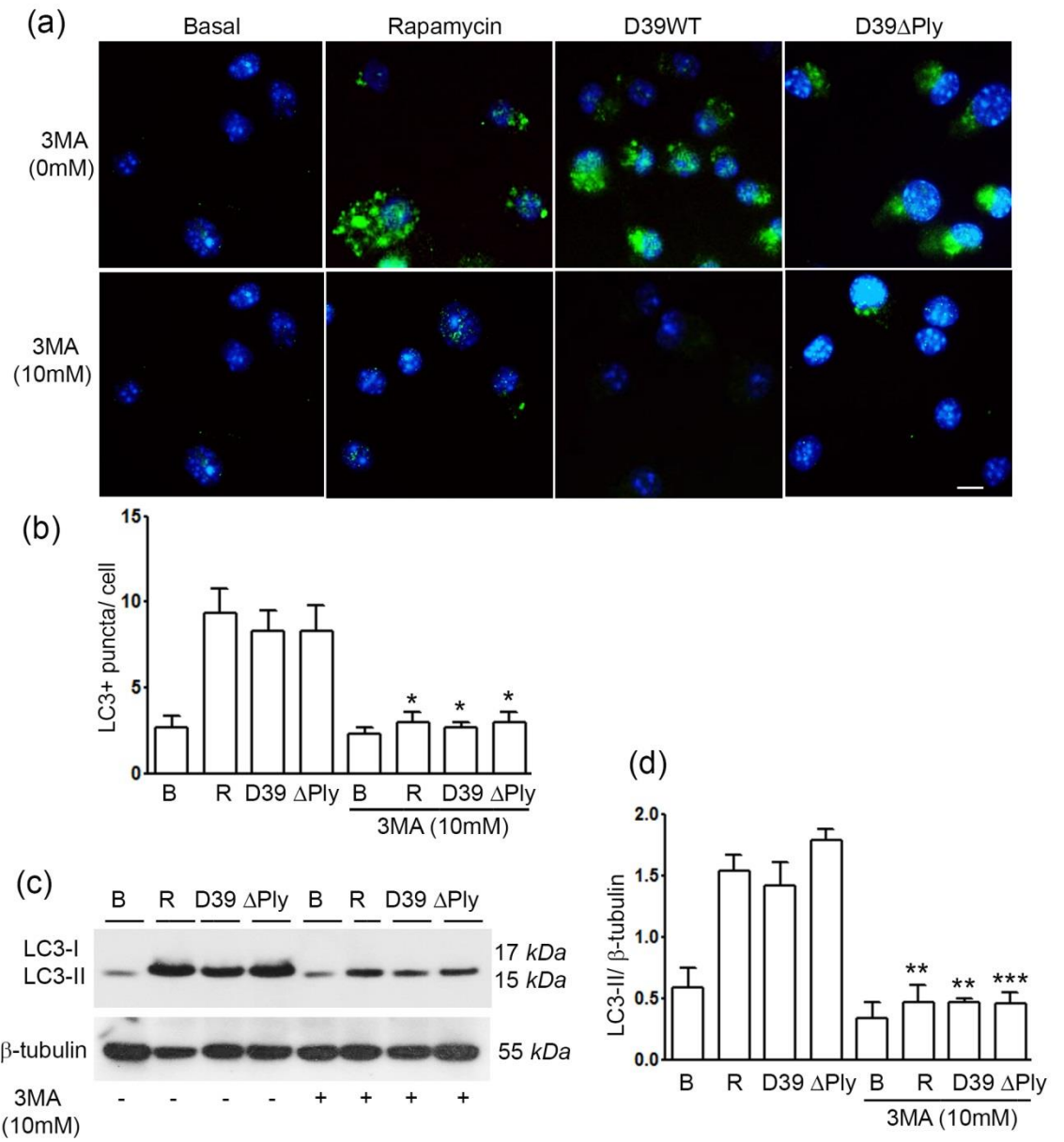


Figure 3.7 3-MA inhibits autophagy in primary murine BMDMs

(a) Representative immunofluorescence images of LC3 puncta in primary murine BMDMs. Cells were left uninfected (Basal), treated with Rapamycin (25 μ g/ ml) or infected with *S. pneumoniae* strains D39 WT and D39 Δ Ply at an MOI of 10 for 4 hours in the presence or absence of 3MA (10mM). Cells were stained with anti-LC3 antibody (green) and DAPI to visualize the nuclei (blue). Scale bar is 50 μ m.

(b) Quantification of average number of LC3 puncta present per cell (counted in 60 cells in different views) following treatments and infections as indicated. * shows significant decrease in puncta/ cell in 3-MA treated cells, ($p < 0.05$).

(c) Western blot analysis of LC3 I and LC3 II proteins in primary murine BMDMs pre-treated with 3-MA and infected with *S. pneumoniae*. Cells were left uninfected (B) or treated with Rapamycin (R; 25 μ g/ ml) or infected with *S. pneumoniae* strains D39 WT and D39 Δ Ply at an MOI of 10 for 4 hours in the presence (+) or absence (-) of (10mM) 3MA.

(d) Densitometry analysis of the autophagy signal in primary murine BMDMs treated with 3MA and without treatment. Columns are mean values of LC3 II determinations; error bars are SEM. Asterisks indicates significant reduction in autophagy in cells treated with 3MA as compared to untreated cells: **, $p < 0.01$; ***, $p < 0.001$ (3 independent experiments).

3.2.5.2 Autophagy knock down in murine BMDMs using siRNA to *Lc3b* gene

Autophagy is dependent on multiple autophagy-related (Atg) proteins. LC3 (Atg8) is one of the most important autophagy protein (Tanida et al., 2008) and a classical marker for the autophagosome formation. Knock down of *Lc3b* gene has been demonstrated to down regulate autophagy in many different types of cell. We studied the effect of *Lc3b* knock down in primary murine BMDMs using control siRNA and *LC3b* siRNA.

Cell viability was determined with Trypan blue after 48 hours of transfection (discussed in material and method section). This showed that > 80 % of the cells were alive after transfection and incubation for the indicated time. With the siRNA treatment, very effective knock down of LC3b was achieved (Fig. 3.8). Although useful for further studies, we wished to show which other autophagy genes were involved.

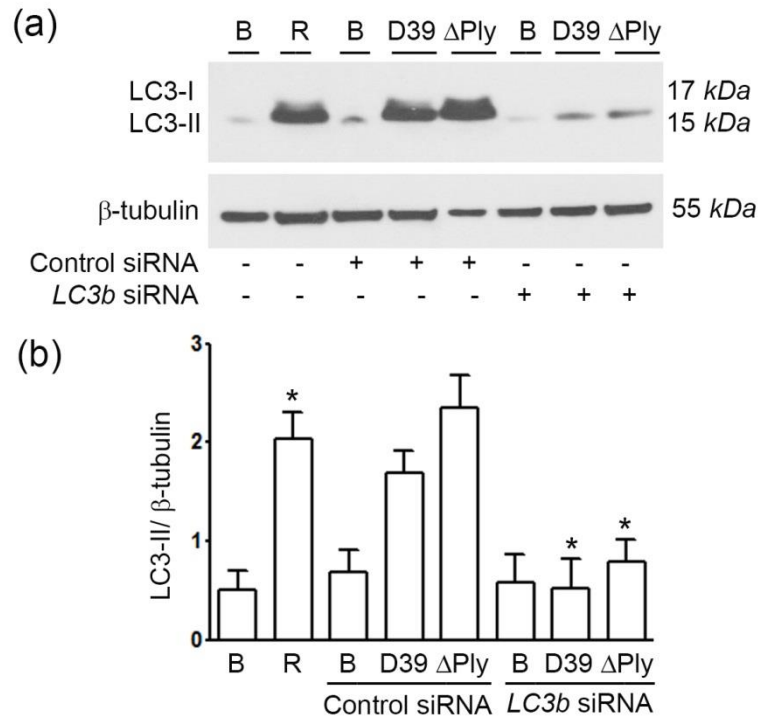


Figure 3.8 *S. pneumoniae* induced autophagy in primary murine BMDMs is LC3 dependent.

(a) Representative western blot analysis from lysates of primary murine BMDMs treated with control siRNA and *Lc3b* siRNA and probed for LC3 I and LC3 II proteins as indicated. Cells were left uninfected (B), treated with Rapamycin (R; 25 μ g/ml) or treated with control siRNA and *Lc3b* siRNA and then left uninfected (B) or infected with *S. pneumoniae* strains D39 WT and D39 Δ Ply at an MOI of 10 for 4 hours. The blot was stripped and re-probed for β -tubulin protein as a loading control.

(b) Densitometry analysis of the autophagy protein LC3 II in primary murine BMDMs knocked down for *Lc3b* gene and control. Columns are the means of LC3 II determinations; error bars are SEM. Asterisks showing significant reduction of LC3 II protein in *Lc3b* knock down cells, $p < 0.05$ (2 independent experiments).

3.2.5.3 Autophagy knock down in primary murine BMDMs using siRNA to *Atg5* gene

Autophagy related-5 (ATG5) protein is one of the classical markers of autophagy and *Atg5* gene knock down can block the autophagy pathway. Following knockdown of *Atg5* gene, we infected cells with *S. pneumoniae* strain D39WT and D39 Δ Ply and followed the progression of autophagy (Fig. 3.9). We found that knock down of ATG5 significantly inhibited autophagy following *S. pneumoniae* infection. Note the band detected by the *Atg5* antibody is in fact the conjugate between ATG5 and ATG12 that forms following the induction of autophagy, accounting for the increase in the signal when autophagy is increased e.g. after rapamycin treatment or pneumococcal infection.

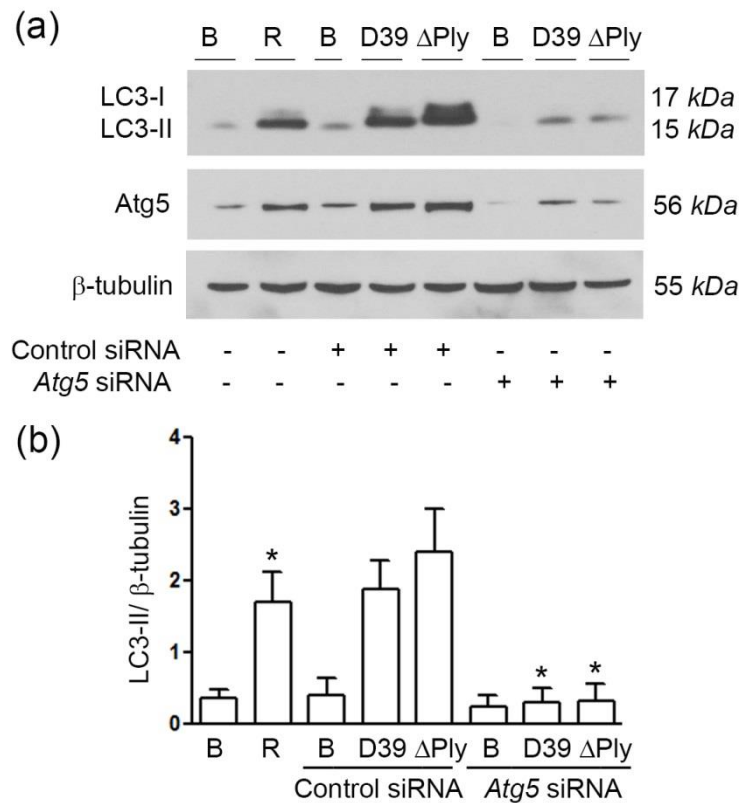


Figure 3.9 *S. pneumoniae* induced autophagy is *Atg5* dependent.

(a) Representative western blot analysis from lysates of primary murine BMDMs treated with control siRNA and *Atg5* siRNA genes and probed for the proteins as indicated. Cells were left uninfected (B), treated with Rapamycin (R; 25 μ g/ml) or transfected with control and *Atg5* siRNA and then left uninfected (B) or infected with *S. pneumoniae* strains D39 WT and D39 Δ Ply at an MOI of 10 for 4 hours. The blot was stripped and re-probed for *Atg5* protein to look for the efficiency of knock down and for β -tubulin protein as a loading control.

(b) Densitometry analysis of the autophagy protein LC3 II in primary murine BMDMs knocked down for *Atg5* gene. Columns are the means of LC3 II determinations; error bars are SEM. Asterisks showing significant reduction of LC3 II in *Atg5* gene knock down cells, * is significant difference from control siRNA, $p < 0.05$ (2 independent experiments).

3.2.5.4 Autophagy is dependent on Atg7 in primary murine BMDMs using *Atg7*^{-/-} mice.

Autophagy related-7 (ATG7) protein is important in the classical autophagy pathway. To explore the role of this protein in autophagy induced by *S. pneumoniae*, we studied this pathway in macrophages derived from animals with selective deletion of the *Atg7* gene (*Vav-Atg7*^{-/-}). Macrophages were grown from WT and *Vav-Atg7*^{-/-} mice and infected with *S. pneumoniae* strain D39 WT and D39 Δ Ply.

Western blot was performed for LC3 I and II using cell lysates from both groups of mice. As shown in (Fig. 3.10a), knock out of the *Atg7* gene effectively inhibited autophagy following infection, as assayed by the conversion of LC3 I to II. Thus, autophagy following *S. pneumoniae* infection of primary murine macrophages is dependent on *Atg5* and *Atg7*, genes that form part of the classical autophagy pathway.

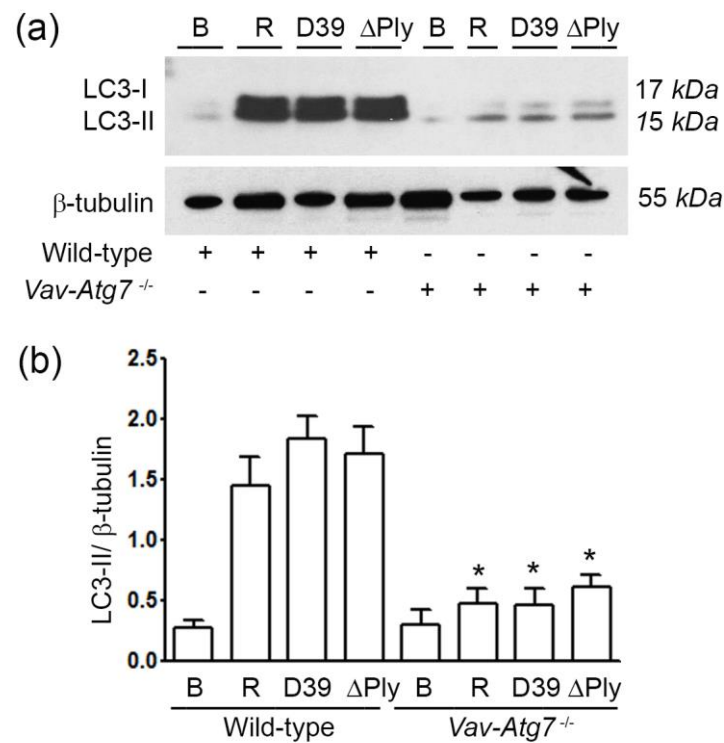


Figure 3.10 *S. pneumoniae* induced autophagy is Atg7 dependent.

(a) Representative western blot analysis of LC3 protein from cell lysates of primary murine BMDMs of WT and *Vav-Atg7*^{-/-} mice. Cells were left uninfected (B), treated with Rapamycin (R; 25 μ g/ml) or infected with *S. pneumoniae* strains D39 WT and D39 Δ Ply at an MOI of 10 for 4 hours. The blot was stripped and re-probed for β -tubulin protein as a loading control.

(b) Densitometry analysis of the autophagy protein LC3 in primary murine BMDMs from WT and *Atg7* gene knock-out mice. Columns are the means of LC3 II determinations; error bars are SEM. Asterisks showing significant reduction of LC3 II protein in *Atg7* gene knock-out mice as compared to the wild-type mice, $p < 0.05$ (2 independent experiments).

3.2.6 Phagocytosis (internalization) of *S. pneumoniae* by primary murine BMDMs

Next, we explored the relationship between induction of autophagy following *S. pneumoniae* infection and phagocytosis of the microbe. Macrophages are large phagocytes and they have the ability to phagocytose invading pathogens. This is an important process and is regulated by a complex mechanism to prevent damage to the host tissues from uncontrolled phagocytosis. Macrophages have evolved a restricted number of phagocytic receptors such as mannose receptors for the recognition of conserved motifs from invading pathogens, and discriminate from self-tissues (Aderem and Underhill, 1999). Pathogens use different strategies to alter their phagocytosis by the innate immune cells - for example, the *S. pneumoniae* capsule protects it from phagocytosis. Immune cells can recognize pathogens, inactivate their virulence factors and then engulf them.

We set out to explore the effects of autophagy on phagocytosis following infection as well as the influence of the virulence determinant pneumolysin on this process. We used strains D39 WT and D39 Δ Ply and followed their phagocytosis by primary murine BMDMs. Cells were infected with bacteria, treated with gentamycin to kill the extracellular bacteria (Vaudaux and Waldvogel, 1979) and the internalized live bacteria were grown and counted as discussed in the material and methods section. *S. pneumoniae* CFU counts were calculated at different time points (Arlehamn et al., 2010).

To demonstrate the relationship between autophagy and phagocytosis, we also studied *S. pneumoniae* phagocytosis in primary murine BMDM with abrogation of autophagy by 3MA and *Lc3b* gene knock down.

3.2.6.1 Comparison of *S. pneumoniae* strains D39 WT and D39 Δ Ply phagocytosis by murine BMDMs

Primary murine BMDMs were infected with *S. pneumoniae* strain D39 WT and D39 Δ Ply. Extracellular bacteria were killed with gentamicin (100 μ g/ ml) for 90 minutes. The phagocytosed live bacterial CFU were counted in the lysates of cells at different time points.

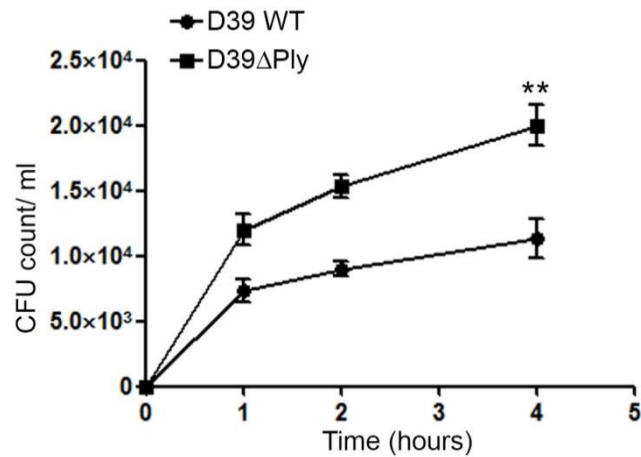


Figure 3.11 *S. pneumoniae* strain D39 WT is resistant to phagocytosis when compared to its pneumolysin deficient counter-part

Representative line graph showing numbers of live phagocytosed *S. pneumoniae* at various times after infection. Primary murine BMDMs (1×10^6) were infected with *S. pneumoniae* strains D39 WT and D39 Δ Ply at an MOI of 10 at time zero. After 1, 2 and 4 hours of *S. pneumoniae* infection, the samples were treated with gentamycin for 90 minutes to kill extracellular bacteria and viable bacteria were then enumerated. CFU counts in the lysates were plotted in triplicate as the mean value; error bars are SEM. ** indicates a significant difference between the two groups when analysed by 2 way ANOVA ($p < 0.01$).

There was a significant difference between the numbers of *S. pneumoniae* strain D39 WT and D39 Δ Ply phagocytosed by murine BMDMs over time as is shown in (Fig. 3.11). Both strains of bacteria accumulated steadily over time in the macrophages, but the numbers of D39 Δ Ply recovered were always significantly higher.

3.2.6.2 *S. pneumoniae* phagocytosis by primary murine BMDMs is up-regulated by blocking pneumococcal surface protein A (*PspA*)

We wished to explore the influence of opsonising antibody on the progress of phagocytosis and autophagy following infection. *S. pneumoniae* D39 WT were pre-treated with anti-pneumococcal surface protein A (anti-*PspA*) for 30 minutes. Primary murine BMDM were infected with *S. pneumoniae* treated with anti-*PspA* and without treatment.

Extracellular bacteria were killed with gentamycin (100 μ g/ ml) for 90 minutes and phagocytosed live bacterial CFU were counted in the cell lysates. CFU counts were compared in cells infected with *S. pneumoniae* treated with and without antibody to *PspA* (Fig. 3.12).

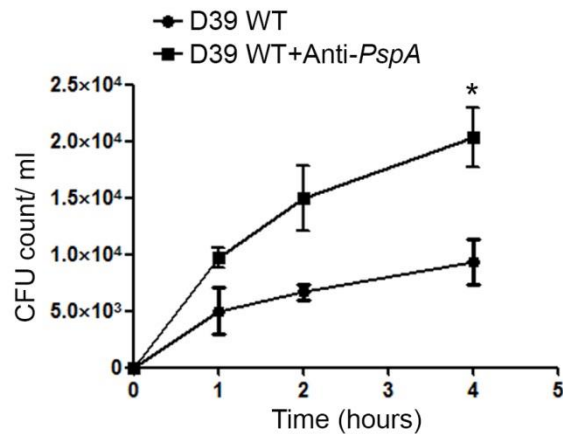


Figure 3.12 Antibody to *PspA* up-regulates phagocytosis of *S. pneumoniae* by murine BMDMs

Representative line graph showing number of phagocytosed live *S. pneumoniae* over time. Primary murine BMDMs (1×10^6) were infected with *S. pneumoniae* strain D39 WT pre-treated with anti-*PspA* ($1 \mu\text{g}/\text{ml}$) for 30 minutes or without treatment, at an MOI of 10 for (1, 2 and 4) hours. After 1, 2 and 4 hours of *S. pneumoniae* infection, the samples were treated with gentamycin for 90 minutes to kill extracellular bacteria and viable bacteria were then enumerated. CFU counts in the lysates were plotted in triplicate with mean and SEM. Asterisks indicate significance between the two groups when analysed by 2 way ANOVA ($p < 0.05$).

This shows that antibody to *PspA* up-regulates phagocytosis of *S. pneumoniae*. There was also some increase in the autophagy signal when *S. pneumoniae* was pre-treated with this antibody as shown in (Fig. 3.6).

3.2.6.3 Effect of 3MA on phagocytosis (internalization) of *S. pneumoniae* by primary murine BMDMs

Next, we explored the relationship between autophagy and phagocytosis using 3-MA to inhibit the autophagocytic pathway. Primary murine BMDMs were pre-treated with 3-MA and then infected with *S. pneumoniae* D39 WT. Extracellular bacteria were killed with gentamicin (100µg/ ml) for 90 minutes and phagocytosed live bacteria were counted in the cell lysates. CFU counts were compared in cells treated with and without 3-MA as shown (Fig. 3.13).

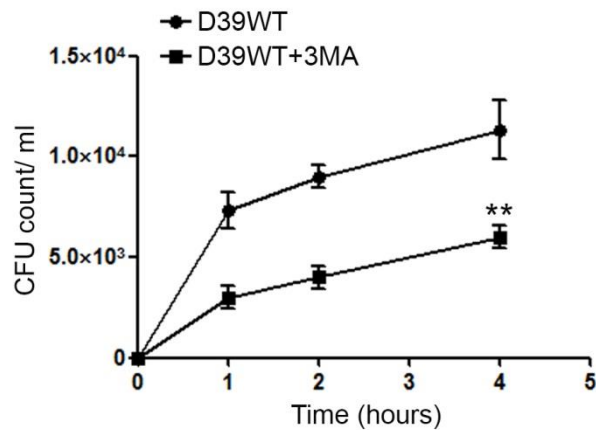


Figure 3.13 3-MA down regulates phagocytosis of *S. pneumoniae* by murine BMDMs

Representative line graph showing counts of phagocytosed live *S. pneumoniae* over time. Primary murine BMDMs (1×10^6) were left untreated and treated with 3-MA (10mM) for 60 minutes. The cells were then infected with *S. pneumoniae* strain D39 WT at an MOI of 10. After 1, 2 and 4 hours of *S. pneumoniae* infection, the samples were treated with gentamycin for 90 minutes to kill extracellular bacteria and viable bacteria were then enumerated. CFU counts in the lysates are plotted as means of triplicates; error bars show SEM. ** indicates a significant difference between cells treated with and without 3-MA when analysed by 2 way ANOVA, ($p < 0.01$).

These data show that inhibition of autophagy with 3-MA significantly reduces the uptake of *S. pneumoniae* by BMDMs. This suggests that autophagy plays a part in the phagocytosis of this microbe.

3.2.6.4 Phagocytosis of *S. pneumoniae* by primary murine BMDMs transfected with siRNA *Lc3b*

Next, we inhibited autophagy by knock-down of *Lc3b* gene using siRNA and determined the effect of this process on phagocytosis of live *S. pneumoniae*. Primary murine BMDMs were transfected with control siRNA or *Lc3b* siRNA for 48 hours and then infected with *S. pneumoniae* at 10 multiplicity of infection for 1, 2 and 4 hours. Extracellular bacteria were killed with gentamicin (100µg/ ml) for 90 minutes and phagocytosed live bacteria were counted in the cell lysates. CFU counts of *S. pneumoniae* were compared in cells transfected with control siRNA and *Lc3b* siRNA as shown (Fig. 3.14).

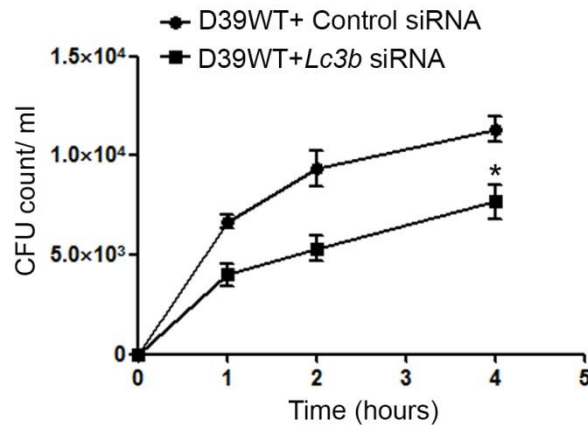


Figure 3.14 Autophagy gene *Lc3b* knock down in murine BMDMs down-regulates phagocytosis of *S. pneumoniae*

Representative line graph showing counts of phagocytosed live *S. pneumoniae*. Primary murine BMDMs (1×10^6) were transfected with control siRNA and *Lc3b* siRNA for 48 hours and then infected with *S. pneumoniae* at an MOI of 10. After 1, 2 and 4 hours of *S. pneumoniae* infection, the samples were treated with gentamycin for 90 minutes to kill extracellular bacteria and viable bacteria were then enumerated. CFU counts in the lysates were plotted as means of triplicates; error bars are SEM. * indicates a significant difference between phagocytosis of cells transfected with control and *Lc3b* siRNA when analysed by 2 way ANOVA, ($p < 0.05$).

The data show that as with chemical inhibition of autophagy with 3-MA, abrogation of autophagy by genetic means with siRNA to *Lc3b* also significantly reduced the phagocytosis of live *S. pneumoniae*. This supports the conclusion that autophagy has a role in the phagocytosis of this organism by macrophages.

3.2.7 Relationship of autophagy with inflammasome activation

As discussed in the Introduction, autophagy and inflammasome activation are both important in the innate immune system. A number of studies have shown that autophagy can down-regulate activation of the NLRP3 inflammasome, as outlined in the Introduction (Saitoh et al., 2008, Nakahira et al., 2011). Additionally, the inflammasome has been shown to inhibit autophagy following infection with *Pseudomonas aeruginosa* (Jabir et al., 2014). We wished to explore the relationship, if any, between autophagy and inflammasome activation following infection of primary murine BMDMs with *S. pneumoniae*.

3.2.7.1 Inflammasome activation by *S. pneumoniae* D39 WT and D39 Δ Ply

First, we determined if infection with *S. pneumoniae* could induce the production of IL-1 β by primary murine BMDMs and the influence of pneumolysin on this production. Primary murine BMDMs were infected with *S. pneumoniae* strains D39 WT and D39 Δ Ply. The cell supernatants were analysed for IL-1 β and TNF- α production (Fig. 3.15). IL-1 β levels were higher after infection with *S. pneumoniae* strain D39 WT as compared to the D39 Δ Ply, a strain lacking pneumolysin (Fig. 3.15a). TNF- α levels were not significantly different in both groups as shown in (Fig. 3.15b).

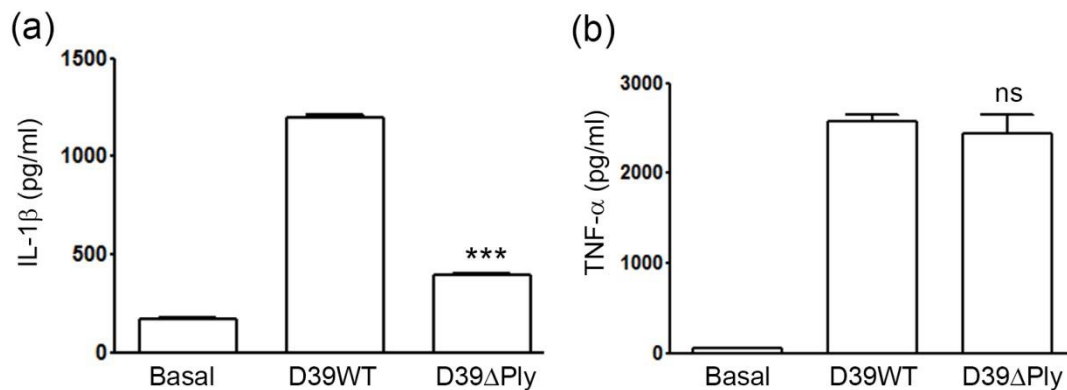


Figure 3.15 Inflammation activation by *S. pneumoniae* strains D39 WT and D39 ΔPly

(a) Bar graph showing inflammatory cytokine interleukin-1 beta (IL-1β) levels released from primary murine BMDMs. Cells were left un-stimulated (Basal), or infected with D39 WT and D39 ΔPly for 4 hours. *** indicates a highly significant decrease in the level of IL-1β secretion by *S. pneumoniae* strain D39 ΔPly as compared to D39 WT, $p < 0.001$. Bars are means of triplicates of IL-1β determinations; error bars are SEM.

(b) As (a) but inflammatory cytokine TNF-α released by primary murine BMDMs. Bars are means of triplicates of TNF-α (pg/ml) determinations; error bars are SEM. ns, non-significant difference between the strains of *S. pneumoniae*

These data confirm the results of McNeela et al who showed that pneumolysin activates the NLRP3 inflammasome independent of TLR4 following *S. pneumoniae* infection (McNeela et al., 2010).

3.2.8 Effects of inflammasome activation on autophagy induction in primary murine BMDMs

S. pneumoniae strains D39 WT and D39 Δ Ply both induce autophagy but this is more pronounced in the pneumolysin deficient strain. We hypothesized that this might be the effect of pneumolysin itself or the associated inflammasome activation. Pneumolysin is responsible for inflammasome activation and production of inflammatory cytokines in *S. pneumoniae* infection (Shoma et al., 2008).

We studied the effect of inflammasome on autophagy induction by blocking of caspase-1 using a specific inhibitor or knock down of *caspase-1* gene. Caspase-1 inhibitor Z-YVAD-FMK (fluoromethyl-ketone) is a selective and irreversible caspase-1 inhibitor (Slee et al., 1996). It blocks caspase-1 activation by inflammasome following microbial infection. Similarly we also tested the role of caspase-1 specifically by knocking down *casapase-1* gene using siRNA and observed its effects on autophagy induction with *S. pneumoniae* infection.

3.2.8.1 Effects of casapase-1 inhibitor Z-YVAD-FMK on autophagy induction in murine BMDMs infected with *S. pneumoniae*

Further to establish that the IL-1 β release produced from murine BMDMs after infection was due to inflammasome activation, we tested the dependence of this cytokine production on the activity of caspase-1. First, primary murine BMDMs were pre-treated with the caspase-1 inhibitor Z-YVAD-FMK. The cells were then infected with *S. pneumoniae* D39 WT at an MOI of 10. Western blot was performed for procaspase-1 and activated caspase-1 (p10) from cell lysates of inhibitor treated and untreated cells. The blot was stripped and re-probed for LC3 autophagy protein and β - tubulin proteins as shown (Fig. 3.16).

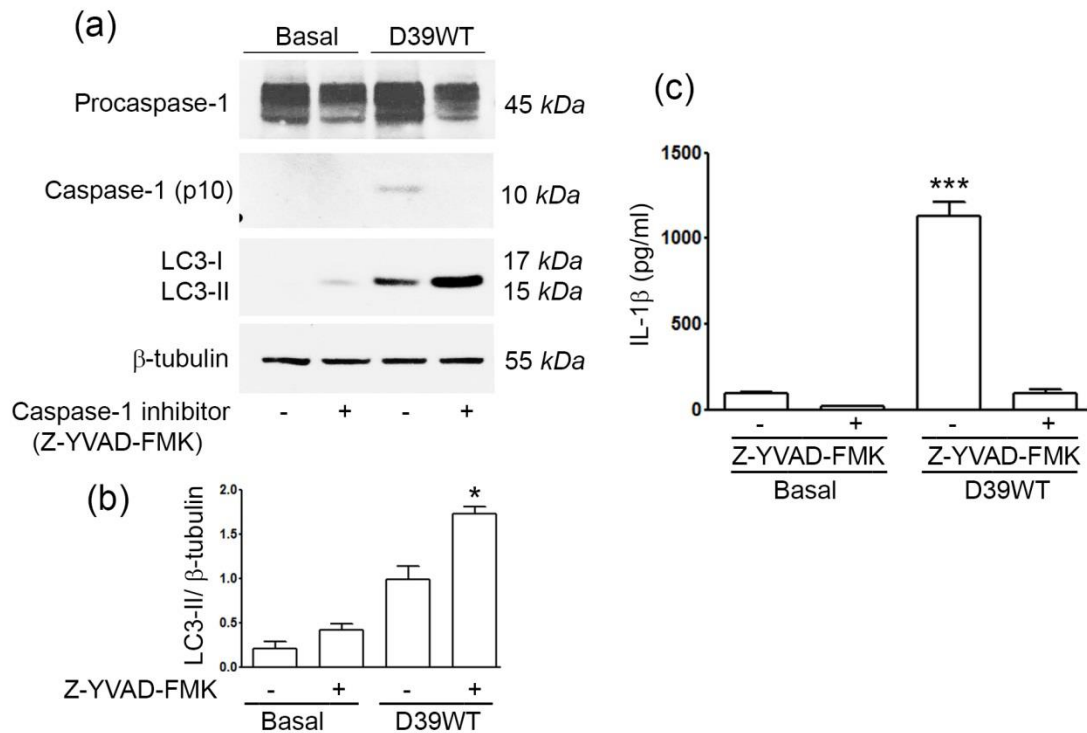


Figure 3.16 Autophagy is up-regulated in the presence of the caspase-1 inhibitor Z-YVAD-FMK in murine BMDM infected with *S. pneumoniae*

(a) Primary murine BMDMs were infected with *S. pneumoniae* at an MOI of 10 for 4 hours in the presence (+) or absence (-) of the caspase-1 inhibitor Z-YVAD-FMK (10 μ M). The panels show western blot of pro-caspase-1, the activated caspase-1 p10 subunit, autophagy protein LC3 II and β -tubulin as a loading control.

(b) Densitometry analysis of LC3 II/ β -tubulin (two independent experiments). Columns are mean values; error bars are SEM. Asterisks indicates significant difference in autophagy induction in cells pre-treated with Z-YVAD-FMK (+) and untreated (-), $p < 0.05$.

(c) ELISA for IL-1 β on cell supernatants from primary murine BMDMs infected with *S. pneumoniae* as indicated in the presence (+) or absence (-) of the caspase-1 inhibitor Z-YVAD-FMK (10 μ M). Columns are means of three independent determinations; error bars are SEM. Asterisks indicates significant difference between the IL-1 β levels in the presence (+) and absence (-) of the inhibitor, $p < 0.001$.

This experiment demonstrates that inhibition of caspase-1 activity results in an inhibition of the production of IL-1 β . It also demonstrates that infection with *S. pneumoniae* produces activation of caspase-1, as shown by the appearance of the p10 fragment of the activated caspase-1 following infection (Fig. 3.16a). This too is inhibited by the caspase-1 inhibitor.

Thus, these data confirm that release of IL-1 β is accompanied by activation of the inflammasome. The experiment also shows that when the inflammasome is inhibited, the amount of autophagy also increases. Thus, this suggests that activation of the inflammasome results in inhibition of the autophagocytic pathway.

3.2.8.2 Autophagy induction in caspase-1 knock-down murine BMDM infected with *S. pneumoniae*.

To confirm these findings, we analysed the effect of knock down of caspase-1 with *Caspase-1* siRNA on infection of primary murine BMDMs with *S. pneumoniae*. Western blot was performed for procaspase-1 and activated caspase-1 proteins from lysates of control and knock down cells. The blot was stripped and re-probed for LC3 and β - tubulin proteins.

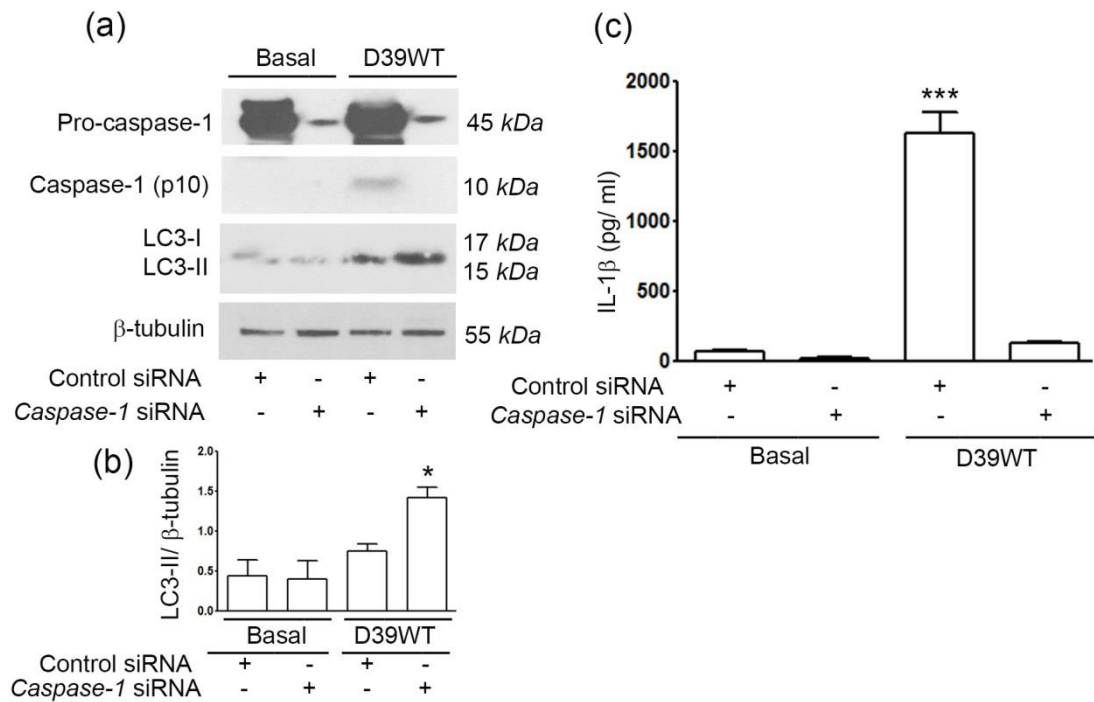


Figure 3.17 *Caspase-1* gene Knock down in primary murine BMDMs up-regulates autophagy in *S. pneumoniae* infection

(a) Primary murine BMDMs were transfected with control siRNA and *caspase-1* siRNA and then infected with *S. pneumoniae* D39 WT at an MOI of 10 for 4 hours. The panels show western blot of procaspase-1 and caspase-1 p10 subunit. The blot was stripped and re-probed for LC3 II autophagy protein and β -tubulin as a loading control.

(b) Densitometry analysis of LC3 II/ β -tubulin (two independent experiments). Columns are mean values; error bars are SEM. Asterisks indicates significant difference in autophagy induction in both groups, ($p < 0.05$).

(c) ELISA for IL-1 β on cell supernatants from primary murine BMDMs. Cells were transfected with control siRNA and *caspase-1* siRNA and then infected with *S. pneumoniae*. Columns are means of triplicate of IL-1 β determinations; error bars are SEM. Asterisks indicate significant differences between the IL-1 β levels in the control and *caspase-1* knock down cells, $p < 0.001$.

The results of this experiment were similar to those seen using the chemical inhibitor of caspase-1. The *caspase-1* siRNA produced an excellent reduction in the amount of pro-caspase-1. This inhibited IL-1 β release to virtually background levels. We also observed an increase in the degree of autophagy following infection when the inflammasome activation was blocked. Again, this suggests that activation of the inflammasome following infection with *S. pneumoniae* results in an inhibition of autophagy.

3.2.9 Influence of autophagy inhibition on inflammasome activation in *S. pneumoniae*

To study the effect of autophagy with inflammasome activation in *S. pneumoniae* infection, we inhibited autophagy in primary murine BMDMs by treating with 3MA or by knock down of the *Lc3b* and *Atg5* genes or using *Atg7* gene knock-out mice. Cells were then infected and analysed for IL-1 β production.

3.2.9.1 Influence of autophagy inhibitor 3-MA on inflammasome activation

Autophagy was inhibited in primary murine BMDMs by treating them with 3-MA. The cells were then infected with *S. pneumoniae* D39 WT for the indicated time. Supernatants from cells infected with *S. pneumoniae* in the presence or absence of 3-MA were analysed for the inflammatory cytokine IL-1 β (Fig. 3.18).

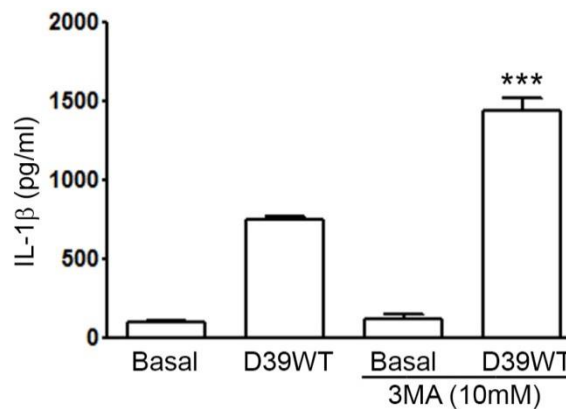


Figure 3.18 Activation of the Inflammasome by *S. pneumoniae* infection in primary murine BMDM pre-treated with 3MA

Representative bar graph showing IL-1B levels produced by primary murine BMDM pre-treated with 3-MA and then infected with *S. pneumoniae*. Cells were left un-infected (Basal), or infected with *S. pneumoniae* strain D39 WT at an MOI of 10 for 4 hours in the presence or absence of 3-MA. *** indicate a significant difference between 3-MA treated and untreated cells, $p < 0.001$. Bars are means of IL-1B triplicate determinations; error bars are SEM.

These data suggest that inhibition of autophagy increases the activation of the inflammasome following infection with *S. pneumoniae*.

3.2.9.2 Influence of genetic knock down of autophagy on inflammasome activation in *S. pneumoniae* infection

Further to investigate the effect of inhibiting autophagy on inflammasome activation, we examined the effect of knock down of the *Lc3b* and *Atg5* genes using siRNA. We observed IL-1 β production in these *LC3b* and *Atg5* gene knock down cells following infection with *S. pneumoniae*. Supernatants from cells transfected with control siRNA and *Lc3b* or *Atg5* siRNA were collected after infection with *S. pneumoniae*, and then analysed for inflammatory cytokine IL-1 β production (Fig. 3.19).

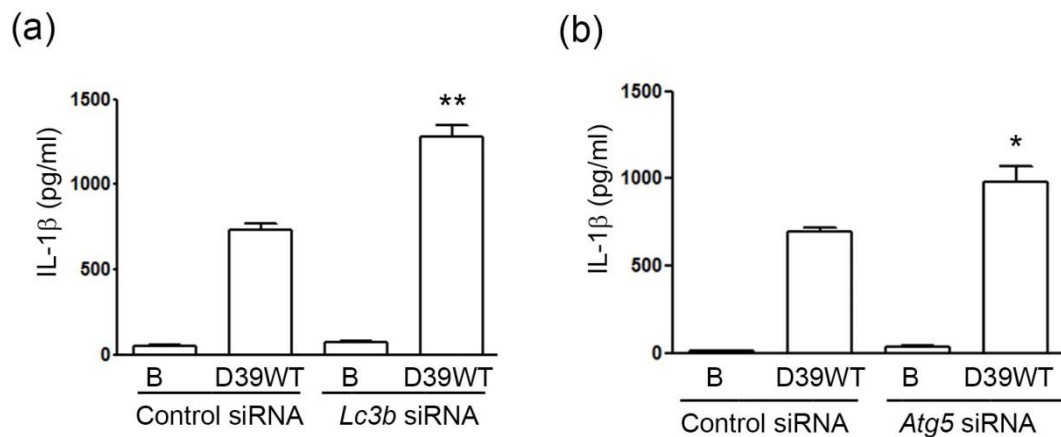


Figure 3.19 Inflammasome activation is up-regulated by knock down of autophagy genes *LC3b* and *Atg5* in murine BMDMs

(a) Representative bar graph showing IL-1 β levels released by primary murine BMDM knocked down for *Lc3b* gene and then infected with *S. pneumoniae*. Transfected cells were left un-infected (B), or infected with *S. pneumoniae* strain D39 WT at an MOI of 10 for 4 hours. ** indicate a significant difference between two groups, $p < 0.01$. Bars are means of triplicate of IL-1 β determinations; error bars are SEM.

(b) As (a) but primary murine BMDMs with *Atg5* gene knock down. * indicates a significant difference between the two groups, $p < 0.05$. Bars are means of triplicate IL-1 β determinations; error bars are SEM.

The experiment shows that with knock down of either LC3b or ATG5, there is a significant increase in inflammasome activation and release of IL-1 β following *S. pneumoniae* infection. This is in agreement with the data obtained from treating cells with 3-MA and supports the conclusion that autophagy acts to limit inflammasome activation following infection with *S. pneumoniae*.

3.2.9.3 Inflammasome activation in primary murine BMDMs from *Vav-Atg7*^{-/-} mice infected with *S. pneumoniae*

Next, we explored the effect of a lack of ATG7 on inflammasome activation following infection of primary murine BMDMs with *S. pneumoniae*. BMDMs were grown from WT and *Vav-Atg7*^{-/-} mice and then infected with *S. pneumoniae* at an MOI of 10. Supernatants from infected cells were analysed for IL-1 β (Fig. 3.20).

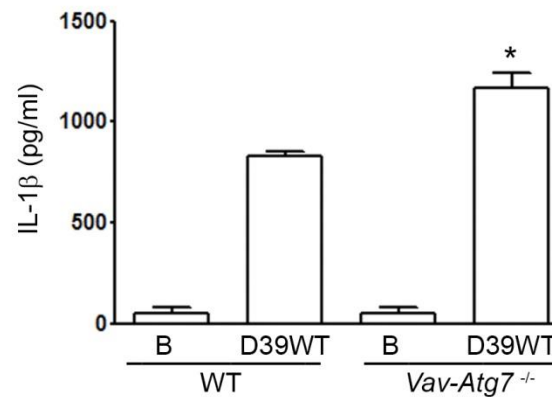


Figure 3.20 Inflammasome activation is up-regulated in *Vav-Atg7*^{-/-} primary murine BMDMs infected with *S. pneumoniae*.

Representative bar graph showing IL-1 β levels released by primary murine BMDM from wild type and *Vav-Atg7*^{-/-} mice. Cells were left un-stimulated (B), or infected with *S. pneumoniae* strain D39 WT at an MOI of 10 for 4 hours. * indicates a significant difference between both groups. Bars are means of IL-1 β triplicate determinations; error bars are SEM, $p < 0.05$.

Levels of released IL-1 β were significantly higher in the BMDMs from the *Vav-Atg7*^{-/-} mice. Thus, data from this experiment confirm our previous observations. It supports the conclusion that autophagy acts to inhibit inflammasome activation following *S. pneumoniae* infection.

3.2.10 The role of TIR-domain-containing adapter-inducing interferon- β (TRIF) in autophagy induction

We wished to determine the intracellular signalling pathways involved in autophagy induction following infection with *S. pneumoniae*. The data presented above shows that inflammasome activation inhibits autophagy induction following *S. pneumoniae* infection. In *P. aeruginosa* infection, our laboratory has previously shown that caspase-1 limits autophagy by cleavage of the signalling adaptor TRIF (Jabir et al., 2014).

We hypothesized that the TRIF pathway may be involved in *S. pneumoniae* autophagy induction as well, which would also explain the reduction in autophagy following inflammasome induction by *S. pneumoniae*. Thus, we tested induction of autophagy by *S. pneumoniae* infection in primary murine BMDMs following knock down of TRIF with siRNA. Western blot was performed for TRIF and LC3 proteins as shown (Fig. 3.21).

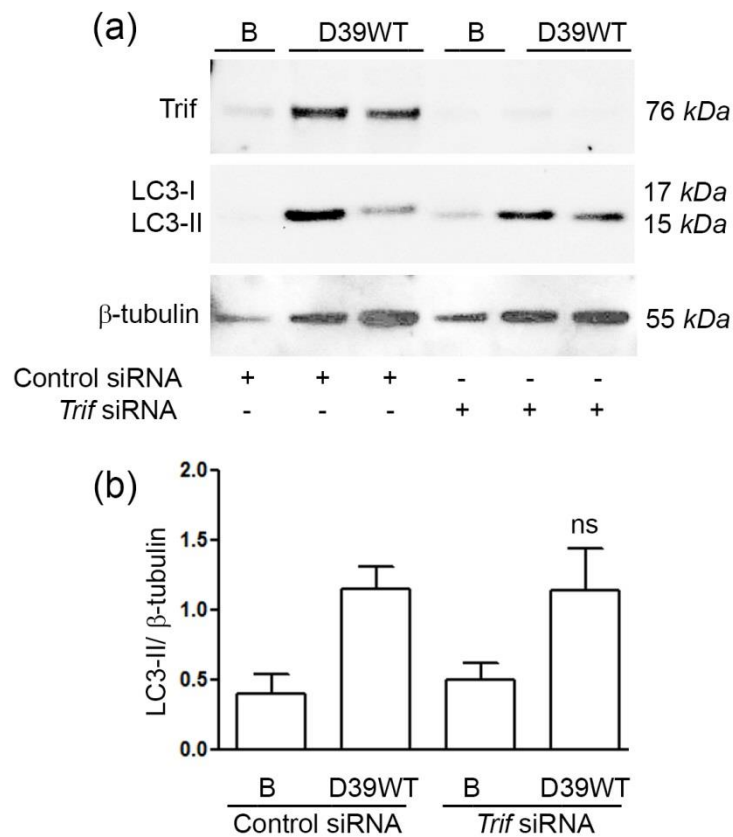


Figure 3.21 Autophagy induction following infection with *S. pneumoniae* is not dependent on TRIF pathway.

(a) Representative western blot image from primary murine BMDM transfected with control siRNA and *Trif* siRNA and then infected with *S. pneumoniae* D39 WT at an MOI of 10 for 4 hours. Western blot was performed for TRIF protein and then stripped and re-probed for LC3 II autophagy protein and β - tubulin as a loading control.

(b) Densitometry analysis of LC3 II/ β - tubulin (two independent experiments). Columns are mean values; error bars are SEM. The results shown here are non-significant (ns) and there is no difference in autophagy induction in the cells transfected with control siRNA and *Trif* siRNA.

The siRNA for *Trif* achieved a good degree of knock down of the TRIF protein following infection (Fig. 3.21a). Baseline levels of TRIF in uninfected cells in the presence of control siRNA were rather low, but this probably reflects a lower amount of total protein in this lane as judged by the β - tubulin loading control. Knock down of TRIF by this means did not produce any reduction of autophagy following infection with *S. pneumoniae*. This suggests that TRIF is not an intermediate in initiation of autophagy following infection with this pathogen.

3.2.10.1 Autophagy induction in primary murine BMDMs from *Trif*^{-/-} mice infected with *S. pneumoniae*

We further investigated the role of TRIF pathway by using *Trif*^{-/-} mice. Autophagy induction was studied in primary murine BMDMs derived from *Trif*^{-/-} mice infected with *S. pneumoniae*. Cells were grown from wild type and *Trif*^{-/-} mice and then infected with *S. pneumoniae* strains D39 WT and D39 Δ Ply. Western blot was performed for LC3 autophagy protein as shown (Fig. 3.22).

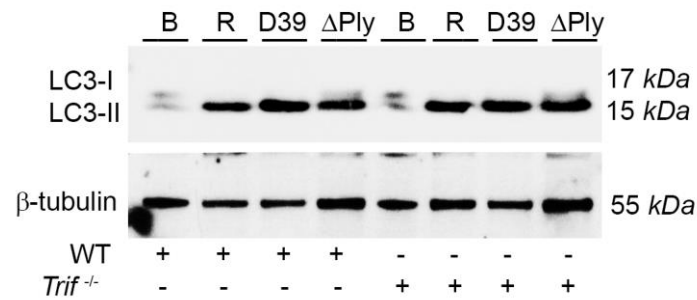


Figure 3.22 TRIF is not required as adaptor protein for autophagy induction in murine BMDMs infected with *S. pneumoniae*.

Representative western blot image using lysates of primary murine BMDM of wild type and $Trif^{-/-}$ mice treated as indicated. Cells were left uninfected (B), treated with Rapamycin (R; 25 μ g/ml) as positive control of autophagy and infected with *S. pneumoniae* D39 WT or D39 Δ Ply at an MOI of 10 for 4 hours. Western blot was performed for LC3 autophagy protein and then stripped and re-probed for β -tubulin as a loading control.

This experiment showed that autophagy proceeded to the same degree even in cells lacking TRIF. This confirms our observations with knock down of TRIF by siRNA, that this intermediate is not required for induction of autophagy following *S. pneumoniae* infection.

3.2.11 Autophagy induction in murine BMDMs from *Myd88* knock-out mice infected with *S. pneumoniae*

TRIF is a signalling intermediate from TLR3 and TLR4. We demonstrated that TRIF is not involved in *S. pneumoniae* induced autophagy (Fig. 3.21, 3.22). Next, we investigated the involvement of another important pathway, Myd88, in autophagy induction with *S. pneumoniae* infection. Myd88 is involved in signalling from all other Toll-like receptors. A variety of TLR agonists that use Myd88 have been found to induce autophagy in macrophages (Shi and Kehrl, 2008).

We used primary murine BMDMs from WT and *Myd88*^{-/-} mice and infected with *S. pneumoniae* strains D39 WT and D39 Δ Ply. Western blot was performed for LC3 protein as shown (Fig. 3.23).

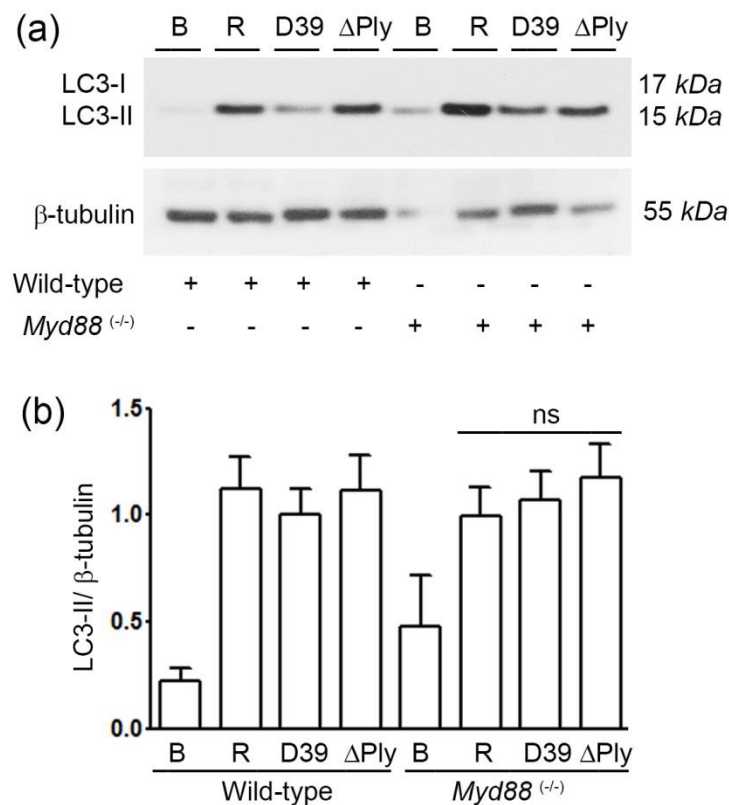


Figure 3.23 MYD88 is not required for autophagy induction in murine BMDMs with *S. pneumoniae* infection.

(a) Representative western blot image from the lysates of primary murine BMDM of WT mice and *Myd88*^(-/-) mice. Cells were left uninfected (B), treated with Rapamycin (R; 25 μ g/ ml) as positive autophagy control or infected with *S. pneumoniae* D39 WT and D39 Δ Ply at an MOI of 10 for 4 hours. Western blot was performed for LC3 protein and the blot was stripped and re-probed for β -tubulin as loading control.

(b) Densitometry analysis of LC3 II/ β -tubulin (two independent experiments). Columns are mean values; error bars are SEM. The results are not significant (ns) with no difference in autophagy induction in both groups.

These results show clearly that autophagy following infection with *S. pneumoniae* is not affected by the lack of MYD88. Thus, given the lack of involvement of TRIF as well in the induction of autophagy by *S. pneumoniae*, suggest that TLRs are not involved in any way with induction of autophagy by this microbe.

3.2.12 Role of TLR4 in autophagy induction in primary murine BMDMs in infection with *S. pneumoniae*

To confirm and extend these findings, we investigated the specific role of TLR4 in autophagy induction by *S. pneumoniae*. TLR4 serves as a sensor for autophagy induction which is mediated through TRIF when stimulated with LPS (Xu et al., 2007) or MyD88. We used TLR4 defective and TLR4^{-/-} mice strains for autophagy induction and found that TLR4 is not used as a sensor for autophagy following *S. pneumoniae* infection.

3.2.12.1 Autophagy induction in primary murine BMDMs from C3H/HeJ (Lps-d) mice in *S. pneumoniae* infection

First, we used primary murine BMDMs from TLR4-defective LPS hypo-responsive mice strains. Cells from LPS responsive C3H/HeNHsd (control) and LPS hypo-responsive C3H/HeJ0laHsd-Tlr4^{-Lps-d} mice strains were infected with *S. pneumoniae* strains D39 WT and D39 Δ Ply. Western blot was performed for LC3 autophagy protein from cell lysates of both strains of mice after *S. pneumoniae* infection as shown (Fig. 3.24).

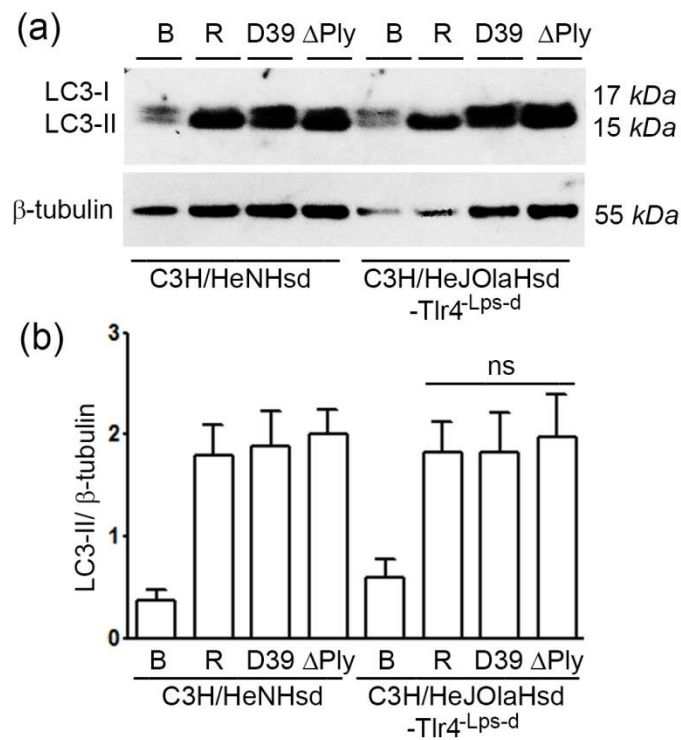


Figure 3.24 Autophagy induction is not affected in TLR4- defective LPS hypo-responsive murine BMDMs in infection with *S. pneumoniae*

(a) Representative western blot image from the lysates of primary murine BMDM of C3H/HeNHsd (control) and C3H/HeJOlaHsd-Tlr4 Lps-d strains of mice. Cell were left uninfected (B), treated with rapamycin (R; 25 μ g/ ml) as positive autophagy control or infected with *S. pneumoniae* D39 WT and D39 Δ Ply at an MOI 10 for 4 hours. Western blot was performed for LC3 autophagy protein and then stripped and re-probed for β -tubulin as loading control.

(b) Densitometry analysis of LC3 II/ β - tubulin (two independent experiments). Columns are mean values; error bars are SEM. The results shown here are non-significant (ns) with no difference in autophagy induction in both groups.

The results show that there was no difference in the induction of autophagy following *S. pneumoniae* infection in the cells from control and TLR4 defective mouse strains. Thus, this confirms that TLR4 signalling is not involved in autophagy induction following this infection.

3.2.12.2 Autophagy induction in primary murine BMDMs from *Tlr4*^{-/-} infected with *S. pneumoniae*

To further investigate the role of TLR4 in autophagy induction by *S. pneumoniae* infection, we infected primary murine BMDMs from *Tlr4*^{-/-} mice. Western blot was performed for LC3 autophagy protein as shown (Fig. 3.25).

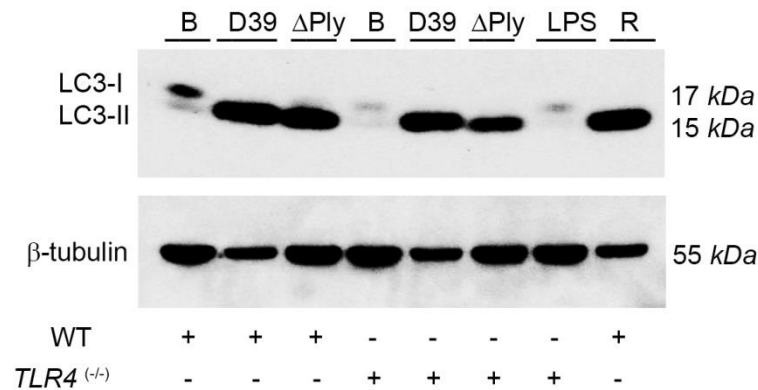


Figure 3.25 Role of TLR4 in autophagy induction in primary murine BMDMs infected with *S. pneumoniae*

Representative western blot image from the lysates of primary murine BMDM from WT mice and *Tlr4*^{-/-} mice infected with *S. pneumoniae*. WT cells were left uninfected (B), treated with rapamycin (R; 25μg/ ml) as positive autophagy control and infected with *S. pneumoniae* D39 WT and D39 ΔPly at an MOI 10 for 4 hours. *TLR4*^{-/-} cells were left uninfected (B) treated with LPS (100ng/ ml) or infected as WT cells. Western blot was performed for LC3 protein. The blot was then stripped and re-probed for β-tubulin as a loading control. There is no difference in the autophagy induction between both groups of mice as shown.

These experiments again showed that a lack of TLR4 did not affect the degree of autophagy following *S. pneumoniae* infection.

3.2.13 Role of TLR2 in autophagy induction in murine BMDMs infected with *S. pneumoniae*

We next investigated whether TLR2 had a specific role in autophagy induction following *S. pneumoniae* infection. TLR2 mediates autophagy induction following infection with *Listeria monocytogenes*, an intracellular gram positive pathogen (Anand et al., 2011). TLR2 receptors are present on innate immune cells and respond to lipid containing PAMPs i.e. lipoteichoic acid released from pathogens.

We tested the effect of TLR2 by treating primary murine BMDMs with a neutralising anti-TLR2 antibody, Pam3CSK4 and Isotype control antibody. Pam3CSK4 is a tri-acylated lipopeptide ligand of TLR2 (Jin et al., 2007) which was used as control. Autophagy was induced in pre-treated primary murine BMDMs with *S. pneumoniae* D39 WT and D39 Δ Ply infection. Western blot was performed for LC3 autophagy protein as shown (Fig. 3.26).

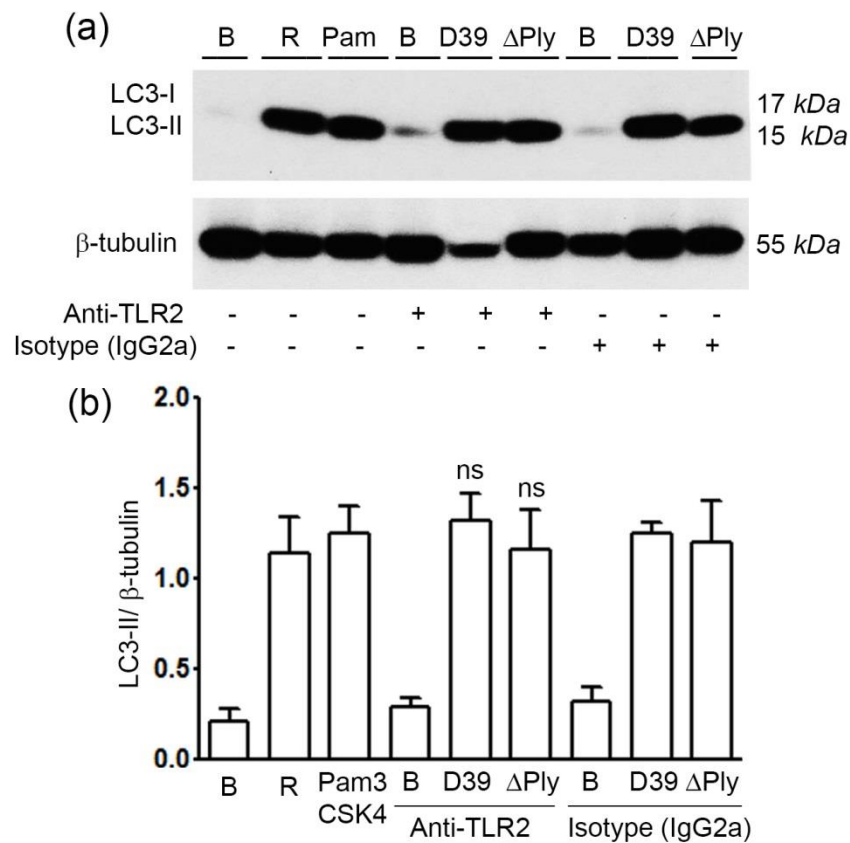


Figure 3.26 TLR2 is not required for autophagy induction in murine BMDMs infected with *S. pneumoniae*

(a) Representative western blot image from primary murine BMDM pre-treated as indicated and then infected with *S. pneumoniae*. Cells were left un-treated (B), treated with Rapamycin (R; 25 μ g/ ml) as positive control of autophagy or with Pam3CSK4 (100ng/ml). Next, cells pre-treated with anti-*TLR2* antibody (1 μ g/ ml), or mouse IgG2a isotype control antibody (1 μ g/ ml) for 60 minutes were then left uninfected (B) or infected with *S. pneumoniae* strains D39 WT and D39 Δ Ply at an MOI of 10 for 4 hours. Western blot was performed for LC3 autophagy protein. The blot was then stripped and re-probed for β - tubulin as loading control.

(b) Densitometry analysis of LC3 II/ β - tubulin (two independent experiments). Columns are mean values; error bars are SEM. The results are non-significant (ns) and there is no difference in autophagy induction in TLR2 blocked cells and ligand activated cells.

This experiment showed that treatment of cells with a neutralizing antibody to TLR2 had no effect on the induction of autophagy induced by *S. pneumoniae*. This excluded a direct role of TLR2 in signalling induction of autophagy following this infection.

3.2.14 Role of NOD2 in autophagy induction in primary murine BMDMs

Given the lack of involvement of the TLRs in autophagy induction following pneumococcal infection we sought involvement of other innate signalling pathways. To explore involvement of the intracellular peptidoglycan sensor NOD2, we used the ligands muramyl dipeptide (MDP) and its control (MDPc). Muramyl dipeptide is a peptidoglycan constituent from bacteria. It is recognized by NOD2 in innate immune cells (Girardin et al., 2003). We treated primary murine BMDMs with MDP and its control MCPc for 6 - 24 hours to observe their effects in induction of autophagy. Western blot was performed for LC3 protein as shown (Fig. 3.27).

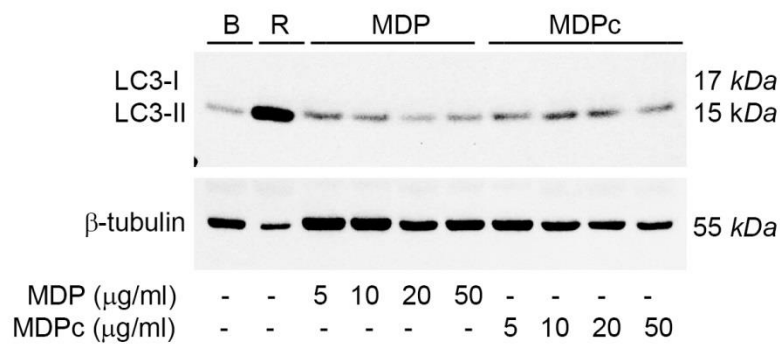


Figure 3.27 NOD2 has no role with the induction of autophagy in primary murine BMDMs

Representative western blot image from the lysates of primary murine BMDM treated with NOD2 ligand. Cells were left untreated (B), treated with rapamycin (R; 25 μ g/ml) as positive autophagy control or treated with MDP or MDPc (5, 10, 20 and 50 μ g/ml) for 24 hours. Western blot was performed for LC3 autophagy protein. The blot was then stripped and re-probed for β -tubulin as a loading control.

These data show that addition of the NOD2 ligand, muramyl dipeptide does not induce autophagy in primary murine BMDMs. Thus, NOD2 is unlikely to be involved in autophagy induction by *S. pneumoniae*.

3.2.15 Influence of a P38MAP Kinase Inhibitor on Autophagy induction in primary murine BMDMs infected with *S. pneumoniae*

We next investigated the effect of an inhibitor of mitogen activated protein kinase p38 (p38-MAPK) on autophagy induction following *S. pneumoniae* infection. This pathway activates transcription factor NF- κ B, and has been shown to be involved in autophagy induction (Matsuzawa et al., 2014). We blocked this pathway by treating primary murine BMDMs with SB203580, a specific inhibitor of p38MAP kinase. We then tested whether this affected the induction of autophagy in primary murine BMDMs infected with *S. pneumoniae* strains D39 WT and D39 Δ Ply.

Cells were pre-treated with SB203580 and then infected with *S. pneumoniae* strains or treated with LPS to compare its effects. Western blot was performed for LC3 protein as shown (Fig. 3.28)

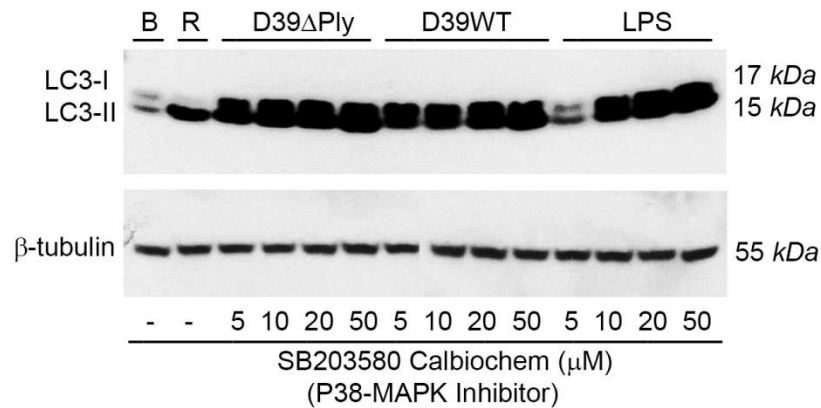


Figure 3.28 P38-mitogen activated protein kinase inhibitor has no effect on autophagy induction in murine BMDMs infected with *S. pneumoniae*

Representative western blot image from the lysates of primary murine BMDM treated with SB203580 and then infected with *S. pneumoniae*. Cells were left uninfected (B) and treated with rapamycin (R; 25 μ g/ml) as positive autophagy control. Next, cells were pre-treated with 5, 10, 20, & 50 μ M of SB203580 for 60 minutes and then infected with *S. pneumoniae* D39 WT and D39 Δ Ply at an MOI 10 for 4 hours or treated with LPS as a control. Western blot was performed for LC3 proteins and then stripped and re-probed for β -tubulin as a loading control.

SB203580 had no effect on the induction of autophagy by *S. pneumoniae* D39 WT and D39 Δ Ply. Thus, p38MAP Kinase is unlikely to be involved in triggering autophagy induced by this infection.

3.3 Discussion and Conclusion

3.3.1 Discussion

We show here that *S. pneumoniae* induces autophagy in primary murine macrophages following infection. It has not previously been demonstrated in infection with this pathogen. We clearly demonstrated the induction of autophagy in infection with *S. pneumoniae* strains D39 WT and D39 Δ Ply in murine BMDMs in a time and dose dependent manner (Fig. 3.1- 3.5). Although the signal tended to be stronger in the pneumolysin deficient strain, this difference was not significant and the absolute difference between the strains was not huge.

We further studied autophagy in *S. pneumoniae* infection by blocking this pathway by different chemical and genetic methods. It was demonstrated here that 3-MA an autophagy inhibitor (Seglen and Gordon, 1982, Wu et al., 2010) blocked this pathway in murine BMDMs infected with *S. pneumoniae* (Fig. 3.7). We also demonstrated that genetic knock down of the autophagy genes *Lc3b* and *Atg5* (Tanida et al., 2008, Walczak and Martens, 2013) inhibited autophagy induction by *S. pneumoniae* infection (Fig. 3.8, 3.9).

Similarly the effect of *Atg7* was studied (Komatsu et al., 2007) and its role was demonstrated in autophagy induction by using *Vav-Atg7*^{-/-} mice. *S. pneumoniae* infection was unable to induce autophagy in *Atg7* knock-out murine BMDMs as compared to WT (Fig. 3.10). All these observations confirmed our hypothesis that infection with *S. pneumoniae* induces autophagy and that this follows a classical pathway.

We have also shown here that autophagy in murine BMDMs is associated with phagocytosis of *S. pneumoniae*. Phagocytosis and internalization is also affected by the virulence factor pneumolysin which may be due to the down-regulation of complement deposition (Yuste et al., 2005). Phagocytosis of the pneumolysin deficient strain was higher as compared to the WT (Fig. 3.11).

We also demonstrated that inhibiting autophagy with pharmacological agent 3-MA or genetic knock down of *Lc3b* gene attenuated phagocytosis of *S. pneumoniae* by murine BMDMs (Fig. 3.13, 3.14). This shows that autophagy and autophagy genes are required for the phagocytosis.

Similarly we have successfully demonstrated a relationship between autophagy and the inflammasome. We demonstrated here that inhibiting autophagy by a chemical method using 3-MA or genetically using siRNA or gene knock-out mice resulted in an increase in inflammasome activation following infection with *S. pneumoniae* (Fig. 3.18- 3.20). This demonstrated that inflammasome and autophagy are associated mechanisms in the innate immune system.

Similarly when we inhibited inflammasome by blocking caspase-1 with its specific inhibitor Z-YVAD-FMK (Slee et al., 1996) or by *caspase-1* siRNA transfection, autophagy was up-regulated (Fig. 3.16, 3.17). These observations demonstrated that autophagy and inflammasome influence on each other. The mechanism by which inflammasome activation acts to limit autophagy is not clearly understood.

Next, we also studied different pathways and receptors to find how the autophagy signal is transferred to the interior of the cell from an extracellular pathogen. We have shown here the roles of TRIF, Myd88 (Piras and Selvarajoo, 2014), TLR4 (Xu et al., 2007) and TLR2 (Fang et al., 2014) pathways (Fig. 3.21- 3.26). We found that none of these pathways are associated with autophagy induction in *S. pneumoniae* infection.

We also studied the role of NOD2 using muramyl dipeptide (Girardin et al., 2003), a bacterial peptidoglycan (Fig.3.7), and found that it does not induce autophagy in murine BMDMs. It may be that extracellular addition of this ligand alone is ineffective in producing intracellular effects and further studies using transfection reagents to enhance intracellular delivery will need to be performed.

Similarly p38MAP kinase was studied by blocking with inhibitor (SB203580) and observed its activity with *S. pneumoniae* infection and LPS activation (Fig.

3.28). It was demonstrated that this enzyme is not involved in *S. pneumoniae* induced autophagy in murine BMDM.

All data shown here in this chapter provide important information regarding autophagy induction in *S. pneumoniae* infection. Manipulation of this emerging immune signalling pathway could possibly treat this important pathogen. Further work may be required to study different PRRs and find the exact pathway involved in transfer of the autophagy signal from this extracellular pathogen to the interior of the cell.

3.3.2 Conclusion

In conclusion, the results shown here in this chapter demonstrate that infection with *S. pneumoniae*, an extracellular Gram positive pathogen induces autophagy in primary murine BMDMs which is a novel finding. Virulence factors of *S. pneumoniae* affect autophagy induction directly or through inflammasome activation. When we block autophagy, inflammasome activation is up-regulated while blocking inflammasome activation enhances autophagy following *S. pneumoniae* infection.

It is now clear that in normal conditions the inflammasome might have a controlling effect on autophagy induction and that autophagy maintains a fine balance in inflammasome activation. We also demonstrated that autophagy acts to increase phagocytosis. The mechanism of this effect is not clear.

4 ***In vivo* Studies of Autophagy following *S. pneumoniae* Infection**

4.1 Introduction

S. pneumoniae infection induces autophagy as was observed in our *in vitro* study presented in this thesis earlier. We wished to further extend our study to analyse this pathway in an *in vivo* mouse model.

Previous studies demonstrate that bacterial infection can induce autophagy *in vivo*. Pharmacological reinforcement of autophagy increases the clearance of pathogens while its inhibition leads to persistent infection (Junkins et al., 2013). Studies from our laboratory using *in vivo* infection models with *Pseudomonas aeruginosa* have also shown that autophagy can be observed *in vivo*. This was also shown that pharmacological manipulation of this process can influence the outcome of infection and the degree of inflammation produced (Jabir et al., 2014). Autophagy induction in *S. pneumoniae* infection has not been studied *in vivo*.

Here, we set out to determine if autophagy could be observed in an *in vivo* model of *S. pneumoniae*. We used an intraperitoneal (i.p) infection model in mice and observed the effects of *S. pneumoniae*. Pulmonary infection in a mouse model is difficult to study since the onset is over 24 - 48 hours with variation in timing between animals. This would necessitate prolonged administration of drugs to alter the level of autophagy with consequent problems in toxicity.

Intraperitoneal infection is a convenient model to determine the presence and role of autophagy after infection, although it is an infrequent site of infection with *S. pneumoniae*. The onset of infection after i.p. inoculation is rapid and synchronous between animals, allowing the effects of drugs to alter the degree of autophagy to be studied much more easily.

4.2 Results

4.2.1 Autophagy induction in *in vivo* mouse model of *S. pneumoniae* infection

We used a mouse model of *S. pneumoniae* infection to observe autophagy induction. We also demonstrated the effects of autophagy inducer and inhibitor drugs. C57BL/6 mice were randomly distributed into six groups (n= 3) mice each. The groups were designated as control groups (n= 3) and study groups (n= 3). The control groups were injected i.p. with sterile PBS, Rapamycin or 3MA (Harris et al., 2011, Kim et al., 2012) while the study groups were injected with D39 WT (1×10^7) alone, or together with Rapamycin or 3MA. Mice were left for 6 hours and observed for vital signs during this time. Blood and peritoneal lavage were then collected from mice aseptically and analysed for autophagy, phagocytosis and inflammasome activation.

First, the cell lysates were analysed for autophagy induction by immunoblotting of LC3 autophagy protein (Fig. 4.1). This showed that infection increased the proportion of LC3 II in the peritoneal lavage cells. The addition of 3-MA inhibited *S. pneumoniae* induced autophagy markedly. Rapamycin on its own also induced an increase in LC3 II as expected. When added in addition to infection, there was a very minor increase in the amount of LC3 II.

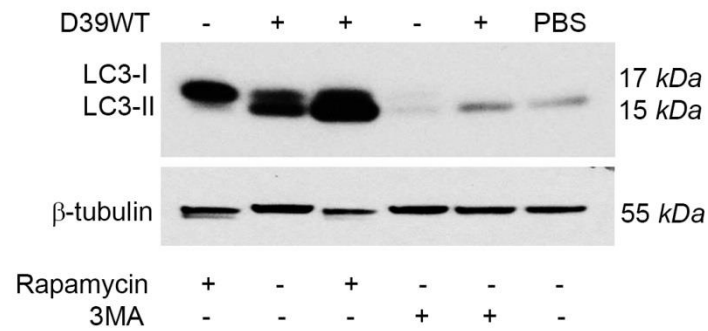


Figure 4.1 3MA inhibits *S. pneumoniae* induced Autophagy *in vivo*

Representative western blot from cells (macrophages) from peritoneal lavage of mice infected with *S. pneumoniae* alone, with Rapamycin or 3MA.

Mice were injected (i.p.) with PBS (5 ml), Rapamycin (1.5 mg/ kg), 3MA (30 mg/ kg) as control or infected with *S. pneumoniae* D39 WT (1×10^7) alone, with Rapamycin or with 3MA for 6 hours. Peritoneal lavage was then collected and cell lysates were analysed for LC3 proteins by western blot. The blot was stripped and re-probed for β -tubulin protein as loading control.

4.2.2 Role of autophagy in *S. pneumoniae* clearance during *in vivo* infection

We next investigated the role of autophagy in *S. pneumoniae* clearance by the peritoneal macrophages and other scavenger cells *in vivo*. Previous studies demonstrate that bacterial clearance during *Pseudomonas aeruginosa* infection is increased by pharmacological reinforcement of autophagy while inhibition of this pathway decreases the clearance (Junkins et al., 2013).

4.2.2.1 Autophagy up-regulated the clearance of *S. pneumoniae in vivo*

Mice were infected with *S. pneumoniae* alone and along with Rapamycin or 3MA. Peritoneal lavage was collected and plated on blood agar to grow the extracellular bacteria. *S. pneumoniae* CFU counts from control and test groups of mice were performed to observe the effect of autophagy as shown (Fig. 4.2).

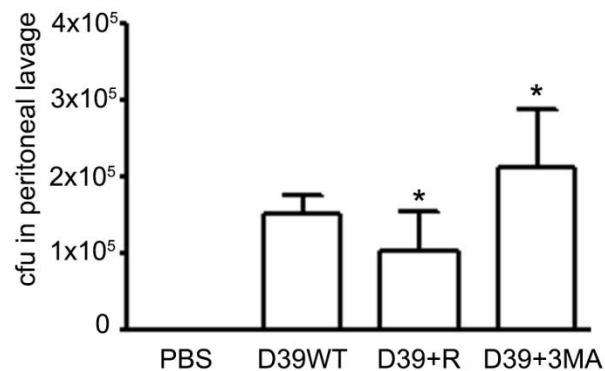


Figure 4.2 Inhibition of Autophagy increased CFU of *S. pneumoniae* in the peritoneal lavage

Representative bar graph of the CFU counts in peritoneal lavage from mice infected with *S. pneumoniae* D39 WT alone and with Rapamycin or 3MA.

Mice were injected with PBS, or infected with *S. pneumoniae* (D39 WT; 1×10^7), D39 with Rapamycin (D39 + R; 1.5 g/ kg) and D39 with 3MA (D39 + 3MA; 30 mg/ kg) for 6 hours. Peritoneal lavage was analysed and bacterial CFU counts performed. The bars show means of CFU counts in in three different mice and error bars are SEM. Asterisks indicate significant difference from infection alone ($p < 0.05$) in the groups.

The results show that inhibition of autophagy with 3-MA produced a small but significant increase in the numbers of bacteria recovered from the peritoneal cavity. Rapamycin produced a small but significant decrease in the numbers of recovered bacteria. These results suggest that autophagy enhances clearance of the organism *in vivo* in this infection model.

4.2.2.2 Effect of autophagy on phagocytosis of *S. pneumoniae*

Mice were infected with *S. pneumoniae* alone and along with Rapamycin or 3MA as above. Peritoneal lavage was collected in centrifuge tubes and spun down at 100g for 5 minutes. The cell pellet was washed three times and re-suspended in PBS. Cells were lysed with 0.1 % Triton- X100 and the lysates were analysed for viable bacterial counts through colony counting.

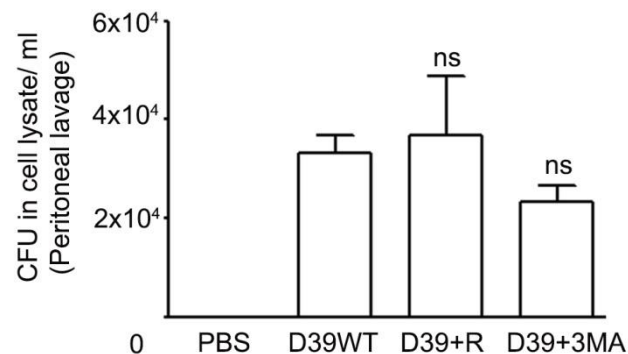


Figure 4.3 Autophagy up-regulates phagocytosis of *S. pneumoniae* in vivo

Representative bar graph of the CFU counts from lysates of peritoneal lavage cells from mice infected with *S. pneumoniae* D39 WT alone and with Rapamycin or 3MA.

Mice were injected with PBS, or infected with *S. pneumoniae* (D39 WT; 1×10^7), D39 with Rapamycin (D39+R; 1.5 mg / kg) and D39 with 3MA (D39+3MA; 30 mg / kg) for 6 hours. Cells were collected from peritoneal lavage and the lysates were analysed for bacterial CFU counts. The bars show means of CFU counts in in three different mice and error bars are SEM. The results are non-significant (ns).

The results show that re-enforcement of autophagy with Rapamycin produced a small non-significant increase in the numbers of bacteria recovered from the peritoneal lavage cell lysates. 3MA produced a small decrease in the numbers of recovered bacteria. These results suggest that autophagy enhances clearance of the *S. pneumoniae* in vivo in this infection model - this needs further confirmation.

4.2.3 Influence of autophagy in *S. pneumoniae* induced inflammasome activation *in vivo*

In *in vitro* experiments, we demonstrated previously that autophagy induction down-regulated inflammasome and vice versa. Next, we investigated the role of autophagy induction in *S. pneumoniae* induced inflammasome activation in this *in vivo* model. Mice were infected with *S. pneumoniae* alone or with Rapamycin or 3MA. Blood was collected from mice and serum samples were analysed for the inflammatory cytokines IL-1 β and TNF- α by ELISA as shown (Fig. 4.4).

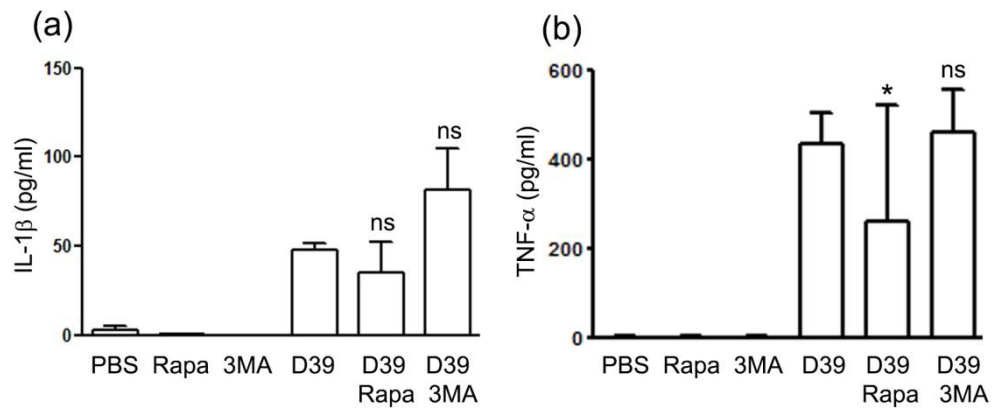


Figure 4.4 Autophagy induction down regulates cytokine production in *in vivo* infection with *S. pneumoniae*

(a) Representative bar graph of IL-1 β in serum of mice infected with *S. pneumoniae* with and without Rapamycin or 3MA. Mice were injected with PBS (5 ml), Rapamycin (Rapa; 1.5 g/ kg), 3MA (30 mg/ kg) or infected with *S. pneumoniae* alone (D39; 1×10^7) or D39 and Rapamycin (D39 Rapa) or D39 and 3MA (D39 3MA) for 6 hours. Bars are means of IL-1 β determinations from three mice and error bars are SEM. ns, not significant.

(b) As (a) but for TNF- α . * indicates a significant difference in Rapamycin (D39 Rapa) form D39 alone when analysed by unpaired t- test, ($p < 0.05$)

This experiment shows that although there was activation of the inflammasome by infection *in vivo*, the levels of IL-1 β produced were rather low. The addition of rapamycin or 3-MA did not produce any significant differences in the levels of IL-1 β . TNF- α production after infection was more robust, and did show a drop in the presence of rapamycin. Although suggesting that increasing autophagy might thus limit TNF production. These results require further confirmation.

4.2.4 Influence of autophagy on protein content of peritoneal fluid in *S. pneumoniae* infection

We also determined the protein content of peritoneal lavage from mice infected with *S. pneumoniae* alone and with Rapamycin or 3MA (Fig. 4.5). This is an indication of the degree of inflammation within the peritoneal cavity. The results show a marked increase in the protein content of peritoneal fluid following infection. This was increased significantly by the inhibitor of autophagy, 3-MA.

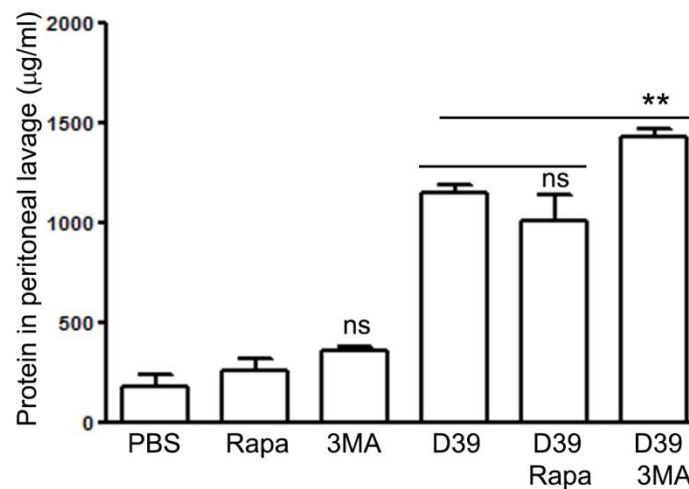


Figure 4.5 Autophagy inhibition increases protein content of peritoneal fluid in *S. pneumoniae* infection

Representative bar graph of protein content in the peritoneal lavage of mice infected with *S. pneumoniae* alone or with Rapamycin and 3MA. Mice were treated and infected as shown. Bars show mean of 3 individual determinations; error bars are SEM. ** indicates a significant difference from D39 infected mice alone ($p < 0.01$). ns, not significant.

4.3 Discussion

Although the experiments contained within this chapter are best viewed as an initial study, they do show that autophagy can be observed *in vivo*. These observations suggest that there may be important biological roles for this pathway in the host defence and inflammation.

The peritoneal infection model was a potent stimulus to induction of autophagy in cells accumulating within the peritoneal cavity. The resident population of cells in this location are macrophages. There will be an influx of neutrophils following infection with *S. pneumoniae*. So it is most likely that the results we obtained are from a composite of these cell types. In further studies, the cell types present would need to be quantified, ideally using cell surface markers and flow cytometry.

Pharmacological manipulation of the autophagocytic response was also successful. 3-MA was a potent inhibitor of autophagy. Rapamycin was an effective inducer of autophagy on its own (Fig. 4.1), although it did not enhance to any great degree the amount of autophagy following infection. In further studies, additional inhibitors and inducers of autophagy could be used to strengthen the conclusions of the studies.

Our *in vitro* experiments have shown that inhibiting autophagy reduced the uptake of viable *S. pneumoniae*, suggesting that autophagy was important in promoting phagocytosis. The results shown in (Fig. 4.2, 4.3) suggest that this is also true *in vivo*. In the presence of 3-MA there was an increase in the numbers of bacteria recovered from the peritoneal cavity and some decrease in the numbers of internalized bacteria. However, further experiments would be required to substantiate these conclusions.

We also examined the influence of infection and autophagy on inflammatory cytokine production. Intraperitoneal infection produced increase in serum levels of both IL-1 β and TNF- α . Manipulating autophagy with 3-MA and rapamycin did not produce a large effect on the production of these cytokines. The variation in the levels measured was also rather large. IL-1 β levels were also

not high, again making interpretation difficult. Further work measuring these cytokine levels over time and at later time points will be required.

- 5 **Infection with *S. pneumoniae* induces autophagy, phagocytosis and neutrophil extracellular traps in human neutrophils**

5.1 Introduction

Polymorphonuclear neutrophils are the first line of defence against infection and provide strong immunity to the body by eliminating invading pathogens using multiple strategies. They are the most abundant cells amongst leukocytes and are one of the principal effectors of the immune system (Kolaczkowska and Kubes, 2013).

Previously, neutrophils were believed to kill pathogens through phagocytosis and secretion of antimicrobial molecules but recently a newer mechanism of trapping and killing invading pathogens called neutrophil extracellular traps (NETs) has emerged. This has links with phagocytosis and possibly the autophagy pathway (Brinkmann et al., 2004).

When neutrophils are activated by some invading pathogens, they commence killing of pathogens by activation of phagocytosis and release of molecules from their intracellular granules. This then leads to release of their nuclear material to form a mesh-like structure - a neutrophil extracellular trap (NET) - through a process called (NETosis) which is used for trapping and killing pathogens (Brinkmann et al., 2004).

The main function of neutrophil leukocytes is to combat invading pathogens (Nathan, 2006). When pathogens invade, they are first detected by resident tissue macrophages and some other sentinel cells, which then initiate a signal to circulating neutrophils by releasing chemical mediators into the blood and body fluids. Neutrophil leukocytes are then activated and rapidly recruited to the site of infection where they start phagocytosis, degranulation and release of chemical mediators, NET formation and possibly autophagy in response to infection.

NETs released by neutrophils are composed of de-condensed nuclear material and antimicrobial proteins which can entrap and kill multiple invading pathogens including bacteria, fungi and parasites (Papayannopoulos and Zychlinsky, 2009). Neutrophils have a short life span and die quickly during infection when they are activated, and NET generation may contribute to this early death (Pillay et al., 2010).

Recent research has suggested a relationship between autophagy and NET formation by neutrophils. Enhancing autophagy with rapamycin, an inhibitor of mammalian target of rapamycin (mTOR) accelerated NET formation when neutrophils were treated with a microbial component (fMLP) formyl-methionyl leucyl phenylalanine (Itakura and McCarty, 2013). This could be a direct action of mTOR as an inhibitor of NETosis or could indicate that autophagy *per se* is essential for NET formation.

We hypothesized that neutrophil activation with *S. pneumoniae* induces phagocytosis, autophagy and NET formation, and that autophagy may be a requirement for NET formation. We have already demonstrated autophagy induction in primary murine BMDMs and in this section we present studies using human neutrophils infected with different strains of *S. pneumoniae*.

The induction of autophagy, phagocytosis and NETosis and their relationship was demonstrated using different techniques and different incubation conditions. We further investigated the relationship of these pathways with inflammasome activation in response to *S. pneumoniae* infection.

5.2 Results

5.2.1 Autophagy induction in human neutrophils infected with *S. pneumoniae* using immunofluorescence (IF) and western blot (WB) techniques

First, we set out to determine whether infection of human neutrophils induced autophagy. We used purified human neutrophils and following infection stained them for LC3 and quantified the numbers of autophagocytic puncta formed (Fig. 5.1a and b). This showed that infection with both D39 WT and D39 Δ Ply induced autophagy, similar to the results seen with the positive control, rapamycin. This was confirmed by immunoblotting for LC3 following infection (Fig. 5.1c). The ratio of LC3 II to tubulin increased significantly (Fig. 5.1d) following infection with both D39 WT and D39 Δ Ply, confirming that infection of human neutrophils by *S. pneumoniae* induced autophagy.

We further demonstrated that there is an increase in LC3 II flux through the autophagocytic pathway by repeating western blot in the presence of inhibitors of lysosomal degradation (Fig. 5.3, 5.4). This further increased the amounts of LC3 II following infection, showing that the increase in observed LC3 was due to greater flux through the autophagocytic pathway. This data showed increased conversion of LC3 I to LC3 II in cells pre-treated with lysosomal inhibitors such as Pepstatin A, E64d, and Bafilomycin A1. These inhibitors prevent loss of LC3 II during lysosomal degradation by preventing fusion between autophagosome with lysosomes.

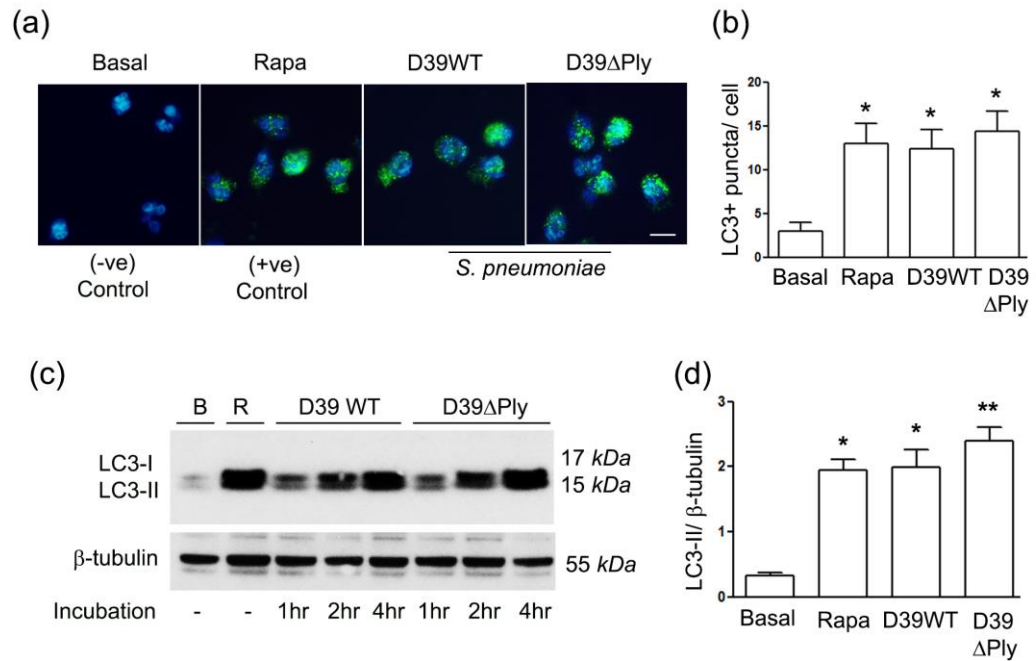


Figure 5.1 Autophagy induction in human neutrophils infected with *S. pneumoniae*.

(a) Immunofluorescence was performed for LC3 protein levels in untreated (basal) neutrophils as negative control, treated with Rapamycin (50 μ g/ ml) as positive control of autophagy and infected with *S. pneumoniae* strains D39 WT and D39 Δ Ply at an MOI of 10 as indicated. Fluorescent microscopy was performed to visualize LC3 (green) and nuclear (blue) staining. Scale bar is 50 μ m.

(b) Bar graph showing numbers of LC3 puncta/ cell (counted in 60 cells in different views). Columns show mean; error bars are SEM. Asterisks indicate statistical significance from basal (p < 0.05).

(c) Western blot analysis of LC3 I and LC3 II proteins in human neutrophils left unstimulated (B), treated with Rapamycin (R; 50 μ g / ml) as positive control of autophagy and infected with *S. pneumoniae* strains D39 WT and D39 Δ Ply at an MOI of 10 as indicated. The same blot was stripped and re-probed for β - tubulin protein as loading control as shown.

(d) Densitometry measurement of the ratio of LC3 II/ β - tubulin for two different representative blots from independent experiments. Asterisks indicates statistically significant difference from basal, * indicates p < 0.05 and ** indicates p < 0.01.

As shown in Figure 5.1, autophagy was effectively induced in human neutrophils following infection with *S. pneumoniae*, as assayed by both the appearance of LC3 puncta (Fig. 5.1a) and conversion of LC3 I to II (Fig. 5.1c). Autophagy signal is higher in pneumolysin deficient strain indicating a relationship with inflammasome activation as shown by immunoblotting for LC3 protein (Fig. 5.1d).

5.2.2 Dependence of autophagy on multiplicity of infection

Next, we determined how autophagy induction depended on the multiplicity of infection. Neutrophils were infected with either D39 WT or D39 Δ Ply at different MOIs and then assayed for the content of LC3 II (Fig. 5.2). At an MOI of 10, both these strains produced a significant increase in the ratio of LC3 II to β - tubulin, indicating an increase in autophagy.

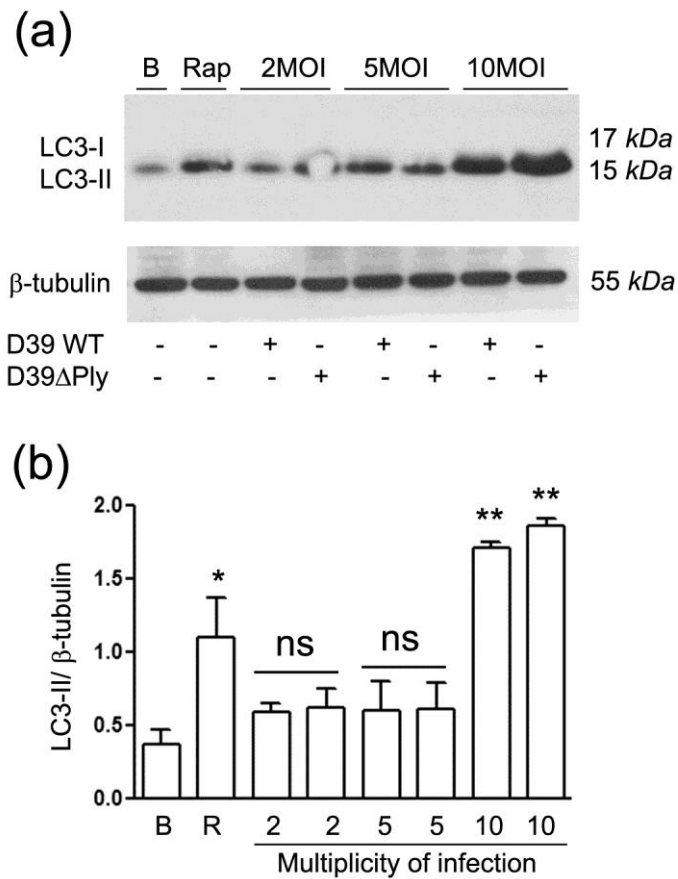


Figure 5.2 Dependence of autophagy on multiplicity of infection

(a) Representative western blot image of LC3 (Atg8) protein using human neutrophils infected with *S. pneumoniae* at different MOIs. Cells left uninfected (B), treated with Rapamycin (R; 25 μ g / ml) or infected with *S. pneumoniae* strains D39 WT and D39 Δ Ply as shown.

(b) Densitometry analysis of LC3 II/ β - tubulin (two independent experiments). Columns are mean values; error bars are SEM. ** indicates significant difference from basal, $p < 0.01$, (ns) non-significant.

As shown in the (Fig. 5.2b), columns of LC3 II relative to β - tubulin, autophagy induction following infection with *S.pneumoniae* is dependent on multiplicity of infection, as assayed by the conversion of LC3 I to LC3 II. Autophagy induction is non- significant at an MOI of 2 and 5 but there is significant increase at an MOI of 10 using *S. pneumoniae* strains D39 WT and D39 Δ Ply as shown.

5.2.3 Autophagy flux is increased following infection of neutrophils with *S. pneumoniae*

To determine if infection with *S. pneumoniae* increased flux through the autophagocytic pathway, lysosomal proteases were inhibited with E64d and Pepstatin A or by preventing fusion autophagosomes with lysosomes using bafilomycin A1. Importantly under these conditions, there was not any significant increase in cell death due to cytotoxicity of the drugs as measured by the release of lactate dehydrogenase (LDH) from both treated and untreated cells (data not shown).

5.2.3.1 Increased autophagy flux measured using lysosomal protease inhibitors E64d and Pepstatin A

The lysosomal degradation of LC3 protein was blocked by pre-treating neutrophils with E64d and Pepstatin A (Tanida et al., 2005) for 60 minutes. The cells were then infected with *S. pneumoniae* strains without changing media as shown in Figure 5.3. This increased the amount of LC3 II produced following infection when analysed by western blot. This indicated that autophagy flux was increased in the infected cells.

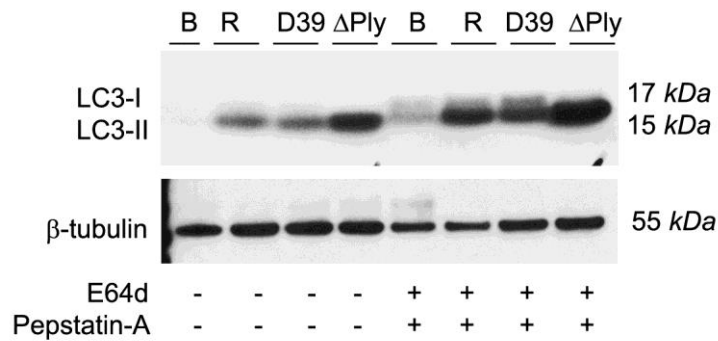


Figure 5.3 Infection with *S. pneumoniae* increases autophagocytic flux in human neutrophils

Representative western blot analysis of LC3 I and LC3 II levels in human neutrophils pre-treated as indicated with E64d (10 μ g/ ml) and Pepstatin A (10 μ g / ml) as compared to untreated cells. Cells were left un-stimulated (B), treated with Rapamycin (R; 25 μ g/ ml), or infected with *S. pneumoniae* strains D39 WT and D39 Δ Ply (10 MOI; 4 hours) in the presence (+) or absence (-) of E64d and Pepstatin A.

The increase in autophagy signal indicated that autophagy flux was increased in cells treated with lysosomal inhibitor drugs.

5.2.3.2 Autophagy flux using lysosomal inhibitor Bafilomycin A1

Bafilomycin A1 is an inhibitor of the late phase of the autophagy pathway. It blocks fusion of the autophagosome with the lysosome (Yamamoto et al., 1998). Cells were pre-treated with Bafilomycin A1 (50 nM) for 60 minutes and then infected with *S. pneumoniae*. As shown in Figure 4.4, bafilomycin A1 treatment increased the amounts of LC3 II produced following infection, indicating an increase in autophagocytic flux.

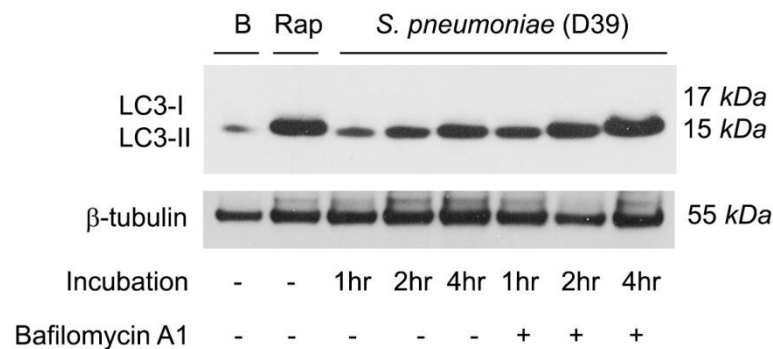


Figure 5.4 Infection with *S. pneumoniae* increases autophagocytic flux in human neutrophils

Representative western blot analysis of LC3 protein levels in human neutrophils pre-treated with of Bafilomycin A1 (50 nM) as indicated. Cells were then left un-stimulated (B), treated with Rapamycin (Rap; 25 μ g / ml), or infected with *S. pneumoniae* D39 WT (10 MOI) for the indicated times with (+) or without (-) inhibitor drug.

The observed autophagic flux is increased in infected cells pre-treated with this inhibitor drug.

5.2.4 Blocking autophagy by chemical and genetic methods

Next, we studied the functional effects of autophagy by inhibiting the process using chemical inhibitors and siRNA knock down. Under these conditions, there was not any significant increase in cell death due to cytotoxicity of 3MA or siRNA as measured by the release of lactate dehydrogenase from both treated and untreated cells (data not shown).

5.2.4.1 Autophagy inhibition by 3-methyladenine (3-MA)

Purified human neutrophils were treated with 3-MA, a pharmacological agent known to block autophagosome formation by inhibiting class-III phosphatidylinositol-3-kinase (PI-3K III). Neutrophils were pre- treated with 3MA (10mM) for 60 minutes (Seglen and Gordon, 1982, Wu et al., 2010) and then infected with *S. pneumoniae*.

Immunofluorescence and western blot techniques were performed on 3MA treated and untreated cells. Fluorescent microscopy was performed to observe LC3 puncta and cell lysates were analysed by western blot for LC3 I and II isoforms. As shown in figure 5.5, 3-MA produced a marked inhibition of autophagy, in both assay of LC3 puncta formation, and in inhibiting the formation of LC3 II.

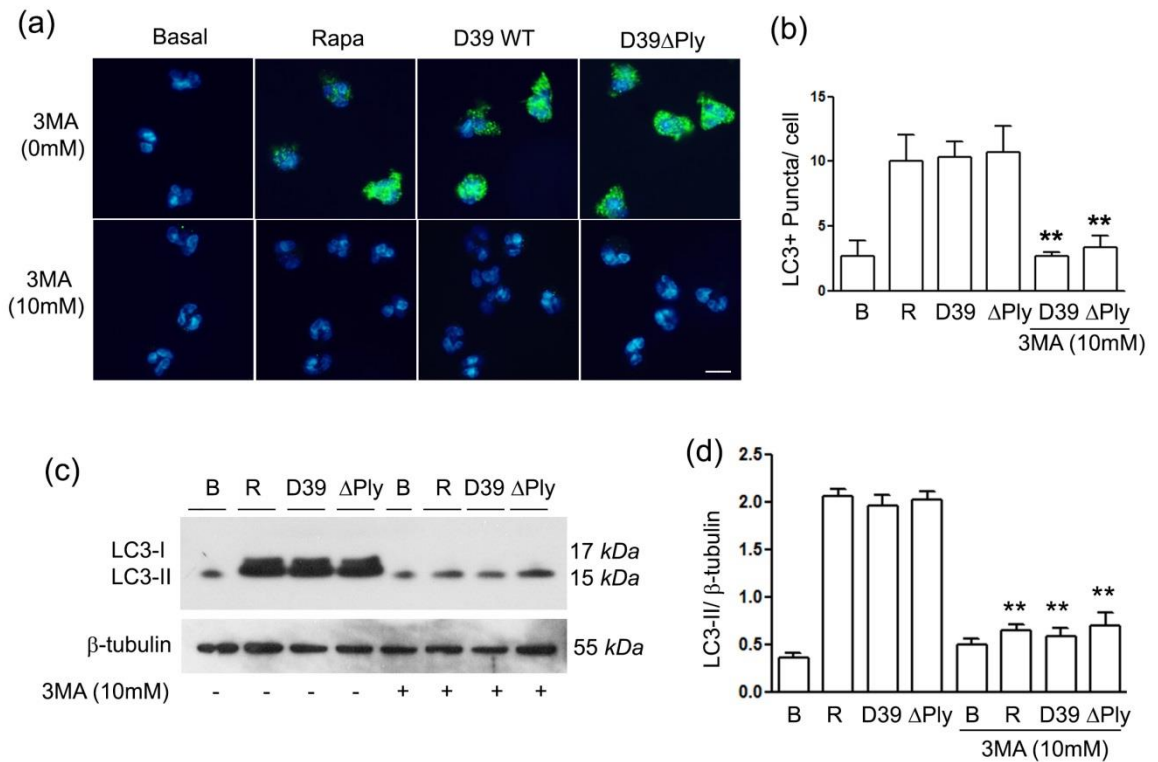


Figure 5.5 3-Methyl-adenine inhibits autophagy in human neutrophils

(a) Representative immunofluorescence images of LC3 puncta in human neutrophils. Cells were left uninfected (Basal), treated with Rapamycin (Rapa; 25 μ g / ml) or infected with *S. pneumoniae* strains D39 WT and D39 Δ Ply at an MOI of 10 for 4 hours in the presence or absence of 3MA. Cells were stained with anti-LC3 (green) and (DAPI) to visualize the nuclei (blue). Scale bar is 50 μ m.

(b) Quantification of average number of LC3 puncta present per cell from three independent experiments (counted in 60 cells in different views) following treatments and infections as indicated. ** shows significant decrease in the number of puncta in cells treated with 3-MA, $p < 0.01$.

(c) Western blot analysis of LC3 I and LC3 II proteins levels in human neutrophils uninfected (B) or treated with Rapamycin (R; 25 μ g/ ml) or infected with *S. pneumoniae* strains D39 WT and D39 Δ Ply (10MOI) for 4 hours in the presence (+) or absence (-) of (10 mM) 3-MA.

(d) Densitometry analysis of the autophagy signal in neutrophils treated with 3MA and without treatment. Columns are means of LC3-II/ β - tubulin determinations; error bars are SEM. ** denotes significant reduction in autophagy signal in cells treated with 3MA as compared to untreated cells, $p < 0.01$ (2 independent experiments).

5.2.4.2 Autophagy knock down using siRNA to Atg5 gene

Autophagy-related (Atg) proteins are responsible for autophagy and genetic knock down of essential *Atg genes* can down regulate autophagy. The *Atg5* autophagy gene in neutrophils was knocked down by electroporation with *Atg5* siRNA. Viability was determined by 7-AAD staining and maintained at > 80 % after overnight incubation as shown in figure 2.5 in material methods section. Cells were then infected with *S. pneumoniae*. Immunofluorescence for LC3 puncta and western blot analysis for LC3 I and II was then performed.

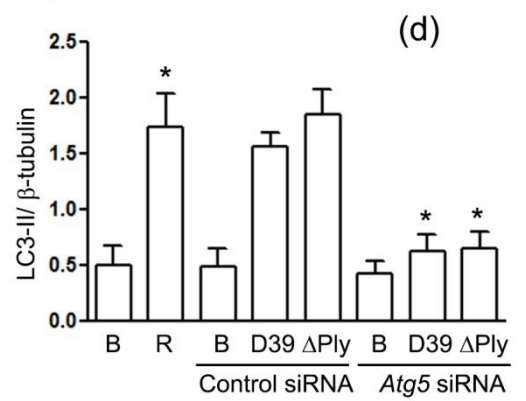
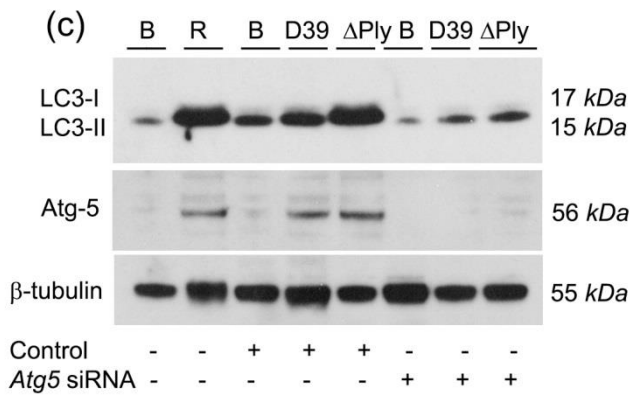
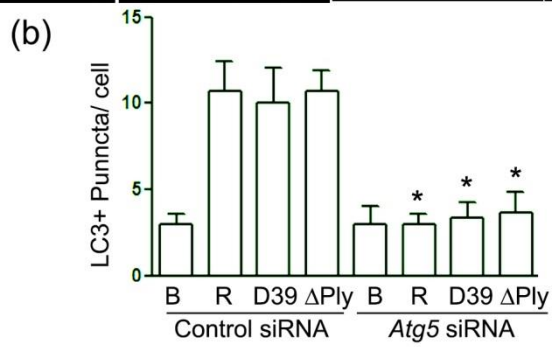
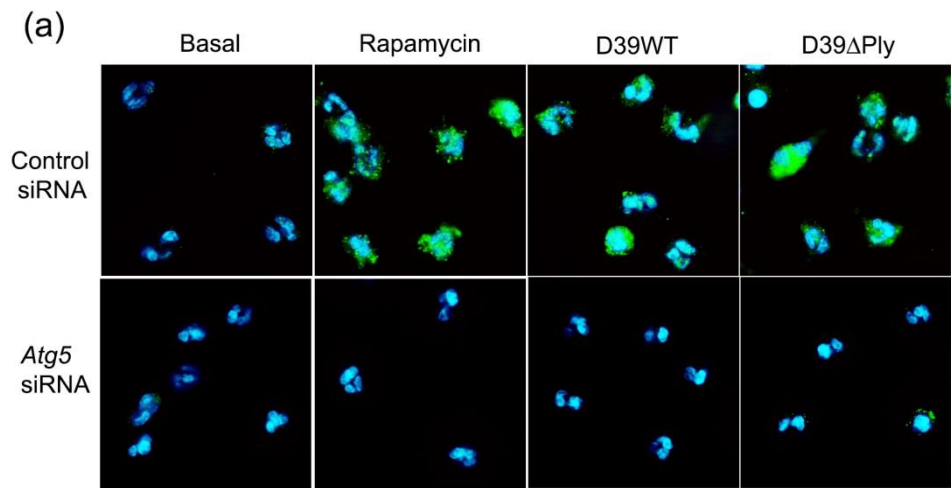


Figure 5.6 *S. pneumoniae* induced autophagy is Atg5 dependent

(a) Representative immunofluorescence images of LC3 puncta in neutrophils treated as indicated. Cells were left uninfected (Basal), treated with Rapamycin (Rapa) or infected with *S. pneumoniae* strains D39 WT and D39 Δ Ply at an MOI of 10. Cells were stained with anti-LC3 (green) and DAPI to visualize nuclei (blue).

(b) Quantification of LC3 puncta present per cell (counted in 60 cells in different views) following treatments and infections as indicated. Asterisks represent significant difference between control siRNA and Atg5 siRNA, $p < 0.005$.

(c) Representative western blot analysis from lysates of neutrophils treated with siRNA for Atg5 and probed for the proteins as indicated. Cells were left uninfected (basal), treated with Rapamycin (25 μ g/ml) or infected with *S. pneumoniae* strains D39 WT and D39 Δ Ply at an MOI of 10. The blot was stripped and re-probed for β - tubulin protein as a loading control.

(d) Densitometry analysis of LC3 signal. Columns are the means of LC3 II determinations; error bars are SEM. The asterisks showing significant reduction in Atg5 knock down cells, $p < 0.05$ (2 independent experiments).

As shown in figure 5.6, knock down of *Atg5* effectively inhibited autophagy following infection, as assayed by both the appearance of LC3 puncta and conversion of LC3 I to II. Efficient knock down of *Atg5* was confirmed by immunoblotting for the Atg5 protein (Fig. 5.6c).

Note that the ATG5 protein is covalently conjugated to ATG12 on the induction of autophagy, and that the signal shown in the immunoblot is the band that represents this ATG5-ATG12 conjugate. This is thus only a signal under conditions where autophagy is induced with rapamycin or infection. When treated with siRNA to *Atg5* this signal is considerably attenuated.

5.2.5 Relationship of autophagy with inflammasome activation

Next, we determined the relationship between induction of autophagy and activation of the inflammasome following infection.

5.2.5.1 Inflammasome activation by *S. pneumoniae* D39 WT and D39 Δ Ply

Neutrophils were infected with *S. pneumoniae* strains D39 WT and D39 Δ Ply and then analysed for inflammatory cytokine IL-1 β production (Fig. 5.7). IL-1 β levels were significantly higher after infection with *S. pneumoniae* strain D39 WT as compared to the D39 Δ Ply strain lacking pneumolysin. Thus, inflammasome activation in neutrophils is dependent on pneumolysin, as found in murine BMDMs.

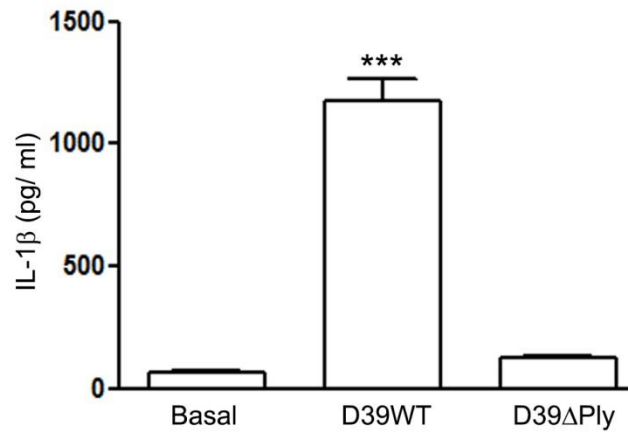


Figure 5.7 Inflammasome activation by *S. pneumoniae* strains D39 WT and D39 ΔPly

Bar graph showing inflammatory cytokine interleukin-1β (IL-1β) levels released from neutrophils left un-stimulated (Basal), or infected with D39 WT and D39 ΔPly for the times indicated. Asterisks indicate highly significant levels of inflammasome activation (IL-1β) in neutrophils stimulated with strain D39 WT as compared its pneumolysin deficient counterpart. Bars are means of triplicates of IL-1β (pg / ml) determinations; error bars are SEM, $p < 0.001$.

5.2.5.2 Influence of autophagy on inflammasome activation by *S. pneumoniae*

To explore the relationship of autophagy with inflammasome activation, autophagy in neutrophils was inhibited by treating them with 3MA or by knock down of the *Atg5* gene using siRNA. Cells were then infected and analysed for IL-1 β production (Fig. 5.8). When neutrophils were treated with the chemical inhibitor 3-MA, there was a significant increase in the amount of IL-1 β released from the cells (Fig. 5.8a).

However, knock down of the essential autophagy gene *Atg5* produced a significant increase in the amount of IL-1 β released (Fig. 5.8b). This was similar to the results seen when autophagy was inhibited in BMDMs. We believe that this disparity in the results obtained with 3-MA and siRNA to *Atg5* most likely reflects a non-specific effect of 3-MA on the neutrophils ability to process pro-IL1 β and that the more specific inhibitory effects of siRNA knockdown of ATG5 suggest that as with BMDMs, autophagy normally acts to limit IL-1 β release following *S. pneumoniae* infection.

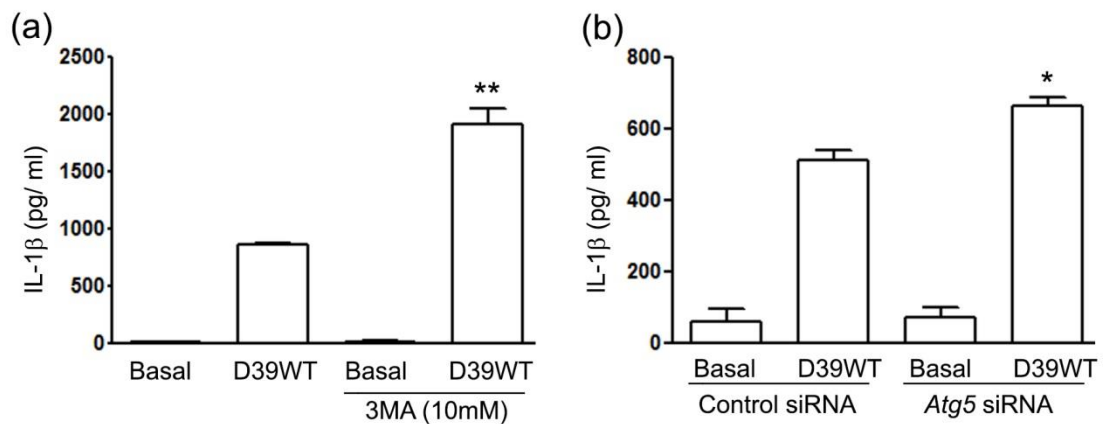


Figure 5.8 Inflammasome activation by *S. pneumoniae* strains D39 WT and D39 Δ Ply in neutrophils knocked down for autophagy

(a) Representative bar graph showing interleukin-1 β (IL-1 β) levels produced by neutrophils left un-stimulated (Basal), or infected with *S. pneumoniae* strain D39 WT for 4 hours in the presence or absence of 3-MA (10 mM). Asterisks indicate a significant difference between 3MA treated and untreated cells. Bars are means of IL-1 β levels in triplicate determinations; error bars are SEM, $p < 0.01$.

(b) As (a) but in cells transfected with control siRNA or *Atg5* siRNA. Asterisks indicate a significant difference between IL-1 β levels produced by these groups. Bars are means of triplicates of IL-1 β determinations; error bars are SEM, * $p < 0.05$, ** $p < 0.01$.

5.2.6 Phagocytosis and killing of *S. pneumoniae* by human neutrophils

Human neutrophils have the ability to phagocytose and kill invading pathogens. Phagocytosis of *S. pneumoniae* strains D39 WT and D39 Δ Ply by neutrophils was demonstrated at different time points according to the method described by (Hampton et al., 1994, Hampton and Winterbourn, 1999), as described in the Materials and Methods. This technique allowed the determination of the rates of uptake and killing of the microbe by neutrophils following incubation with *S. pneumoniae*.

5.2.6.1 Comparison of phagocytosis and killing of *S. pneumoniae* strains D39 WT and D39 Δ Ply by human neutrophils

First, we measured the rates of phagocytosis and killing of *S. pneumoniae* D39 WT and D39 Δ Ply by human neutrophils (Fig. 5.9).

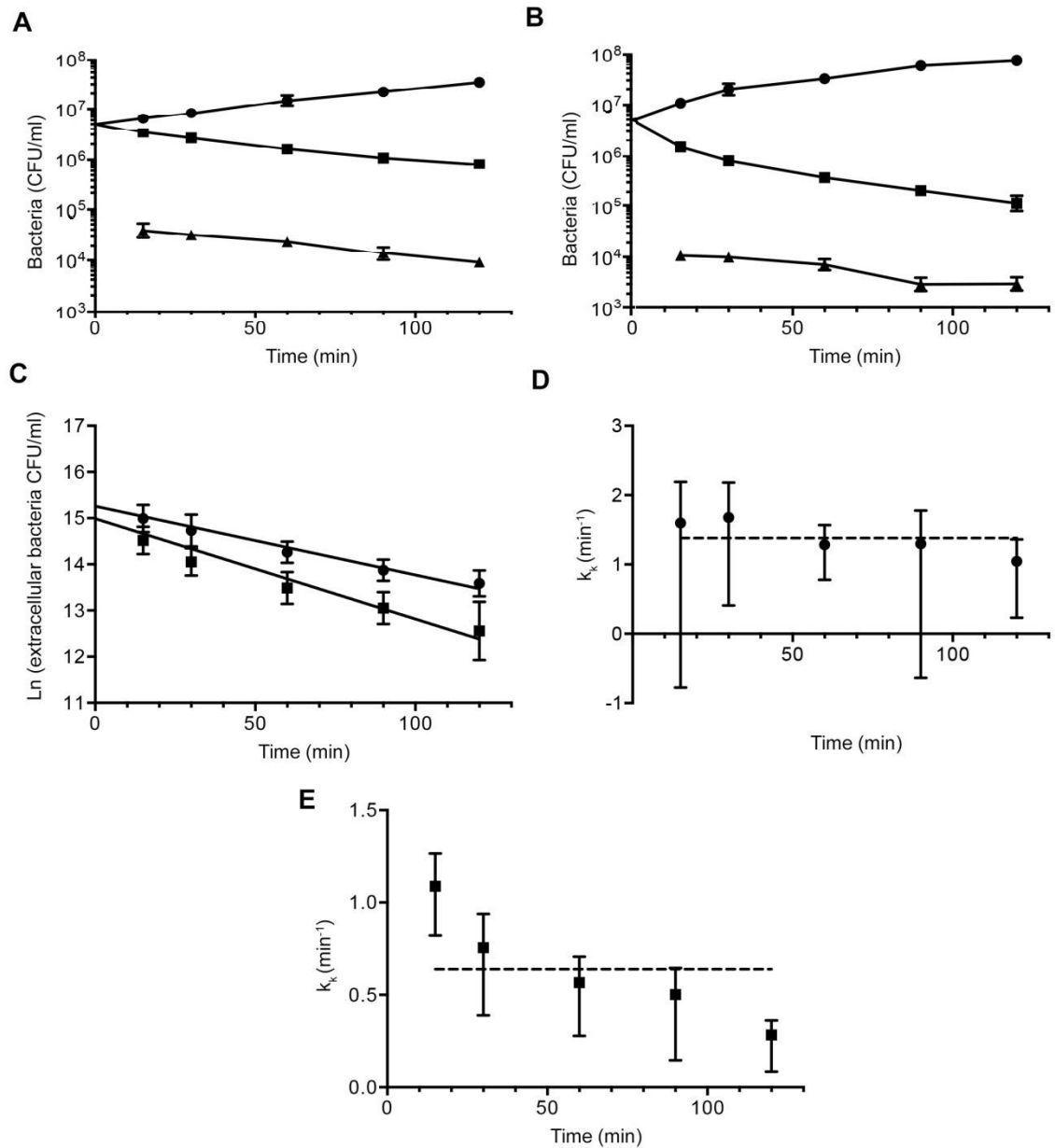


Figure 5.9 Phagocytosis and killing of *S. pneumoniae* strains D39 WT and D39 Δ Ply by human neutrophils

S. pneumoniae strains D39 WT and D39 Δ Ply were grown alone in medium as control or with neutrophils infected at a MOI of 10.

(a) CFU count of *S. pneumoniae* D39 WT in complete medium alone (circles), or in cell supernatant (squares) and cell lysates (triangles) from infected neutrophils at different time points. CFU counts shown are the mean of triplicates for each time point; error bars are SEM.

(b) As (a), but with *S. pneumoniae* D39 Δ Ply.

(c) Comparison of \ln (extracellular bacteria) over time for *S. pneumoniae* strains D39 WT (circles) and D39 Δ Ply (squares).

(d) Calculated values for k_k at indicated time points for *S. pneumoniae* D39 WT. Points are means of triplicate determinations; error bars are SD. Dotted line shows the mean value across all time points.

(e) As (d), but for the *S. pneumoniae* strain D39 Δ Ply.

The analysis of these data allows the rates of phagocytosis and intracellular killing for the two strains to be derived. The rate of phagocytosis is calculated from the slope of the graphs shown in Figure 5.9c. The calculated rate constant of phagocytosis, k_p , for D39 WT was 0.0149 min^{-1} (95 % confidence limits 0.0120 - 0.0178) and for D39 Δ Ply was 0.0217 min^{-1} (95 % confidence limits 0.0169 - 0.0266). This difference was significant when the data were compared using a non-linear regression best fit model ($p < 0.016$).

Thus, the rate of phagocytosis of the D39 Δ Ply strain was significantly higher than the D39 WT strain, indicating that Ply reduces the rate of phagocytosis by human neutrophils. The rate constant for intracellular killing was calculated at each time point, as described in the Methods section and shown for the two strains in Fig 5.9d and e. The mean value for all the time points was 1.381 min^{-1} (sem 0.115) for the D39 WT strain and 0.639 min^{-1} (sem 0.135) for the D39 Δ Ply strain, a significant difference ($p < 0.0031$, two-sample t test).

Thus, intracellular killing was significantly slower in the D39 Δ Ply strain, suggesting that Ply acts to accelerate intracellular killing. This is considered further in the discussion.

5.2.6.2 Effects of blocking autophagy on the phagocytosis and killing of *S. pneumoniae* by human neutrophils

Autophagy in neutrophils was inhibited using 3MA and colony counts of extra- and intra- cellular bacteria determined as before (Fig. 5.10).

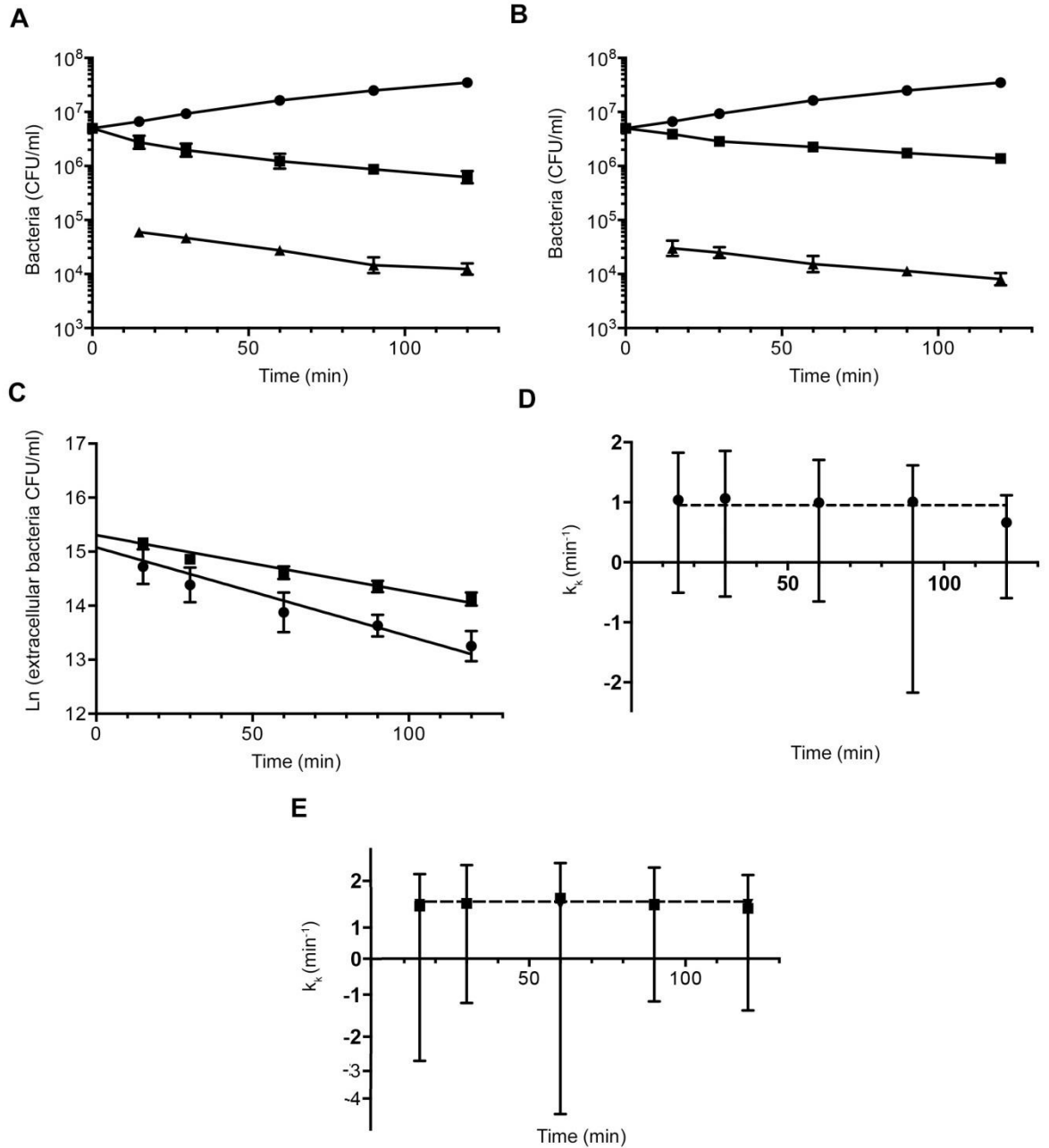


Figure 5.10 Effect of 3-MA on phagocytosis and killing of *S. pneumoniae* strain D39 WT by human neutrophils

S. pneumoniae strains D39 WT were grown alone in medium as control or with 3MA treated and untreated neutrophils infected at an MOI of 10.

(a) CFU count of *S. pneumoniae* D39 WT in complete medium alone (circles), or in cell supernatant (squares) and cell lysates (triangles) from infected neutrophils at different time points. CFU counts shown are the mean of triplicates for each time point; error bars are SEM.

(b) As (a) in the presence of 10 mM 3-MA.

(c) Comparison of $\ln(\text{extracellular bacteria})$ over time in cell supernatant without 3-MA (circles) or in the presence of 3-MA (squares).

(d) Calculated values for k_k at indicated time points for *S. pneumoniae* D39 WT grown in neutrophils without 3MA treatment. Points are means of triplicate determinations; error bars are SD. Dotted line shows the mean value across all time points.

(e) As (d), but for growth in 3-MA treated neutrophils

The analysis of these data allow the rates of phagocytosis and intracellular killing in the presence and absence of 3-MA to be derived. The rate of phagocytosis is calculated from the slope of the graphs shown in Figure 5.10c. The calculated rate constant of phagocytosis, k_p , for cells grown in medium alone was 0.01646 min⁻¹ (95 % confidence limits 0.0109 to 0.0220) and in the presence of 3-MA was 0.0104 min⁻¹ (95 % confidence limits 0.00851 to 0.0124). This difference was significant when the data were compared using a non-linear regression best fit model ($p < 0.0001$).

Thus, the rate of phagocytosis in the presence of 3-MA was significantly lower than the control value, indicating that when autophagy is inhibited the rate of phagocytosis of *S. pneumoniae* by human neutrophils is significantly reduced. The rate constant for intracellular killing was calculated at each time point, as described in the material and methods section and shown for the two strains in Fig. 5.10d and e. The mean value for the control at all the time points was 0.954 min⁻¹ (sem 0.0738) and in the presence of 3-MA was 1.612 min⁻¹ (sem 0.0503), a significant difference ($p < 0.0001$, two-sample t- test).

Thus, intracellular killing was significantly faster in the presence of 3-MA, suggesting that autophagy acts to limit intracellular killing. This is considered further in the discussion.

5.2.6.3 Effect of *Atg5* knock down on the phagocytosis and killing of *S. pneumoniae* by human neutrophils

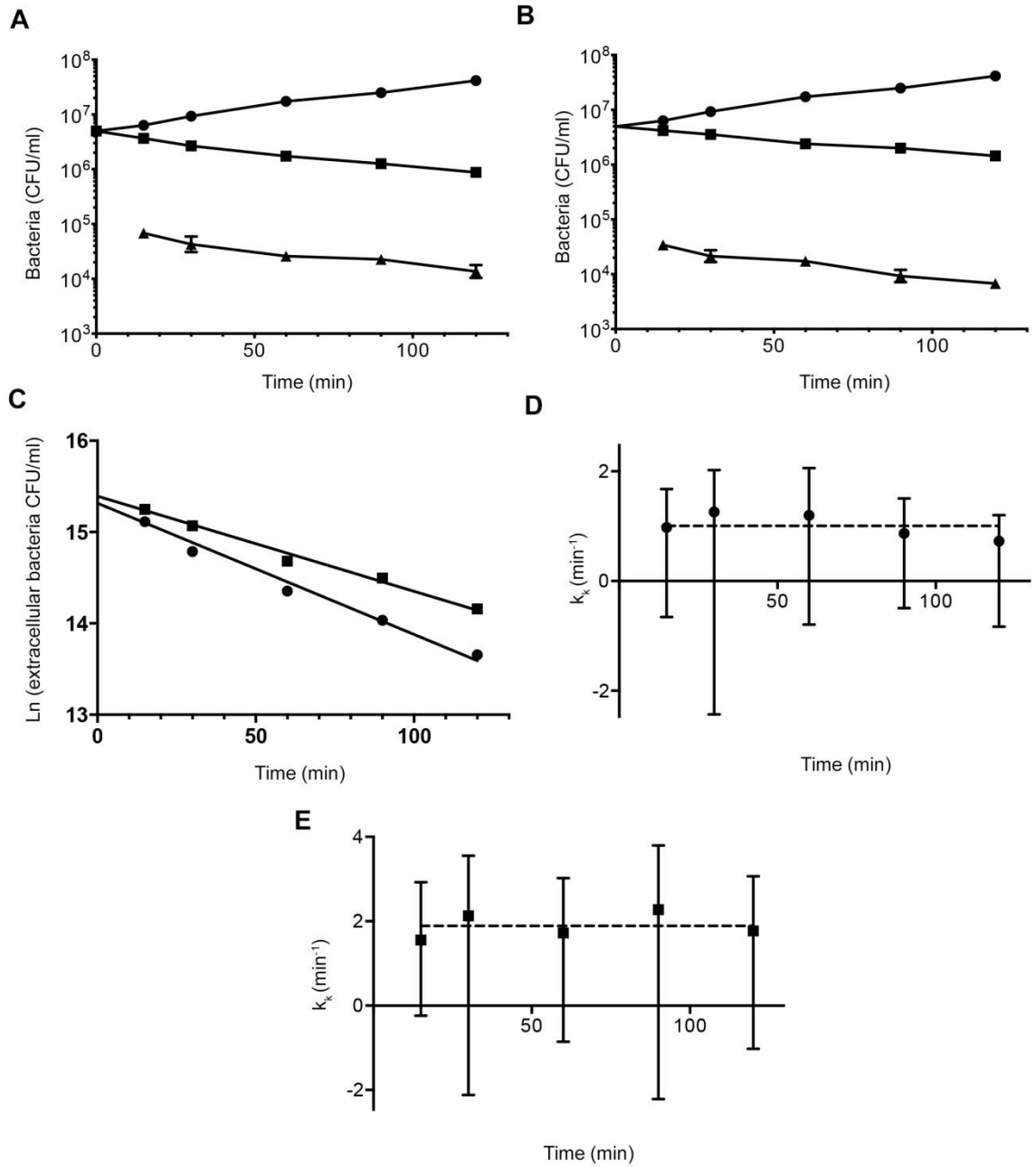


Figure 5.11 Phagocytosis and killing of *S. pneumoniae* D39 WT by human neutrophils knocked down for (*Atg5*) autophagy gene.

As Figure 5.10, but comparing rates of phagocytosis and killing in cells in the presence and absence of siRNA to *Atg5*.

We then inhibited autophagy by using knock down of *Atg5* using siRNA and assayed the effects on uptake and killing of *S. pneumoniae* by human neutrophils.

The analysis of these data allows the effects of *Atg5* knock down on the rates of phagocytosis and intracellular killing to be derived. The rate of phagocytosis is calculated from the slope of the graphs shown in Figure 5.11c. The calculated rate constant of phagocytosis, k_p , for cells grown with control siRNA alone was 0.01437 min^{-1} (95 % confidence limits 0.0118 to 0.0169) and in the presence of the *Atg5* siRNA was 0.0104 min^{-1} (95 % confidence limits 0.00904 to 0.0118). This difference was significant when the data were compared using a non-linear regression best fit model ($p = 0.0053$).

Thus, the rate of phagocytosis when *Atg5* was knocked down was significantly lower than the control value, indicating that when autophagy is inhibited the rate of phagocytosis of *S. pneumoniae* by human neutrophils is significantly reduced. The rate constant for intracellular killing was calculated at each time point, as described in the Materials and Methods section and shown for the two conditions in Figure 5.11 d and e. The mean value for the control siRNA at all the time points was 1.006 min^{-1} (sem 0.100) and in the presence of *Atg5* siRNA was 1.890 min^{-1} (sem 0.134), a significant difference ($p = 0.0007$, two-sample t- test).

Thus, intracellular killing was significantly faster when *Atg5* was knocked down, suggesting that autophagy acts to limit intracellular killing. This is a very similar result to that seen when autophagy was inhibited using 3-MA. These results are considered further in the discussion.

5.2.7 Neutrophil extracellular trap (NET) generation by human neutrophils following infection with *S. pneumoniae*

5.2.7.1 *S. pneumoniae* induces NETs

Purified human neutrophils were re-suspended in RPMI medium containing human serum and infected with *S. pneumoniae* strains D39 WT. NET generation was assessed by staining preparations of cells for the neutrophil protein neutrophil elastase and for DNA using DAPI, as outlined in the Materials and Methods section. PMA was used as a positive control, as it is known to induce NET formation (Brinkmann et al., 2004).

Following *S. pneumoniae* infection, we observed classical NET generation by human neutrophils, with the appearance of long strands of nuclear material decorated with neutrophil elastase (Fig. 5.12a) which was visualized from 1 hour and increased after 4 hours incubation. This was identical in appearance to NETs formed following administration of PMA. Quantification of NET formation showed a highly significant rise in their formation following either PMA or pneumococcal infection (Fig. 5.12b).

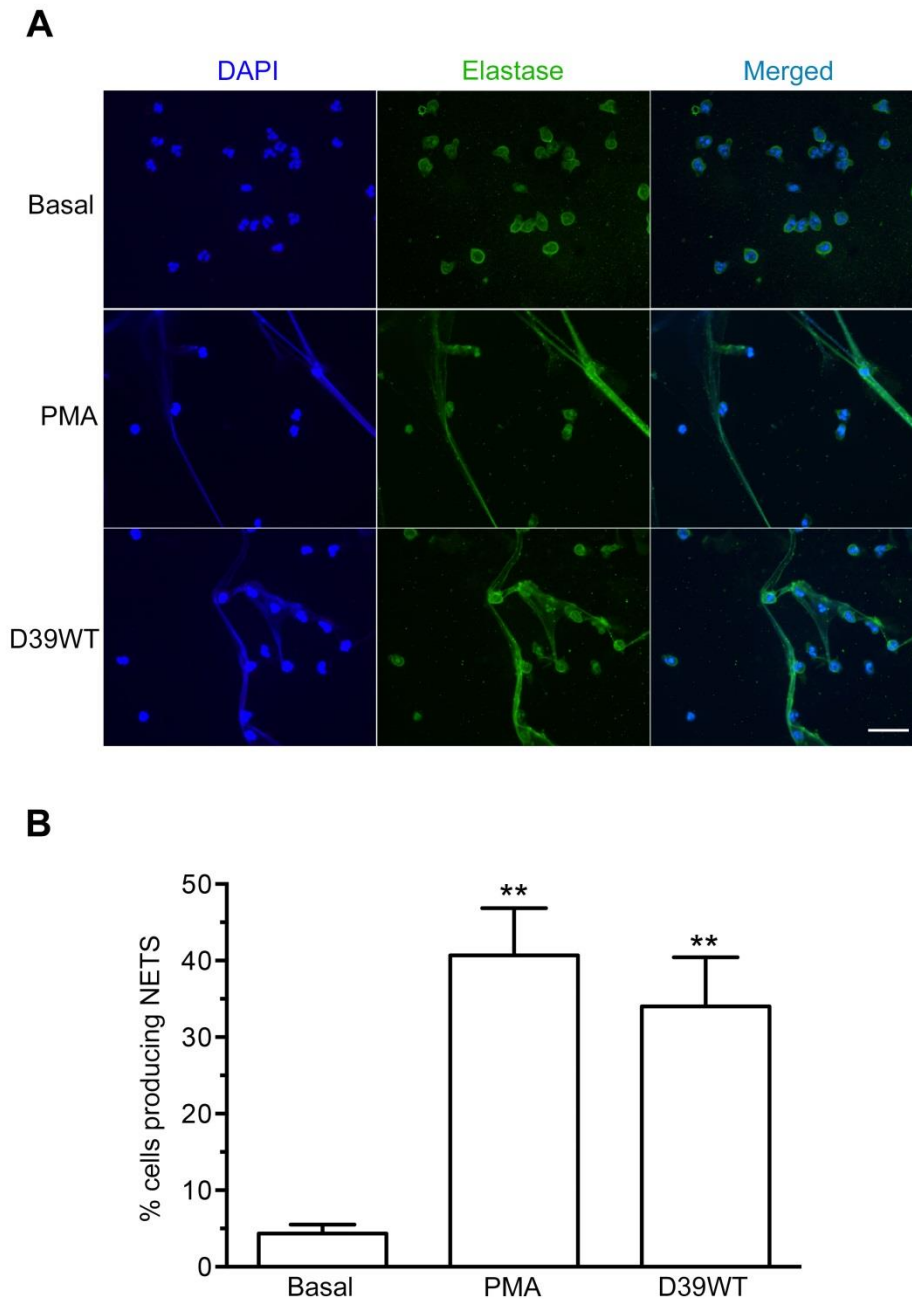


Figure 5.12 Human neutrophils generate NETs in infection with *S. pneumoniae*.

(a) Immunofluorescence image of neutrophils left untreated (Basal), treated with PMA (1 μ g/ ml) or infected with *S. pneumoniae* D39 WT at a MOI of 10 for 4 hours as indicated. Cells were stained with anti-neutrophil elastase antibody (green) and the nuclear material with DAPI (blue). Scale bar is 50 μ m.

(b) Number of neutrophils producing NETs per 100 of total cells in 3 different views with treatments as indicated; columns show mean and error bars are SEM. The asterisks show significant difference ($p < 0.01$, unpaired t- test) from basal.

5.2.8 Inhibition of autophagy attenuates NET generation in human neutrophils following infection with *S. pneumoniae*

Recent research has shown that NET generation in neutrophils has some association with autophagy through the mTOR pathway (Itakura and McCarty, 2013), but the exact mechanism is still unknown. We hypothesized that inhibition of autophagy by chemical or genetic methods might block NET generation by human neutrophils.

5.2.8.1 Blocking autophagy with 3MA down regulate NETs generation

When autophagy was inhibited using 3-MA, NET generation in neutrophils following infection with *S. pneumoniae* was significantly down regulated (Fig. 5.13). This suggests that induction of autophagy is required for NET generation following infection.

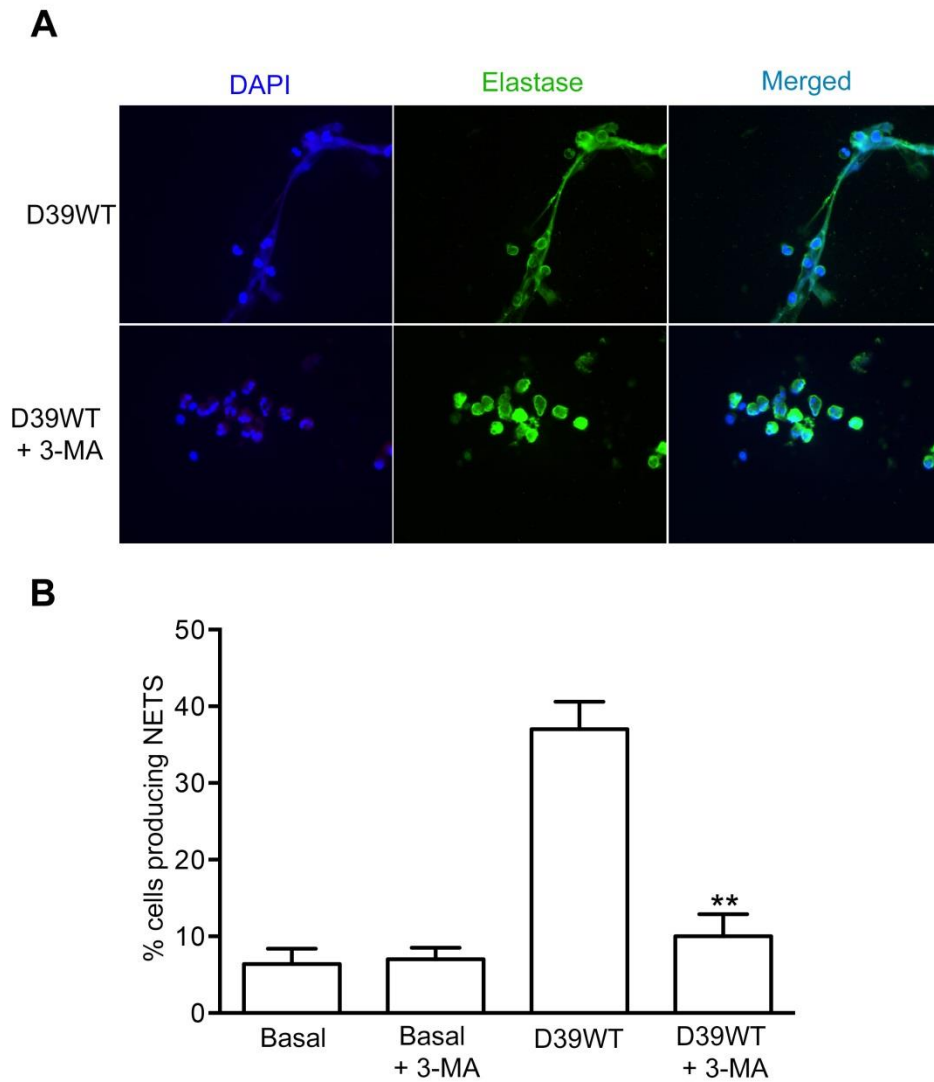


Figure 5.13 NET generation in human neutrophils following infection is down regulated by inhibition of autophagy with 3MA.

(a) Representative immunofluorescence image of human neutrophils infected with *S. pneumoniae* D39 WT at an MOI of 10 in the presence or absence of 3-MA. Cells were stained as in Figure 5.12a.

(b) Number of neutrophils producing NETs per 100 of total in 3 different views with indicated treatments as in Figure 5.12b. ** indicates a significant difference from untreated cells ($p < 0.01$, unpaired t- test).

5.2.8.2 Knock down of *Atg5* inhibits NET generation following infection

Further to explore the relationship between autophagy and NET formation, we inhibited autophagy by knock down of *Atg5* using siRNA. Following inhibition of autophagy by this means, NET formation following infection was again significantly down regulated (Fig. 5.14).

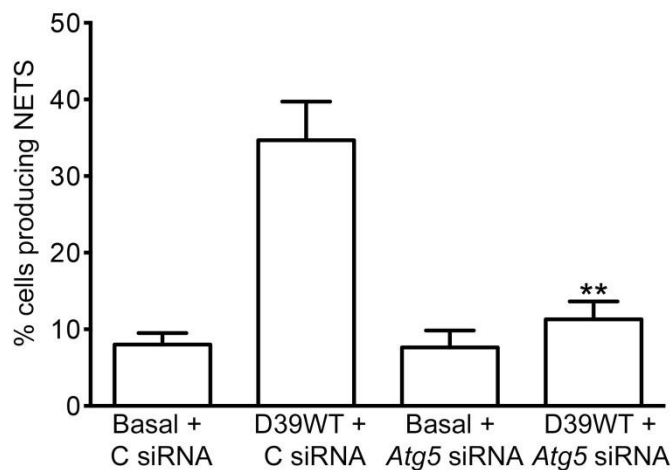


Figure 5.14 Autophagy gene *Atg5* knock down in human neutrophils down-regulates NETs generation in infection with *S. pneumoniae*.

As Fig 5.13b, but using knock down of ATG5 with *Atg5* siRNA or control (C siRNA) as indicated with treatments and infections as shown. ** indicates a significant difference ($p < 0.01$, unpaired t- test) from control siRNA.

5.2.8.3 Effects of pneumococcal virulence factor pneumolysin on NETs trapping of bacteria.

To investigate whether pneumolysin has an effect on bacterial trapping by NETs, bacterial strains D39 WT and D39 Δ Ply were pre-stained with vibrant Blue and then used to infect neutrophils. NET formation was then visualised as before and the numbers of bacteria entrapped in the NETS enumerated (Fig. 5.15). Significantly more of the D39 Δ Ply bacteria were present in NETs compared to the D39 WT. This indicates that pneumolysin attenuates bacterial trapping by NETs.

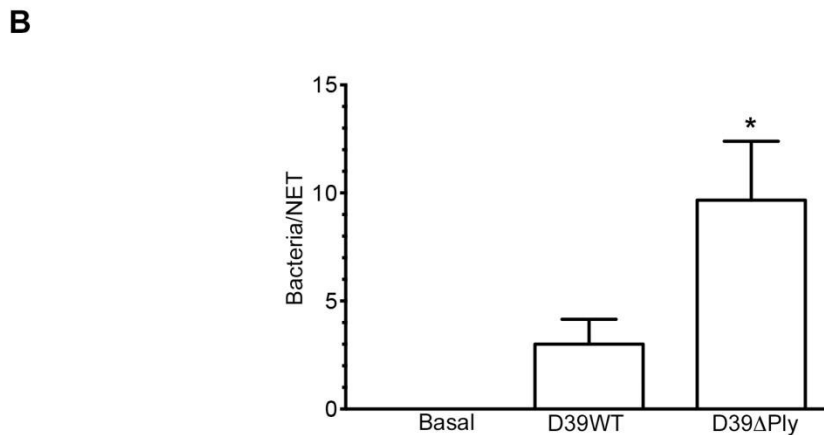
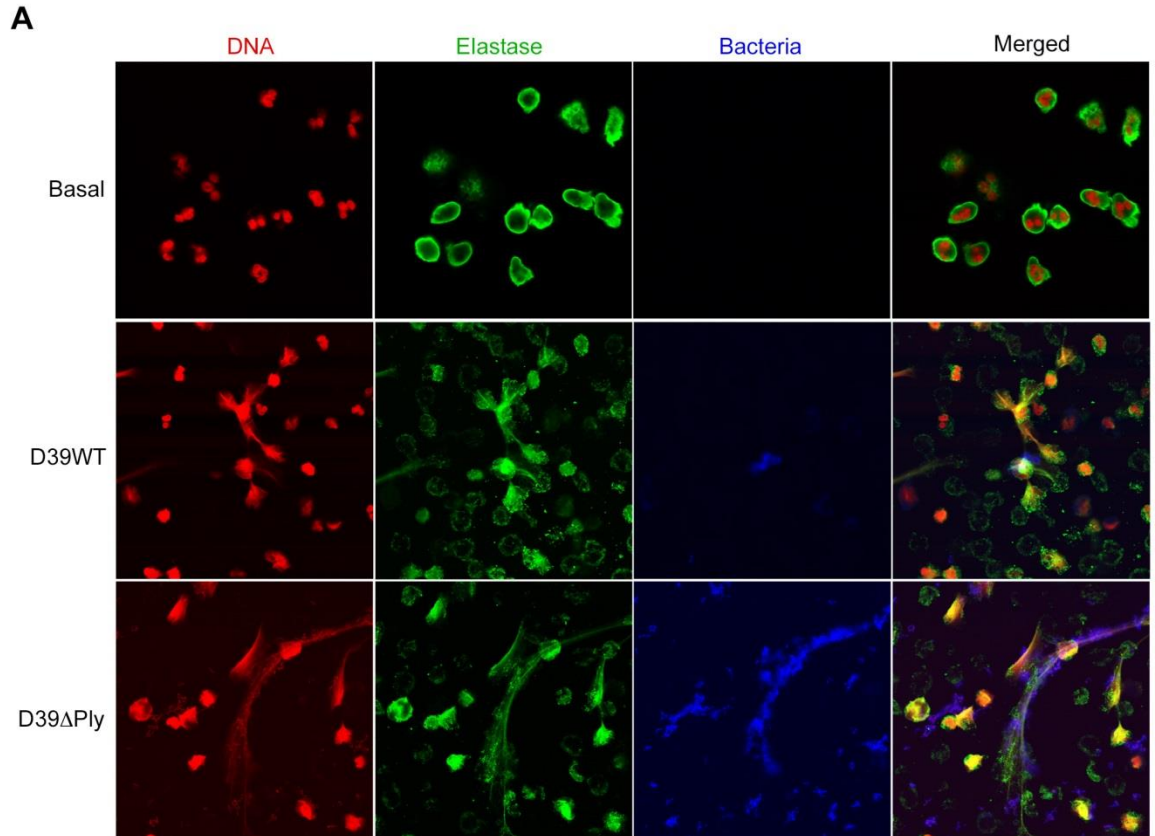


Figure 5.15 NET trapping of *S. pneumoniae* D39 WT and D39 Δ Ply in human neutrophils

(a) Immunofluorescence image of human neutrophils left untreated (Basal) or infected with *S. pneumoniae* D39 WT and D39 Δ Ply (stained blue) at an MOI of 10 for 4 hours. Cells were stained with anti-neutrophil elastase antibody (green) and Sytox orange nucleic acid stain (red).

(b) Bacterial counts (blue stained dots) of *S. pneumoniae* D39 WT and D39 Δ Ply were taken at multiple views and mean SEM of counts were calculated per NET from different experiments. Columns are means of three independent views; error bars are SEM. Asterisks indicates a significant difference from D39 WT, $p < 0.05$ (unpaired t-test).

5.3 Discussion and conclusion

Autophagy induction in human neutrophils following infection with *S. pneumoniae* was clearly demonstrated *in vitro* (Fig. 5.1 - 5.4). There was a stronger induction of autophagy with *S. pneumoniae* strain D39 Δ Ply compared to D39 WT. This suggests that pneumolysin and associated inflammasome activation may affect autophagy induction in infection with this pathogen. Although this difference was not significant, the absolute difference between the strains was not huge. Pneumolysin is required for inflammasome activation following infection, and this may be responsible for the down regulation of autophagy. Equally, another mechanism may be responsible.

We have shown here that autophagy plays an important role in the ability of human neutrophils to kill *S. pneumoniae*. Calculations from the kinetic analysis of killing by neutrophils suggests that when autophagy is inhibited there is a reduction in the rate constant for phagocytosis, k_p but increase in the rate constant of intracellular killing, k_k (Fig. 5.10 and 5.11). This would imply that autophagy is required for efficient phagocytosis of *S. pneumoniae*, but slows intracellular killing.

Phagocytosis is known to have a relationship with autophagy. The study of (Sanjuan et al., 2007) found that LC3 was rapidly recruited to phagosomes which were then targeted to lysosomes, leading to formation of a phagolysosome and enhanced killing of the ingested organism. Interestingly, this occurred apparently without formation of the typical double-membrane autophagosomal structure. This process has been termed LC3- assisted phagocytosis.

The results presented here seem to suggest an alternative mechanism is operating. In our experiments, autophagy increased the efficiency of phagocytosis of the pneumococcus. Given that it is an extracellular bacterium that is able to cause pathological effects, this difference in phagocytic rate is the most important in controlling of infection. Once internalised by neutrophils, even if the bacteria are not killed, they are not able to cause further damage.

Autophagy also seemed to result in a diminution of intracellular killing. This could be because bacteria contained within autophagocytic vacuoles slow

down the direct entry of phagocytosed organisms into the lysosomal degradation pathway. It may also be because of an inhibitory effect of phagocytosed microbes on killing such that when phagocytosis is slowed, killing can proceed more rapidly.

The results reported here also link autophagy with a novel mechanism in neutrophils for pathogen killing called NETosis, the generation of a mesh-like structure formed of nuclear material for trapping and killing bacteria (Brinkmann et al., 2004). *S. pneumoniae* strains D39 WT and D39 Δ Ply induced NET generation, which was similar in both strains (Fig. 5.12). We made two novel observations relating to the role of NETs in killing of *S. pneumoniae*.

Firstly, the formation of NETS within neutrophils following infection was dependent on the autophagy pathway, since 3-MA and *Atg5* knock down significantly inhibited NET formation (Fig. 5.13 and 5.14). Previous studies have suggested that autophagy is essential for NETosis induced by PMA. Typical autophagocytic vesicles are observed during the induction of NETs and inhibiting autophagy with wortmannin prevented NET formation (Remijnsen et al., 2011).

We extend these observations to show that autophagy is essential for NET formation following infection with *S. pneumoniae*. The exact role for autophagy in NET formation is not clear. A role for autophagy in NET formation may also account for the reduction in apparent phagocytosis when autophagy is inhibited, since under these conditions there will be fewer NETs and thus reduced extracellular killing.

Secondly, pneumolysin inhibited the entrapment of bacteria within the NETs (Fig. 5.15). It is not yet clear exactly what actions of pneumolysin are important in evading capture by NETs. In general, pneumolysin acts on membranes to form a pore structure, accounting for its cytolytic activity. Although NETs induced by bacteria with and without pneumolysin appeared morphologically similar, it may be that alteration of the membrane structure of neutrophils by pneumolysin prevents effective NET formation allowing the bacteria to escape entrapment. Further work will help define the molecular mechanisms by which pneumolysin evades NETs.

To conclude, *S. pneumoniae* different strains activate and induce autophagy, phagocytosis and NETosis in human neutrophils which were demonstrated in this chapter. These finding clarified that autophagy is not only induced in murine BMDMs and some cell lines but can also be activated in human neutrophils which are important defence cells.

6 **General Discussion and Conclusions**

6.1 Discussion

S. pneumoniae is a significant human pathogen causing invasive disease in young children, elderly and immunocompromised people. Traditionally pneumococcal diseases are treated with antibiotics or prevented by pneumococcal vaccines. According to the NHS, pneumococcal conjugate vaccines (PCV) are effective against 13 serotypes while pneumococcal polysaccharide vaccines (PPV) provide protection from up to 23 serotypes in 50-70 % of severe diseases. The emerging resistant strains of *S. pneumoniae* can be difficult to treat and alternative antimicrobial strategies are required in high risk individuals.

Autophagy is a conserved degradation pathway which has emerged as a potential new strategy for the control of a variety of microbial infections. This pathway has a potential role in treating many inflammatory and infectious diseases. Reinforcing autophagy with the use of rapamycin increases the clearance of certain microbes *in vitro* and *in vivo* (Junkins et al., 2014). Induction of autophagy in *S. pneumoniae* infection may help prevent lengthy antibiotic treatments and emergence of new multi-drug resistant strains.

The main hypothesis of my study was that *S. pneumoniae* infection induces autophagy. We tested this hypothesis *in vitro* and *in vivo*, and the results presented in this thesis indicate that *S. pneumoniae* infection induced autophagy in primary murine BMDMs, human neutrophils and in a mouse model. We further studied autophagy in *S. pneumoniae* infection by inhibiting it pharmacologically with 3-methyladenine (3MA). It blocks autophagosome formation through the inhibition of type III phosphatidylinositol 3-kinases (PI3K III) required in the early stage of autophagosome formation. Inhibition of PI3K III by 3MA has been shown to inhibit starvation-induced autophagy (Lum et al., 2005).

Our results here showed that 3MA is also able to block *S. pneumoniae* induced autophagy as detected by immunofluorescence and western blot techniques. Many drugs including 3MA induce cell death at doses used for inhibition of autophagy (Sheng et al., 2013), but in our experiments the cell viability measured by LDH release was similar in murine BMDM and human

neutrophils treated and untreated with 3MA. We further confirmed autophagy induction in *S. pneumoniae* infection by studying of different *Atg* genes knock down and autophagy knock-out mice.

We used two strains of *S. pneumoniae* D39 WT and D39 Δ Ply (a pneumolysin deficient strain) and hypothesized that pneumolysin or associated inflammasome activation may down regulate autophagy induction. Pneumolysin intact and deficient strains were first confirmed by haemolysis activity assay and then used for infection.

Our results demonstrated that autophagy induction was present in both D39 WT and D39 Δ Ply strains of *S. pneumoniae*. The pneumolysin intact strain consistently induced a weaker signal as compared to its pneumolysin deficient counterpart, although the absolute difference between these strains was not huge. This effect of ply on the autophagy induction may be direct or due to the associated inflammasome activation. Pneumolysin is a pore-forming toxin and important virulence factor of *S. pneumoniae* which activates the inflammasome and induces the release of inflammatory cytokines (Shoma et al., 2008).

To further confirm the effect of inflammasome and associated caspase-1 activation, we manipulated inflammasome activation and observed its effects on the induction of autophagy in murine BMDMs infected with *S. pneumoniae* D39 WT. We first inhibited inflammasome activation by blocking caspase-1 with an irreversible inhibitor Z-YVAD-FMK (Slee et al., 1996) or genetic knock down by siRNA transfection. We observed a significant increase in autophagy with *S. pneumoniae* infection when the activation of the inflammasome was blocked. The exact mechanism of autophagy up-regulation with inflammasome inhibition is not clearly understood.

Next, we studied the effect of autophagy on inflammasome activation. Autophagy was inhibited pharmacologically with 3MA or genetically with siRNA transfection. Inhibition of *S. pneumoniae* induced autophagy up-regulated inflammasome activation. The exact mechanism by which autophagy induction inhibits inflammasome activation is not clearly understood. One possibility could be a direct interaction between autophagy proteins and inflammasome components, or may be an indirect inhibition of the inflammasome activity via

autophagic sequestration of mitochondria (Sun et al., 2014) and suppression of mitochondrial ROS required for inflammasome activation, or autophagic degradation of PAMPs and danger signals that are required for inflammasome activation. In the latter model, autophagic degradation of mutant superoxide dismutase, linked to a disease Amyotrophic-lateral-sclerosis has been proposed to limit the activation of caspase-1 and IL-1 β production (Meissner et al., 2008). All these findings indicate that both autophagy and inflammasome maintain a fine balance during infection.

Next, we studied phagocytosis of *S. pneumoniae* by murine BMDM and human neutrophils. We hypothesized that autophagy may influence phagocytosis of *S. pneumoniae*. A previous study demonstrated that LC3 was rapidly recruited to phagosomes targeted to lysosomes and then leading to phagolysosome formation. Ingested microorganisms are killed without the formation of a double membrane autophagosome through this process of LC3-associated phagocytosis (Sanjuan et al., 2007). We investigated the role of autophagy in phagocytosis and found that its inhibition with 3MA or knock down with siRNA transfection down regulated phagocytosis of *S. pneumoniae* in both murine BMDM and human neutrophils.

We also investigated the role of *S. pneumoniae* virulence factors in phagocytosis. Previous studies demonstrate that inhibition of virulence factors enhance pneumococcal clearance and phagocytosis (Quin et al., 2007). Our study here also shown the same results and found that inhibition of Ply up-regulated phagocytosis of *S. pneumoniae* which may be a direct effect or due to the associated inflammasome and complement activation. Furthermore, pneumolysin appears to aid the bacterium in avoiding killing by the innate immune cells.

We further investigated a novel mechanism in neutrophils for extracellular trapping and killing pathogens called neutrophil extracellular traps or NETosis (Brinkmann et al., 2004). Previous studies have indicated that autophagy is essential for phorbol myristate acetate (PMA) induced NETosis, and inhibiting autophagy with wortmannin prevented NET formation (Remijsen et al., 2011).

We hypothesized that NETs induced in *S. pneumoniae* infection may have a link with autophagy induction. We tested NET generation in infection with *S. pneumoniae* strains D39 WT and D39 Δ Ply and found that both strains induced morphologically similar NETs. We made two novel observations relating to the role of NETs in killing of *S. pneumoniae*.

Firstly, NETs formation following infection with *S. pneumoniae* were dependent on the autophagy pathway, since 3MA and *Atg5* gene knock down significantly inhibited NET generation. The exact role of autophagy in NET formation is not clearly understood.

Secondly, we also found that pneumolysin inhibited the entrapment of *S. pneumoniae* D39 WT within the NETs. In general, pneumolysin is a pore-forming cytolytic toxin (Marriott et al., 2008) and its exact action in evading capture of *S. pneumoniae* by NETs is not clearly understood. Further work is needed to understand the exact molecular mechanisms by which pneumolysin evades NETs.

Next, we studied the role of some TLR signalling pathways in autophagy induction with *S. pneumoniae* infection. TLRs are a major class of trans-membrane receptors in the mammalian innate immune system. They detect pathogen-associated molecular patterns (PAMPs) and trigger signal transduction cascades to neutralize danger by the invading pathogen (Piras and Selvarajoo, 2014).

Firstly, we investigated the role of major adaptor proteins of TLR signalling in autophagy induction with *S. pneumoniae* infection. There are two major adaptors that bind to the TLR intracellular domain i.e. the myeloid differentiation primary response protein (MyD88) and TIR- domain-containing adapter-inducing interferon- β (TRIF) which upon activation lead to an inflammatory cascade and release inflammatory cytokines (Piras and Selvarajoo, 2014).

We inhibited TRIF and MyD88 using siRNA transfection or gene knock-out mice and then induced autophagy in BMDMs infected with *S. pneumoniae* strains D39 WT and D39 Δ Ply. Our results demonstrated that autophagy induction in *S. pneumoniae* infection is independent of the key adaptor molecules TRIF and

MyD88. *S. pneumoniae* may use some unknown pathway to invoke intracellular response for autophagy induction.

To further expand our understanding of the TLRs, we investigated the role of TLR4 which is believed to be activated by LPS and associates with both TRIF and MyD88 pathways for induction of inflammatory cytokines and type-1 interferon secretion (Bell, 2008). TLR4 is also believed to serve as a sensor for autophagy induction through adaptor protein TRIF when stimulated with LPS (Xu et al., 2007).

We first investigated autophagy induction in macrophages from TLR4-defective (C3H/HeJ) mice having a mutation in the *Lps* gene. Macrophages from the control and mutated strains of these mice both induced autophagy in *S. pneumoniae* infection when followed by the conversion of LC3 I to LC3 II.

To further extend these observations, we used TLR4^{-/-} mice and induced autophagy in BMDMs with *S. pneumoniae* infection. We found that TLR4^{-/-} mice induced autophagy exactly the same way as WT mice when infected with *S. pneumoniae* strains D39 WT and D39 ΔPly. Our results indicated that autophagy induction with *S. pneumoniae* infection is independent of TLR4 pathway and some other unknown pathway may be used by this pathogen.

Next, we also studied the role of TLR2 in autophagy induction. Previous studies have demonstrated that TLR2 is necessary for efficient clearance of *S. pneumoniae* colonisation and is critical for induction of autophagy and phagocytosis in *S. aureus* (van Rossum et al., 2005, Fang et al., 2014). We blocked TLR2 in murine BMDMs and induced autophagy with *S. pneumoniae* infection compared to an important TLR2 ligand Pam3CSK4.

We found that autophagy was induced equally in TLR2 blocked cells and its isotype control when stimulated with *S. pneumoniae* strains D39 WT and D39 ΔPly when compared with Pam3CSK4. These observations indicated that TLR2 pathway is not used by *S. pneumoniae* for autophagy induction and some other unknown signalling pathway may be used which needs further exploration.

To further extend our search for the PRR signalling in *S. pneumoniae* induced autophagy, we studied the role of an intracellular PRR NOD2 which recognizes molecules containing a specific structure muramyl dipeptide present in peptidoglycans from certain bacteria (Girardin et al., 2003). We activated NOD2 using muramyl dipeptide (MDP) and its control (MDPc) for 6-24 hours. Our results demonstrated that autophagy was not induced in murine BMDMs in cells treated with MDP and MDPc. This indicated that NOD2 has no role in autophagy induction.

Next, we investigated another potential pathway and looked for the effect of a Mitogen-activated protein kinase (P38-MAPK) in autophagy induction with *S. pneumoniae* infection. P38-MAP kinase pathway is involved in regulation of inflammasome and production of inflammatory cytokines (Yang et al., 2014). This pathway is also believed to induce autophagy in response to IFN- γ in macrophages (Matsuzawa et al., 2014).

We blocked p38MAP kinase with its specific inhibitor SB203580 and autophagy was induced with *S. pneumoniae* D39 WT and D39 Δ Ply, and LPS. Autophagy induction was not affected in cells blocked with p38MAP kinase inhibitor when infected with *S. pneumoniae* D39 WT and D39 Δ Ply. This indicated that this pathway has no role in autophagy induction with *S. pneumoniae* infection.

Finally we studied autophagy pathway in an *in vivo* mouse model and found that *S. pneumoniae* infection induced autophagy which was up-regulated by Rapamycin and inhibited by 3MA. Furthermore autophagy induction was associated with increased clearance of *S. pneumoniae* from the peritoneal cavity while blocking this pathway decreased the clearance of bacteria.

Next, we also studied inflammasome activation *in vivo* and found that *S. pneumoniae* induced autophagy has some inhibitory effect as shown by the decrease of inflammatory cytokines in serum and protein content of peritoneal lavage. Furthermore, autophagy inhibition produced the opposite effects and inflammsome was up-regulated.

These findings confirmed our hypothesis both *in vitro* and *in vivo*. Autophagy and inflammasome maintain a fine balance which could be manipulated and used for controlling *S. pneumoniae* infections.

6.2 Conclusion

In conclusion, this thesis demonstrates that *S. pneumoniae* induces autophagy both *in vitro* and *in vivo*. Autophagy induction is a novel finding in *S. pneumoniae* infection. Both D39 WT and D39 Δ Ply strains of *S. pneumoniae* induced autophagy and phagocytosis in murine bone marrow derived macrophages and human neutrophils. There was a clear difference in the autophagy signal and phagocytosis induced by both these strains. Pneumolysin deficient strain induced stronger autophagy and phagocytosis as compared to the wild type strain. This indicates that pneumolysin might have some effect on these immune pathways besides the inflammasome activation against invading pathogens.

When the inflammasome was chemically or genetically inhibited, *S. pneumoniae* induced autophagy was up-regulated. This suggests that pneumolysin induced inflammasome activation normally inhibits autophagy. Similarly, autophagy inhibition by chemical methods and siRNA knock down produced an inhibitory effect on the inflammasome activation. These findings indicate that both these immune pathways maintain a fine balance, and disturbance in any of these pathways may lead to abnormal immune responses against invading pathogens.

Autophagy inhibition in murine BMDMs and human neutrophils down regulated phagocytosis, which indicates an association between these two pathways. We found that autophagy plays a regulatory role in bacterial phagocytosis and clearance rather than early internalisation of *S. pneumoniae*. Both autophagy and phagocytosis are intracellular killing pathways for the elimination of invading pathogens. Our data shows that autophagy increases phagocytosis of *S. pneumoniae*, but decreases its killing. The exact mechanism is not clearly understood but once the microbe is phagocytosed, its chances of spread decreases which explains the importance of these pathways. When autophagosome and phagosome fuses with the lysosome to form autolysosome

and phagolysosome, the internalised microbe is then degraded by the action of lysosomal proteases.

Furthermore, our data shows that activation of neutrophils with *S. pneumoniae* induces neutrophil extracellular traps (NETs) generation. NETs are used as an extracellular microbial trapping and killing strategy by the activated neutrophils. We found that *S. pneumoniae* induced NET generation depends on autophagy. When we blocked autophagy by chemical method or genetic knock down, *S. pneumoniae* induced NET generation was down regulated. This indicates that this extracellular microbial killing mechanism works in association with the intracellular pathways. This explains that these intracellular and extracellular microbial killing strategies of the immune cells are activated by sensing microbial PAMPs, which function in association for the host defence.

It is possible that different pathogens may react differently to the autophagy pathway and will show different patterns of its activation. However autophagy could play different roles with different types of pathogens and different cells. Our study herein represents the evidence for autophagy induction by *S. pneumoniae*, an extracellular gram positive bacterium. This suggests that this ancient defence mechanism plays a role against extracellular pathogens as well.

Thus, *S. pneumoniae* could be used as a model pathogen to investigate the impact of autophagy on different important protective cellular events such as phagocytosis, NETosis, destroying the microbial virulence factors, killing bacteria and finally clearance of microbes for the host defence. Study of autophagy pathway in neutrophils may also prove helpful to investigate the neutrophil- induced inflammatory diseases

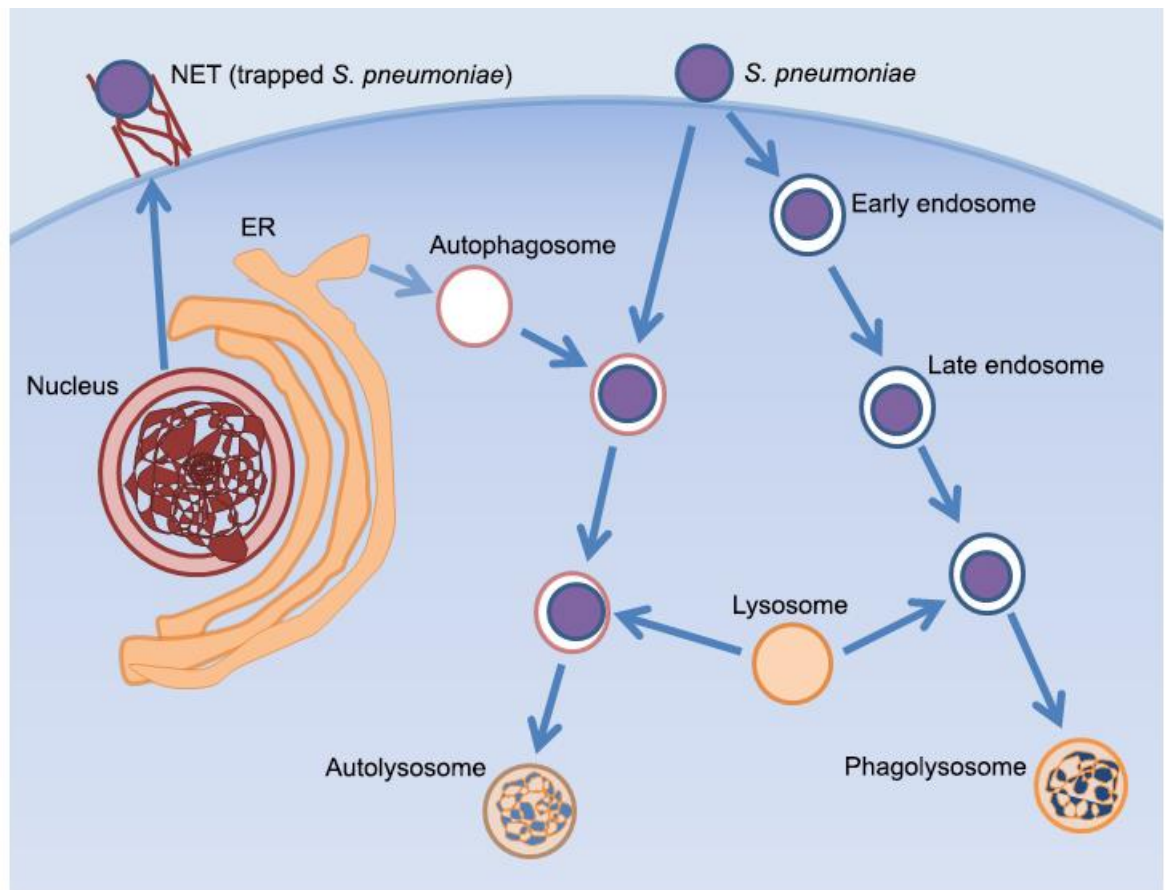


Figure 6.1 Schematic representation of autophagy, phagocytosis and NETosis

Invading pathogens are internalised and taken up by endosome or autophagosome. Autophagosome and phagosome then fuses with the lysosome to form autolysosome and phagosome respectively. Invading pathogen is then degraded by the release of lysosomal proteases.

Neutrophils are activated by the invading pathogens which release neutrophil extracellular traps from the nuclei. NETs then trap and kill invading microbes extracellularly, figure adapted from (Ham et al., 2011).

6.3 Future Plans

The following studies may help in investigating autophagy in *S. pneumoniae* infection.

- i. Investigating autophagy and associated pathways *in vivo*.
- ii. Investigating the role of different autophagy inducer and inhibitor drugs in *S. pneumoniae* induced autophagy *in vivo*.

- iii. Study of pharmacological manipulation of *S. pneumoniae* induced autophagy and its therapeutic benefits.
- iv. Study of multiple PRRs and their role in *S. pneumoniae* induced autophagy
- v. Study of autophagy in different pathogenic and non-pathogenic *S. pneumoniae* strains
- vi. Study of the molecular mechanisms involved in inflammasome down-regulation with autophagy induction and vice versa.
- vii. Investigating the role of *S. pneumoniae* induced autophagy in innate and adaptive immunity.
- viii. Exploration of molecular mechanisms of autophagy, phagocytosis and NETosis to further link these important immune pathways.

References

- ADEREM, A. & UNDERHILL, D. M. 1999. Mechanisms of phagocytosis in macrophages. *Annu Rev Immunol*, 17, 593-623.
- AKIRA, S. & TAKEDA, K. 2004. Toll-like receptor signalling. *Nat Rev Immunol*, 4, 499-511.
- AKIRA, S., UEMATSU, S. & TAKEUCHI, O. 2006. Pathogen Recognition and Innate Immunity. *Cell*, 124, 783-801.
- ALBIGER, B., DAHLBERG, S., SANDGREN, A., WARTHA, F., BEITER, K., KATSURAGI, H., AKIRA, S., NORMARK, S. & HENRIQUES-NORMARK, B. 2007. Toll-like receptor 9 acts at an early stage in host defence against pneumococcal infection. *Cellular Microbiology*, 9, 633-644.
- AMULIC, B., CAZALET, C., HAYES, G. L., METZLER, K. D. & ZYCHLINSKY, A. 2012. Neutrophil Function: From Mechanisms to Disease. *Annual Review of Immunology*, 30, 459-489.
- ANAND, P. K., TAIT, S. W. G., LAMKANFI, M., AMER, A. O., NUNEZ, G., PAGÈS, G., POUYSSÉGUR, J., MCGARGILL, M. A., GREEN, D. R. & KANNEGANTI, T.-D. 2011. TLR2 and RIP2 Pathways Mediate Autophagy of *Listeria monocytogenes* via Extracellular Signal-regulated Kinase (ERK) Activation. *Journal of Biological Chemistry*, 286, 42981-42991.
- AO, X., ZOU, L. & WU, Y. 2014. Regulation of autophagy by the Rab GTPase network. *Cell Death Differ*, 21, 348-58.
- ARANCIBIA, S. A., BELTRAN, C. J., AGUIRRE, I. M., SILVA, P., PERALTA, A. L., MALINARICH, F. & HERMOSO, M. A. 2007. Toll-like receptors are key participants in innate immune responses. *Biol Res*, 40, 97-112.
- ARLEHAMN, C. S. L., PÉTRILLI, V., GROSS, O., TSCHOPP, J. & EVANS, T. J. 2010. The Role of Potassium in Inflammasome Activation by Bacteria. *Journal of Biological Chemistry*, 285, 10508-10518.
- ARULANANDAM, B. P., LYNCH, J. M., BRILES, D. E., HOLLINGSHEAD, S. & METZGER, D. W. 2001. Intranasal vaccination with pneumococcal surface protein A and interleukin-12 augments antibody-mediated opsonization and protective immunity against *Streptococcus pneumoniae* infection. *Infect Immun*, 69, 6718-24.
- AUSTYN, J. M. & GORDON, S. 1981. F4/80, a monoclonal antibody directed specifically against the mouse macrophage. *European Journal of Immunology*, 11, 805-815.

- AXE, E. L., WALKER, S. A., MANIFAVA, M., CHANDRA, P., RODERICK, H. L., HABERMANN, A., GRIFFITHS, G. & KTISTAKIS, N. T. 2008. Autophagosome formation from membrane compartments enriched in phosphatidylinositol 3-phosphate and dynamically connected to the endoplasmic reticulum. *J Cell Biol*, 182, 685-701.
- BALACHANDRAN, P., BROOKS-WALTER, A., VIROLAINEN-JULKUNEN, A., HOLLINGSHEAD, S. K. & BRILES, D. E. 2002. Role of Pneumococcal Surface Protein C in Nasopharyngeal Carriage and Pneumonia and Its Ability To Elicit Protection against Carriage of *Streptococcus pneumoniae*. *Infection and immunity*, 70, 2526-2534.
- BELL, E. 2008. Innate immunity: TLR4 signalling. *Nat Rev Immunol*, 8, 241-241.
- BELLA, J., HINDLE, K. L., MCEWAN, P. A. & LOVELL, S. C. 2008. The leucine-rich repeat structure. *Cellular and Molecular Life Sciences*, 65, 2307-2333.
- BELODU, R., S, N., R, R., KUMAR, R. & B, A. C. 2013. A pneumococcal brain abscess: a case report. *J Clin Diagn Res*, 7, 1694-5.
- BENOIT, M., DESNUES, B. & MEGE, J.-L. 2008. Macrophage Polarization in Bacterial Infections. *The Journal of Immunology*, 181, 3733-3739.
- BENTLEY, S. D., AANENSEN, D. M., MAVROIDI, A., SAUNDERS, D., RABBINOWITSCH, E., COLLINS, M., DONOHOE, K., HARRIS, D., MURPHY, L., QUAIL, M. A., SAMUEL, G., SKOVSTED, I. C., KALTOFT, M. S., BARRELL, B., REEVES, P. R., PARKHILL, J. & SPRATT, B. G. 2006. Genetic analysis of the capsular biosynthetic locus from all 90 pneumococcal serotypes. *PLoS Genet*, 2, e31.
- BLASIUS, A. L. & BEUTLER, B. 2010. Intracellular toll-like receptors. *Immunity*, 32, 305-15.
- BOGAERT, D., DE GROOT, R. & HERMANS, P. W. 2004. *Streptococcus pneumoniae* colonisation: the key to pneumococcal disease. *Lancet Infect Dis*, 4, 144-54.
- BONARDI, V., CHERKIS, K., NISHIMURA, M. T. & DANGL, J. L. 2012. A new eye on NLR proteins: focused on clarity or diffused by complexity? *Curr Opin Immunol*, 24, 41-50.
- BOURNE, H. R. & WEINER, O. 2002. Cell polarity: A chemical compass. *Nature*, 419, 21.
- BOUZA, E., PINTADO, V., RIVERA, S., BLAZQUEZ, R., MUNOZ, P., CERCENADO, E., LOZA, E., RODRIGUEZ-CREIXEMS, M., MORENO, S. & SPANISH PNEUMOCOCCAL INFECTION STUDY, N. 2005. Nosocomial bloodstream infections caused by *Streptococcus pneumoniae*. *Clin Microbiol Infect*, 11, 919-24.

- BOYTON, R. J. & OPENSHAW, P. J. 2002. Pulmonary defences to acute respiratory infection. *British Medical Bulletin*, 61, 1-12.
- BRAUN, J. S., NOVAK, R., GAO, G., MURRAY, P. J. & SHENEP, J. L. 1999. Pneumolysin, a protein toxin of *Streptococcus pneumoniae*, induces nitric oxide production from macrophages. *Infect Immun*, 67, 3750-6.
- BRILES, D. E., NOVAK, L., HOTOMI, M., VAN GINKEL, F. W. & KING, J. 2005. Nasal colonization with *Streptococcus pneumoniae* includes subpopulations of surface and invasive pneumococci. *Infect Immun*, 73, 6945-51.
- BRINKMANN, V., REICHARD, U., GOOSMANN, C., FAULER, B., UHLEMANN, Y., WEISS, D. S., WEINRAUCH, Y. & ZYCHLINSKY, A. 2004. Neutrophil extracellular traps kill bacteria. *Science*, 303, 1532-5.
- BROOK, I. 2011. Microbiology of sinusitis. *Proc Am Thorac Soc*, 8, 90-100.
- BROWN, G. D. 2006. Dectin-1: a signalling non-TLR pattern-recognition receptor. *Nat Rev Immunol*, 6, 33-43.
- BRUEGGEMANN, A. B., PAI, R., CROOK, D. W. & BEALL, B. 2007. Vaccine escape recombinants emerge after pneumococcal vaccination in the United States. *PLoS Pathog*, 3, e168.
- BRYANT, C. & FITZGERALD, K. A. 2009. Molecular mechanisms involved in inflammasome activation. *Trends in cell biology*, 19, 455-464.
- CAMPOY, E. & COLOMBO, M. 2009. Autophagy Subversion by Bacteria. In: LEVINE, B., YOSHIMORI, T. & DERETIC, V. (eds.) *Autophagy in Infection and Immunity*. Springer Berlin Heidelberg.
- CARDOZO, D. M., NASCIMENTO-CARVALHO, C. M., ANDRADE, A. L., SILVANYNETO, A. M., DALTRO, C. H., BRANDAO, M. A., BRANDAO, A. P. & BRANDILEONE, M. C. 2008. Prevalence and risk factors for nasopharyngeal carriage of *Streptococcus pneumoniae* among adolescents. *J Med Microbiol*, 57, 185-9.
- CARTWRIGHT, K. 2002. Pneumococcal disease in western Europe: burden of disease, antibiotic resistance and management. *Eur J Pediatr*, 161, 188-95.
- CHAN, E. Y., KIR, S. & TOOZE, S. A. 2007. siRNA screening of the kinome identifies ULK1 as a multidomain modulator of autophagy. *J Biol Chem*, 282, 25464-74.
- CHEW, L. & YIP, C. 2014. Structural biology of the macroautophagy machinery. *Frontiers in Biology*, 9, 18-34.

- CLARKE, T. B., FRANCELLA, N., HUEGEL, A. & WEISER, J. N. 2011. Invasive bacterial pathogens exploit TLR-mediated downregulation of tight junction components to facilitate translocation across the epithelium. *Cell Host Microbe*, 9, 404-14.
- COHEN, G. M. 1997. Caspases: the executioners of apoptosis. *Biochem J*, 326 (Pt 1), 1-16.
- CORNICK, J. E., EVERETT, D. B., BROUGHTON, C., DENIS, B. B., BANDA, D. L., CARROL, E. D. & PARRY, C. M. 2011. Invasive *Streptococcus pneumoniae* in children, Malawi, 2004-2006. *Emerg Infect Dis*, 17, 1107-9.
- DAVIS, K. M., NAKAMURA, S. & WEISER, J. N. 2011. Nod2 sensing of lysozyme-digested peptidoglycan promotes macrophage recruitment and clearance of *S. pneumoniae* colonisation in mice. *J Clin Invest*, 121, 3666-76.
- DELGADO, M. A., ELMAOUED, R. A., DAVIS, A. S., KYEI, G. & DERETIC, V. 2008. Toll-like receptors control autophagy. *The EMBO journal*, 27, 1110-21.
- DERETIC, V. 2006. Autophagy as an immune defense mechanism. *Current Opinion in Immunology*, 18, 375-382.
- DERETIC, V. 2012. Autophagy as an innate immunity paradigm: expanding the scope and repertoire of pattern recognition receptors. *Curr Opin Immunol*, 24, 21-31.
- DERETIC, V., DELGADO, M., VERGNE, I., MASTER, S., DE HARO, S., PONPUAK, M. & SINGH, S. 2009a. Autophagy in immunity against mycobacterium tuberculosis: a model system to dissect immunological roles of autophagy. *Curr Top Microbiol Immunol*, 335, 169-88.
- DERETIC, V., LEVINE, B., DERETIC, V. & LEVINE, B. 2009b. Autophagy, immunity, and microbial adaptations. *Cell Host & Microbe*, 5, 527-49.
- DESSING, M. C., SCHOUTEN, M., DRAING, C., LEVI, M., VON AULOCK, S. & VAN DER POLL, T. 2008. Role played by Toll-like receptors 2 and 4 in lipoteichoic acid-induced lung inflammation and coagulation. *J Infect Dis*, 197, 245-52.
- DETER, R. L. & DE DUVE, C. 1967. Influence of glucagon, an inducer of cellular autophagy, on some physical properties of rat liver lysosomes. *J Cell Biol*, 33, 437-49.
- DINARELLO, C. A. 1988. Biology of interleukin 1. *The FASEB Journal*, 2, 108-15.
- DINARELLO, C. A. 2009. Immunological and inflammatory functions of the interleukin-1 family. *Annu Rev Immunol*, 27, 519-50.

- DINARELLO, C. A. 2011. Interleukin-1 in the pathogenesis and treatment of inflammatory diseases. *Blood*, 117, 3720-32.
- DOCKRELL, D. H., LEE, M., LYNCH, D. H. & READ, R. C. 2001. Immune-Mediated Phagocytosis and Killing of *Streptococcus pneumoniae* Are Associated with Direct and Bystander Macrophage Apoptosis. *Journal of Infectious Diseases*, 184, 713-722.
- DOCKRELL, D. H., WHYTE, M. K. & MITCHELL, T. J. 2012. Pneumococcal pneumonia: mechanisms of infection and resolution. *Chest*, 142, 482-91.
- DREUX, M., GASTAMINZA, P., WIELAND, S. F. & CHISARI, F. V. 2009. The autophagy machinery is required to initiate hepatitis C virus replication. *Proc Natl Acad Sci U S A*, 106, 14046-51.
- DUPONT, N., LACAS-GERVAIS, S., BERTOUT, J., PAZ, I., FRECHE, B., VAN NHIEU, G. T., VAN DER GOOT, F. G., SANSONETTI, P. J. & LAFONT, F. 2009. *Shigella* phagocytic vacuolar membrane remnants participate in the cellular response to pathogen invasion and are regulated by autophagy. *Cell host & microbe*, 6, 137-49.
- EARNSHAW, W. C., MARTINS, L. M. & KAUFMANN, S. H. 1999. Mammalian caspases: structure, activation, substrates, and functions during apoptosis. *Annu Rev Biochem*, 68, 383-424.
- EDER, C. 2009. Mechanisms of interleukin-1 β release. *Immunobiology*, 214, 543-53.
- FADEEL, B., ÅHLIN, A., HENTER, J.-I., ORRENIUS, S. & HAMPTON, M. B. 1998. Involvement of Caspases in Neutrophil Apoptosis: Regulation by Reactive Oxygen Species. *Blood*, 92, 4808-4818.
- FAIRWEATHER, D. & CIHAKOVA, D. 2009. Alternatively activated macrophages in infection and autoimmunity. *Journal of Autoimmunity*, 33, 222-230.
- FANG, L., WU, H. M., DING, P. S. & LIU, R. Y. 2014. TLR2 mediates phagocytosis and autophagy through JNK signaling pathway in *Staphylococcus aureus*-stimulated RAW264.7 cells. *Cell Signal*, 26, 806-14.
- FANG, R., TSUCHIYA, K., KAWAMURA, I., SHEN, Y., HARA, H., SAKAI, S., YAMAMOTO, T., FERNANDES-ALNEMRI, T., YANG, R., HERNANDEZ-CUELLAR, E., DEWAMITTA, S. R., XU, Y., QU, H., ALNEMRI, E. S. & MITSUYAMA, M. 2011. Critical roles of ASC inflammasomes in caspase-1 activation and host innate resistance to *Streptococcus pneumoniae* infection. *J Immunol*, 187, 4890-9.
- FAUSTIN, B., LARTIGUE, L., BRUEY, J.-M., LUCIANO, F., SERGIENKO, E., BAILLY-MAITRE, B., VOLKMANN, N., HANEIN, D., ROUILLER, I. & REED, J. C. 2007.

Reconstituted NALP1 Inflammasome Reveals Two-Step Mechanism of Caspase-1 Activation. *Molecular Cell*, 25, 713-724.

- FENOLL, A., MUÑOZ, R., GARCIA, E. & DE LA CAMPA, A. G. 1994. Molecular basis of the optochin-sensitive phenotype of pneumococcus: characterization of the genes encoding the F0 complex of the *S. pneumoniae* *S. oralis* H⁺-ATPases. *Molecular Microbiology*, 12, 587-598.
- FERNANDES-ALNEMRI, T., YU, J.-W., DATTA, P., WU, J. & ALNEMRI, E. S. 2009. AIM2 activates the inflammasome and cell death in response to cytoplasmic DNA. *Nature*, 458, 509-513.
- FERRERO-MILIANI, L., NIELSEN, O. H., ANDERSEN, P. S. & GIRARDIN, S. E. 2007. Chronic inflammation: importance of NOD2 and NALP3 in interleukin-1beta generation. *Clin Exp Immunol*, 147, 227-35.
- FIMIA, G. M., STOYKOVA, A., ROMAGNOLI, A., GIUNTA, L., DI BARTOLOMEO, S., NARDACCI, R., CORAZZARI, M., FUOCO, C., UCAR, A., SCHWARTZ, P., GRUSS, P., PIACENTINI, M., CHOWDHURY, K. & CECCONI, F. 2007. Ambra1 regulates autophagy and development of the nervous system. *Nature*, 447, 1121-5.
- FINK, S. L. & COOKSON, B. T. 2005. Apoptosis, Pyroptosis, and Necrosis: Mechanistic Description of Dead and Dying Eukaryotic Cells. *Infection and Immunity*, 73, 1907-1916.
- FRANCHI, L., MUNOZ-PLANILLO, R. & NUNEZ, G. 2012. Sensing and reacting to microbes through the inflammasomes. *Nat Immunol*, 13, 325-332.
- FRANCHI, L., PARK, J. H., SHAW, M. H., MARINA-GARCIA, N., CHEN, G., KIM, Y. G. & NUNEZ, G. 2008. Intracellular NOD-like receptors in innate immunity, infection and disease. *Cell Microbiol*, 10, 1-8.
- FRITZ, T., NIEDERREITER, L., ADOLPH, T., BLUMBERG, R. S. & KASER, A. 2011. Crohn's disease: NOD2, autophagy and ER stress converge. *Gut*, 60, 1580-1588.
- FUCHS, T. A., ABED, U., GOOSMANN, C., HURWITZ, R., SCHULZE, I., WAHN, V., WEINRAUCH, Y., BRINKMANN, V. & ZYCHLINSKY, A. 2007. Novel cell death program leads to neutrophil extracellular traps. *The Journal of Cell Biology*, 176, 231-241.
- FUJITA, N., ITOH, T., OMORI, H., FUKUDA, M., NODA, T. & YOSHIMORI, T. 2008. The Atg16L complex specifies the site of LC3 lipidation for membrane biogenesis in autophagy. *Molecular biology of the cell*, 19, 2092-100.
- GELDHOFF, M., MOOK-KANAMORI, B. B., BROUWER, M. C., TROOST, D., LEEMANS, J. C., FLAVELL, R. A., VAN DER ENDE, A., VAN DER POLL, T. & VAN DE BEEK, D. 2013. Inflammasome activation mediates inflammation

and outcome in humans and mice with pneumococcal meningitis. *BMC Infect Dis*, 13, 358.

- GIRARDIN, S. E., BONECA, I. G., VIALA, J., CHAMAILLARD, M., LABIGNE, A., THOMAS, G., PHILPOTT, D. J. & SANSONETTI, P. J. 2003. Nod2 Is a General Sensor of Peptidoglycan through Muramyl Dipeptide (MDP) Detection. *Journal of Biological Chemistry*, 278, 8869-8872.
- GIRARDIN, S. E. & PHILPOTT, D. J. 2004. Mini-review: the role of peptidoglycan recognition in innate immunity. *Eur J Immunol*, 34, 1777-82.
- GOMES, LIGIA C. & DIKIC, I. 2014. Autophagy in Antimicrobial Immunity. *Molecular cell*, 54, 224-233.
- GORDON, S. & MARTINEZ, F. O. 2010. Alternative Activation of Macrophages: Mechanism and Functions. *Immunity*, 32, 593-604.
- GORDON, S. B., JAGOE, R. T., JARMAN, E. R., NORTH, J. C., PRIDMORE, A., MUSAYA, J., FRENCH, N., ZIJLSTRA, E. E., MOLYNEUX, M. E. & READ, R. C. 2013. The alveolar microenvironment of patients infected with *human immunodeficiency virus* does not modify alveolar macrophage interactions with *Streptococcus pneumoniae*. *Clin Vaccine Immunol*, 20, 882-91.
- GRAY, B. M., CONVERSE, G. M., 3RD & DILLON, H. C., JR. 1980. Epidemiologic studies of *Streptococcus pneumoniae* in infants: acquisition, carriage, and infection during the first 24 months of life. *J Infect Dis*, 142, 923-33.
- GRÉGOIRE, I. P., RICHETTA, C., MEYNIEL-SCHICKLIN, L., BOREL, S., PRADEZYNSKI, F., DIAZ, O., DELOIRE, A., AZOCAR, O., BAGUET, J., LE BRETON, M., MANGEOT, P. E., NAVRATIL, V., JOUBERT, P.-E., FLACHER, M., VIDALAIN, P.-O., ANDRÉ, P., LOTTEAU, V., BIARD-PIECHACZYK, M., RABOURDIN-COMBE, C. & FAURE, M. 2011. IRGM Is a Common Target of RNA Viruses that Subvert the Autophagy Network. *PLoS Pathog*, 7, e1002422.
- HAILEY, D. W., RAMBOLD, A. S., SATPUTE-KRISHNAN, P., MITRA, K., SOUGRAT, R., KIM, P. K. & LIPPINCOTT-SCHWARTZ, J. 2010. Mitochondria supply membranes for autophagosome biogenesis during starvation. *Cell*, 141, 656-67.
- HAM, H., SREELATHA, A. & ORTH, K. 2011. Manipulation of host membranes by bacterial effectors. *Nat Rev Microbiol*, 9, 635-46.
- HAMANN, J., KONING, N., POWWELS, W., ULFMAN, L. H., VAN EIJK, M., STACEY, M., LIN, H.-H., GORDON, S. & KWAKKENBOS, M. J. 2007. EMR1, the human homolog of F4/80, is an eosinophil-specific receptor. *European Journal of Immunology*, 37, 2797-2802.

- HAMERS, M., BOT, A., WEENING, R., SIPS, H. & ROOS, D. 1984. Kinetics and mechanism of the bactericidal action of human neutrophils against *Escherichia coli*. *Blood*, 64, 635-641.
- HAMPTON, M. B., VISSERS, M. C. & WINTERBOURN, C. C. 1994. A single assay for measuring the rates of phagocytosis and bacterial killing by neutrophils. *J Leukoc Biol*, 55, 147-52.
- HAMPTON, M. B. & WINTERBOURN, C. C. 1999. Methods for quantifying phagocytosis and bacterial killing by human neutrophils. *J Immunol Methods*, 232, 15-22.
- HARRIS, J., HARTMAN, M., ROCHE, C., ZENG, S. G., O'SHEA, A., SHARP, F. A., LAMBE, E. M., CREAGH, E. M., GOLENBOCK, D. T., TSCHOPP, J., KORNFELD, H., FITZGERALD, K. A. & LAVELLE, E. C. 2011. Autophagy controls IL-1 β secretion by targeting pro-IL-1 β for degradation. *J Biol Chem*, 286, 9587-97.
- HAUSDORFF, W. P., YOTHERS, G., DAGAN, R., KILPI, T., PELTON, S. I., COHEN, R., JACOBS, M. R., KAPLAN, S. L., LEVY, C., LOPEZ, E. L., MASON, E. O., JR., SYRIOPOULOU, V., WYNNE, B. & BRYANT, J. 2002. Multinational study of pneumococcal serotypes causing acute otitis media in children. *Pediatr Infect Dis J*, 21, 1008-16.
- HEATH, R. J. & XAVIER, R. J. 2009. Autophagy, immunity and human disease. *Current opinion in gastroenterology*, 25, 512-20.
- HENDERSON, P. & STEVENS, C. 2012. The role of autophagy in Crohn's disease. *Cells*, 1, 492-519.
- HEYWORTH, P. G., CROSS, A. R. & CURNUTTE, J. T. 2003. Chronic granulomatous disease. *Current Opinion in Immunology*, 15, 578-584.
- HILLER, N. L., AHMED, A., POWELL, E., MARTIN, D. P., EUTSEY, R., EARL, J., JANTO, B., BOISSY, R. J., HOGG, J., BARBADORA, K., SAMPATH, R., LONERGAN, S., POST, J. C., HU, F. Z. & EHRLICH, G. D. 2010. Generation of genic diversity among *Streptococcus pneumoniae* strains via horizontal gene transfer during a chronic polyclonal pediatric infection. *PLoS Pathog*, 6, e1001108.
- HOCHREIN, H. & KIRSCHNING, C. J. 2013. Bacteria evade immune recognition via TLR13 and binding of their 23S rRNA by MLS antibiotics by the same mechanisms. *Oncoimmunology*, 2, e23141.
- HOFFMAN, H. M., ROSENGREN, S., BOYLE, D. L., CHO, J. Y., NAYAR, J., MUELLER, J. L., ANDERSON, J. P., WANDERER, A. A. & FIRESTEIN, G. S. 2004. Prevention of cold-associated acute inflammation in familial cold autoinflammatory syndrome by interleukin-1 receptor antagonist. *Lancet*, 364, 1779-85.

- HOMER, C. R., RICHMOND, A. L., REBERT, N. A., ACHKAR, J. P. & MCDONALD, C. 2010. ATG16L1 and NOD2 Interact in an Autophagy-Dependent Antibacterial Pathway Implicated in Crohn's Disease Pathogenesis. *Gastroenterology*, 139, 1630-1641.e2.
- HOPKINSON-WOOLLEY, J., HUGHES, D., GORDON, S. & MARTIN, P. 1994. Macrophage recruitment during limb development and wound healing in the embryonic and foetal mouse. *Journal of Cell Science*, 107, 1159-1167.
- HORNUNG, V., ABLASSER, A., CHARREL-DENNIS, M., BAUERNFEIND, F., HORVATH, G., CAFFREY, D. R., LATZ, E. & FITZGERALD, K. A. 2009. AIM2 recognizes cytosolic dsDNA and forms a caspase-1-activating inflammasome with ASC. *Nature*, 458, 514-518.
- HOULDSWORTH, S., ANDREW, P. W. & MITCHELL, T. J. 1994. Pneumolysin stimulates production of tumor necrosis factor alpha and interleukin-1 beta by human mononuclear phagocytes. *Infect Immun*, 62, 1501-3.
- HSIEH, Y. C., LEE, W. S., SHAO, P. L., CHANG, L. Y. & HUANG, L. M. 2008. The transforming *Streptococcus pneumoniae* in the 21st century. *Chang Gung Med J*, 31, 117-24.
- HUETT, A., NG, A., CAO, Z., KUBALLA, P., KOMATSU, M., DALY, M. J., PODOLSKY, D. K. & XAVIER, R. J. 2009. A novel hybrid yeast-human network analysis reveals an essential role for FBNP1L in antibacterial autophagy. *J Immunol*, 182, 4917-30.
- HYAMS, C., CAMBERLEIN, E., COHEN, J. M., BAX, K. & BROWN, J. S. 2010. The *Streptococcus pneumoniae* Capsule Inhibits Complement Activity and Neutrophil Phagocytosis by Multiple Mechanisms. *Infection and immunity*, 78, 704-715.
- HYTTINEN, J. M. T., NIITTYKOSKI, M., SALMINEN, A. & KAARNIRANTA, K. 2013. Maturation of autophagosomes and endosomes: A key role for Rab7. *Biochimica et Biophysica Acta (BBA) - Molecular Cell Research*, 1833, 503-510.
- IANNELLI, F., CHIAVOLINI, D., RICCI, S., OGGIONI, M. R. & POZZI, G. 2004. Pneumococcal surface protein C contributes to sepsis caused by *Streptococcus pneumoniae* in mice. *Infect Immun*, 72, 3077-80.
- INOHARA, N., KOSEKI, T., DEL PESO, L., HU, Y., YEE, C., CHEN, S., CARRIO, R., MERINO, J., LIU, D., NI, J. & NÚÑEZ, G. 1999. Nod1, an Apaf-1-like Activator of Caspase-9 and Nuclear Factor- κ B. *Journal of Biological Chemistry*, 274, 14560-14567.
- ISHII, K. J., KOYAMA, S., NAKAGAWA, A., COBAN, C. & AKIRA, S. 2008. Host Innate Immune Receptors and Beyond: Making Sense of Microbial Infections. *Cell host & microbe*, 3, 352-363.

- ITAKURA, A. & MCCARTY, O. J. 2013a. Pivotal role for the mTOR pathway in the formation of neutrophil extracellular traps via regulation of autophagy. *Am J Physiol Cell Physiol*, 305, C348-54.
- ITAKURA, E. & MIZUSHIMA, N. 2010. Characterization of autophagosome formation site by a hierarchical analysis of mammalian Atg proteins. *Autophagy*, 6, 764-76.
- JABIR, M. S., RITCHIE, N. D., LI, D., BAYES, H. K., TOURLMOUSIS, P., PULESTON, D., LUPTON, A., HOPKINS, L., SIMON, A. K., BRYANT, C. & EVANS, T. J. 2014. Caspase-1 cleavage of the TLR adaptor TRIF inhibits autophagy and beta-interferon production during *Pseudomonas aeruginosa* infection. *Cell Host Microbe*, 15, 214-27.
- JACOBS, S. R. & DAMANIA, B. 2012. NLRs, inflammasomes, and viral infection. *Journal of leukocyte biology*, 92, 469-477.
- JANEWAY JR, C. A. 1992. The immune system evolved to discriminate infectious nonself from noninfectious self. *Immunology Today*, 13, 11-16.
- JIN, M. S., KIM, S. E., HEO, J. Y., LEE, M. E., KIM, H. M., PAIK, S. G., LEE, H. & LEE, J. O. 2007. Crystal structure of the TLR1-TLR2 heterodimer induced by binding of a tri-acetylated lipopeptide. *Cell*, 130, 1071-82.
- JOHNSON, H. L., DELORIA-KNOLL, M., LEVINE, O. S., STOSZEK, S. K., FREIMANIS HANCE, L., REITHINGER, R., MUENZ, L. R. & O'BRIEN, K. L. 2010. Systematic evaluation of serotypes causing invasive pneumococcal disease among children under five: the pneumococcal global serotype project. *PLoS Med*, 7.
- JUNKINS, R. D., MCCORMICK, C. & LIN, T. J. 2014. The emerging potential of autophagy-based therapies in the treatment of cystic fibrosis lung infections. *Autophagy*, 10, 538-47.
- JUNKINS, R. D., SHEN, A., ROSEN, K., MCCORMICK, C. & LIN, T.-J. 2013. Autophagy Enhances Bacterial Clearance during *P. aeruginosa* Lung Infection. *PLoS One*, 8, e72263.
- KASTENBAUER, S. & PFISTER, H. W. 2003. Pneumococcal meningitis in adults: spectrum of complications and prognostic factors in a series of 87 cases. *Brain*, 126, 1015-25.
- KAWAI, T. & AKIRA, S. 2006. TLR signaling. *Cell Death Differ*, 13, 816-25.
- KELLY, T., DILLARD, J. P. & YOTHER, J. 1994. Effect of genetic switching of capsular type on virulence of *Streptococcus pneumoniae*. *Infect Immun*, 62, 1813-9.

- KIM, W. Y., NAM, S. A., SONG, H. C., KO, J. S., PARK, S. H., KIM, H. L., CHOI, E. J., KIM, Y. S., KIM, J. & KIM, Y. K. 2012. The role of autophagy in unilateral ureteral obstruction rat model. *Nephrology (Carlton)*, 17, 148-59.
- KIMURA, S., NODA, T. & YOSHIMORI, T. 2008. Dynein-dependent movement of autophagosomes mediates efficient encounters with lysosomes. *Cell Struct Funct*, 33, 109-22.
- KIRKEGAARD, K., TAYLOR, M. P. & JACKSON, W. T. 2004. Cellular autophagy: surrender, avoidance and subversion by microorganisms. *Nat Rev Micro*, 2, 301-314.
- KOLACZKOWSKA, E. & KUBES, P. 2013. Neutrophil recruitment and function in health and inflammation. *Nat Rev Immunol*, 13, 159-75.
- KOMATSU, M., WANG, Q. J., HOLSTEIN, G. R., FRIEDRICH, V. L., JR., IWATA, J., KOMINAMI, E., CHAIT, B. T., TANAKA, K. & YUE, Z. 2007. Essential role for autophagy protein Atg7 in the maintenance of axonal homeostasis and the prevention of axonal degeneration. *Proc Natl Acad Sci U S A*, 104, 14489-94.
- KRAUSGRUBER, T., BLAZEK, K., SMALLIE, T., ALZABIN, S., LOCKSTONE, H., SAHGAL, N., HUSSELL, T., FELDMANN, M. & UDALOVA, I. A. 2011. IRF5 promotes inflammatory macrophage polarization and TH1-TH17 responses. *Nat Immunol*, 12, 231-238.
- KUMAR, H., KAWAI, T. & AKIRA, S. 2009. Pathogen recognition in the innate immune response. *Biochem J*, 420, 1-16.
- KUNDU, M., THOMPSON, C. B., KUNDU, M. & THOMPSON, C. B. 2008. Autophagy: basic principles and relevance to disease. *Annual Review Of Pathology*, 3, 427-55.
- LANIE, J. A., NG, W.-L., KAZMIERCZAK, K. M., ANDRZEJEWSKI, T. M., DAVIDSEN, T. M., WAYNE, K. J., TETTELIN, H., GLASS, J. I. & WINKLER, M. E. 2007. Genome Sequence of Avery's Virulent Serotype 2 Strain D39 of *S. pneumoniae* and Comparison with That of Unencapsulated Laboratory Strain R6. *Journal of Bacteriology*, 189, 38-51.
- LATERRE, P. F., GARBER, G., LEVY, H., WUNDERINK, R., KINASEWITZ, G. T., SOLLET, J. P., MAKI, D. G., BATES, B., YAN, S. C., DHAINAUT, J. F. & COMMITTEE, P. C. E. 2005. Severe community-acquired pneumonia as a cause of severe sepsis: data from the PROWESS study. *Crit Care Med*, 33, 952-61.
- LEAVY, O. 2011. Inflammasome: NAIPs: pathogen-sensing proteins. *Nat Rev Immunol*, 11, 644-644.

- LEE, H.-Y., ANDALIBI, A., WEBSTER, P., MOON, S.-K., TEUFERT, K., KANG, S.-H., LI, J.-D., NAGURA, M., GANZ, T. & LIM, D. 2004. Antimicrobial activity of innate immune molecules against *Streptococcus pneumoniae*, *Moraxella catarrhalis* and nontypeable *Haemophilus influenzae*. *BMC Infect Dis*, 4, 1-12.
- LEE, N. Y., SONG, J. H., KIM, S., PECK, K. R., AHN, K. M., LEE, S. I., YANG, Y., LI, J., CHONGTHALEONG, A., TIENGRIM, S., ASWAPOKEE, N., LIN, T. Y., WU, J. L., CHIU, C. H., LALITHA, M. K., THOMAS, K., CHERIAN, T., PERERA, J., YEE, T. T., JAMAL, F., WARSA, U. C., VAN, P. H., CARLOS, C. C., SHIBL, A. M., JACOBS, M. R. & APPELBAUM, P. C. 2001. Carriage of antibiotic-resistant pneumococci among Asian children: a multinational surveillance by the Asian Network for Surveillance of Resistant Pathogens (ANSORP). *Clin Infect Dis*, 32, 1463-9.
- LEE, Y. R., HU, H. Y., KUO, S. H., LEI, H. Y., LIN, Y. S., YEH, T. M., LIU, C. C. & LIU, H. S. 2013. *Dengue virus* infection induces autophagy: an in vivo study. *J Biomed Sci*, 20, 65.
- LEENEN, P. J. M., DE BRUIJN, M. F. T. R., VOERMAN, J. S. A., CAMPBELL, P. A. & VAN EWIJK, W. 1994. Markers of mouse macrophage development detected by monoclonal antibodies. *Journal of Immunological Methods*, 174, 5-19.
- LEGRAND, C., BOUR, J. M., JACOB, C., CAPIAUMONT, J., MARTIAL, A., MARC, A., WUDTKE, M., KRETZMER, G., DEMANGEL, C., DUVAL, D. & ET AL. 1992. Lactate dehydrogenase (LDH) activity of the cultured eukaryotic cells as marker of the number of dead cells in the medium [corrected]. *J Biotechnol*, 25, 231-43.
- LEHRER, R. I. & GANZ, T. 1999. Antimicrobial peptides in mammalian and insect host defence. *Current Opinion in Immunology*, 11, 23-27.
- LEVINE, B. 2005. Eating Oneself and Uninvited Guests: Autophagy-Related Pathways in Cellular Defence. *Cell*, 120, 159-162.
- LEVINE, B. & KROEMER, G. 2008. Autophagy in the pathogenesis of disease. *Cell*, 132, 27-42.
- LEVINE, B., MIZUSHIMA, N. & VIRGIN, H. W. 2011. Autophagy in immunity and inflammation. *Nature*, 469, 323-335.
- LIANG, C., FENG, P., KU, B., DOTAN, I., CANAANI, D., OH, B. H. & JUNG, J. U. 2006. Autophagic and tumour suppressor activity of a novel Beclin1-binding protein UVRAG. *Nat Cell Biol*, 8, 688-99.
- LIANG, C., LEE, J. S., INN, K. S., GACK, M. U., LI, Q., ROBERTS, E. A., VERGNE, I., DERETIC, V., FENG, P., AKAZAWA, C. & JUNG, J. U. 2008. Beclin1-binding UVRAG targets the class C Vps complex to coordinate

autophagosome maturation and endocytic trafficking. *Nat Cell Biol*, 10, 776-87.

- LITTMANN, M., ALBIGER, B., FRENTZEN, A., NORMARK, S., HENRIQUES-NORMARK, B. & PLANT, L. 2009. *Streptococcus pneumoniae* evades human dendritic cell surveillance by pneumolysin expression. *EMBO Mol Med*, 1, 211-22.
- LORD, K. A., HOFFMAN-LIEBERMANN, B. & LIEBERMANN, D. A. 1990. Nucleotide sequence and expression of a cDNA encoding MyD88, a novel myeloid differentiation primary response gene induced by IL6. *Oncogene*, 5, 1095-7.
- LUM, J. J., BAUER, D. E., KONG, M., HARRIS, M. H., LI, C., LINDSTEN, T. & THOMPSON, C. B. 2005. Growth factor regulation of autophagy and cell survival in the absence of apoptosis. *Cell*, 120, 237-48.
- LUTZ, M. B., KUKUTSCH, N., OGILVIE, A. L. J., RAYNER, S., KOCH, F., ROMANI, N. & SCHULER, G. 1999. An advanced culture method for generating large quantities of highly pure dendritic cells from mouse bone marrow. *Journal of Immunological Methods*, 223, 77.
- MA, C., WANG, N., DETRE, C., WANG, G., O'KEEFFE, M. & TERHORST, C. 2012. SLAM is a microbial sensor which regulates bacterial phagosome functions in macrophages by recruiting a Vps34/beclin 1/UVRAG complex. *The Journal of Immunology*, 188, 112.8.
- MALLEY, R., HENNEKE, P., MORSE, S. C., CIESLEWICZ, M. J., LIPSITCH, M., THOMPSON, C. M., KURT-JONES, E., PATON, J. C., WESSELS, M. R. & GOLENBOCK, D. T. 2003. Recognition of pneumolysin by Toll-like receptor 4 confers resistance to pneumococcal infection. *Proc Natl Acad Sci U S A*, 100, 1966-71.
- MANZANERO, S. 2012. Generation of Mouse Bone Marrow-Derived Macrophages. *In: ASHMAN, R. B. (ed.) Leucocytes*. Humana Press.
- MARRIOTT, H. M., MITCHELL, T. J. & DOCKRELL, D. H. 2008. Pneumolysin: a double-edged sword during the host-pathogen interaction. *Curr Mol Med*, 8, 497-509.
- MARTINEZ, F. O., HELMING, L. & GORDON, S. 2009. Alternative activation of macrophages: an immunologic functional perspective. *Annu Rev Immunol*, 27, 451-83.
- MARTINON, F., BURNS, K. & TSCHOPP, J. 2002. The inflammasome: a molecular platform triggering activation of inflammatory caspases and processing of proIL-beta. *Mol Cell*, 10, 417-26.

- MARTINON, F., GAIDE, O., PETRILLI, V., MAYOR, A. & TSCHOPP, J. 2007. NALP inflammasomes: a central role in innate immunity. *Semin Immunopathol*, 29, 213-29.
- MARTINON, F., MAYOR, A. & TSCHOPP, J. 2009. The Inflammasomes: Guardians of the Body. *Annual Review of Immunology*, 27, 229-265.
- MARTINON, F., PETRILLI, V., MAYOR, A., TARDIVEL, A. & TSCHOPP, J. 2006. Gout-associated uric acid crystals activate the NALP3 inflammasome. *Nature*, 440, 237-241.
- MARTINON, F. & TSCHOPP, J. 2005. NLRs join TLRs as innate sensors of pathogens. *Trends Immunol*, 26, 447-54.
- MATSUNAGA, K., SAITOH, T., TABATA, K., OMORI, H., SATOH, T., KURATORI, N., MAEJIMA, I., SHIRAHAMA-NODA, K., ICHIMURA, T., ISOBE, T., AKIRA, S., NODA, T. & YOSHIMORI, T. 2009. Two Beclin 1-binding proteins, Atg14L and Rubicon, reciprocally regulate autophagy at different stages. *Nature cell biology*, 11, 385-96.
- MATSUZAWA, T., FUJIWARA, E. & WASHI, Y. 2014a. Autophagy activation by interferon-gamma via the p38 mitogen-activated protein kinase signalling pathway is involved in macrophage bactericidal activity. *Immunology*, 141, 61-9.
- MATSUZAWA, T., FUJIWARA, E. & WASHI, Y. 2014b. Autophagy activation by interferon- γ via the p38 mitogen-activated protein kinase signalling pathway is involved in macrophage bactericidal activity. *Immunology*, 141, 61-69.
- MATZINGER, P. 2002. The Danger Model: A Renewed Sense of Self. *Science*, 296, 301-305.
- MCDONALD, C., INOHARA, N. & NUNEZ, G. 2005. Peptidoglycan signaling in innate immunity and inflammatory disease. *J Biol Chem*, 280, 20177-80.
- MCFARLANE, S., AITKEN, J., SUTHERLAND, J. S., NICHOLL, M. J., PRESTON, V. G. & PRESTON, C. M. 2011. Early Induction of Autophagy in Human Fibroblasts after Infection with Human *Cytomegalovirus* or *Herpes Simplex Virus 1*. *Journal of virology*, 85, 4212-4221.
- MCNEELA, E. A., BURKE, Á., NEILL, D. R., BAXTER, C., FERNANDES, V. E., FERREIRA, D., SMEATON, S., EL-RACHKIDY, R., MCLOUGHLIN, R. M., MORI, A., MORAN, B., FITZGERALD, K. A., TSCHOPP, J., PÉTRILLI, V., ANDREW, P. W., KADIOGLU, A. & LAVELLE, E. C. 2010. Pneumolysin Activates the NLRP3 Inflammasome and Promotes Proinflammatory Cytokines Independently of TLR4. *PLoS Pathog*, 6, e1001191.

- MEDZHITOV, R., PRESTON-HURLBURT, P. & JANEWAY, C. A., JR. 1997. A human homologue of the *Drosophila* Toll protein signals activation of adaptive immunity. *Nature*, 388, 394-7.
- MEIFFREN, G., JOUBERT, P.-E., GREGOIRE, I. P., RABOURDIN-COMBE, C. & FAURE, M. 2010. Pathogen recognition by the cell surface receptor CD46 induces autophagy. *Autophagy*, 6, 299-300.
- MEISSNER, F., MOLAWI, K. & ZYCHLINSKY, A. 2008. Superoxide dismutase 1 regulates caspase-1 and endotoxic shock. *Nat Immunol*, 9, 866-872.
- MITCHELL, A. M. & MITCHELL, T. J. 2010. *Streptococcus pneumoniae*: virulence factors and variation. *Clin Microbiol Infect*, 16, 411-8.
- MITCHELL, T. J., ANDREW, P. W., SAUNDERS, F. K., SMITH, A. N. & BOULNOIS, G. J. 1991. Complement activation and antibody binding by pneumolysin via a region of the toxin homologous to a human acute-phase protein. *Mol Microbiol*, 5, 1883-8.
- MIZUSHIMA, N., LEVINE, B., CUERVO, A. M. & KLIONSKY, D. J. 2008. Autophagy fights disease through cellular self-digestion. *Nature*, 451, 1069-75.
- MOINE, P., VERCKEN, J. B., CHEVRET, S. & GAJDOS, P. 1995. Severe community-acquired pneumococcal pneumonia. The French Study Group of Community-Acquired Pneumonia in ICU. *Scand J Infect Dis*, 27, 201-6.
- MOLLOY, S. 2011. Bacterial pathogenicity: Pneumolysin: stimulating protection. *Nat Rev Micro*, 9, 4-4.
- MONASTA, L., RONFANI, L., MARCHETTI, F., MONTICO, M., VECCHI BRUMATTI, L., BAVCAR, A., GRASSO, D., BARBIERO, C. & TAMBURLINI, G. 2012. Burden of Disease Caused by Otitis Media: Systematic Review and Global Estimates. *PloS one*, 7, e36226.
- MOSSER, D. M. & EDWARDS, J. P. 2008. Exploring the full spectrum of macrophage activation. *Nat Rev Immunol*, 8, 958-969.
- MUKERJI, R., MIRZA, S., ROCHE, A. M., WIDENER, R. W., CRONEY, C. M., RHEE, D. K., WEISER, J. N., SZALAI, A. J. & BRILES, D. E. 2012. Pneumococcal surface protein A inhibits complement deposition on the pneumococcal surface by competing with the binding of C-reactive protein to cell-surface phosphocholine. *J Immunol*, 189, 5327-35.
- MURRAY, P. J. & WYNN, T. A. 2011. Obstacles and opportunities for understanding macrophage polarization. *J Leukoc Biol*, 89, 557-63.
- MYERS, C. & GERVAIX, A. 2007. *Streptococcus pneumoniae* bacteraemia in children. *Int J Antimicrob Agents*, 30 Suppl 1, S24-8.

- NAKAHIRA, K., HASPEL, J. A., RATHINAM, V. A., LEE, S. J., DOLINAY, T., LAM, H. C., ENGLERT, J. A., RABINOVITCH, M., CERNADAS, M., KIM, H. P., FITZGERALD, K. A., RYTER, S. W. & CHOI, A. M. 2011. Autophagy proteins regulate innate immune responses by inhibiting the release of mitochondrial DNA mediated by the NALP3 inflammasome. *Nat Immunol*, 12, 222-30.
- NAKHAEI, P., GENIN, P., CIVAS, A. & HISCOTT, J. 2009. RIG-I-like receptors: Sensing and responding to RNA virus infection. *Seminars in Immunology*, 21, 215-222.
- NATHAN, C. 2006. Neutrophils and immunity: challenges and opportunities. *Nat Rev Immunol*, 6, 173-82.
- NAUSEEF, W. 2014. Isolation of Human Neutrophils from Venous Blood. In: QUINN, M. T. & DELEO, F. R. (eds.) *Neutrophil Methods and Protocols*. Humana Press.
- NEDJIC, J., AICHINGER, M., EMMERICH, J., MIZUSHIMA, N. & KLEIN, L. 2008. Autophagy in thymic epithelium shapes the T-cell repertoire and is essential for tolerance. *Nature*, 455, 396-400.
- NELSON, A. L., ROCHE, A. M., GOULD, J. M., CHIM, K., RATNER, A. J. & WEISER, J. N. 2007. Capsule enhances pneumococcal colonisation by limiting mucus-mediated clearance. *Infect Immun*, 75, 83-90.
- NODA, T., FUJITA, N. & YOSHIMORI, T. 2009. The late stages of autophagy: how does the end begin? *Cell Death Differ*, 16, 984-90.
- O'BRIEN, K. L., WOLFSON, L. J., WATT, J. P., HENKLE, E., DELORIA-KNOLL, M., MCCALL, N., LEE, E., MULHOLLAND, K., LEVINE, O. S., CHERIAN, T., HIB & PNEUMOCOCCAL GLOBAL BURDEN OF DISEASE STUDY, T. 2009. Burden of disease caused by *Streptococcus pneumoniae* in children younger than 5 years: global estimates. *Lancet*, 374, 893-902.
- OGUNNIYI, A. D., LEMESSURIER, K. S., GRAHAM, R. M. A., WATT, J. M., BRILES, D. E., STROEHER, U. H. & PATON, J. C. 2007. Contributions of Pneumolysin, Pneumococcal Surface Protein A (PspA), and PspC to Pathogenicity of *Streptococcus pneumoniae* D39 in a Mouse Model. *Infection and Immunity*, 75, 1843-1851.
- OLIVEIRA, M. L., AREAS, A. P., CAMPOS, I. B., MONEDERO, V., PEREZ-MARTINEZ, G., MIYAJI, E. N., LEITE, L. C., AIRES, K. A. & LEE HO, P. 2006. Induction of systemic and mucosal immune response and decrease in *Streptococcus pneumoniae* colonisation by nasal inoculation of mice with recombinant lactic acid bacteria expressing pneumococcal surface antigen A. *Microbes Infect*, 8, 1016-24.

- ORVEDAHL, A., MACPHERSON, S., SUMPTER, R., JR., TALLOCZY, Z., ZOU, Z. & LEVINE, B. 2010. Autophagy protects against *Sindbis virus* infection of the central nervous system. *Cell Host Microbe*, 7, 115-27.
- OSTERGAARD, C., KONRADSEN, H. B. & SAMUELSSON, S. 2005. Clinical presentation and prognostic factors of *Streptococcus pneumoniae* meningitis according to the focus of infection. *BMC Infect Dis*, 5, 93.
- PAPAYANNOPOULOS, V. & ZYCHLINSKY, A. 2009. NETs: a new strategy for using old weapons. *Trends in Immunology*, 30, 513-521.
- PAREJA, M. E. & COLOMBO, M. I. 2013. Autophagic clearance of bacterial pathogens: molecular recognition of intracellular microorganisms. *Front Cell Infect Microbiol*, 3, 54.
- PARK, H. H., LO, Y.-C., LIN, S.-C., WANG, L., YANG, J. K. & WU, H. 2007. The Death Domain Superfamily in Intracellular Signalling of Apoptosis and Inflammation. *Annual Review of Immunology*, 25, 561-586.
- PATEL, I. S., SEEMUNGAL, T. A., WILKS, M., LLOYD-OWEN, S. J., DONALDSON, G. C. & WEDZICHA, J. A. 2002. Relationship between bacterial colonisation and the frequency, character, and severity of COPD exacerbations. *Thorax*, 57, 759-64.
- PILLAY, J., DEN BRABER, I., VRISEKOOP, N., KWAST, L. M., DE BOER, R. J., BORGHANS, J. A., TESSELAAR, K. & KOENDERMAN, L. 2010. In vivo labeling with $2\text{H}_2\text{O}$ reveals a human neutrophil lifespan of 5.4 days. *Blood*, 116, 625-7.
- PIRAS, V. & SELVARAJOO, K. 2014. Beyond MyD88 and TRIF Pathways in Toll-Like Receptor Signaling. *Front Immunol*, 5, 70.
- POLSON, H. E., DE LARTIGUE, J., RIGDEN, D. J., REEDIJK, M., URBE, S., CLAGUE, M. J. & TOOZE, S. A. 2010. Mammalian Atg18 (WIPI2) localizes to omegasome-anchored phagophores and positively regulates LC3 lipidation. *Autophagy*, 6.
- POYET, J. L., SRINIVASULA, S. M., TNANI, M., RAZMARA, M., FERNANDES-ALNEMRI, T. & ALNEMRI, E. S. 2001. Identification of Ipaf, a human caspase-1-activating protein related to Apaf-1. *J Biol Chem*, 276, 28309-13.
- PRACHT, D., ELM, C., GERBER, J., BERGMANN, S., ROHDE, M., SEILER, M., KIM, K. S., JENKINSON, H. F., NAU, R. & HAMMERSCHMIDT, S. 2005. PavA of *Streptococcus pneumoniae* modulates adherence, invasion, and meningeal inflammation. *Infect Immun*, 73, 2680-9.

- PROELL, M., RIEDL, S. J., FRITZ, J. H., ROJAS, A. M. & SCHWARZENBACHER, R. 2008. The Nod-like receptor (NLR) family: a tale of similarities and differences. *PLoS One*, 3, e2119.
- PUCHTA, A., VERSCHOOR, C. P., THURN, T. & BOWDISH, D. M. 2014. Characterization of inflammatory responses during intranasal colonisation with *Streptococcus pneumoniae*. *J Vis Exp*, e50490.
- PULESTON, D. J. & SIMON, A. K. 2014. Autophagy in the immune system. *Immunology*, 141, 1-8.
- QU, X., ZOU, Z., SUN, Q., LUBY-PHELPS, K., CHENG, P., HOGAN, R. N., GILPIN, C. & LEVINE, B. 2007. Autophagy Gene-Dependent Clearance of Apoptotic Cells during Embryonic Development. *Cell*, 128, 931-946.
- QUAN, W., JUNG, H. S. & LEE, M. S. 2013. Role of autophagy in the progression from obesity to diabetes and in the control of energy balance. *Arch Pharm Res*, 36, 223-9.
- QUIN, L. R., MOORE, Q. C. & MCDANIEL, L. S. 2007. Pneumolysin, PspA, and PspC Contribute to Pneumococcal Evasion of Early Innate Immune Responses during Bacteraemia in Mice. *Infection and Immunity*, 75, 2067-2070.
- RAVIKUMAR, B., MOREAU, K., JAHREISS, L., PURI, C. & RUBINSZTEIN, D. C. 2010. Plasma membrane contributes to the formation of pre-autophagosomal structures. *Nat Cell Biol*, 12, 747-57.
- REMIJSEN, Q., VANDEN BERGHE, T., WIRAWAN, E., ASSELBERGH, B., PARTHOENS, E., DE RYCKE, R., NOPPEN, S., DELFORGE, M., WILLEMS, J. & VANDENABEELE, P. 2011. Neutrophil extracellular trap cell death requires both autophagy and superoxide generation. *Cell Res*, 21, 290-304.
- REN, B., LI, J., GENSCHEMER, K., HOLLINGSHEAD, S. K. & BRILES, D. E. 2012. The absence of PspA or presence of antibody to PspA facilitates the complement-dependent phagocytosis of pneumococci in vitro. *Clin Vaccine Immunol*, 19, 1574-82.
- ROBERTSON, O. H., VAN SANT, H. & PETERSON, G. 1939. A Comparative Study of Phagocytosis and Digestion of Pneumococci by Macrophages and Polymorphonuclear Leucocytes in Normal and Immune Dogs. *The Journal of Immunology*, 37, 571-597.
- RUDAN, I., BOSCHI-PINTO, C., BILOGLAV, Z., MULHOLLAND, K. & CAMPBELL, H. 2008. Epidemiology and etiology of childhood pneumonia. *Bull World Health Organ*, 86, 408-16.
- SAGULENKO, V., THYGESEN, S. J., SESTER, D. P., IDRIS, A., CRIDLAND, J. A., VAJJHALA, P. R., ROBERTS, T. L., SCHRODER, K., VINCE, J. E., HILL, J. M., SILKE, J. & STACEY, K. J. 2013. AIM2 and NLRP3 inflammasomes

activate both apoptotic and pyroptotic death pathways via ASC. *Cell Death Differ*, 20, 1149-1160.

- SAITOH, T. & AKIRA, S. 2010. Regulation of innate immune responses by autophagy-related proteins. *The Journal of cell biology*, 189, 925-35.
- SAITOH, T., FUJITA, N., JANG, M. H., UEMATSU, S., YANG, B. G., SATOH, T., OMORI, H., NODA, T., YAMAMOTO, N., KOMATSU, M., TANAKA, K., KAWAI, T., TSUJIMURA, T., TAKEUCHI, O., YOSHIMORI, T. & AKIRA, S. 2008. Loss of the autophagy protein Atg16L1 enhances endotoxin-induced IL-1 β production. *Nature*, 456, 264-8.
- SANJUAN, M. A., DILLON, C. P., TAIT, S. W. G., MOSHIACH, S., DORSEY, F., CONNELL, S., KOMATSU, M., TANAKA, K., CLEVELAND, J. L., WITHOFF, S. & GREEN, D. R. 2007. Toll-like receptor signalling in macrophages links the autophagy pathway to phagocytosis. *Nature*, 450, 1253-1257.
- SCHAFF, U. S. S. 2008. Electroporation parameters for transfection of HL-60 leukocytic cell line with siRNA using the Gene Pulser MXcell system. *Bio-Rad Bulletin*. 5778.
- SEGAL, A. W. 2005. HOW NEUTROPHILS KILL MICROBES. *Annual Review of Immunology*, 23, 197-223.
- SEGAL, A. W. & ABO, A. 1993. The biochemical basis of the NADPH oxidase of phagocytes. *Trends in Biochemical Sciences*, 18, 43-47.
- SEGLIN, P. O. & GORDON, P. B. 1982. 3-Methyladenine: Specific inhibitor of autophagic/lysosomal protein degradation in isolated rat hepatocytes. *Proceedings of the National Academy of Sciences*, 79, 1889-1892.
- SERHAN, C. N. & SAVILL, J. 2005. Resolution of inflammation: the beginning programs the end. *Nat Immunol*, 6, 1191-1197.
- SHAHNAZARI, S., YEN, W. L., BIRMINGHAM, C. L., SHIU, J., NAMOLOVAN, A., ZHENG, Y. T., NAKAYAMA, K., KLIONSKY, D. J. & BRUMELL, J. H. 2010. A diacylglycerol-dependent signaling pathway contributes to regulation of antibacterial autophagy. *Cell Host Microbe*, 8, 137-46.
- SHAPER, M., HOLLINGSHEAD, S. K., BENJAMIN, W. H., JR. & BRILES, D. E. 2004. PspA protects *Streptococcus pneumoniae* from killing by apolactoferrin, and antibody to PspA enhances killing of pneumococci by apolactoferrin [corrected]. *Infect Immun*, 72, 5031-40.
- SHENG, Y., SUN, B., GUO, W. T., ZHANG, Y. H., LIU, X., XING, Y. & DONG, D. L. 2013. 3-Methyladenine induces cell death and its interaction with chemotherapeutic drugs is independent of autophagy. *Biochem Biophys Res Commun*, 432, 5-9.

- SHI, C. S. & KEHRL, J. H. 2008. MyD88 and Trif target Beclin 1 to trigger autophagy in macrophages. *J Biol Chem*, 283, 33175-82.
- SHOMA, S., TSUCHIYA, K., KAWAMURA, I., NOMURA, T., HARA, H., UCHIYAMA, R., DAIM, S. & MITSUYAMA, M. 2008. Critical involvement of pneumolysin in production of interleukin-1alpha and caspase-1-dependent cytokines in infection with *Streptococcus pneumoniae* in vitro: a novel function of pneumolysin in caspase-1 activation. *Infect Immun*, 76, 1547-57.
- SHUI, W., SHEU, L., LIU, J., SMART, B., PETZOLD, C. J., HSIEH, T.-Y., PITCHER, A., KEASLING, J. D. & BERTOZZI, C. R. 2008. Membrane proteomics of phagosomes suggests a connection to autophagy. *Proceedings of the National Academy of Sciences*, 105, 16952-16957.
- SICA, A. & MANTOVANI, A. 2012. Macrophage plasticity and polarization: in vivo veritas. *J Clin Invest*, 122, 787-95.
- SINGH, S. B., DAVIS, A. S., TAYLOR, G. A. & DERETIC, V. 2006. Human IRGM induces autophagy to eliminate intracellular mycobacteria. *Science (New York, N.Y.)*, 313, 1438-41.
- SIR, D., TIAN, Y., CHEN, W. L., ANN, D. K., YEN, T. S. & OU, J. H. 2010. The early autophagic pathway is activated by *hepatitis B virus* and required for viral DNA replication. *Proc Natl Acad Sci U S A*, 107, 4383-8.
- SLEE, E. A., ZHU, H., CHOW, S. C., MACFARLANE, M., NICHOLSON, D. W. & COHEN, G. M. 1996. Benzylloxycarbonyl-Val-Ala-Asp (OMe) fluoromethylketone (Z-VAD.FMK) inhibits apoptosis by blocking the processing of CPP32. *Biochem J*, 315 (Pt 1), 21-4.
- SONG, J. H., JUNG, S. I., KO, K. S., KIM, N. Y., SON, J. S., CHANG, H. H., KI, H. K., OH, W. S., SUH, J. Y., PECK, K. R., LEE, N. Y., YANG, Y., LU, Q., CHONGTHALEONG, A., CHIU, C. H., LALITHA, M. K., PERERA, J., YEE, T. T., KUMARASINGHE, G., JAMAL, F., KAMARULZAMAN, A., PARASAKTHI, N., VAN, P. H., CARLOS, C., SO, T., NG, T. K. & SHIBL, A. 2004. High prevalence of antimicrobial resistance among clinical *Streptococcus pneumoniae* isolates in Asia (an ANSORP study). *Antimicrob Agents Chemother*, 48, 2101-7.
- SONG, W., HAN, Z., SUN, Y. & CHAI, J. 2014. Crystal structure of a plant leucine rich repeat protein with two island domains. *Science China Life Sciences*, 57, 137-144.
- SRINIVASULA, S. M., POYET, J. L., RAZMARA, M., DATTA, P., ZHANG, Z. & ALNEMRI, E. S. 2002. The PYRIN-CARD protein ASC is an activating adaptor for caspase-1. *J Biol Chem*, 277, 21119-22.
- STEIN, M., KESHAV, S., HARRIS, N. & GORDON, S. 1992. Interleukin 4 potently enhances murine macrophage mannose receptor activity: a marker of

alternative immunologic macrophage activation. *The Journal of Experimental Medicine*, 176, 287-292.

- STEINBERG, B. E. & GRINSTEIN, S. 2007. Assessment of phagosome formation and maturation by fluorescence microscopy. *Methods Mol Biol*, 412, 289-300.
- SUN, Y., GUO, W. & XU, Q. 2014. Mitophagy-mediated NLRP3 inflammasome inhibition by andrographolide contributes to the prevention of colitis-associated cancer (1052.3). *The FASEB Journal*, 28.
- TAKEMURA, R. & WERB, Z. 1984. Secretory products of macrophages and their physiological functions. *Am J Physiol*, 246, C1-9.
- TANIDA, I., MINEMATSU-IKEGUCHI, N., UENO, T. & KOMINAMI, E. 2005. Lysosomal turnover, but not a cellular level, of endogenous LC3 is a marker for autophagy. *Autophagy*, 1, 84-91.
- TANIDA, I., UENO, T. & KOMINAMI, E. 2008. LC3 and Autophagy. *Methods Mol Biol*, 445, 77-88.
- TATTOLI, I., TRAVASSOS, L. H., CARNEIRO, L. A., MAGALHAES, J. G. & GIRARDIN, S. E. 2007. The Nodosome: Nod1 and Nod2 control bacterial infections and inflammation. *Semin Immunopathol*, 29, 289-301.
- THURSTON, T. L., RYZHAKOV, G., BLOOR, S., VON MUHLINEN, N. & RANDOW, F. 2009. The TBK1 adaptor and autophagy receptor NDP52 restricts the proliferation of ubiquitin-coated bacteria. *Nat Immunol*, 10, 1215-21.
- TIAN, Y., LI, Z., HU, W., REN, H., TIAN, E., ZHAO, Y., LU, Q., HUANG, X., YANG, P., LI, X., WANG, X., KOVACS, A. L., YU, L. & ZHANG, H. 2010. *C. elegans* screen identifies autophagy genes specific to multicellular organisms. *Cell*, 141, 1042-55.
- TING, J. P., LOVERING, R. C., ALNEMRI, E. S., BERTIN, J., BOSS, J. M., DAVIS, B. K., FLAVELL, R. A., GIRARDIN, S. E., GODZIK, A., HARTON, J. A., HOFFMAN, H. M., HUGOT, J. P., INOHARA, N., MACKENZIE, A., MALTAIS, L. J., NUNEZ, G., OGURA, Y., OTTEN, L. A., PHILPOTT, D., REED, J. C., REITH, W., SCHREIBER, S., STEIMLE, V. & WARD, P. A. 2008. The NLR gene family: a standard nomenclature. *Immunity*, 28, 285-7.
- TOOZE, S. A. & YOSHIMORI, T. 2010. The origin of the autophagosomal membrane. *Nat Cell Biol*, 12, 831-835.
- TRAVASSOS, L. H., CARNEIRO, L. A., RAMJEET, M., HUSSEY, S., KIM, Y. G., MAGALHÃES, J. G., YUAN, L., SOARES, F., CHEA, E., LE BOURHIS, L., BONECA, I. G., ALLAOUI, A., JONES, N. L., NUAEZ, G., GIRARDIN, S. E. & PHILPOTT, D. J. 2010. Nod1 and Nod2 direct autophagy by recruiting ATG16L1 to the plasma membrane at the site of bacterial entry. *Nature immunology*, 11, 55-62.

- TSANG, M., PERERA, S., LONN, E. & DOKAINISH, H. 2013. Pneumococcal endocarditis causing valve destruction in the absence of vegetations on transesophageal echocardiography: a series of 3 consecutive cases. *Can J Cardiol*, 29, 519 e7-9.
- TSCHOPP, J., MARTINON, F. & BURNS, K. 2003. NALPs: a novel protein family involved in inflammation. *Nat Rev Mol Cell Biol*, 4, 95-104.
- TSUCHIYA, K. & HARA, H. 2014. The inflammasome and its regulation. *Crit Rev Immunol*, 34, 41-80.
- TU, A.-H. T., FULGHAM, R. L., MCCRORY, M. A., BRILES, D. E. & SZALAI, A. J. 1999. Pneumococcal Surface Protein A Inhibits Complement Activation by *Streptococcus pneumoniae*. *Infection and Immunity*, 67, 4720-4724.
- VAN GINKEL, F. W., MCGHEE, J. R., WATT, J. M., CAMPOS-TORRES, A., PARISH, L. A. & BRILES, D. E. 2003. Pneumococcal carriage results in ganglioside-mediated olfactory tissue infection. *Proc Natl Acad Sci U S A*, 100, 14363-7.
- VAN ROSSUM, A. M. C., LYSENKO, E. S. & WEISER, J. N. 2005. Host and Bacterial Factors Contributing to the Clearance of Colonization by *Streptococcus pneumoniae* in a Murine Model. *Infection and Immunity*, 73, 7718-7726.
- VAUDAUX, P. & WALDVOGEL, F. A. 1979. Gentamicin antibacterial activity in the presence of human polymorphonuclear leukocytes. *Antimicrob Agents Chemother*, 16, 743-9.
- VIRGIN, H. W. & LEVINE, B. 2009. Autophagy genes in immunity. *Nature Immunology*, 10, 461-470.
- WALCZAK, M. & MARTENS, S. 2013. Dissecting the role of the Atg12-Atg5-Atg16 complex during autophagosome formation. *Autophagy*, 9, 424-5.
- WEN, H., MIAO, E. A. & TING, J. P. 2013. Mechanisms of NOD-like receptor-associated inflammasome activation. *Immunity*, 39, 432-41.
- WHO 2008. 23-valent pneumococcal polysaccharide vaccine. Position paper. *Wkly Epidemiol Rec*, 83, 373-84.
- WILLIAMSON, Y. M., MOURA, H., WOOLFITT, A. R., PIRKLE, J. L., BARR, J. R., CARVALHO MDA, G., ADES, E. P., CARLONE, G. M. & SAMPSON, J. S. 2008. Differentiation of *Streptococcus pneumoniae* conjunctivitis outbreak isolates by matrix-assisted laser desorption ionization-time of flight mass spectrometry. *Appl Environ Microbiol*, 74, 5891-7.
- WINK, D. A., HINES, H. B., CHENG, R. Y., SWITZER, C. H., FLORES-SANTANA, W., VITEK, M. P., RIDNOUR, L. A. & COLTON, C. A. 2011. Nitric oxide and redox mechanisms in the immune response. *J Leukoc Biol*, 89, 873-91.

- WU, Y.-T., TAN, H.-L., SHUI, G., BAUVY, C., HUANG, Q., WENK, M. R., ONG, C.-N., CODOGNO, P. & SHEN, H.-M. 2010. Dual Role of 3-Methyladenine in Modulation of Autophagy via Different Temporal Patterns of Inhibition on Class I and III Phosphoinositide 3-Kinase. *Journal of Biological Chemistry*, 285, 10850-10861.
- XU, F., DROEMANN, D., RUPP, J., SHEN, H., WU, X., GOLDMANN, T., HIPPENSTIEL, S., ZABEL, P. & DALHOFF, K. 2008. Modulation of the inflammatory response to *Streptococcus pneumoniae* in a model of acute lung tissue infection. *Am J Respir Cell Mol Biol*, 39, 522-9.
- XU, Y., JAGANNATH, C., LIU, X.-D., SHARAFKHANEH, A., KOLODZIEJSKA, K. E. & EISSA, N. T. 2007. Toll-like Receptor 4 Is a Sensor for Autophagy Associated with Innate Immunity. *Immunity*, 27, 135-144.
- YAMAGUCHI, H., NAKAGAWA, I., YAMAMOTO, A., AMANO, A., NODA, T. & YOSHIMORI, T. 2009. An initial step of GAS-containing autophagosome-like vacuoles formation requires Rab7. *PLoS pathogens*, 5, e1000670.
- YAMAMOTO, A., TAGAWA, Y., YOSHIMORI, T., MORIYAMA, Y., MASAKI, R. & TASHIRO, Y. 1998. Bafilomycin A1 prevents maturation of autophagic vacuoles by inhibiting fusion between autophagosomes and lysosomes in rat hepatoma cell line, H-4-II-E cells. *Cell Struct Funct*, 23, 33-42.
- YANG, Y., KIM, S. C., YU, T., YI, Y. S., RHEE, M. H., SUNG, G. H., YOO, B. C. & CHO, J. Y. 2014. Functional roles of p38 mitogen-activated protein kinase in macrophage-mediated inflammatory responses. *Mediators Inflamm*, 2014, 352371.
- YU, H. B., CROXEN, M. A., MARCHIANDO, A. M., FERREIRA, R. B., CADWELL, K., FOSTER, L. J. & FINLAY, B. B. 2014. Autophagy facilitates *Salmonella* replication in HeLa cells. *MBio*, 5, e00865-14.
- YUSTE, J., BOTTO, M., PATON, J. C., HOLDEN, D. W. & BROWN, J. S. 2005. Additive Inhibition of Complement Deposition by Pneumolysin and PspA Facilitates *Streptococcus pneumoniae* Septicemia. *The Journal of Immunology*, 175, 1813-1819.
- ZHANEL, G. G., PALATNICK, L., NICHOL, K. A., BELYOU, T., LOW, D. E. & HOBAN, D. J. 2003. Antimicrobial resistance in respiratory tract *Streptococcus pneumoniae* isolates: results of the Canadian Respiratory Organism Susceptibility Study, 1997 to 2002. *Antimicrob Agents Chemother*, 47, 1867-74.
- ZHOU, X.-J. & ZHANG, H. 2012. Autophagy in immunity: Implications in etiology of autoimmune/autoinflammatory diseases. *Autophagy*, 8, 1286-1299.